

Appendix C

**UPRC - STRATOS FED UNIT #1
SPECIAL CORE ANALYSIS STUDY**

Prepared For

Union Pacific Resources Corporation

Prepared By

Hycal Energy Research Laboratories Ltd.

August 23, 1996

TABLE OF CONTENTS (cont'd)

| | <u>Page</u> |
|--|--------------------|
| Fracture Tests..... .. | 26 |
| Geomechanical Tests | 27 |
| Mercury Injection Capillary Pressure Tests | 27 |

List of Figures

- | | | |
|--------|----|---|
| FIGURE | 1 | Core #6B - Fracture Fluid Leakoff with Halliburton Frac Gel 2 Permeability Summary |
| FIGURE | 2 | Core #7A - Fracture Fluid Leakoff with BJ Titan Borate HT 4500 Permeability Summary |
| FIGURE | 3 | Core #31A - Fracture Fluid Leakoff with BJ Titan Borate HT 4500 Permeability Summary |
| FIGURE | 4 | Core #31B - Fracture Fluid Leakoff with Halliburton Frac Gel 2 Permeability Summary |
| FIGURE | 5 | Core #6A - Incremental Phase Trap Relative Permeability Test Permeability Summary - Threshold Pressure Regains |
| FIGURE | 5A | Core #6A - Incremental Phase Trap Relative Permeability Test Permeability vs Water Saturation |
| FIGURE | 6 | Core #37 - Incremental Phase Trap Relative Permeability Test Permeability Summary - Threshold Pressure Regains |
| FIGURE | 6A | Core #37 - Incremental Phase Trap Relative Permeability Test Permeability vs Water Saturation |
| FIGURE | 7 | Core #9 - Water-Gas Relative Permeability Test Cuml Production vs Cuml Injection |
| FIGURE | 8 | Core #9 - Water-Gas Relative Permeability Test Pressure vs Cuml Injection |
| FIGURE | 9 | Core #9 - Water-Gas Relative Permeability Test Relative Permeability vs Water Saturation (Cartesian) |
| FIGURE | 10 | Core #9 - Water-Gas Relative Permeability Test Relative Permeability vs Water Saturation (Semi-Log) |
| FIGURE | 11 | Core #48B - Water-Gas Relative Permeability Test Cuml Production vs Cuml Injection |
| FIGURE | 12 | Core #48B - Water-Gas Relative Permeability Test Pressure vs Cuml Injection |

List of Figures (cont'd)

- FIGURE 13 Core #48B - Water-Gas Relative Permeability Test
Relative Permeability vs Water Saturation (Cartesian)
- FIGURE 14 Core #48B - Water-Gas Relative Permeability Test
Relative Permeability vs Water Saturation (Semi-Log)
- FIGURE 15 Core #12 - Fracture Permeability vs Overburden and Fluid Saturation Test
Permeability Summary - Threshold Pressure Regains
- FIGURE 16 Core #32 - Fracture Permeability vs Overburden and Fluid Saturation Test
Permeability Summary - Threshold Pressure Regains

List of Tables

| | | |
|-------|-----|---|
| TABLE | 1: | Routine Porosity and Gas Permeability |
| TABLE | 2: | Core #6B - Fracture Fluid Leakoff with Halliburton Frac Gel 2 Core and Test Parameters |
| TABLE | 3: | Core #6B - Fracture Fluid Leakoff with Halliburton Frac Gel 2 Permeability Summary |
| TABLE | 4 | Core #6B - Fracture Fluid Leakoff with Halliburton Frac Gel 2 Leakoff Summary |
| TABLE | 5 | Core #7A - Fracture Fluid Leakoff with BJ Titan Borate HT 4500 Core and Test Parameters |
| TABLE | 6 | Core #7A - Fracture Fluid Leakoff with BJ Titan Borate HT 4500 Permeability Summary |
| TABLE | 7: | Core #7A - Fracture Fluid Leakoff with BJ Titan Borate HT 4500 Leakoff Summary |
| TABLE | 8. | Core #31A - Fracture Fluid Leakoff with BJ Titan Borate HT 4500 Core and Test Parameters |
| TABLE | 9: | Core #31A - Fracture Fluid Leakoff with BJ Titan Borate HT 4500 Permeability Summary |
| TABLE | 10. | Core #31A - Fracture Fluid Leakoff with BJ Titan Borate HT 4500 Leakoff Summary |
| TABLE | 11 | Core #31B - Fracture Fluid Leakoff with Halliburton Frac Gel 2 Core and Test Parameters |
| TABLE | 12 | Core #31B - Fracture Fluid Leakoff with Halliburton Frac Gel 2 Permeability Summary |
| TABLE | 13 | Core #31B - Fracture Fluid Leakoff with Halliburton Frac Gel 2 Leakoff Summary |
| TABLE | 14: | Core #6A - Incremental Phase Trap Relative Permeability Test Core and Test Parameters |

List of Tables (cont'd)

| | | |
|-------|-----|---|
| TABLE | 15 | Core #6A - Incremental Phase Trap Relative Permeability Test Permeability Summary - Threshold Pressure Regains |
| TABLE | 16 | Core #37 - Incremental Phase Trap Relative Permeability Test Core and Test Parameters |
| TABLE | 17: | Core #37 - Incremental Phase Trap Relative Permeability Test Permeability Summary - Threshold Pressure Regains |
| TABLE | 18 | Core #9 - Water-Gas Relative Permeability Test Core and Test Parameters |
| TABLE | 19: | Core #9 - Water-Gas Relative Permeability Test Saturation and Permeability Summary |
| TABLE | 20: | Core #9 - Water-Gas Relative Permeability Test Experimental Pressure and Production History |
| TABLE | 21: | Core #9 - Water-Gas Relative Permeability Data |
| TABLE | 22: | Core #48B - Water-Gas Relative Permeability Test Core and Test Parameters |
| TABLE | 23: | Core #48B - Water-Gas Relative Permeability Test Saturation and Permeability Summary |
| TABLE | 24 | Core #48B - Water-Gas Relative Permeability Test Experimental Pressure and Production History |
| TABLE | 25 | Core #48B - Water-Gas Relative Permeability Data |
| TABLE | 26 | Core #12 - Fracture Permeability vs Overburden and Fluid Saturation Test Core and Test Parameters |
| TABLE | 27: | Core #12 - Fracture Permeability vs Overburden and Fluid Saturation Test Permeability Summary - Threshold Pressure Regains |
| TABLE | 28: | Core #32 - Fracture Permeability vs Overburden and Fluid Saturation Test Core and Test Parameters |

List of Tables (cont'd)

| | | |
|-------|----|---|
| TABLE | 29 | Core #32 - Fracture Permeability vs Overburden and Fluid Saturation Test Permeability Summary - Threshold Pressure Regains |
| TABLE | 30 | Results of Geomechanical Testing |

List of Appendices

- APPENDIX A Results of Mercury Injection Capillary Pressure Measurements
- APPENDIX B. Petrographic Analysis Summary
- APPENDIX C Technical Papers
- 1 "Recent Improvements In Experimental Laboratory Techniques
In The Analysis Of Unsteady-State Relative Permeability Data"
- 2 "Low Permeability Gas Reservoirs Problems, Opportunities and
Solutions for Drilling, Completion, Stimulation and Production" - SPE35577
3. "Remediation of Water and Hydrocarbon Phase Trapping
Problems in Low Permeability Gas Reservoirs" - CIM96-80
- 4 "Reductions in the Productivity of Oil and Low Permeability Gas
Reservoirs Due to Aqueous Phase Trapping"

SUMMARY

At the request of Mr Frank Lim of Union Pacific Resources Corporation, Hycal Energy Research Laboratories Ltd conducted an extensive series of special core analysis tests to quantify formation damage mechanisms and reservoir quality and productivity on core samples received from the 16025 25 to 16180 3 ft interval of UPRC Stratos Federal Unit well #1

Tests were conducted to evaluate the formation sensitivity to two crosslinked fracture fluids (Halliburton Frac Gel 2 and BJ Titan Borate HT 4500 to quantify the effects of invasion of these fluids into the formation. Additional tests were conducted to quantify phase trapping potential and determine the water-gas relative permeability characteristics of the formation under consideration

Tests were also conducted on fractured full diameter cores to quantify the effect of closure stress on effective fracture permeability at reservoir conditions and the effect of water influx on microfracture permeability

The tests were conducted on samples from the upper (fluvial) interval and the lower (marine) interval. For some tests, the lower (marine) interval was subdivided into upper (clean) and a lower (dirty) lithofacies. The tests results indicated that

1 In-situ reservoir quality was extremely poor in the absence of any microfractures in the system. Matrix permeabilities to air in an unstressed, clean and dry condition at 100% gas saturation ranged from approximately 0.08 mD to a high of approximately 0.4 mD with porosities ranging from approximately 4 - 10%. The presence of fractures in the samples tended to enhance permeability, but later tests indicated that most of the fracture permeability was compromised when overburden stress was applied to the fractures

2 A detailed petrographic assessment of the reservoir quality of the UPRC Stratos Federal #1 samples from the fluvial and clean and dirty marine facies is contained in Appendix "B". In general, the petrographic work indicated that the sandstone samples represented sequences of slightly to moderately feldspathic, highly quartzose sublitharenite to atharenites with fair core measured porosity, low effective porosity and extremely low permeability. The smallest to mean grain sizes occurred in the dirty marine facies with an average diameter of 0.211 mm and largest grain sizes in the quartzose samples in the fluvial facie with an average mean diameter of 0.26 mm

The samples had moderate to high volumes of clay, ranging from 5 to 18% of the bulk overall reservoir matrix that tended to greatly lower reservoir quality, particularly in the marine facies samples. Low to high volumes of pore filling cements, ranging from 3 to 25%, also lowered the reservoir quality in the fluvial facies. There was no evidence of any pore occluding bitumen in any of the samples evaluated.

3 The petrology indicated that the dominant clay in the pore system appeared to be illitic in nature with some mixed layer illite-smectite expandable clay. This would indicate that the facies of the UPRC Stratos Federal #1 well would be moderately to highly sensitive to contact with fresh or low salinity water. Petrography indicates that the sandstones would not be sensitive to HCl stimulation in mineralogical terms, however, due to the highly quartzose nature of the system, it is not expected that any significant permeability enhancement would result by contact with HCl and, due to the very low permeability nature of the porous media, it is likely that acid trapping associated with adverse relative permeability phenomena could result in significant permeability reductions. Therefore, acidization with conventional hydrochloric acid is not recommended as a viable stimulation technique for the sandstone units evaluated.

A more detailed summary and review of the formation petrography is contained in Appendix "B"

Fracture Fluid Tests

A series of core displacement tests were conducted on the Stratos core material to quantify the sensitivity to two proposed fracture fluids which were supplied by UPRC. These fracture fluids were prepared according to the instructions supplied by the specified service companies (Halliburton and BJ) and contained the appropriate crosslinkers and encapsulated breaker systems. The tests were applied to quantify the invasion of fracture fluid at a net overbalance pressure of 1800 psi into the formation to simulate the gradient incurred during a normal fracture exposure job. The tests were conducted at the full reservoir temperature of 285°F utilizing 3200 psi of net confining overburden pressure and a 200 psi backpressure to avoid the volatilization of connate water from the core samples. Initial water saturations were fixed in the samples using a 5% KCl solution. Initial water saturations varied from approximately 50 to 60% depending on sample quality and initial expected water saturation data in the various zones as supplied to Hycal by UPRC. The results of the fracture fluid tests are summarized in the following table.

| FRACTURE FLUID EVALUATION TESTS | | | | | | | | | | |
|---------------------------------|----------|---------|------------------------|-------------------------|-------------------|--------------------------|-------------------------|------------------------|-----------------|-------------|
| Sample | Depth | Facies | Frac Fluid | Initial Sw _i | Initial Perm (mD) | Threshold Pressure (psi) | Invasion Depth (inches) | Maximum Drawdown (psi) | Final Perm (mD) | % Reduction |
| 6B | 16025 45 | Fluvial | Halliburton Frac Gel 2 | 0 48 | 0 0055 | 300 | 0 00 | 1700 | 0 0055 | 0 0 |
| 7A | 16025 80 | Fluvial | BJ Titan Borate HT4500 | 0 60 | 0 0028 | 600 | 0 00 | 1700 | 0 0028 | 0 0 |
| 31A | 16063 20 | Marine | BJ Titan Borate HT4500 | 0 50 | 0 00234 | 2200 | 0 84 | 2200 | 0 00228 | -2 6 |
| 31B | 16063 30 | Marine | Halliburton Frac Gel 2 | 0 50 | 0 00257 | 2200 | 0 00 | 2200 | 0 00253 | -1 6 |

Examination of the data from the frac fluid tests indicated that both the fluvial and marine zones appeared to sustain damage due to minimal frac fluid invasion, but at maximum pressure drawdowns of 1700 psi for the fluvial facies and 2200 for the marine facies the majority of the invaded damage appeared to be mobilized and removed from the formation. This would suggest that the major mechanism of damage associated with the frac fluid contact is a localized aqueous phase trap caused by the physical invasion and transient entrapment of a portion of the broken gelled frac fluid in the porous media resulting in adverse relative permeability effects which impair gas productivity. A more detailed discussion of the mechanism of aqueous phase trapping is contained in the technical papers which are contained in Appendix "C". Examination of the frac fluid data indicated that, with the exception of the BJ Titan fluid tested on sample 31A, no significant measurable losses of frac fluid to the formation were encountered. It is likely that some small physical invasion and imbibition effects occurred (perhaps approximately a 1/32" of invasion) which were too small to measure with the accuracy of the experimental equipment which was being utilized, but the test results indicate that, in general, the rheology of the frac fluids, coupled with the low formation permeability, appeared to be quite effective at reducing significant losses of fluid to the formation during the normal exposure period of approximately 30 minutes which would be utilized in a conventional frac. It should be noted that if frac fluid was allowed to "break" in the formation, resulting in a significant loss in apparent viscosity, invasion depth may be considerably more significant and fluid losses and trapping would be severe.

Even with relatively minimal invasion depth it can be seen that between 300 - 600 psi of effective drawdown pressure had to be applied to the formation to begin to mobilize the damage and total cleanup was not achieved until a pressure drawdown of up 1700 psi was applied to the upper fluvial facies samples. Due to the high pressures that were present in the Stratos formation, it appears likely that drawdowns of this magnitude could be applied relatively easily across the damaged zone at the formation face.

The marine zone appeared to be much more sensitive to phase trapping and a 2200 psi gradient had to be applied across the damaged zone in the samples to even begin to mobilize the damage. Cleanup was relatively rapid after the threshold pressure was achieved, with minimal damage occurring. This indicates that significant physical losses of filtrate into the dirty or lower marine zones may result in significantly greater damage than the fluvial facies. If invasion depth is significant, it may not be possible to have sufficient drawdown pressures in the field to mobilize the damage, resulting in a high degree of damage occurring in this particular area.

Overall reservoir quality was marginal with average initial permeabilities of the samples at stressed conditions with initial water saturation in place in the 2 to 5 mD range. This would suggest that, even if an effective fracture fluid treatment could be conducted in a non-damaging fashion (which the test results appear to indicate could be obtained) inherent formation permeability appears to be too low to allow for effective and economic production rates of gas, even in the presence of a large scale hydraulic fracturing treatment. The presence of naturally existing microfractures in the formation, which may be penetrated by the hydraulic frac, would significantly enhance the productivity of the formation, however, this effect has not been evaluated in these particular tests, which evaluated exclusively low permeability matrix.

The test results indicate that both fluids performed fairly comparably but that the Halliburton Frac Gel 2 appeared to cleanup easier in the fluvial facies sample and had better invasion characteristics and residual damage characteristics in both the marine and fluvial facies than the BJ Titan Borate HT4500 system.

Incremental Phase Trap Tests

The next tests which were conducted as a portion of the UPRC Stratos program were incremental phase trap evaluation tests. The purpose of these experiments was to quantify the effective permeability to gas in the Stratos fluvial and marine facies as a function of the water saturation which was present in the system. The initial water saturation in the reservoir was thought to be in the approximately 50 to 60% region but some uncertainty was present as to the exact saturations which exist in-situ. These tests were conducted to allow the quantification of effective in-situ permeability as a function of increasing water saturation in the tight matrix in both the fluvial and marine samples. The tests were conducted at the maximum temperature allowable without the use of backpressure (176°F) at a 3200 psi net confining stress to simulate net effective rock stress at downhole conditions. A 5% KCl solution was utilized to simulate the connate water in these experiments. The results of the experiments are summarized in the following table.

| INCREMENTAL PHASE TRAP EVALUATION TESTS | | | | | |
|---|-----------------------|----------|------------------------------------|-----------------------|----------|
| Fluvial - Sample 6A 16025.25 ft. | | | Marine - Sample 37 16069.20 ft. | | |
| Sw _i | Gas Permeability (mD) | % Change | Sw _i | Gas Permeability (mD) | % Change |
| 0 00 (unstressed) | 0 2000 | 0 0 | 0 00 (unstressed) | 0 1300 | 0 0 |
| 0 30 | 0 0116 | -94 2 | 0 30 | 0 0104 | -92 0 |
| 0 40 | 0 0091 | -95 4 | 0 40 | 0 0054 | -95 8 |
| 0 50 | 0 0052 | -97 4 | 0 50 | 0 0022 | -98 3 |
| 0 60 | 0 0023 | -98 8 | 0 60 | 0 0007 | -99 4 |
| 0 70 | 0 0017 | -99 2 | 0 70 | 0 0005 | -99 6 |

It can be seen that even relatively small water saturations of 30% in both the fluvial and the marine samples caused significant reductions of over 90% in the effective gas permeabilities in comparison to the normal dry unstressed routine core analysis air permeabilities. A portion of this reduction in permeability may be due to a combination of clay hydration and overburden compression effects in the transition from a 100% gas saturated sample to a fully reservoir stressed and partially water saturated gas permeability measurement. However, the permeability measurements presented here probably provide good estimations of the in-situ effective matrix permeabilities to gas at the saturation conditions which are indicated, and provide good scaling criteria for the translation of routine core analysis air permeabilities (the values at 0% water

saturation) back to full reservoir condition in-situ values. It can be seen that as water saturation increased, permeabilities steadily declined as would be expected by classical relative permeability theory. At a water saturation of 70%, gas permeability was approximately 1.7 mD for the fluvial facies and about 0.5 mD for the marine facies, both representing over a 99% reduction from the original routine core analysis permeabilities. At this condition of a 70% water saturation, no mobile water production was observed from either core sample, indicating that "critical" water saturation, at which water mobility would be obtained, had still not been achieved. This indicates that significant invasion of water-based fluids into the UPRC Stratos matrix, if the water saturation is in fact in the 40 to 50% initial region, would result in the significant potential for permanent retention of these fluids and large reductions in potential gas phase productivity. For example, on the marine facies sample #37, if the initial water saturation was 40%, this would result in an initial effective gas permeability of 0.0054 mD. Invasion of water-based drilling completion or stimulation fluid into the near wellbore frac face region might result in a large increase in water saturation. It can be seen that increasing the water saturation to 70% results in over a 90% reduction in the original permeability to 0.0005 mD. It is likely that the trapped water saturation would be significantly greater than 70% in this situation resulting in total blockage of the pore system and the establishment of a true aqueous phase block. Therefore, test results indicate that although reservoir quality appears to be marginal in the Stratos matrix, the use of water-based fluids (where significant invasion of water-based filtrate into the formation would occur) would likely be highly damaging to the formation both from a chemical (clay sensitivity) perspective as well as from a relative permeability and phase trapping viewpoint.

Unsteady State Water-Gas Relative Permeability Tests

The next set of experiments conducted in the Stratos study was a series of unsteady-state water increasing relative permeability experiments to quantify displacement efficiency of gas by encroaching water (likely from underlying water zones) into the tight Stratos matrix. It should be emphasized at this point that, due to the extremely low matrix and in-situ permeabilities, effective pressure support or water injection would likely not be a viable recovery mechanism in the Stratos system.

The tests were conducted with 3200 psi of confining stress at the full reservoir temperature of 285°F, utilizing humidified nitrogen gas to simulate the reservoir gas phase and 5% KCl as both the initial saturation phase (which was set at 50% saturation) and the simulated water injection phase. The test results are summarized in the following table.

| WATER-GAS RELATIVE PERMEABILITY RESULTS | | | | | |
|--|-----------|-----------|------------------------------|-----------------------------------|------------------------------------|
| Fluvial - Core 9 16028.60 ft | | | | | |
| Test Phase | Sw | Sg | Permeability (mD) | Relative Permeability* | % Recovery Gas in Place |
| Initial Gas | 0.500 | 0.500 | 0.000462 | 0.1525 | - |
| Waterflood | 0.824 | 0.176 | 0.000703 | 0.2320 | 64.8 |
| Marine - Core 48B 16080.30 ft | | | | | |
| Test Phase | Sw | Sg | Permeability (mD) | Relative Permeability* | % Recovery Gas In Place |
| Initial Gas | 0.500 | 0.500 | 0.001660 | 0.3320 | - |
| Waterflood | 0.862 | 0.138 | 0.000422 | 0.0844 | 72.4 |
| * Using estimated "absolute" fluid permeability of 0.003 mD | | | | | |
| ** Using estimated "absolute" fluid permeability of 0.005 mD | | | | | |

It can be seen from the examination of this data that, once again initial in-situ stressed permeability at the 50% water saturation was quite low: approximately 0.0005 mD for the fluvial sample and about 0.0017 mD for the slightly better quality marine sample which was evaluated in this study. Waterflood displacement efficiency was quite good, considering the low permeability of the matrix, although extremely high pressure gradients were required in order to force the high viscosity water through the microDarcy permeability matrix. Recovery efficiency of gas ranged from approximately 65% for the lower quality fluvial sample to about 72% for the better quality marine sample. Trapped critical gas saturations were relatively low for a low permeability matrix of this type, with a value of about 17.6% being observed in the fluvial sample and 13.8% for the marine sample. This would indicate that water influx would generally be fairly efficient in sweeping the majority of the gas saturated pore system. The dominant mechanism is likely capillary imbibition due to the very small pore size distribution which exists in the rock and the natural water wetting infinity associated when water contacts the matrix. This would result in imbibition, rather than displacement, being the dominant mechanism of the high recovery efficiency associated with water saturation increasing displacements which were conducted.

Full Diameter Fractured Core Tests

The final two experiments of the UPRC Stratos project were conducted on full diameter fractured core samples. Both samples contained hairline vertical microfractures. The objective of this set of experiments was to evaluate the effect of reservoir overburden stress on fracture permeability to quantify if, at fully stressed conditions and also during a reservoir depletion process where net overburden stress would be increasing, in-situ fracture connectivity would be maintained. Once these measurements were complete, the samples were saturated with 5% KCl, at approximately overburden stress, and a regain permeability to gas was conducted to determine if phase trapping would cause a significant additional reduction in the effective gas permeability of the conductive fracture system. These tests were conducted at a temperature of 176°F (the maximum possible without any applied backpressure) and with variable overburden pressures varying from 375 to 11,200 psi. The results of these experiments are summarized in the following table.

| FULL DIAMETER FRACTURE PERMEABILITY MEASUREMENTS | | | |
|---|--------------------------------------|----------------------------------|-------------------------------------|
| Sw₁ (%) | Overburden Pressure (psi) | Gas Permeability (mD) | % Change in Permeability |
| Fluvial Facies - FD #12 - 16042 ft | | | |
| 0 | 375 | 0.06000 | 0.00 (baseline) |
| 0 | 1880 | 0.00823 | -86.3 |
| 0 | 3750 | 0.00455 | -92.4 |
| 0 | 5640 | 0.00346 | -94.2 |
| 0 | 7500 | 0.00290 | -95.2 |
| 0 | 11200 | 0.00265 | -95.6 |
| 100 | 3750 | 0.00032 | -99.5 |
| Sw _{irr} | 3750 | 0.00031 | -99.5 |
| Marine Facies - FD #32 - 16064 ft | | | |
| 0 | 375 | 0.010000 | 0.00 |
| 0 | 1880 | 0.001350 | -86.5 |
| 0 | 3750 | 0.000850 | -91.5 |
| 0 | 5640 | 0.000670 | -93.3 |
| 0 | 7500 | 0.000420 | -95.8 |
| 0 | 11200 | 0.000350 | -96.5 |
| 100 | 3750 | 0.000044 | -99.6 |
| Sw _{irr} | 3750 | <0.000010 | -99.9 |

Examination of the data indicates that fracture permeability for both microfractured samples in the fluvial and marine facies was significantly impacted by increasing overburden stresses. It can be seen that going from an unstressed condition to approximately 3750 psi overburden stress (approximating the average current reservoir stress) caused over 90% reduction in fracture permeability in both the fluvial and marine facies situations. Increasing overburden stresses caused additional reductions in permeability with reductions at 11200 psi net confining stress of 95.6% and 96.5% respectively for the two facies. The saturations of the samples with 5% KCl resulted in very low effective brine permeability of 0.00032 mD for the fluvial facies and approximately 0.00004 mD for the marine facies indicating exceptionally poor water conductivity in the microfracture system. This is partially beneficial as it indicates that water mobility in the microfracture system, if present and of a similar size to those evaluated in the two full diameter samples tested here, will be very low. This will tend to reduce potential for premature water coning, even at relatively high drawdowns.

A final gas displacement was conducted to reduce the water saturation in the fracture system to an irreducible value and quantify the effect on fracture permeability. Some gas permeability was retained in the slightly better quality, full diameter fluvial facies sample which was evaluated with a residual gas permeability of approximately 0.0003 mD remaining in the fracture system after water saturation had occurred. This compares to an equivalent value at an overburden stress of approximately 0 00455 mD and indicates that over a 90% reduction in effective fracture conductivity had occurred due to the entrainment of a trapped water saturation in the fracture system. Much more significant damage was observed in the marine facies with near total occlusion of the fracture occurring due to significant aqueous phase trapping effects on a post-water influx basis. This indicates that the loss of water-based drilling, completion or stimulation fluids into the microfractured zone could cause significant permeability impairment, particularly in very small microfractures as evaluated in the marine facies sample FD #32. The presence of larger macrofractures, not contained in the core samples which were evaluated in this study, would probably exhibit less sensitivity to phase trapping and damage, however, fracture size would need to be significant (larger than 200 to 300 microns) before phase trapping effects could be negated as a potential source of reduced productivity in the transmissive microfracture system which may exist in the formation. This would mean that fluid loss concerns and phase trapping concerns would still be problematic when attempting to complete zones in the field of expected higher fracture density than encountered in the Federal Unit #1 well evaluated in this work.

Geomechanical Tests

A series of geomechanical measurements were also conducted on selected samples from the fluvial and clean and dirty marine facies. Young's modulus measurements and compressive strength measurements were conducted on three samples and results are summarized in the following table

| RESULTS OF GEOMECHANICAL TESTS | | | | |
|---------------------------------------|--------------|----------------|---|--|
| Sample | Depth | Facies | Young's Modulus psi x 10⁶ | Compressive Strength psi x 10³ |
| 7C | 16026 90 | Fluvial | 3 79 | 177 0 |
| 31B | 16063 30 | Marine (clean) | 2 92 | 44 1 |
| 48B | 16080 30 | Marine (dirty) | 4 23 | 61 8 |

These test results indicate relatively uniform Young's modulus but significant variation in compressive strength of the samples with the fluvial facies exhibiting the highest compressive strength and the clean marine sample exhibiting the lowest strength. Variation in compressive strength may be due to individual sample heterogeneities due to the presence of microlaminations in the individual plugs, rather than significant distinct variations in zone wide lithology. Additional samples would need to be evaluated to quantify this effect on a rigorous basis.

Mercury injection capillary pressure tests were conducted on four samples, two from the upper fluvial zone and one from the clean marine and one from the dirty marine zone. Mercury injection was conducted up to a maximum pressure of 60000 psi and detailed results are summarized in Appendix "A". Tests results are summarized in the following table.

| RESULTS OF MERCURY CAPILLARY PRESSURE MEASUREMENTS | | | | | |
|---|--------------|----------------|---|--|--|
| Sample | Depth | Facies | Average Pore Throat Radius (microns) | Median Pore Throat Radius (microns) | Degree of Pore Throat Variation |
| 7B | 16026 85 | Fluvial | ≈ 0 18 μ | ≈ 0 45 μ | High |
| 7C | 16026 90 | Fluvial | ≈ 0 22 μ | ≈ 0 45 μ | High |
| 30 | 16062 20 | Marine (clean) | ≈ 0 027 μ | ≈ 0 03 μ | Moderate |
| 48B | 16080 30 | Marine (dirty) | ≈ 0 060 μ | ≈ 0 037 μ | Moderate |

Analysis of these results indicated that the fluvial samples exhibited larger average pore throat radius (defined as the total average pore size above which 50% of the pores are larger and 50% of the pores are smaller) and median pore size (defined as the most common single pore size which exists in the pore system) in comparison to the marine facies which exhibited significantly

smaller average pore throat radii and median pore throat diameters. The degree of variation in pore throat size was significantly higher in the fluvial system than the marine systems indicating a greater degree of randomness and tortuosity in the fluvial system, even in light of the larger pore size distributions which existed.

Final Conclusions

The results of the Stratos study indicate that the reservoir exhibits extremely low in-situ permeability. Test results indicate that, although fracturing could be conducted in a non-damaging fashion, in-situ permeability in the absence of any significant natural fracturing is likely too low to sustain viable economic production rates from low permeability matrix of the quality evaluated from the Stratos Federal #1 well.

The presence of high water saturations in the porous media has a significant reducing effect on the effective permeability to gas and the tight microporous nature of the matrix indicates significant invasion of water-based fluids into either a tight matrix or microfractured system could have severely reducing effects on permeability. Economic production from matrix may be possible if large hydraulic fracture treatments could be propagated in zones where significantly enhanced reservoir quality due to the presence of larger natural fractures exists.

RESULTS AND DISCUSSION

Preliminary Preparations

Table 1 provides a summary of the initial core sample parameters determined on the plug core samples which were utilized in the UPRC Stratos study. The core samples were drilled using an inert 5% KCl solution from a total nine full diameter samples from the 16025.25 to 16080.3 ft interval of Stratos Federal Unit #1 well. Samples 6 through 9 represented the upper fluvial facies, samples 30 through 37 the clean marine facies and samples 46 and 48 the dirty marine facies.

Fracture Fluid Leakoff Tests

Table 2 provides a summary of core and fluid parameters for core sample 6B which was evaluated with Halliburton Frac Gel 2. The results of the fracture fluid leakoff test are summarized in Table 3 and have been plotted and appear as Figure 1. Table 4 summarizes the

invasion depth data for the fracture fluid leakoff experiment. It can be seen that original gas permeability was fairly low at 0.0055 mD. Fracture fluid exposure at 1800 psi overbalance resulted in a minimum drawdown pressure of 300 psi being required to re-initiate flow. Damage due to core face filtrate imbibition and entrainment was significant at this point with over a 98% reduction in permeability being observed. Permeability increased with increasing drawdown pressure, resulting in production of additional entrained frac fluid from the core. At 1200 psi of drawdown pressure, permeability was still 20% impaired at 0.0044 mD but by the time a 1700 psi drawdown had been applied, the original permeability of 0.0055 mD had been restored. No measurable leakoff volume was observed during the 30 minute frac fluid exposure period.

Table 5 summarizes the results of the fracture fluid leakoff conducted with the BJ Titan Borate HT 4500 system on fluvial facies core 7A. Table 6 summarizes the permeability and percent change in permeability data for the test and this data also appears as Figure 2. Examination of this data indicated a similar profile to that observed previously with the Halliburton fluid on the fluvial facies, with the exception that a slightly higher drawdown pressure of 600 psi was required to initiate flow from the core material. Once again, no discernible permeability impairment was observed at the maximum drawdown pressure of 1700 psi. As summarized in Table 7, minimal filtrate invasion characteristics were observed with the frac fluid.

Table 8 summarizes core and fluid parameters for the test conducted on marine facies core 31A using the BJ Titan Borate HT 4500 system. The test results are summarized in Table 9. As shown, original gas permeability was 0.0023 mD and significant entrainment and damage occurred requiring a drawdown pressure of 2200 psi to mobilize fluid from the core material. Once fluid mobilization occurred, the core samples appeared to clean up fairly readily with only a 2.6% ultimate reduction in permeability. This was the only one of the four tests in which discernible leakoff volume during the frac fluid exposure period with a linear invasion depth of approximately 0.84 inches computed.

Table 11 summarizes the parameters for marine facies core 31B which was evaluated with the Halliburton Frac Gel 2 system. The test results are summarized in Table 12. In a manner similar to the BJ Titan fluid, a significant drawdown pressure (2200 psi) was required to mobilize entrained or imbibed frac fluid after the frac fluid exposure phase although only a 1.6% residual reduction in permeability was observed at 2200 psi drawdown after invasion had occurred. The results of Table 12 have been plotted and appear as Figure 4.

General Discussion

In general, test results indicate that the Halliburton Frac Gel 2 appeared to perform in a marginally better fashion than the BJ Titan Borate HT 4500 system requiring lower drawdown pressures to remobilize gas and resulting in slightly less residual damage. High threshold mobilization pressures were required to overcome slight invasion or imbibition of filtrate in the marine facies tests which were conducted. If significant depth of invasion of broken gelled frac fluid occurred during a fracture job, it is likely that insufficient mobilization pressure could be applied in the field to overcome the capillary phase trap which is established, which may result in a near total reduction in gas permeability on the fracture face. The test results indicate that if fracture fluid rheology is maintained, invasion depth will be minimal. With minimal invasion depth, the high natural reservoir pressure which exists in the Stratos reservoir appears to be capable of mobilizing the very localized damage which occurs on the fracture face. In-situ matrix permeabilities at initial saturation conditions of approximately 50% water saturation are in the 0.002 mD range, which would generally be classified as too low for effective and economic gas production rates unless assisted by the presence of significant natural fracturing which would enhance drainage on a large scale from the reservoir system.

Therefore, although the test results indicate that well designed crosslinked water-based systems could be effectively used to place large scale hydraulic fractures in the Stratos matrix in a relatively non-damaging fashion, matrix permeability is likely too low to directly contribute to economic production rates from a well of this type.

Incremental Phase Trap Tests

Table 14 provides a summary of core and fluid parameters for the incremental phase trap tests conducted on fluvial facies core 6A. The results of the incremental phase trap test are summarized in Table 15 and have been plotted and appear as Figure 5. Examination of this data indicates that the permeability dropped from the original dry unstressed routine core analysis air permeability of 0.2 mD by 94.2% to approximately 0.0116 mD at a condition of 30% water saturation. As water saturation continued to be increased, fluid permeabilities continued to decline. Even at a water saturation of 70%, the mobile water saturation had not yet been achieved indicating that significant potential for permanent imbibition and phase trapping damage existed in the Stratos matrix. The data of Table 15 and Figures 5 and 5A provide a comparative plot of the potential matrix transmissivity at full reservoir conditions for the Stratos matrix at a

variety of water saturation conditions. Since the initial water saturation in the field is somewhat ambiguous, this provides a good indication of potential in-situ gas conductivity at a variety of potential saturation conditions. It can be seen that at a 50% water saturation, effective permeability to gas is approximately 0.005 mD which is considered to be marginal for economic production rates. In communication with UPRC, it has been indicated that in-situ water saturations from some evaluations have tended into saturations as high as 60 or 70%. The large reductions in both reserves and effective gas transitivity, if water saturation is in fact this high in the reservoir, would likely indicate that effective matrix production would be non-viable.

Table 16 provides a summary of core and fluid parameters for the incremental phase trap test conducted on marine facies core 37. The results of this experiment are summarized in Table 17 and have been plotted in Figures 6 and 6A. General test profiles are similar to that observed on the previous fluvial facies with the exception that reservoir quality is slightly lower, and reductions in effective permeability appear to be somewhat greater. Effective in-situ gas permeability at 50% water saturation is only 0.0022 mD in this situation

Water-Gas Relative Permeability Experiments

Table 18 provides a summary of core and fluid parameters for the unsteady-state water-gas relative permeability displacement tests conducted on fluvial facies core 9. The saturation and permeability results of the water saturation increasing relative permeability experiment have been summarized and appear as Table 19. It can be seen from this evaluation that the water saturation increasing relative permeability test was relatively efficient at recovering over 65% of the original gas in place and resulting in a residual trapped gas saturation of approximately 17.6%. The dominant mechanism of recovery is likely related more to capillary imbibition effects due to the water-wet nature of the tight microporous system rather than direct displacement efficiency. Due to the very low permeability of the sample, and higher viscosity characteristics of a water-based media, it is unlikely that direct aquifer influx or any type of water injection and pressure support would be possible due to the very high pressure gradients which would be required to institute effective water flow in the porous media.

Table 20 provides a summary of the experimental pressure and transient production history data from the water saturation increasing relative permeability displacement tests conducted on core 9. This data has been plotted and appears as Figures 7 and 8 respectively. A computer history matching algorithm was used to generate the water-gas relative permeability

curves which are contained in Table 21 for core 9. A detailed discussion is contained in a technical paper entitled, "Recent Improvements In Experimental Laboratory Techniques In The Analysis Of Unsteady-State Relative Permeability Data" which is contained in Appendix "C". This provides a detailed mathematical description of the numerical models and regression analysis used to generate the relative permeability data from the unsteady-state transient pressure and production history which was utilized for the Stratos project. The relative permeability data of Table 21 for core 9 have been plotted on both semi-log and Cartesian coordinates and appear as Figures 9 and 10 respectively.

Table 22 provides a summary of core and fluid parameters for marine facies core 48B which was utilized for water-gas relative permeability displacement and Table 23 provides a summary of saturation and permeability data for the experiment. This sample exhibited marginally better quality than the fluvial sample 9 evaluated previously which may explain the slightly better recovery efficiency of gas (approximately 75% of the gas in place) and the somewhat lower residual trapped gas saturation of 13.8% in comparison to the fluvial facies sample. The experimental pressure and production data are summarized in Table 24 for core 48B and have been plotted and appear as Figures 11 and 12 respectively. The computed water-gas relative permeability data are summarized in Table 25 and have been plotted on Cartesian and semi-log coordinates in Figures 13 and 14 respectively. The comments regarding the difficulty of pressure support and water displacement discussed previously for core sample 9 would also apply to the marine facies.

Fracture Permeability vs Overburden Measurements

Table 26 provides a summary of core and fluid parameters for the fracture overburden permeability measurements conducted on full diameter core sample 12 from the fluvial facies. The objective of these measurements was to quantify if microfracture permeability would be maintained as the reservoir is depleted and overburden stress (and closure stress on the fracture system) increases. As well, tests were conducted to evaluate potential for water coning or rapid influx of water from a wet zone up to the production wells, and if the invasion of water-based drilling, completion or stimulation fluids into the microfracture system occurred, how adversely this invasion would affect fracture conductivity. This was accomplished by measuring regain permeability to gas on a microfracture system at increasing overburden stress followed by increasing water saturation at field net overburden stress.

The results of the fluvial facies tests conducted on core sample 12 are summarized in Table 27 and have been plotted and appear as Figure 15. Examination of this data indicated that the permeability was radically influenced by increasing overburden pressure with over 90% reduction in permeability being observed from a low stress condition to a 3750 psi overburden stress condition (which generally approximates current reservoir stresses which exist in the virgin reservoir at this time). As reservoir depletion continues, and overburden stress increases, it can be seen that permeability continues to decline. Effective permeability to brine was very low in the fractured system at 0.0003 mD indicating there would not be a significant tendency for rapid water coning or transmission of water from wet zones up the fracture system to the wellbore (which is obviously advantageous). Unfortunately, once water is introduced into the fracture system, a large potential reduction in permeability was observed. Comparing pre- and post-water exposure permeabilities at an equivalent net overburden pressure condition of 3750 psi, it can be seen that permeability dropped by more than 90% from 0.00455 mD to 0.00031 mD in the fracture system.

In a similar fashion, Table 28 provides a summary of core and fluid parameters for the marine facies full diameter fracture core test conducted on core sample 32. Table 29 summarizes the permeability measurements for this displacement test and this data has been plotted and appears as Figure 16. The original fracture permeability was poor in this marine facies sample and damage appeared to be more significant. Once again, over 90% reduction in permeability was observed going from a low stress to a normal reservoir stress condition. Effective permeability to brine was very low at 0.00004 mD and gas regain permeability was virtually zero indicating that invasion of a water-based drilling, completion, kill or stimulation fluid into very small microfractures of this type may cause virtually total occlusion of the pore system and a near 100% phase block and significant resulting reduction in effective permeability.

Geomechanical Measurements

Table 30 provides a summary of the geomechanical testing which was conducted on three samples representing the fluvial, clean and dirty marine facies. Young's Modulus was fairly uniform throughout the sample set ranging from 2.9 to 4.23 x 10⁶ psi. There was a significant variation in compressive strength with the clean marine facies having the lowest compressive strength of 44,100 psi and the fluvial facies having the highest compressive strength of 177,000 psi. Variation in compressive strength may be a reflection on individual sample laminations and heterogeneity, rather than distinct variations in lithology between the individual zones. A more comprehensive suite of measurements would likely be required in order to definitely draw conclusions with respect to the geomechanical properties of the formation.

Mercury Injection Capillary Pressure Tests

Four mercury injection capillary pressure tests were conducted on samples from the Stratos Federal Unit #1 well. Two samples were evaluated from the fluvial facies and a sample from the clean and dirty marine facies was also evaluated. The results of the mercury injection capillary pressure tests have been summarized and appear as Appendix "A". Detailed numerical data in a Lotus 1-2-3 format of mercury wetting phase saturation vs capillary pressure appears as a portion of the data diskette contained at the end of the report.

Petrographic Work

Appendix "B" provides a summary of the pre-test petrography which was conducted on samples of fluvial, clean marine and dirty marine Stratos core material. A detailed discussion as to reservoir quality potential sensitivity, matrix composition, grain size distribution and depositional history are contained in the detailed petrographic analysis which is summarized in Appendix "B".

Technical Papers

A number of technical papers relevant to aqueous phase trapping, tight gas reservoir exploitation and relative permeability are contained in Appendix "C". A paper describing the relative permeability analysis, data reduction and reporting techniques utilized to reduce the unsteady-state relative permeability data, which were utilized as a portion of the Stratos study, is also contained in Appendix "C".

DESCRIPTION OF EQUIPMENT

General Displacement Test Equipment

Equipment that is used in conventional displacement experiments is common to most core flow evaluation techniques. Detailed schematics of the specific apparatus configurations are provided in Figure 17 of this report. General descriptions of the laboratory equipment utilized for these tests appear in the following paragraphs.

Core Mounting

The core sample to be tested is placed in a 1½" ID flexible confining sleeve. The ductility of the sleeve allows a confining external overburden pressure to be transferred to the core in a radial and axial mode to simulate reservoir pressure. The core, mounted within the sleeve, is placed inside a 4" ID steel core holder that can simulate reservoir pressures of up to 10000 psi. This pressure is applied by filling the annular space between the core sleeve and the core holder with non-damaging saline brine. The water is then compressed with a hydraulic pump to obtain the desired overburden pressure. The core holder ends each contain two ports to facilitate fluid displacement and pressure measurements at each end of the core.

Conventional Core Flow Heads

The portions of the core holder directly adjacent to the injection and production ends of the core are equipped with radial distribution plates to ensure that fluid flow is uniformly distributed into and out of the core sample. These heads are used for experiments which involve fluids that are prefiltered to remove large suspended solids which could entrain in the flow ports. All wetted surfaces of the flow equipment use conventional 316 SS.

High Capacity Core Flow Heads

For experiments which utilize highly viscous fluids and/or which contain a significant suspended solids load, specially designed high capacity core flow heads are used to conduct fluid with solids or additives to the rock face to minimize the potential for flow impedance in the apparatus. Conventional 316 SS is used to fabricate this equipment for applications where reservoir operating conditions are not extreme.

Pressure Measurement

Pressure differential is monitored using Validyne pressure transducers. The transducers are mounted directly across the core and measure the pressure differential between the injection and production ends. The pressure transducers have ranges of sensitivity ranging from 0 to 5 and 0 to 3800 psi and is rated as accurate to 0.01% of the full scale value. The appropriate transducer size is selected based upon the expected permeability and associated range of accompanying differential pressures for a given core sample. The signal from the pressure transducer appears on a multi-channel digital Validyne terminal from which the test operator records pressure readings during the displacement processes. The signal can also be downloaded to a computerized continuing data acquisition system for long term runs.

Temperature Control

The core holder and associated injection fluids are contained in a temperature controlled air bath to simulate reservoir temperature. The oven contains a circulating air system to eliminate internal temperature gradients and can control at temperatures from 70 to 500°F with a rated accuracy of $\pm 1^\circ\text{F}$.

Gas Displacement

A regulated high pressure gas source is used to conduct gas into the porous media at a constant pressure. For systems where displacement gas composition is specifically designed for the experiment, buffer fluids are placed between the test gas and the drive gas so as to maintain compositional integrity.

For systems which are used on porous media containing aqueous fluids, high pressure humidification systems are used to eliminate desiccation of the porous media when necessary.

EXPERIMENTAL PROCEDURE

Preliminary Preparations

UPRC supplied Hycal with a number of full diameter core samples from selected intervals of the UPRC Stratos Federal Unit #1 well. A total of 16, 1.5" OD diameter samples were cored using an inert 5% KCl solution from nine of the full diameter samples. Two other full diameter samples with hairline existing vertical microfractures were retained in a full diameter, unaltered state for potential sensitivity testing. As no free mobile water was produced from the formation and no water compositional samples were available, a 5% KCl solution was used to simulate the formation water phase present in the matrix to ensure that damage or swelling of reactive clays due to the use of non-compatible brine did not occur.

Petrographic Work

Three endcap core samples from the fluvial facies zone, dirty marine and clean marine facies zone were forwarded for detailed petrographic analysis for reservoir quality and sensitivity evaluations. On all three zones, detailed thin section analysis and reservoir description, scanning electron microscopy and X-ray diffraction on both a bulk and glycolated basis were conducted to quantify reservoir quality and sensitivity.

Fracture Fluid Leakoff Evaluation Tests

Four fracture fluid leakoff evaluation tests were conducted, two from the fluvial facies zone and two from the marine facies zone to quantify the effects of two potential water-based crosslinked fracturing fluids. One was supplied by Halliburton Services with the trade name Frac Gel 2 and a second by BJ Titan with the trade name Borate HT 4500. The gelled fluids, complete with encapsulated breaker system, were supplied to Hycal by the respective service companies for testing. The breaker was added in the appropriate concentration immediately prior to the displacement tests, as per the instructions provided by the service companies.

Initially, water saturations were fixed in the range of 60 to 70% as this was thought to be the approximate in-situ water saturation based on field log evaluation determinations. However, very low permeabilities were obtained due to the high water saturation and adverse relative permeability effects and, subsequently, initial water saturations which were instituted in the

samples were lowered to the 50% region for most of the tests conducted in the study. The initial water saturations were fixed by gravimetrically instituting a fixed mass of 5% KCl solution into the samples and dynamically displacing the samples with humidified gas at high pressure drawdown rates for an extended period of time in a multidirectional fashion through the core material to ensure that the water saturation was uniformly and evenly distributed.

The fracture fluid tests were conducted by originally determining a baseline permeability to gas at full reservoir conditions of 285°C with 3200 psi of net confining overburden pressure. The fracture fluid exposure test was conducted by circulating the crosslinked fracture based fluid, complete with encapsulated breaker, at a differential pressure of 1800 psi (to simulate the net fracture gradient overbalance during a typical fracture job) for a period of 30 minutes across the core face. The pressure was then released and, in the opposite direction to the frac fluid exposure, a threshold regain gas permeability measurement was conducted where gradually increasing gas pressures were applied across the core sample to determine both the mobilization point (where gas would originally flow through the damaged zone), as well as to quantify the effect of increasing of drawdown pressure on effective gas permeability and cleanup rate.

Incremental Phase Trap Tests

Two incremental phase trap tests were conducted on samples from the fluvial and marine facies. The incremental phase trap tests were conducted by originally mounting the core samples and determining gas permeability in a totally dry and unstressed condition at reservoir conditions of 3200 psi net confining overburden pressure with zero backpressure at a temperature of 176°F. A somewhat lower temperature was utilized for these experiments due to the fact that no backpressure was utilized to avoid volatilization of the in-situ connate water saturations.

Phase trap tests were conducted by gravimetrically instituting and subsequently dispersing fixed uniform saturation values within the samples. Values of 30, 40, 50, 60 and 70% water saturation were utilized. After each saturation had been dispersed, the effective gas permeability was measured to quantify the effect of the increased water saturation on gas permeability. During each gas displacement, the effluent of the core was examined and the final post-test masses were checked to determine if the mobile water saturation had been exceeded.

Relative Permeability Displacement Tests

Two water saturation increasing relative permeability tests were conducted, one on the fluvial facies sample and one on the marine facies sample. Tests were conducted at full reservoir conditions of 285°F with 200 psi backpressure and 3200 psi net confining overburden pressure. A 50% initial water saturation was instituted in each sample prior to testing. Initial permeability measurements were conducted with humidified gas and an unsteady-state water saturation increasing relative permeability test was conducted by injecting 5% KCl at a low stabilized displacement rate of approximately 1 cc/hr into the core samples and collecting transient gas production and differential pressure history to compute the water and gas-oil relative permeability curves via dynamic computer history matching technique. Post-test trapped residual gas and water saturations were evaluated by direct saturation analysis via Dean Stark on the post-test core material.

Fracture Tests

Two tests were conducted on full diameter vertically oriented samples with vertical hairline fractures present. One sample was from the fluvial facies, the second sample from the marine facies. Full diameter samples were utilized due to the fact that hairline fractures were not present or continuous in small plug samples which were obtained in the study.

The full diameter core sample was mounted and the test was conducted at a temperature of 176°F (to obviate the use of backpressure) and at a variety of overburden pressures, ranging from a nominal value of 375 psi to a maximum value corresponding to a condition of maximum reservoir depletion of 11200 psi. Original gas permeability measurements in the fracture system at nominal stress were conducted at 375 psi net overburden stress, followed by equivalent gas permeability measurements at a condition of 0% water saturation at gradually increasing overburden pressures of 1880, 3750, 5640, 7500 and 11200 psi to quantify the effect of net closure stress on effective fracture permeability. To determine brine permeability to evaluate aquifer influx in a fracture system, the samples were evacuated to remove any trapped residual gas saturation and then pressure saturated with brine to a condition of 100% water saturation. A brine permeability measurement was then conducted to quantify the fractured sample brine permeability at a net 3750 psi overburden pressure condition.

Following this, a gas regain permeability measurement was conducted to quantify the degree of expected damage which would occur to the fracture system at a net overburden pressure of 3750 psi after aqueous fluid invasion had occurred.

Geomechanical Tests

Plug samples from the fluvial facies and the dirty and clean marine facies were subjected to geomechanical tests to quantify Young's Modulus and compressive strength.

Mercury Injection Capillary Pressure Tests

Four endcap samples, two from the fluvial facies and one from the clean marine and one from the dirty marine facies were subjected to 60000 psi mercury capillary pressure tests to quantify pore entry radii and pore throat size distribution for the porous media.

FIGURE 1
UPRC - STRATOS
SPECIAL CORE STUDY
CORE #6B - FRACTURE FLUID LEAKOFF WITH HALLIBURTON FRAC GEL 2
PERMEABILITY SUMMARY

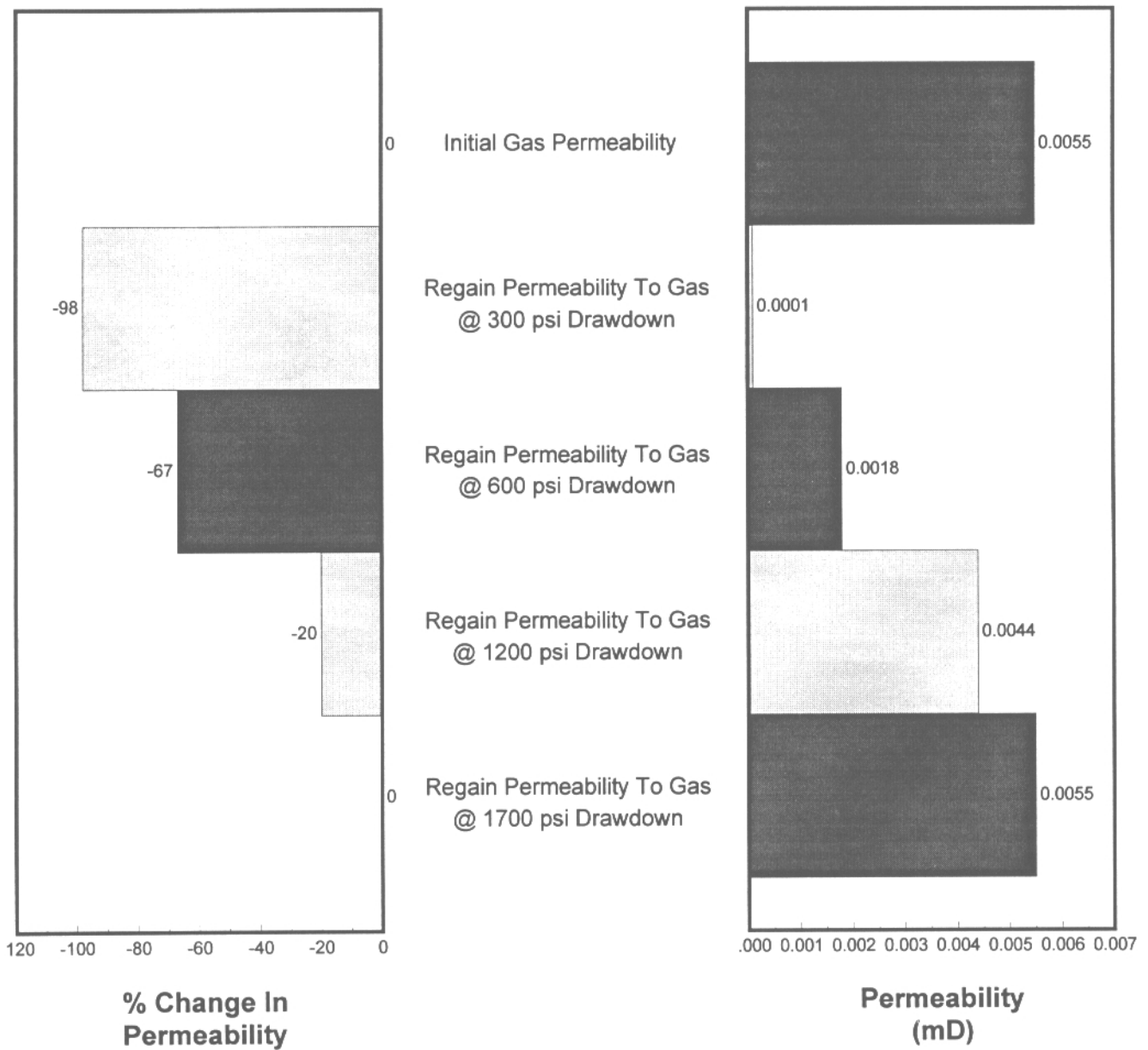


FIGURE 2
UPRC - STRATOS
SPECIAL CORE STUDY
CORE #7A - FRACTURE FLUID LEAKOFF WITH BJ TITAN BORATE HT 4500
PERMEABILITY SUMMARY

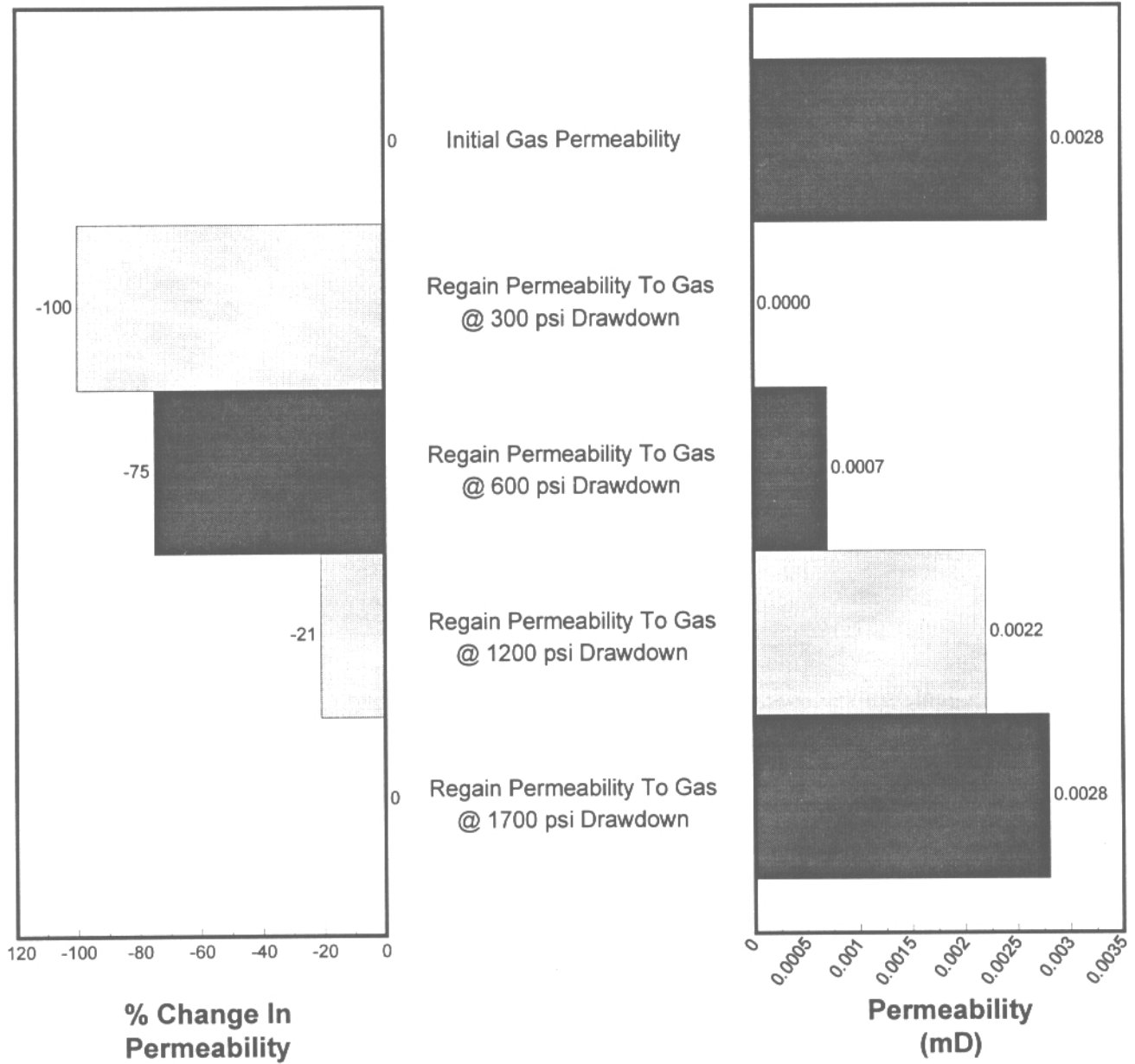


FIGURE 3
UPRC - STRATOS
SPECIAL CORE STUDY
CORE #31A - FRACTURE FLUID LEAKOFF WITH BJ TITAN BORATE HT 4500
PERMEABILITY SUMMARY

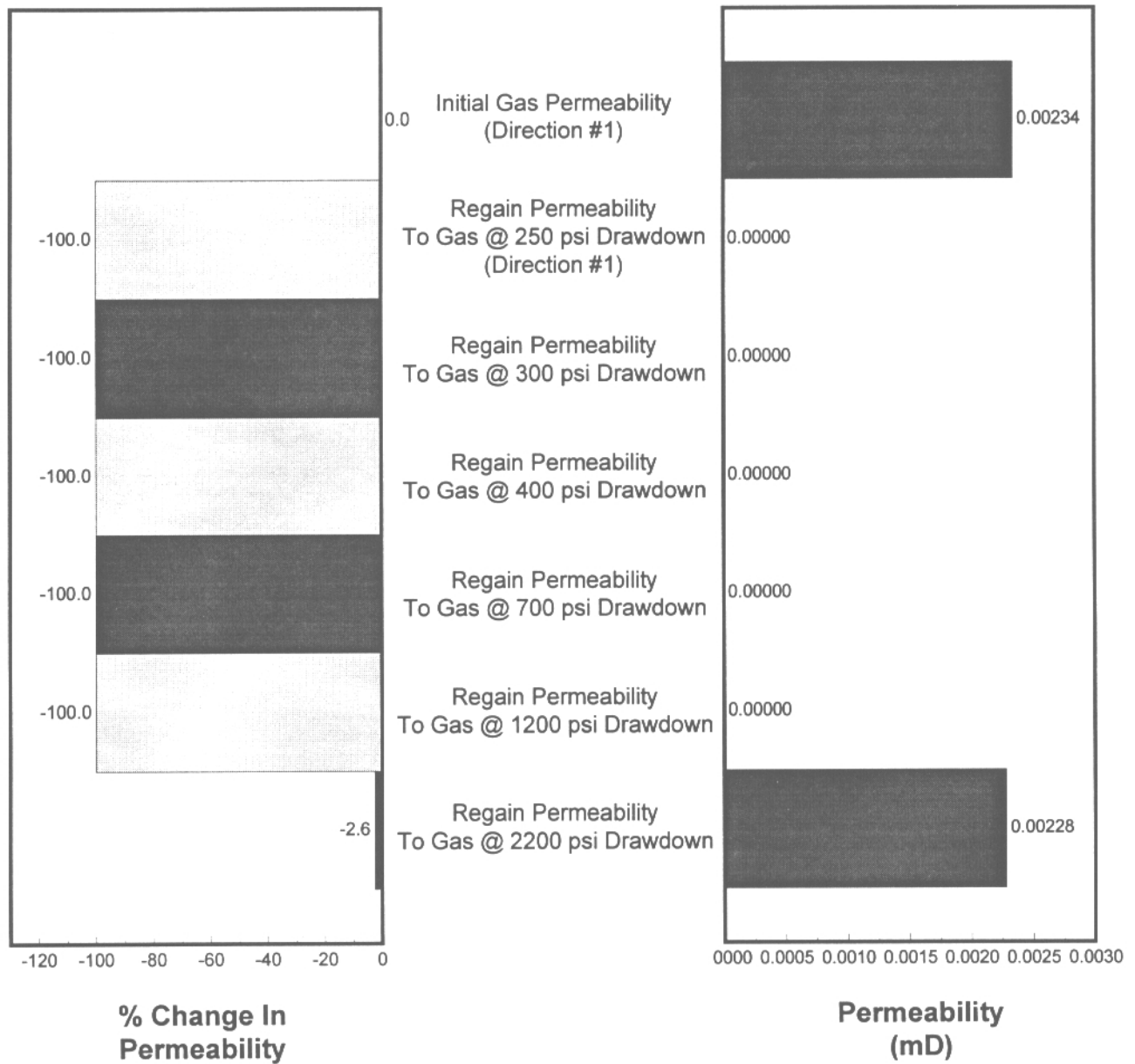


FIGURE 4
UPRC - STRATOS
SPECIAL CORE STUDY
CORE #31B - FRACTURE FLUID LEAKOFF WITH HALLIBURTON FRAC GEL 2
PERMEABILITY SUMMARY

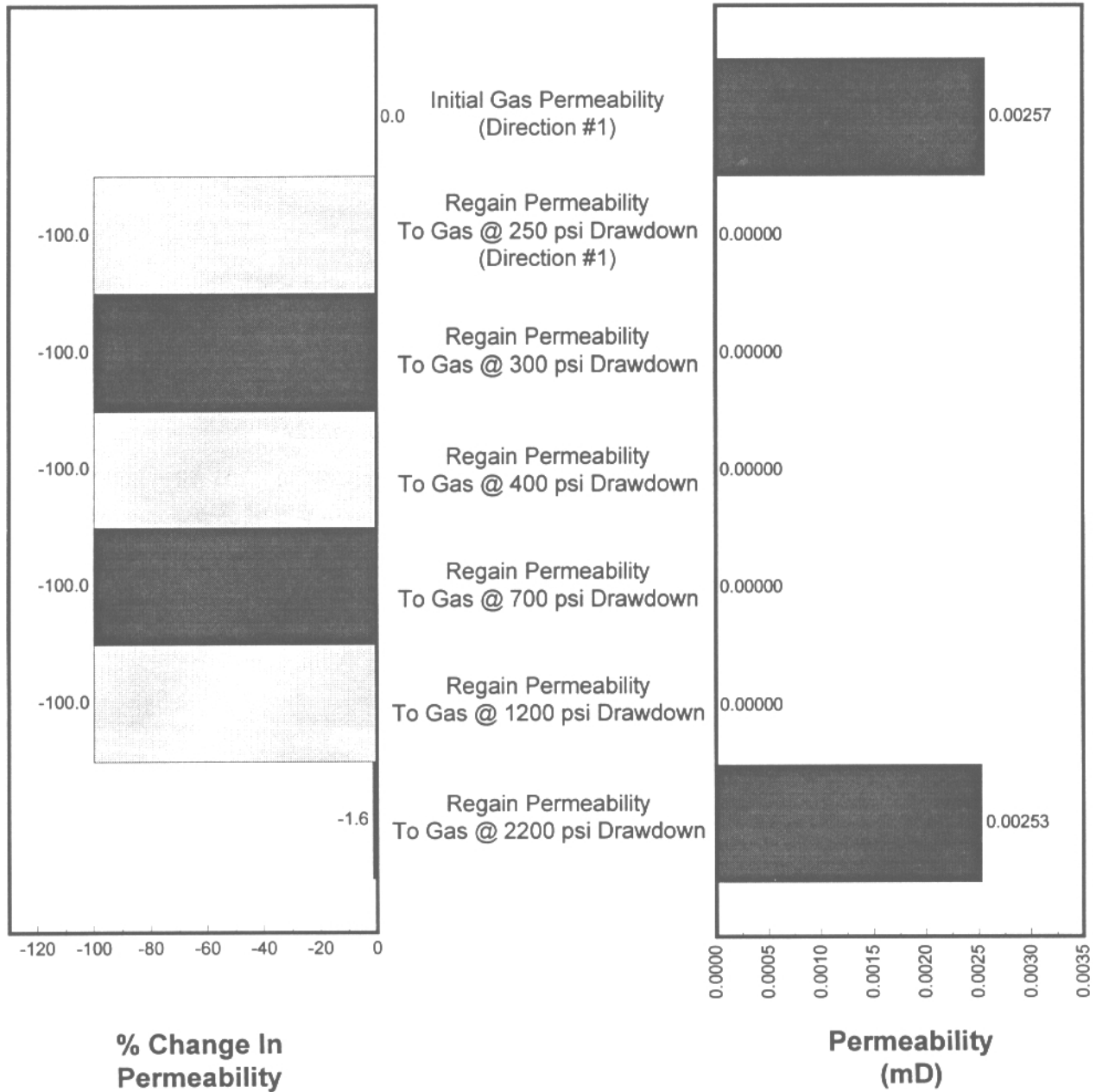


FIGURE 5
UPRC - STRATOS
SPECIAL CORE STUDY
CORE #6A - INCREMENTAL PHASE TRAP RELATIVE PERMEABILITY TEST
PERMEABILITY SUMMARY - THRESHOLD PRESSURE REGAINS

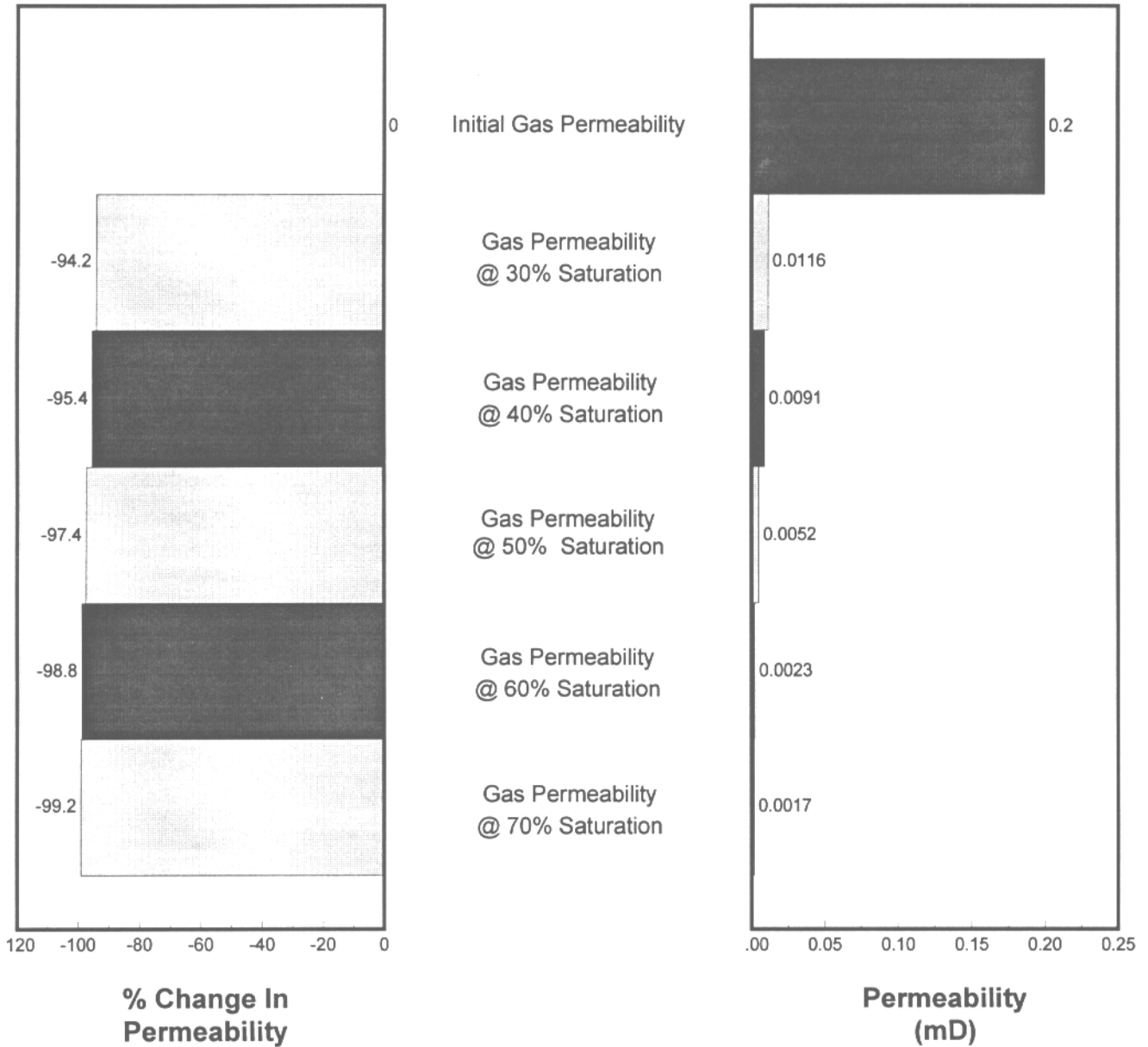


FIGURE 5A
UPRC - STRATOS
SPECIAL CORE STUDY
CORE #6A - INCREMENTAL PHASE TRAP RELATIVE PERMEABILITY
PERMEABILITY vs WATER SATURATION

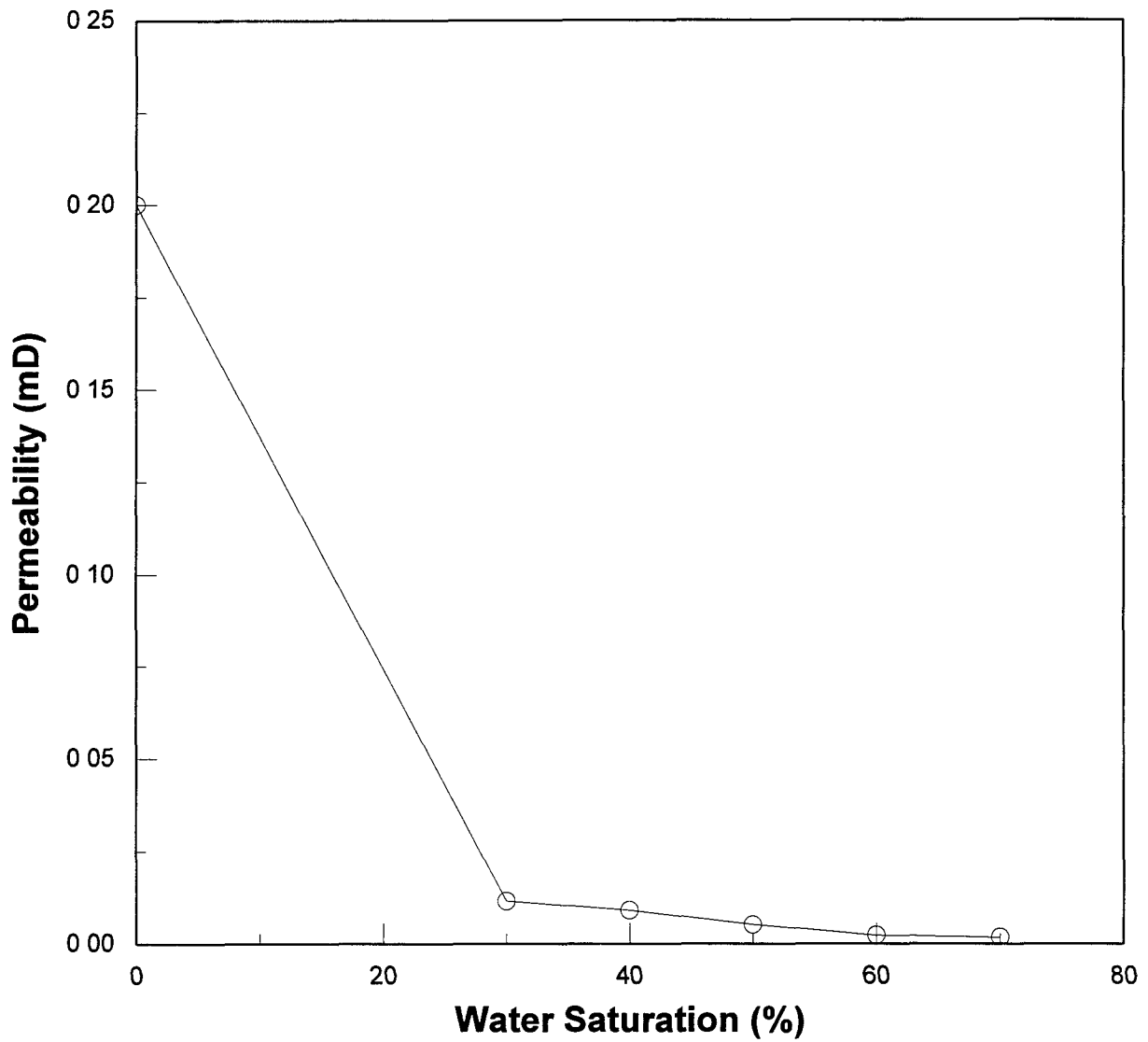


FIGURE 6
UPRC - STRATOS
SPECIAL CORE STUDY
CORE #37 - INCREMENTAL PHASE TRAP RELATIVE PERMEABILITY TEST
PERMEABILITY SUMMARY - THRESHOLD PRESSURE REGAINS

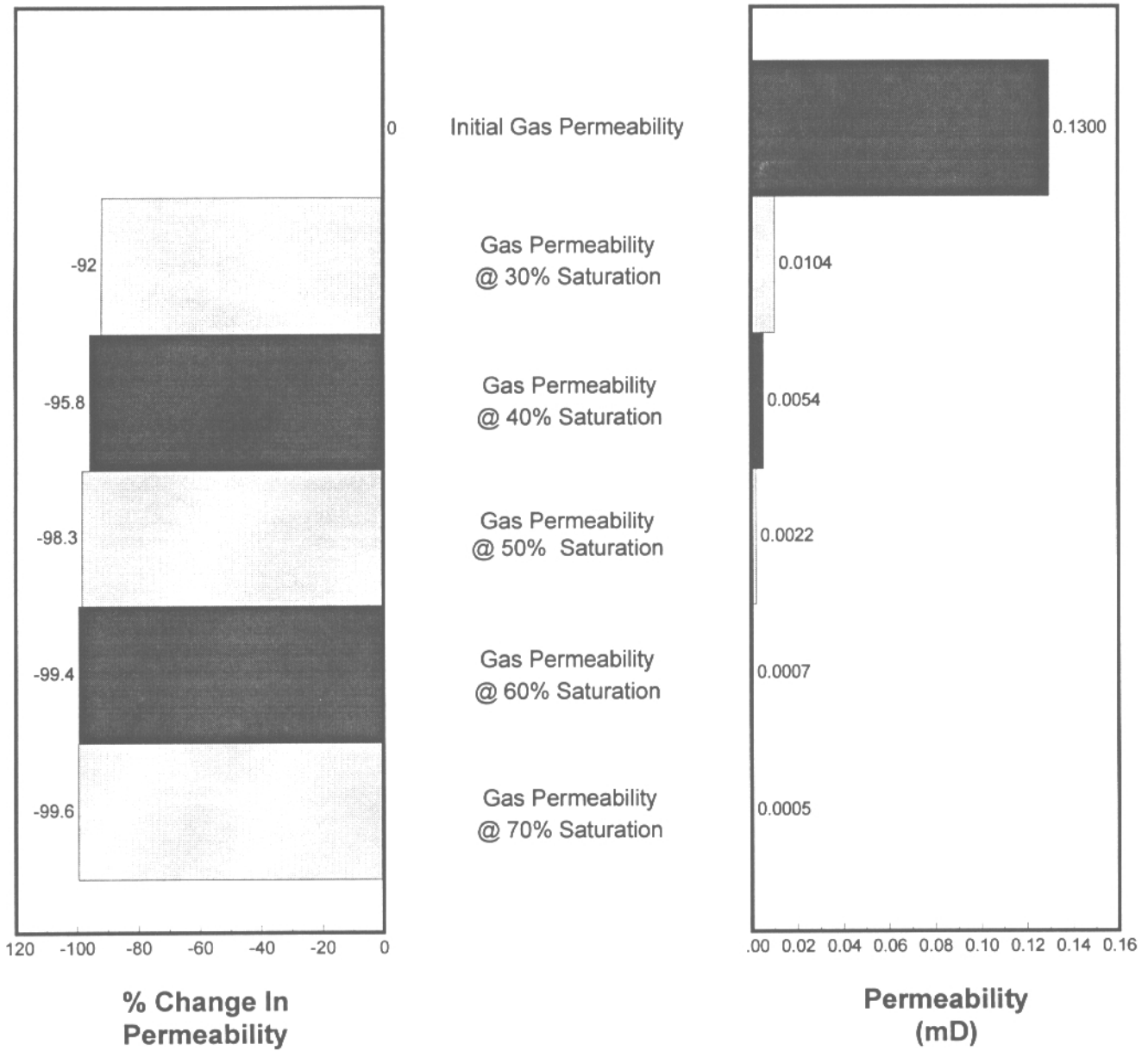


FIGURE 6A
UPRC - STRATOS
SPECIAL CORE STUDY
CORE #37 - INCREMENTAL PHASE TRAP RELATIVE PERMEABILITY
PERMEABILITY vs WATER SATURATION

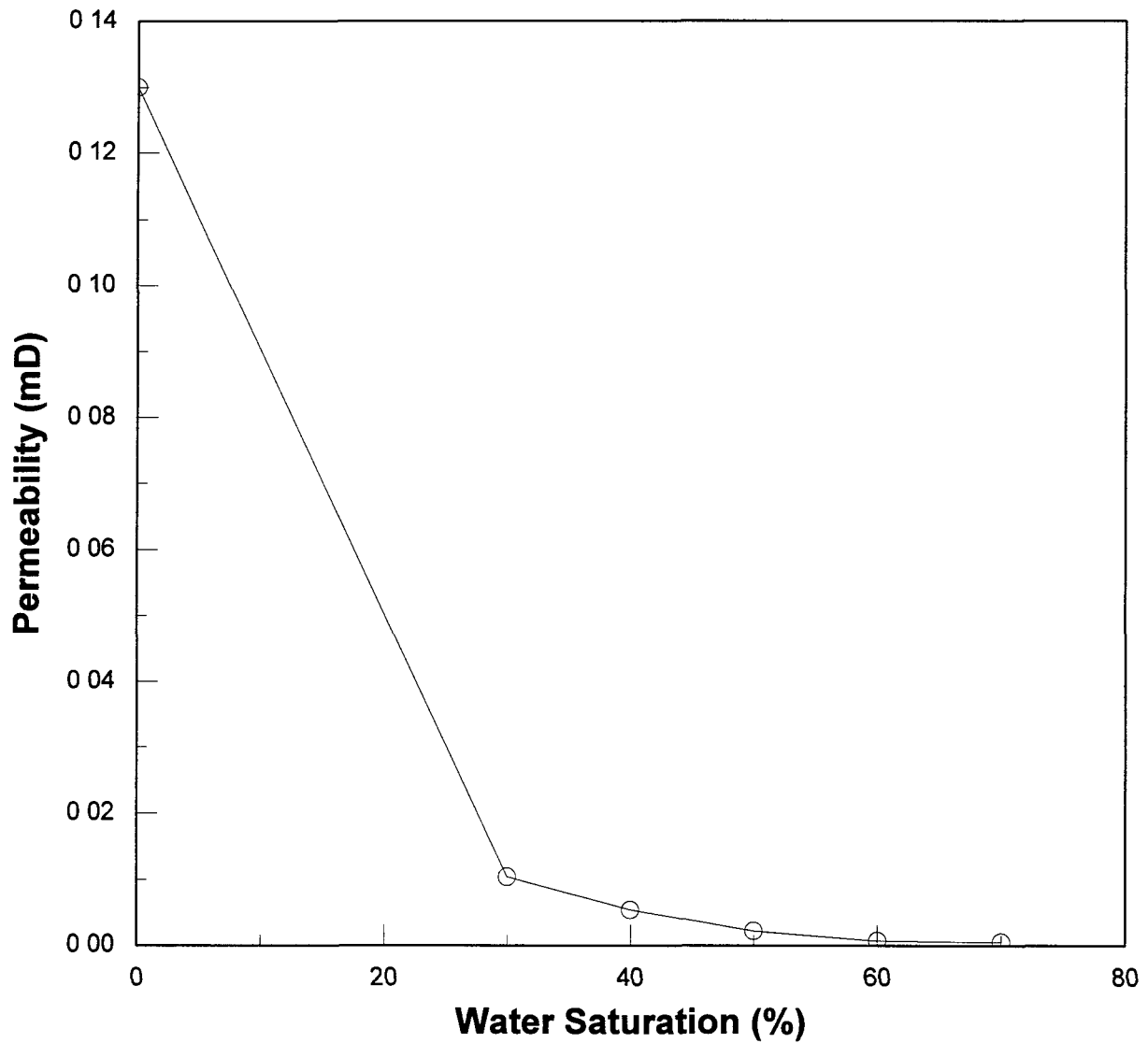


FIGURE 7
UPRC - STRATOS
SPECIAL CORE STUDY
CORE #9 - WATER-GAS RELATIVE PERMEABILITY TEST
CUML PRODUCTION vs CUML INJECTION

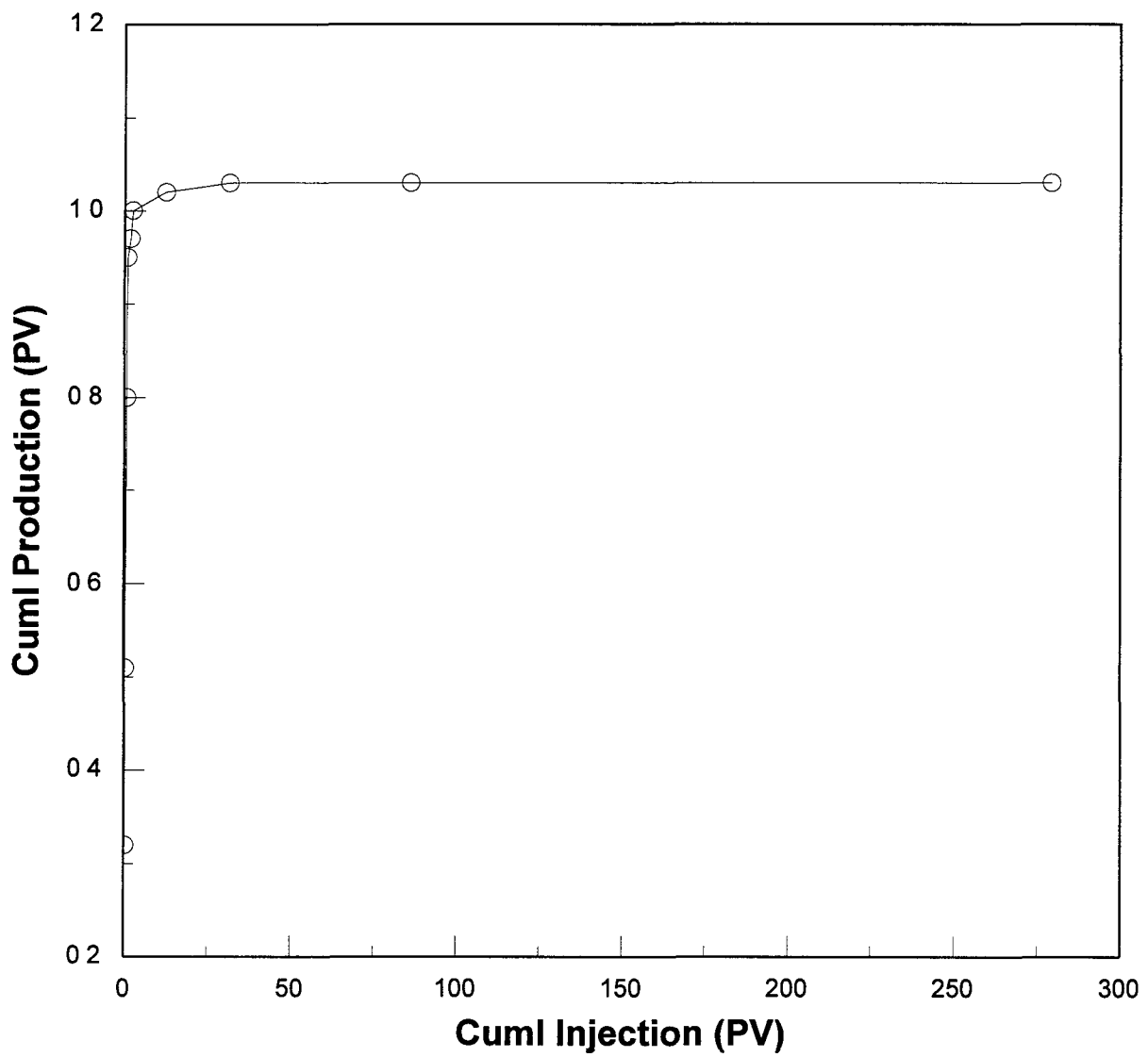


FIGURE 8
UPRC - STRATOS
SPECIAL CORE STUDY
CORE #9 - WATER-GAS RELATIVE PERMEABILITY TEST
PRESSURE vs CUMULATIVE INJECTION

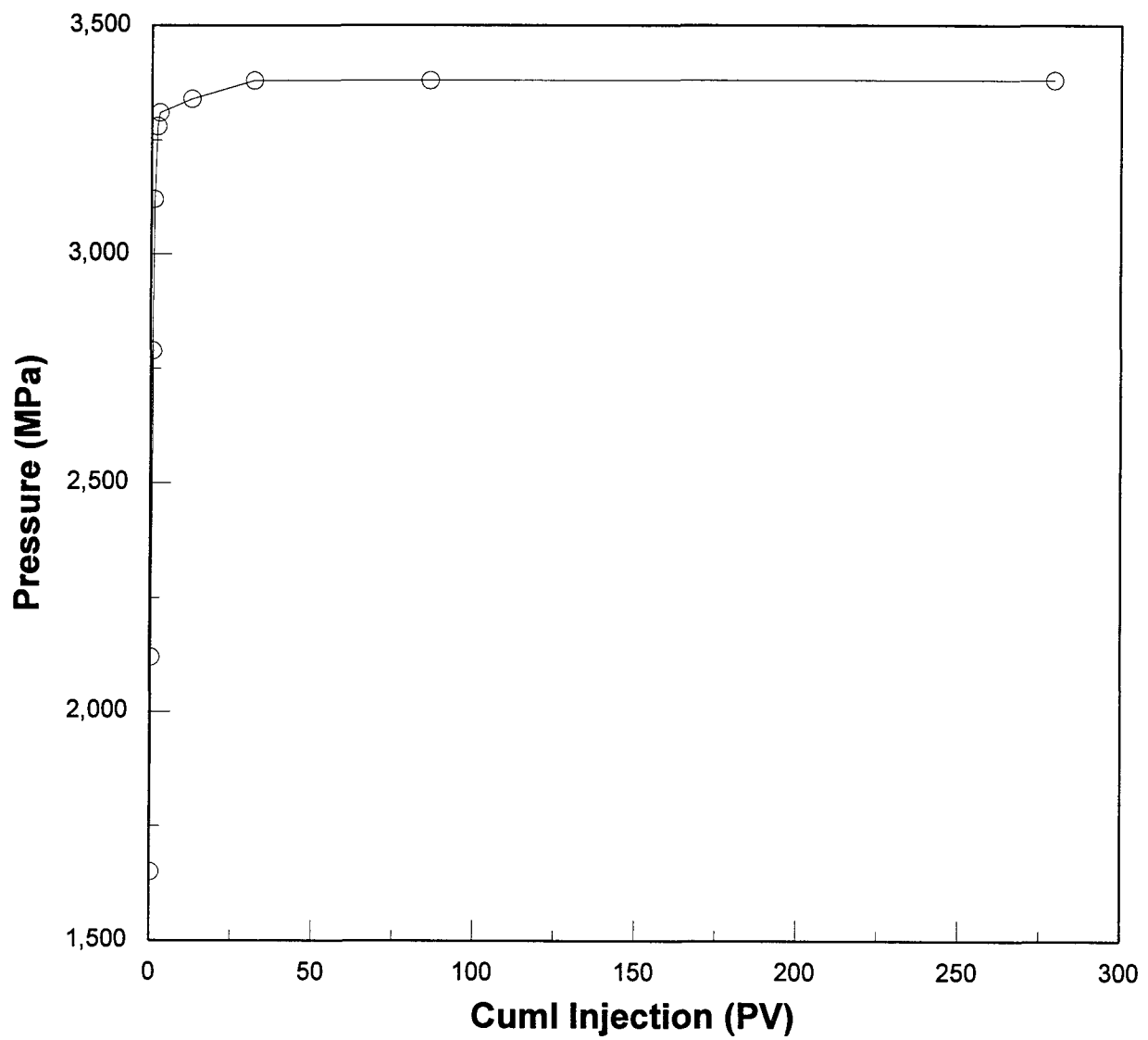


FIGURE 9
UPRC - STRATOS
SPECIAL CORE STUDY
CORE #9 - WATER-GAS RELATIVE PERMEABILITY TEST
RELATIVE PERMEABILITY vs WATER SATURATION

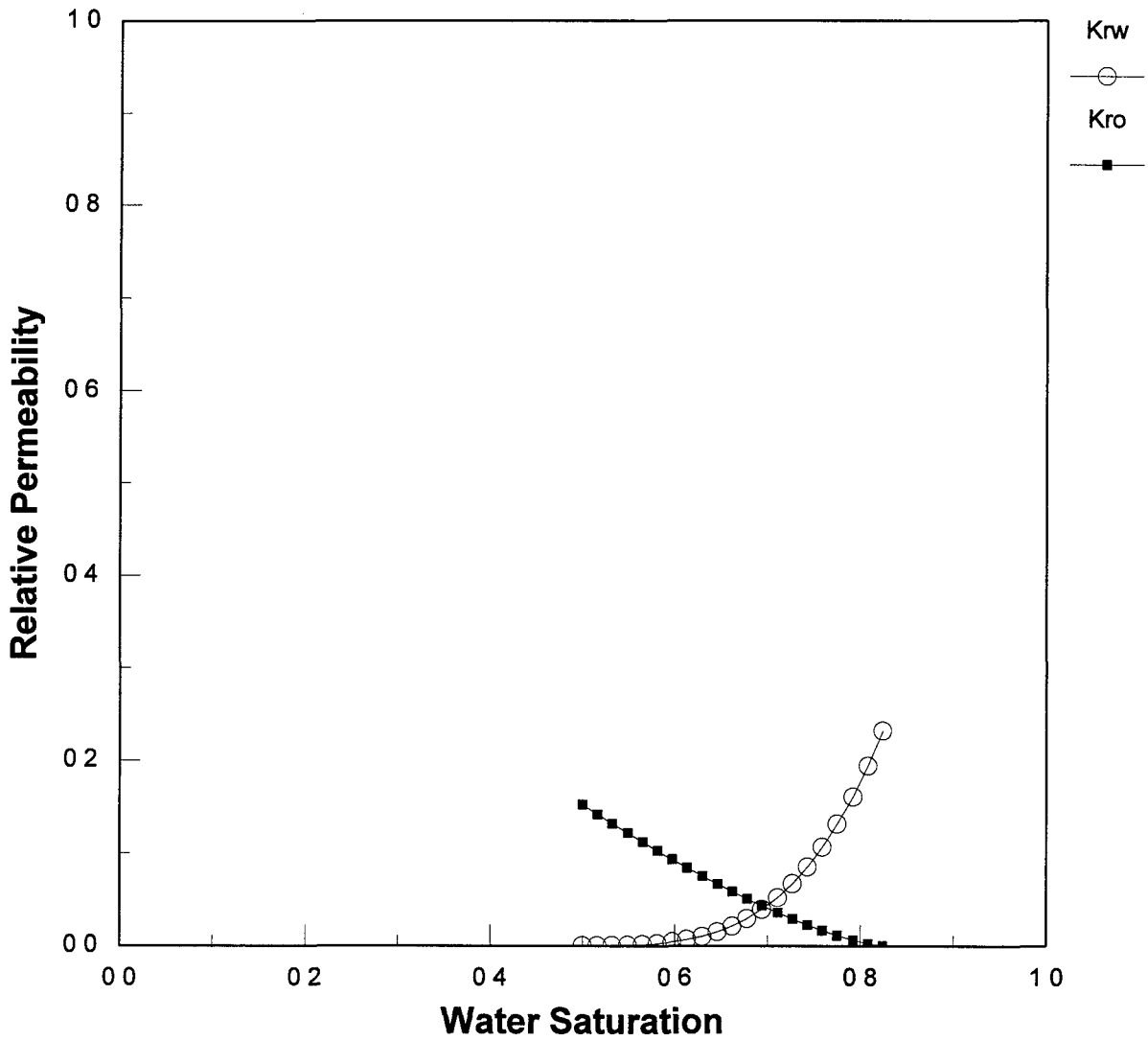


FIGURE 10
UPRC - STRATOS
SPECIAL CORE STUDY
CORE #9 - WATER-GAS RELATIVE PERMEABILITY TEST
RELATIVE PERMEABILITY vs WATER SATURATION

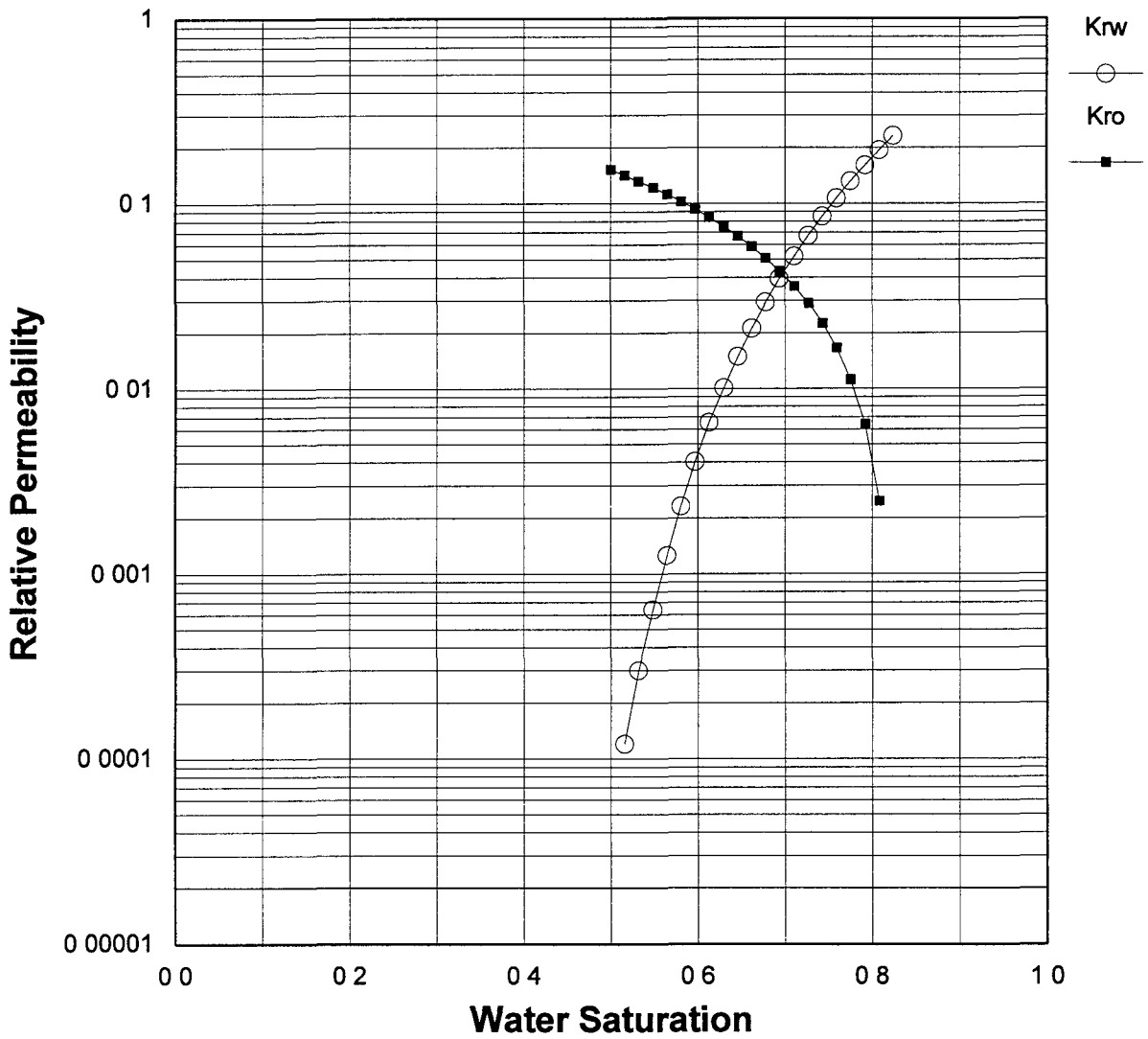


FIGURE 11
UPRC - STRATOS
SPECIAL CORE STUDY
CORE #48B - WATER-GAS RELATIVE PERMEABILITY TEST
CUML PRODUCTION vs CUML INJECTION

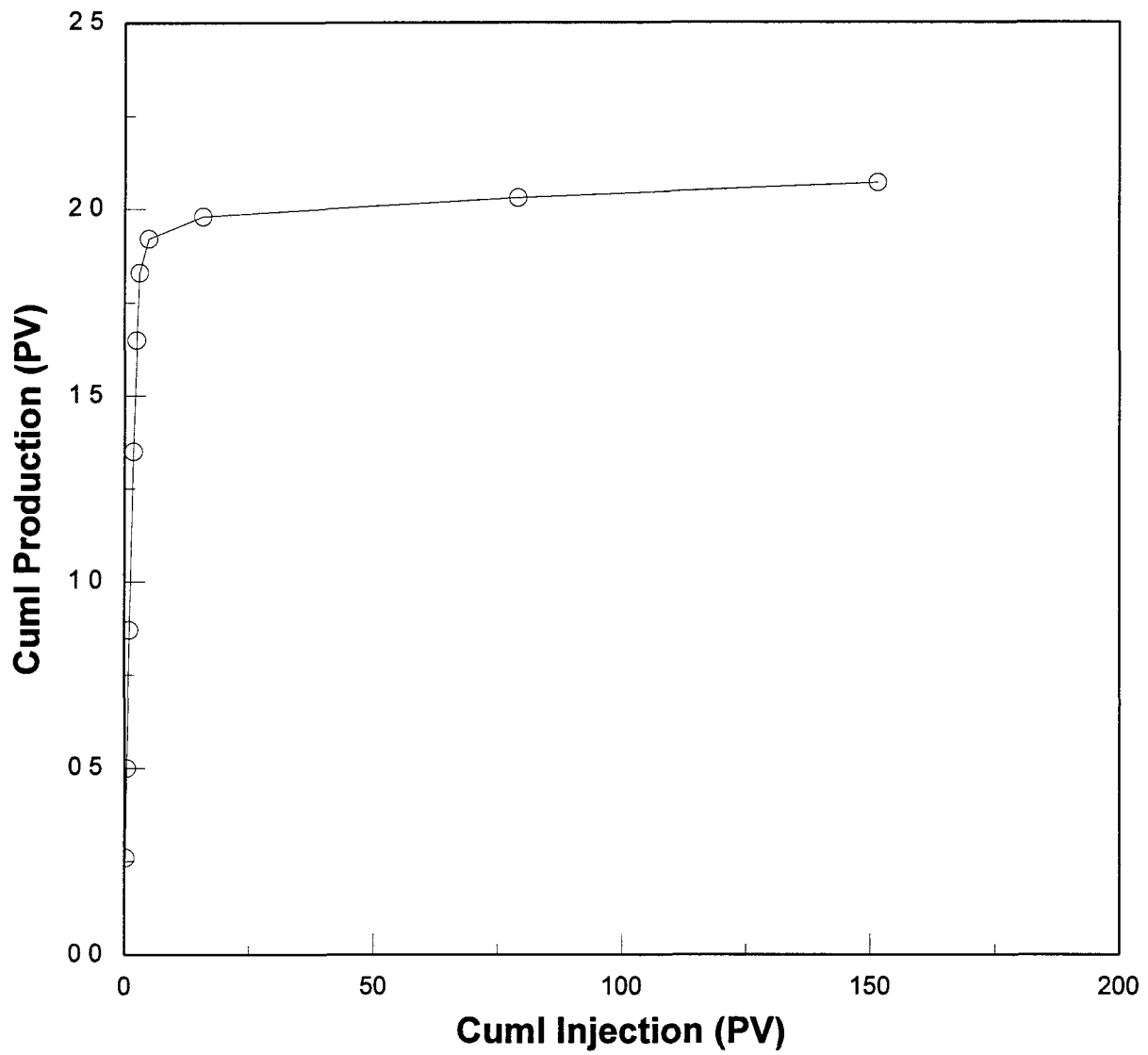


FIGURE 12
UPRC - STRATOS
SPECIAL CORE STUDY
CORE #48B - WATER-GAS RELATIVE PERMEABILITY TEST
PRESSURE vs CUMI INJECTION

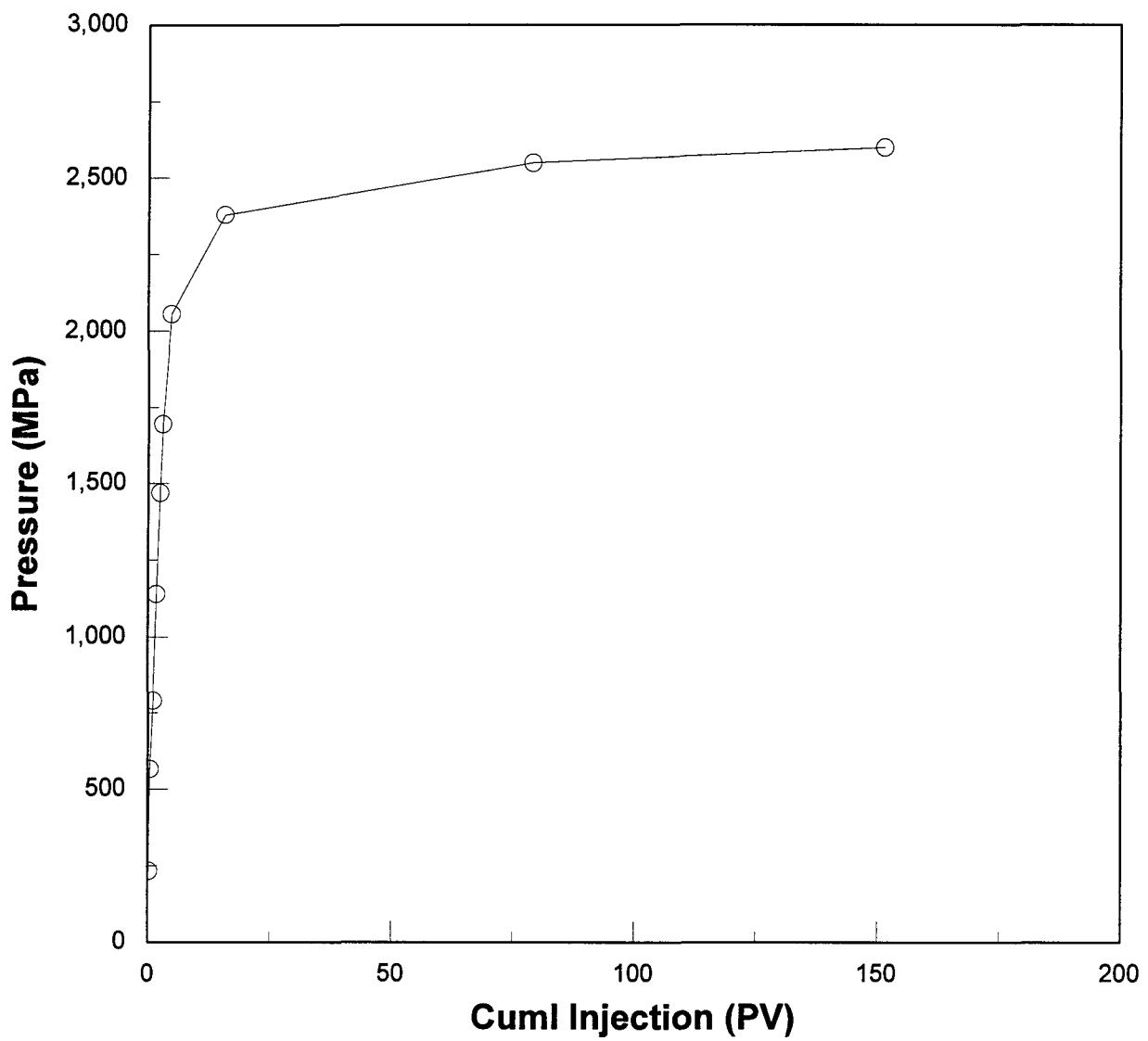


FIGURE 13
UPRC - STRATOS
SPECIAL CORE STUDY
CORE #48B - WATER-GAS RELATIVE PERMEABILITY TEST
RELATIVE PERMEABILITY vs WATER SATURATION

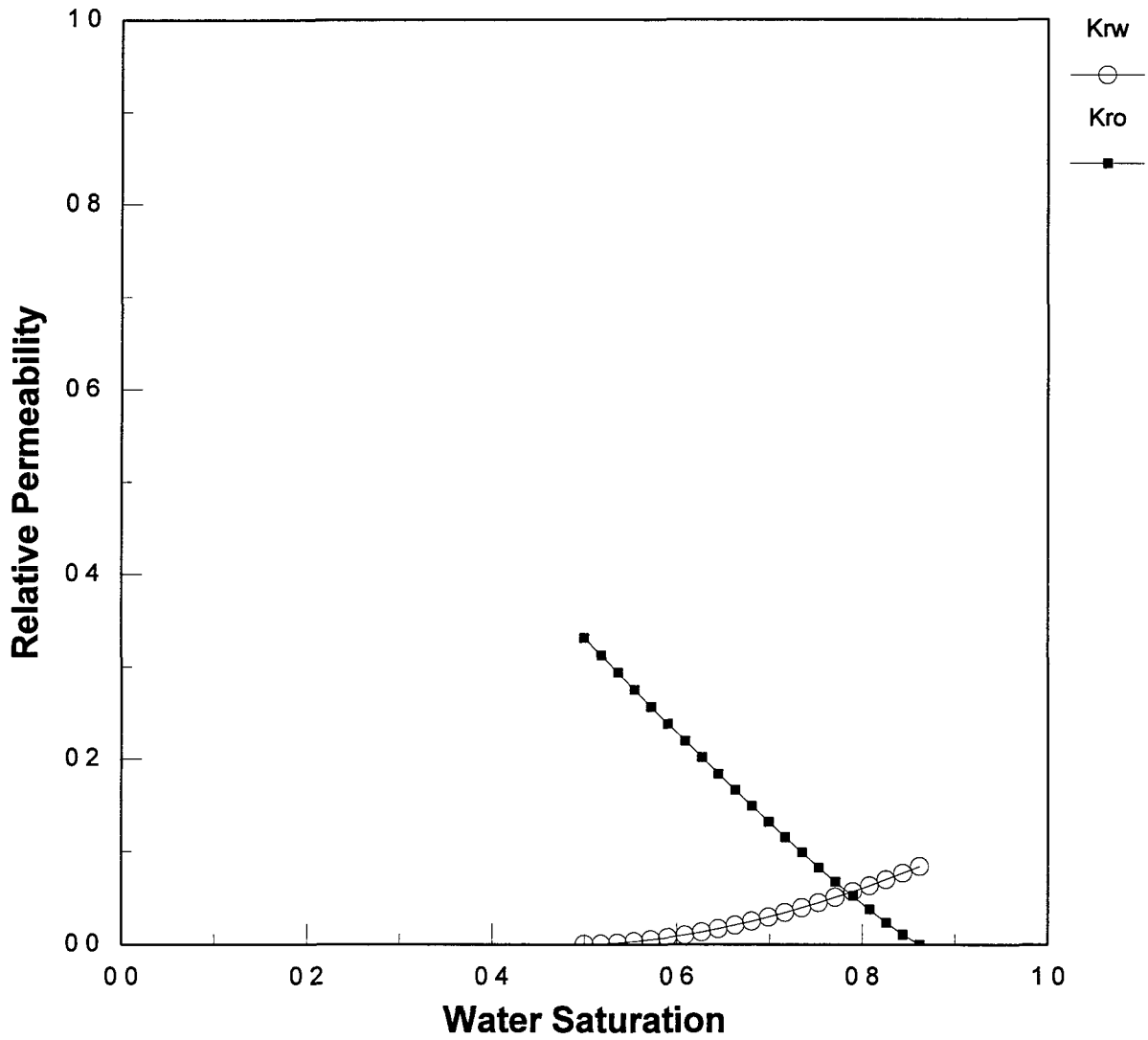


FIGURE 14
UPRC - STRATOS
SPECIAL CORE STUDY
CORE #48B - WATER-GAS RELATIVE PERMEABILITY TEST
RELATIVE PERMEABILITY vs WATER SATURATION

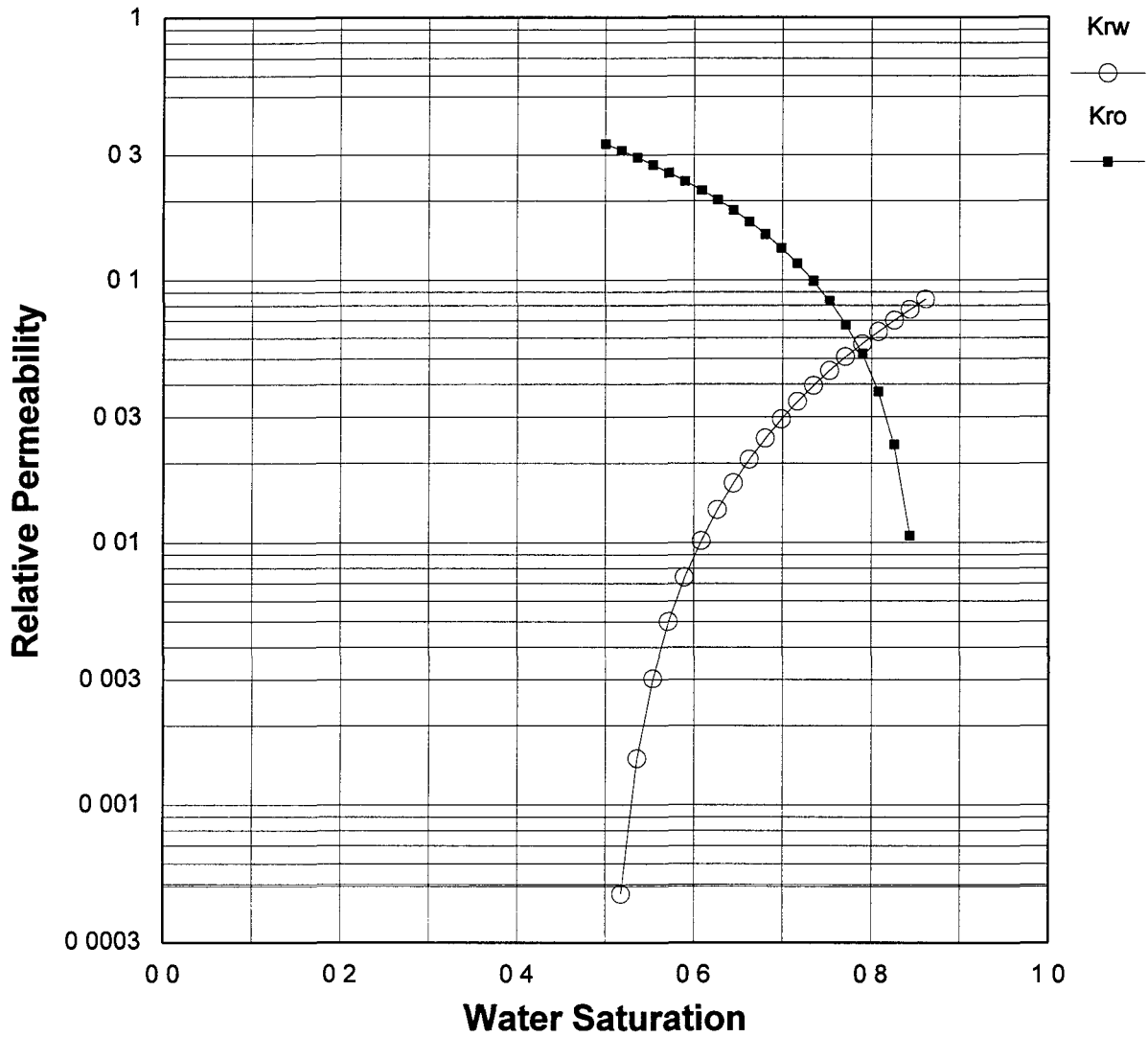


FIGURE 15
UPRC - STRATOS
SPECIAL CORE STUDY
CORE #12 - FRACTURE PERMEABILITY vs OVERBURDEN
AND FLUID SATURATION TEST
PERMEABILITY SUMMARY - THRESHOLD PRESSURE REGAINS

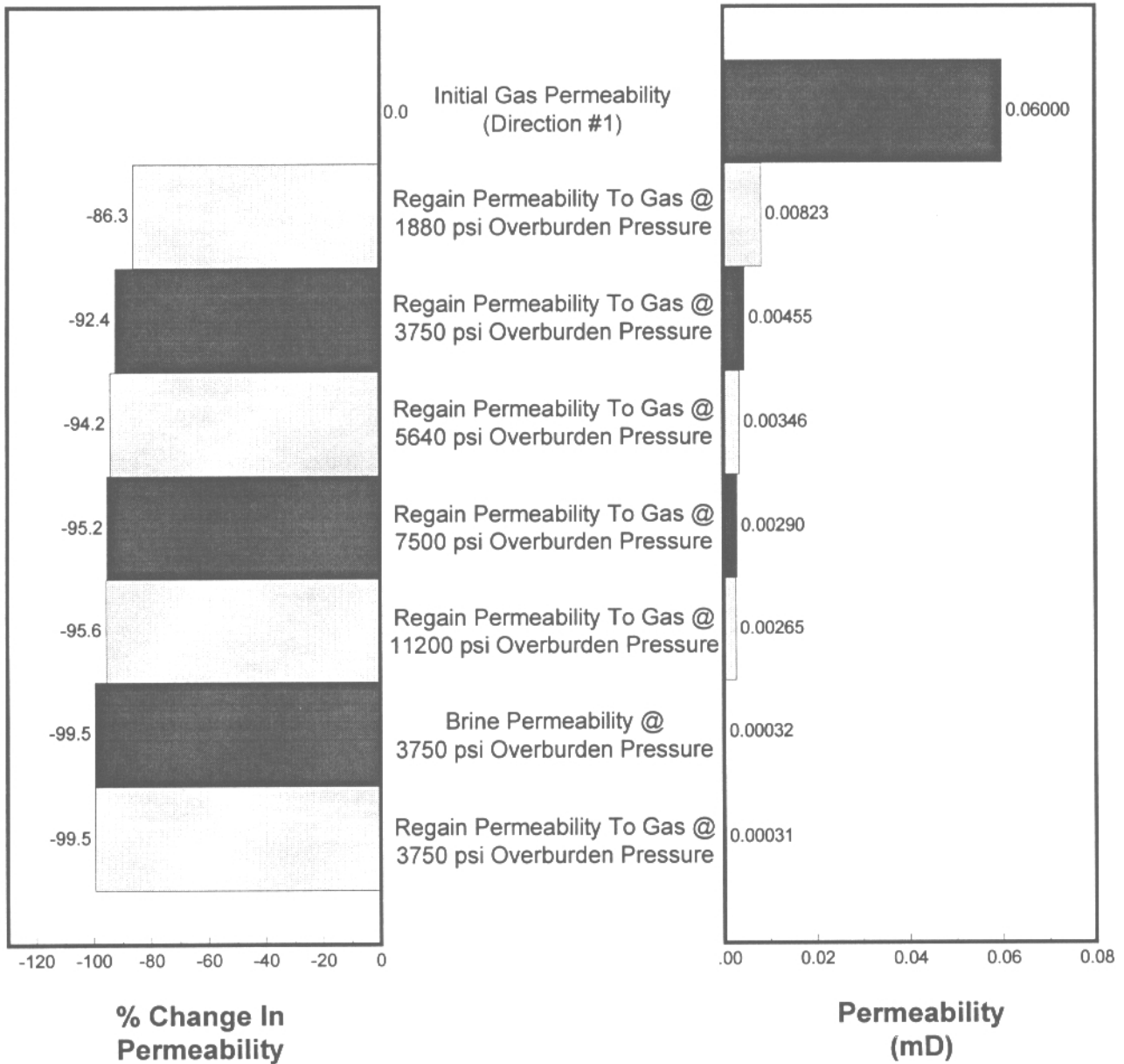


FIGURE 16
UPRC - STRATOS
SPECIAL CORE STUDY
CORE #32 - FRACTURE PERMEABILITY vs OVERBURDEN
AND FLUID SATURATION TEST
PERMEABILITY SUMMARY - THRESHOLD PRESSURE REGAINS

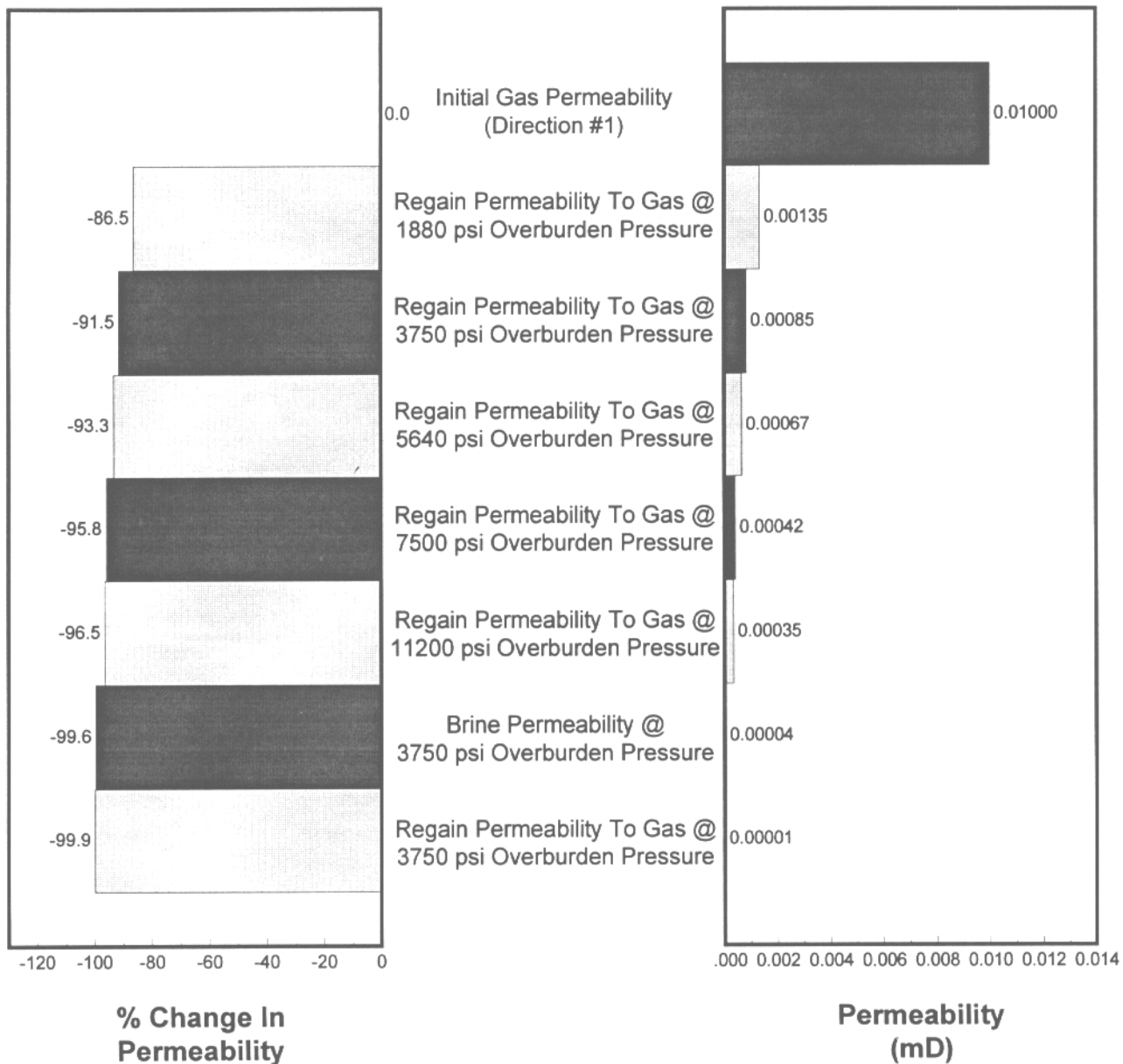


TABLE 1
UPRC - STRATOS
SPECIAL CORE STUDY
ROUTINE POROSITY & GAS PERMEABILITY

| Sample No. | Depth (ft) | Permeability (mD) | Porosity (fraction) | Grain Density (kg/m ³) | Comments | Core Usage |
|--|------------|-------------------|---------------------|------------------------------------|----------------|------------|
| 6A | 16025 25 | 0 20 | 0 062 | 2650 | ss,vf | Rel Perm* |
| 6B | 16025 45 | 0 16 | 0 060 | 2650 | ss,vf | Frac Fluid |
| 7A | 16026 80 | 0 17 | 0 052 | 2650 | ss,vf | Frac Fluid |
| 7B | 16026 85 | 0 39 | 0 054 | 2650 | ss,vf,lam | |
| 7C | 16026 90 | 0 12 | 0 048 | 2650 | ss,vf | |
| 7D | 16026 95 | 0 59 | 0 055 | 2650 | ss,vf,frac | |
| 8 | 16027 70 | 4 94 | 0 041 | 2650 | fractured | |
| 9 | 16028 60 | 0 08 | 0 040 | 2650 | ss,vf | Rel Perm |
| 30 | 16062 20 | 0 11 | 0 077 | 2660 | ss,vf | |
| 31A | 16063 20 | 0 11 | 0 077 | 2660 | ss,vf | Frac Fluid |
| 31B | 16063 30 | 0 10 | 0 077 | 2660 | ss,vf | Frac Fluid |
| 37 | 16069 20 | 0 13 | 0 109 | 2650 | ss,vf,shy | Rel Perm* |
| 46A | 16078 20 | 0 44 | 0 079 | 2660 | ss,vf,shy,frac | |
| 46B | 16078 30 | 0 11 | 0 080 | 2660 | ss,vf,shy | |
| 48A | 16080 20 | 0 10 | 0 087 | 2660 | ss,vf,shy | |
| 48B | 16080 30 | 0 08 | 0 078 | 2660 | ss,vf,shy | Rel Perm |
| * With initial incremental phase trap evaluation | | | | | | |

TABLE 2
UPRC - STRATOS
SPECIAL CORE STUDY
CORE #6B - FRACTURE FLUID LEAKOFF WITH HALLIBURTON FRAC GEL 2
CORE AND TEST PARAMETERS

| | |
|---|-----------------------|
| Core Number | 6B |
| Depth (ft) | 16025 45 |
| Well Location | UPRC - Stratos Fed #1 |
| Length (in) | 2.65 |
| Diameter (in) | 1.49 |
| Effective Flow Area (in ²) | 1 74 |
| Bulk Volume (in ³) | 4.61 |
| Porosity (fraction) | 0.060 |
| Pore Volume (in ³) | 0.277 |
| Initial Air Permeability (mD) | 0 160 |
| Initial Fixed Water Saturation (fraction) | 0.480 |
| Test Temperature (°F) | 285 |
| Gas Viscosity @ 285°F (mPa·s) | 0.0225 |
| Backpressure (psi) | 200 |
| Net Overburden Pressure (psi) | 3200 |
| Overbalance Fracture Pressure (psi) | 1800 |

TABLE 3
UPRC - STRATOS
SPECIAL CORE STUDY
CORE #6B - FRACTURE FLUID LEAKOFF WITH HALLIBURTON FRAC GEL 2
PERMEABILITY SUMMARY

| Test Phase | Permeability (mD) | % Change In Permeability |
|--|-------------------|--------------------------|
| Initial Gas Permeability (Direction #1) | 0.0055 | *0.00 |
| Fracture Fluid Leakoff (Direction #2) | -- | -- |
| Regain Permeability to Gas @ 300 psi Drawdown | 0.0001 | -98 |
| Regain Permeability To Gas @ 600 psi Drawdown | 0.0018 | -67 |
| Regain Permeability to Gas @ 1200 psi Drawdown | 0.0044 | -20 |
| Regain Permeability to Gas @ 1700 psi Drawdown | 0.0055 | 0 |
| * Baseline | | |

TABLE 4
UPRC - STRATOS
SPECIAL CORE STUDY
CORE #6B - FRACTURE FLUID LEAKOFF WITH HALLIBURTON FRAC GEL 2
LEAKOFF SUMMARY

| | |
|---|----------------------|
| Total Leakoff Volume (30 minutes) | 0.00 in ³ |
| (Linear Fluid Penetration Depth (30 minutes) | 0.00 in |
| * Assuming 100% filtrate sweep efficiency | |

TABLE 5
UPRC - STRATOS
SPECIAL CORE STUDY
CORE #7A - FRACTURE FLUID LEAKOFF WITH BJ TITAN BORATE HT 4500
CORE AND TEST PARAMETERS

| | |
|---|-----------------------|
| Core Number | 7A |
| Depth (ft) | 16025.80 |
| Well Location | UPRC - Stratos Fed #1 |
| Length (in) | 2.85 |
| Diameter (in) | 1.49 |
| Effective Flow Area (in ²) | 1.74 |
| Bulk Volume (in ³) | 4.96 |
| Porosity (fraction) | 0.065 |
| Pore Volume (in ³) | 0.322 |
| Initial Air Permeability (mD) | 0.170 |
| Initial Fixed Water Saturation (fraction) | 0.600 |
| Test Temperature (°F) | 285 |
| Gas Viscosity @ 285°F (mPa·s) | 0.0225 |
| Backpressure (psi) | 200 |
| Net Overburden Pressure (psi) | 3200 |
| Overbalance Fracture Pressure (psi) | 1800 |

TABLE 6
UPRC - STRATOS
SPECIAL CORE STUDY
CORE #7A - FRACTURE FLUID LEAKOFF WITH BJ TITAN BORATE HT 4500
PERMEABILITY SUMMARY

| Test Phase | Permeability (mD) | % Change In Permeability |
|--|-------------------|--------------------------|
| Initial Gas Permeability (Direction #1) | 0.0028 | *0.00 |
| Fracture Fluid Leakoff (Direction #2) | -- | -- |
| Regain Permeability To Gas @ 300 psi Drawdown | 0.0000 | -100 |
| Regain Permeability To Gas @ 600 psi Drawdown | 0.0007 | -75 |
| Regain Permeability To Gas @ 1200 psi Drawdown | 0.0022 | -21 |
| Regain Permeability To Gas @ 1700 psi Drawdown | 0.0028 | 0 |
| * Baseline | | |

TABLE 7
UPRC - STRATOS
SPECIAL CORE STUDY
CORE #7A - FRACTURE FLUID LEAKOFF WITH BJ TITAN BORATE HT 4500
LEAKOFF SUMMARY

| | |
|--|------------------------|
| Total Leakoff Volume (30 minutes) | 0.00 in ³ * |
| Linear Fluid Penetration Depth (30 minutes) | 0.00 in |
| * Assuming 100% filtrate sweep efficiency | |

TABLE 8
UPRC - STRATOS
SPECIAL CORE STUDY
CORE #31A - FRACTURE FLUID LEAKOFF WITH BJ TITAN BORATE H5 4500
CORE AND TEST PARAMETERS

| | |
|---|-----------------------|
| Core Number | 31A |
| Depth (ft) | 16063.20 |
| Well Location | UPRC - Stratos Fed #1 |
| Length (in) | 2.65 |
| Diameter (in) | 1.49 |
| Effective Flow Area (in ²) | 1.74 |
| Bulk Volume (in ³) | 4.62 |
| Porosity (fraction) | 0.079 |
| Pore Volume (in ³) | 0.365 |
| Routine Air Permeability (mD) | 0.11 |
| Test Temperature (°F) | 285 |
| Gas Viscosity @ 285°F (mPa·s) | 0.0224 |
| Initial Water Saturation - Fixed (fraction) | 0.50 |
| Backpressure (psi) | 200 |
| Net Overburden Pressure (psi) | 3200 |
| Overbalance Fracture Pressure (psi) | 1800 |

TABLE 9
UPRC - STRATOS
SPECIAL CORE STUDY
CORE #31A - FRACTURE FLUID LEAKOFF WITH BJ TITAN BORATE HT 4500
PERMEABILITY SUMMARY

| Test Phase | Permeability (mD) | % Change In Permeability |
|---|----------------------|-----------------------------|
| Initial Gas Permeability (Direction #1) | 0.00234 | *0.00 |
| Fracture Fluid Leakoff (Direction #2) | -- | -- |
| Regain Permeability To Gas @ 250 psi Drawdown (Direction #1) | 0.00000 | -100 |
| Regain Permeability To Gas @ 300 psi Drawdown | 0.00000 | -100 |
| Regain Permeability To Gas @ 400 psi Drawdown | 0.00000 | -100 |
| Regain Permeability To Gas @ 700 psi Drawdown | 0.00000 | -100 |
| Regain Permeability To Gas @ 1200 psi Drawdown | 0.00000 | -100 |
| Regain Permeability To Gas @ 2200 psi Drawdown | 0.00228 | -2.56 |
| * Baseline | | |

TABLE 10
UPRC - STRATOS
SPECIAL CORE STUDY
CORE #31A - FRACTURE FLUID LEAKOFF WITH BJ TITAN BORATE HT 4500
LEAKOFF SUMMARY

| | |
|--|----------------------|
| Total Leakoff Volume (30 minutes) | 0.12 in ³ |
| Linear Fluid Penetration Depth (30 minutes) | *0.84 in |
| * Assuming 100% filtrate sweep efficiency | |

TABLE 11
UPRC - STRATOS
SPECIAL CORE STUDY
CORE #31B - FRACTURE FLUID LEAKOFF WITH HALLIBURTON FRAC GEL 2
CORE AND TEST PARAMETERS

| | |
|---|-----------------------|
| Core Number | 31B |
| Depth (ft) | 16063.30 |
| Well Location | UPRC - Stratos Fed #1 |
| Length (in) | 2.55 |
| Diameter (in) | 1.49 |
| Effective Flow Area (in ²) | 1.73 |
| Bulk Volume (in ³) | 4.43 |
| Porosity (fraction) | 0.079 |
| Pore Volume (in ³) | 0.350 |
| Routine Air Permeability (mD) | 0.10 |
| Test Temperature (°F) | 285 |
| Gas Viscosity @ 285°F (mPa·s) | 0.0224 |
| Initial Water Saturation - Fixed (fraction) | 0.50 |
| Backpressure (psi) | 200 |
| Net Overburden Pressure (psi) | 3200 |
| Overbalance Fracture Pressure (psi) | 1800 |

TABLE 12
UPRC - STRATOS
SPECIAL CORE STUDY
CORE #31B - FRACTURE FLUID LEAKOFF WITH HALLIBURTON FRAC GEL 2
PERMEABILITY SUMMARY

| Test Phase | Permeability (mD) | % Change In Permeability |
|--|-------------------|--------------------------|
| Initial Gas Permeability (Direction #1) | 0.00257 | *0.00 |
| Fracture Fluid Leakoff (Direction #2) | -- | -- |
| Regain Permeability To Gas @ 250 psi Drawdown (Direction #1) | 0.00000 | -100 |
| Regain Permeability To Gas @ 300 psi Drawdown | 0.00000 | -100 |
| Regain Permeability To Gas @ 400 psi Drawdown | 0.00000 | -100 |
| Regain Permeability To Gas @ 700 psi Drawdown | 0.00000 | -100 |
| Regain Permeability To Gas @ 1200 psi Drawdown | 0.00000 | -100 |
| Regain Permeability To Gas @ 2200 psi Drawdown | 0.00253 | -1.56 |
| * Baseline | | |

TABLE 13
UPRC - STRATOS
SPECIAL CORE STUDY
CORE #31B - FRACTURE FLUID LEAKOFF WITH HALLIBURTON FRAC GEL 2
LEAKOFF SUMMARY

| | |
|--|----------------------|
| Total Leakoff Volume (30 minutes) | 0.00 in ³ |
| Linear Fluid Penetration Depth (30 minutes) | *0.00 in |
| * Assuming 100% filtrate sweep efficiency | |

TABLE 14
UPRC - STRATOS
SPECIAL CORE STUDY
CORE #6A - INCREMENTAL PHASE TRAP RELATIVE PERMEABILITY TEST
CORE AND TEST PARAMETERS

| | |
|--|-----------------------|
| Core Number | 6A |
| Depth (ft) | 16025.25 |
| Field Name | Stratos |
| Well Location | UPRC - Stratos Fed #1 |
| Length (in) | 2.57 |
| Diameter (in) | 1.49 |
| Effective Flow Area (in ²) | 1.74 |
| Bulk Volume (in ³) | 4.47 |
| Porosity (fraction) | 0.062 |
| Pore Volume (in ³) | 0.28 |
| Routine Air Permeability (mD) | 0.20 |
| Test Temperature (°F)* | 176 |
| Gas Viscosity @ 176°F (mPa·s) | 0.0200 |
| Net Overburden Pressure (psig) | 3200 |
| * Maximum temperature attainable without use of backpressure | |

TABLE 15
UPRC - STRATOS
SPECIAL CORE STUDY
CORE #6A - INCREMENTAL PHASE TRAP RELATIVE PERMEABILITY TEST
PERMEABILITY SUMMARY - THRESHOLD PRESSURE REGAINS

| Displacement Phase | Permeability (mD) | % Change In Permeability |
|---|------------------------------|-------------------------------------|
| Initial Gas Permeability (unstressed, 0% Sw _i) | 0.2000 | *0.0 |
| Gas Permeability @ 30% Saturation | 0.0116 | -94.2 |
| Gas Permeability @ 40% Saturation | 0.0091 | -95.4 |
| Gas Permeability @ 50% Saturation | 0.0052 | -97.4 |
| Gas Permeability @ 60% Saturation | 0.0023 | -98.8 |
| Gas Permeability @ 70% Saturation | 0.0017 | -99.2 |

TABLE 16
UPRC - STRATOS
SPECIAL CORE STUDY
CORE #37 - INCREMENTAL PHASE TRAP RELATIVE PERMEABILITY TEST
CORE AND TEST PARAMETERS

| | |
|--|-----------------------|
| Core Number | 37 |
| Depth (ft) | 16069.20 |
| Field Name | Stratos |
| Well Location | UPRC - Stratos Fed #1 |
| Length (in) | 2.57 |
| Diameter (in) | 1.49 |
| Effective Flow Area (in ²) | 1.75 |
| Bulk Volume (in ³) | 4.50 |
| Porosity (fraction) | 0.109 |
| Pore Volume (in ³) | 0.49 |
| Routine Air Permeability (mD) | 0.13 |
| Test Temperature (°F)* | 176 |
| Gas Viscosity @ 176°F (mPa-s) | 0.0200 |
| Net Overburden Pressure (psig) | 3200 |
| * Maximum temperature attainable without use of backpressure | |

TABLE 17
UPRC - STRATOS
SPECIAL CORE STUDY
CORE #37 - INCREMENTAL PHASE TRAP RELATIVE PERMEABILITY TEST
PERMEABILITY SUMMARY - THRESHOLD PRESSURE REGAINS

| Displacement Phase | Permeability (mD) | % Change In Permeability |
|---|------------------------------|-------------------------------------|
| Initial Gas Permeability (Unstressed, 0% Sw _i) | 0.1300 | *0.0 |
| Gas Permeability @ 30% Saturation | 0.0104 | -92.0 |
| Gas Permeability @ 40% Saturation | 0.0054 | -95.8 |
| Gas Permeability @ 50% Saturation | 0.0022 | -98.3 |
| Gas Permeability @ 60% Saturation | 0.0007 | -99.4 |
| Gas Permeability @ 70% Saturation | 0.0005 | -99.6 |

TABLE 18
UPRC - STRATOS
SPECIAL CORE STUDY
CORE #9 - WATER-GAS RELATIVE PERMEABILITY TEST
CORE AND TEST PARAMETERS

| | |
|--|-----------------------|
| Core Number | 9 |
| Depth (ft) | 16028 60 |
| Field Name | Stratos |
| Well Location | UPRC - Stratos Fed #1 |
| Length (in) | 2.81 |
| Diameter (in) | 1.48 |
| Effective Flow Area (in ²) | 1.73 |
| Bulk Volume (in ³) | 4.86 |
| Porosity (fraction) | 0.040 |
| Pore Volume (in ³) | 0.194 |
| Routine Air Permeability (mD) | 0.08 |
| Test Temperature (°F)* | 285 |
| Gas Viscosity @ 176°F (mPa·s) | 0.0224 |
| Net Overburden Pressure (psig) | 3200 |

TABLE 19
UPRC - STRATOS
SPECIAL CORE STUDY
CORE #9 - WATER-GAS RELATIVE PERMEABILITY TEST
SATURATION AND PERMEABILITY SUMMARY

| Test Phase | Sw | Sg | Permeability (mD) | Relative Permeability* |
|---|-----------|-----------|------------------------------|-----------------------------------|
| Initial Gas | 0.500 | 0.500 | 0.000462 | 0.1525 |
| Waterflood | 0.824 | 0.176 | 0.000703 | 0.2320 |
| * Based on estimated absolute fluid permeability of 0.003 mD. | | | | |

TABLE 20
UPRC - STRATOS
SPECIAL CORE STUDY
CORE #9 - WATER-GAS RELATIVE PERMEABILITY TEST
EXPERIMENTAL PRESSURE AND PRODUCTION HISTORY

| Cuml Injection (PV) | Cuml Production (PV) | Pressure (MPa) |
|------------------------|-------------------------|-------------------|
| 0.32 | 0.32 | 1650.00 |
| 0.52 | 0.51 | 2120.00 |
| 0.80 | 0.80 | 2790.00 |
| 1.05 | 0.95 | 3120.00 |
| 1.88 | 0.97 | 3280.00 |
| 2.55 | 1.00 | 3310.00 |
| 12.55 | 1.02 | 3340.00 |
| 31.77 | 1.03 | 3380.00 |
| 86.27 | 1.03 | 3380.00 |
| 279.45 | 1.03 | 3380.00 |

TABLE 21
UPRC - STRATOS
SPECIAL CORE STUDY
CORE #9 - WATER-GAS RELATIVE PERMEABILITY TEST
WATER-GAS RELATIVE PERMEABILITY DATA

| Water Saturation | Relative Permeability | |
|------------------|-----------------------|----------|
| | k_{rw} | k_{ro} |
| 0.500 | 0.00000 | 0.15246 |
| 0.516 | 0.00012 | 0.14203 |
| 0.532 | 0.00030 | 0.13184 |
| 0.549 | 0.00064 | 0.12184 |
| 0.565 | 0.00126 | 0.11207 |
| 0.581 | 0.00233 | 0.10253 |
| 0.597 | 0.00403 | 0.09323 |
| 0.613 | 0.00654 | 0.08418 |
| 0.630 | 0.01009 | 0.07537 |
| 0.646 | 0.01492 | 0.06686 |
| 0.662 | 0.02125 | 0.05864 |
| 0.678 | 0.02936 | 0.05072 |
| 0.694 | 0.03953 | 0.04313 |
| 0.711 | 0.05204 | 0.03587 |
| 0.727 | 0.06719 | 0.02901 |
| 0.743 | 0.08531 | 0.02258 |
| 0.759 | 0.10669 | 0.01661 |
| 0.775 | 0.13170 | 0.01118 |
| 0.792 | 0.16068 | 0.00640 |
| 0.808 | 0.19397 | 0.00247 |
| 0.824 | 0.23199 | 0.00000 |

TABLE 22
UPRC - STRATOS
SPECIAL CORE STUDY
CORE #48B - WATER-GAS RELATIVE PERMEABILITY TEST
CORE AND TEST PARAMETERS

| | |
|--|-----------------------|
| Core Number | 48B |
| Depth (m) | 16080.30 |
| Field Name | Stratos |
| Well Location | UPRC - Stratos Fed #1 |
| Length (cm) | 2.60 |
| Diameter (cm) | 1.48 |
| Effective Flow Area (in ²) | 1.73 |
| Bulk Volume (in ³) | 4.50 |
| Porosity (fraction) | 0.078 |
| Pore Volume (in ³) | 0.351 |
| Routine Air Permeability (mD) | 0.08 |
| Test Temperature (°F) | 285 |
| Gas Viscosity @ 176°F (mPa·s) | 0.0225 |
| Net Overburden Pressure (psig) | 3200 |

TABLE 23
UPRC - STRATOS
SPECIAL CORE STUDY
CORE #48B - WATER-GAS RELATIVE PERMEABILITY TEST
SATURATION AND PERMEABILITY SUMMARY

| Test Phase | Sw | Sg | Permeability (mD) | Relative Permeability* |
|---|-----------|-----------|------------------------------|-----------------------------------|
| Initial Gas | 0.500 | 0.500 | 0.00166 | 0.3320 |
| Waterflood | 0.862 | 0.138 | 0.000422 | 0.0844 |
| * Based on estimated absolute fluid permeability of 0.005 mD. | | | | |

TABLE 24
UPRC - STRATOS
SPECIAL CORE STUDY
CORE #48B - WATER-GAS RELATIVE PERMEABILITY TEST
EXPERIMENTAL PRESSURE AND PRODUCTION HISTORY

| Cuml Injection (PV) | Cuml Production (PV) | Pressure (MPa) |
|------------------------|-------------------------|-------------------|
| 0.26 | 0.26 | 233.00 |
| 0.49 | 0.50 | 566.00 |
| 1.06 | 0.87 | 790.00 |
| 1.81 | 1.35 | 1140.00 |
| 2.51 | 1.65 | 1470.00 |
| 3.02 | 1.83 | 1695.00 |
| 4.86 | 1.92 | 2056.00 |
| 15.76 | 1.98 | 2380.00 |
| 79.20 | 2.03 | 2550.00 |
| 151.55 | 2.07 | 2600.00 |

TABLE 25
UPRC - STRATOS
SPECIAL CORE STUDY
CORE #48B - WATER-GAS RELATIVE PERMEABILITY TEST
WATER-GAS RELATIVE PERMEABILITY DATA

| Water Saturation | Relative Permeability | |
|------------------|-----------------------|----------|
| | k_{rw} | k_{ro} |
| 0.500 | 0.00000 | 0.33120 |
| 0.518 | 0.00046 | 0.31220 |
| 0.536 | 0.00150 | 0.29340 |
| 0.554 | 0.00303 | 0.27480 |
| 0.572 | 0.00501 | 0.25640 |
| 0.590 | 0.00739 | 0.23800 |
| 0.609 | 0.01017 | 0.21980 |
| 0.627 | 0.01332 | 0.20200 |
| 0.645 | 0.01684 | 0.18420 |
| 0.663 | 0.02070 | 0.16670 |
| 0.681 | 0.02492 | 0.14940 |
| 0.699 | 0.02946 | 0.13238 |
| 0.717 | 0.03434 | 0.11564 |
| 0.735 | 0.03952 | 0.09920 |
| 0.753 | 0.04504 | 0.08310 |
| 0.771 | 0.05084 | 0.06740 |
| 0.790 | 0.05696 | 0.05218 |
| 0.808 | 0.06338 | 0.03750 |
| 0.826 | 0.07010 | 0.02354 |
| 0.844 | 0.07710 | 0.01063 |
| 0.862 | 0.08440 | 0.00000 |

TABLE 26
UPRC - STRATOS
SPECIAL CORE STUDY
CORE #12 - FRACTURE PERMEABILITY Versus OVERBURDEN
AND FLUID SATURATION TEST
CORE AND TEST PARAMETERS

| | |
|---|-----------------------|
| Core Number | 12 |
| Depth (ft) | 16042 |
| Field Name | Stratos |
| Well Location | UPRC - Stratos Fed #1 |
| Length (in) | 4.06 |
| Diameter (in) | 4.00 |
| Effective Flow Area (in ²) | 12.56 |
| Bulk Volume (in ³) | 50.99 |
| Porosity (fraction) | 0.079 |
| Pore Volume (in ³) | 4.03 |
| Routine Air Permeability (mD) | 0.06 |
| Test Temperature (°F)* | 176 |
| Gas Viscosity @ 176°F (cP) | 0.0200 |
| Brine Viscosity @ 176°F (cP) | 0.392 |
| Net Overburden Pressure (psig) | 375 - 11200 |
| * Maximum temperature attainable without use of backpressure. | |

TABLE 27
UPRC - STRATOS
SPECIAL CORE STUDY
CORE #12 - FRACTURE PERMEABILITY Versus OVERBURDEN
AND FLUID SATURATION TEST
PERMEABILITY SUMMARY - THRESHOLD PRESSURE REGAINS

| Test Phase | Permeability (mD) | % Change In Permeability |
|--|----------------------|-----------------------------|
| Initial Gas Permeability (0% Sw _i , 375 psi OBP) | 0.06000 | *0.00 |
| Gas Permeability (0% Sw _i , 1880 psi OBP) | 0.00823 | -86.3 |
| Gas Permeability (0% Sw _i , 3750 psi OBP) | 0.00455 | -92.4 |
| Gas Permeability (0% Sw _i , 5640 psi OBP) | 0.00346 | -94.2 |
| Gas Permeability (0% Sw _i , 7500 psi OBP) | 0.00290 | -95.2 |
| Gas Permeability (0% Sw _i , 11200 psi OBP) | 0.00265 | -95.6 |
| Brine Permeability (100% Sw _i , 3750 psi OBP) | 0.00032 | -99.5 |
| Gas Regain Permeability (Sw _{irr} , 3750 psi OBP) | 0.00031 | -99.5 |

TABLE 28
UPRC - STRATOS
SPECIAL CORE STUDY
CORE #32 - FRACTURE PERMEABILITY Versus OVERBURDEN
AND FLUID SATURATION TEST
CORE AND TEST PARAMETERS

| | |
|---|-----------------------|
| Core Number | 32 |
| Depth (m) | 16064.0 |
| Field Name | Stratos |
| Well Location | UPRC - Stratos Fed #1 |
| Length (in) | 4 72 |
| Diameter (in) | 4 00 |
| Effective Flow Area (in ²) | 12.56 |
| Bulk Volume (in ³) | 59.31 |
| Porosity (fraction) | 0 059 |
| Pore Volume (in ³) | 3 49 |
| Routine Air Permeability (mD) | <0.01 |
| Test Temperature (°F)* | 176 |
| Gas Viscosity @ 176°F (cP) | 0.0200 |
| Brine Viscosity @ 176°F (cP) | 0.392 |
| Net Overburden Pressure (psig) | 375 - 11200 |
| * Maximum temperature attainable without use of backpressure. | |

TABLE 29
UPRC - STRATOS
SPECIAL CORE STUDY
CORE #32 - FRACTURE PERMEABILITY Versus OVERBURDEN
AND FLUID SATURATION TEST
PERMEABILITY SUMMARY - THRESHOLD PRESSURE REGAINS

| Test Phase | Permeability (mD) | % Change In Permeability |
|--|-------------------|--------------------------|
| Initial Gas Permeability (0% Sw _i , 375 psi OBP) | 0.01000 | *0.00 |
| Gas Permeability (0% Sw _i , 1880 psi OBP) | 0.00135 | -86.5 |
| Gas Permeability (0% Sw _i , 3750 psi OBP) | 0.00085 | -91.5 |
| Gas Permeability (0% Sw _i , 5640 psi OBP) | 0.00067 | -93.3 |
| Gas Permeability (0% Sw _i , 7500 psi OBP) | 0.00042 | -95.8 |
| Gas Permeability (0% Sw _i , 11200 psi OBP) | 0.00035 | -96.5 |
| Brine Permeability (100% Sw _i , 3750 psi OBP) | 0.000044 | -99.6 |
| Gas Regain Permeability (Sw _{irr} , 3750 psi OBP) | <0.00001 | -99.9 |

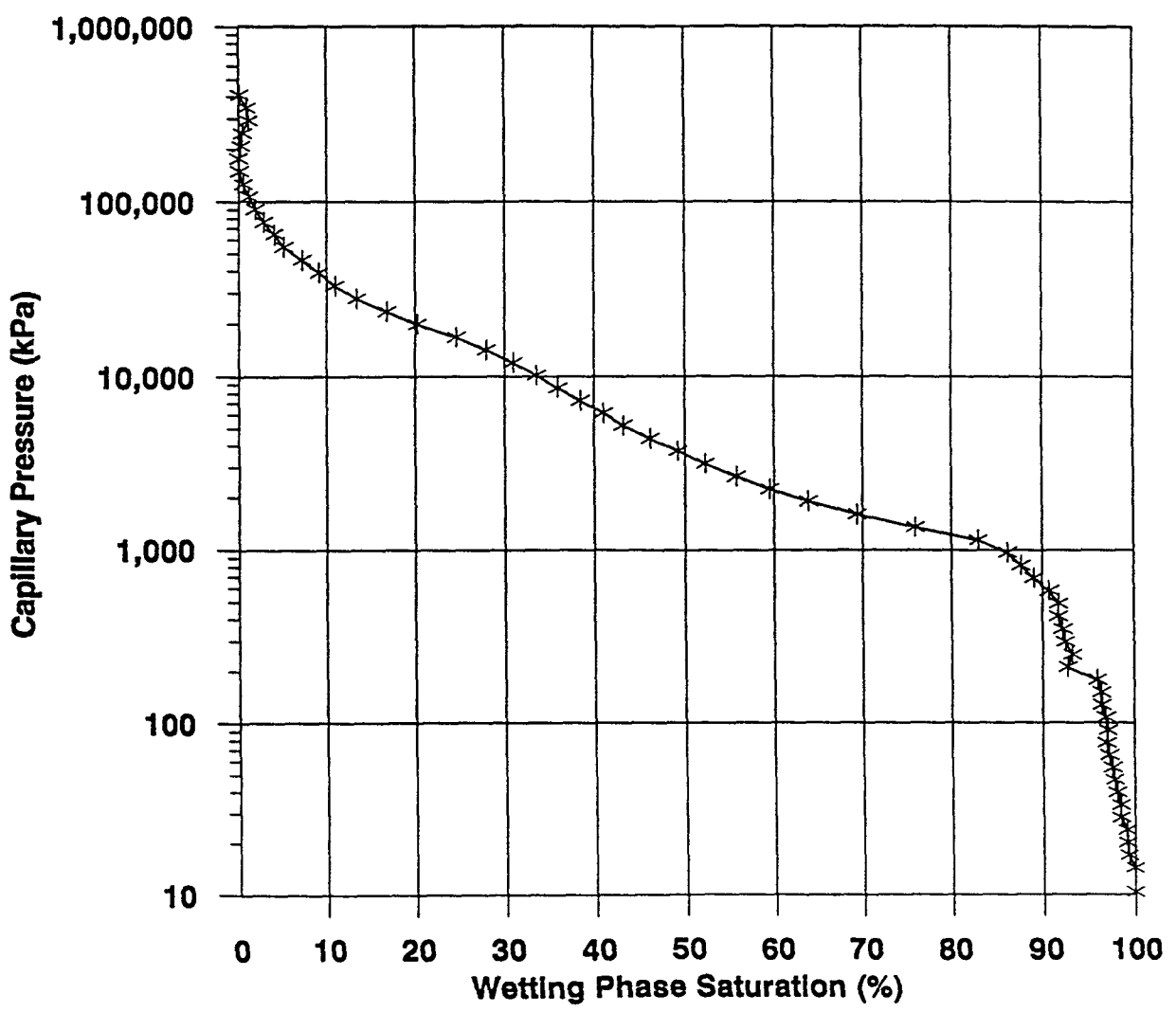
TABLE 30
UPRC - STRATOS
SPECIAL CORE STUDY
RESULTS OF GEOMECHANICAL TESTING

| Sample # | Depth (ft) | Young's Modulus (psi x 10⁶) | Compressive Strength (psi x 10³) |
|-----------------|-----------------------|---|--|
| 7C | 16026.90 | 3.79 | 177.0 |
| 31B | 16063.30 | 2.92 | 44.1 |
| 48B | 16080.30 | 4.23 | 61.8 |

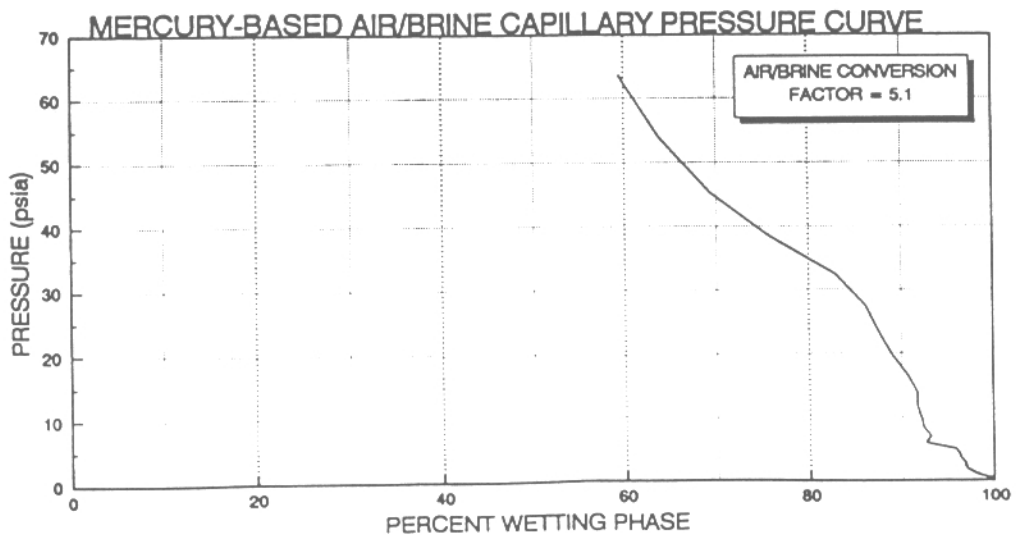
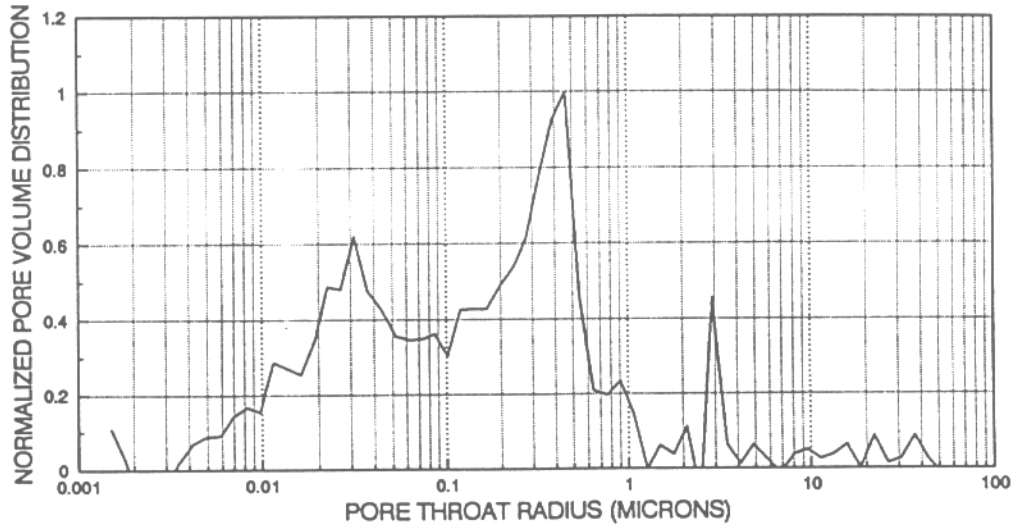
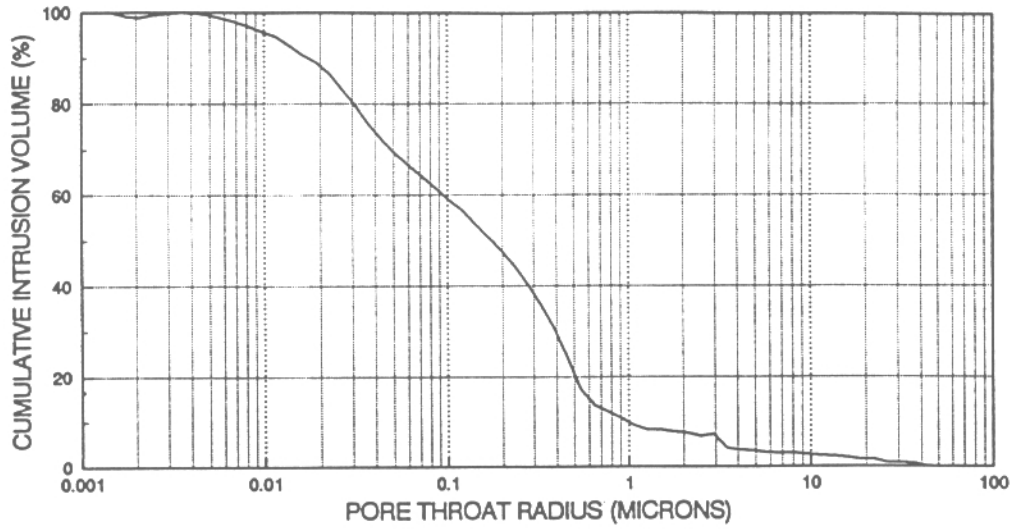
Appendix A
Within Appendix C

UPRC - STRATOS
SPECIAL CORE STUDY
CORE #7B

Mercury Injection Capillary Pressure
Standard Plot

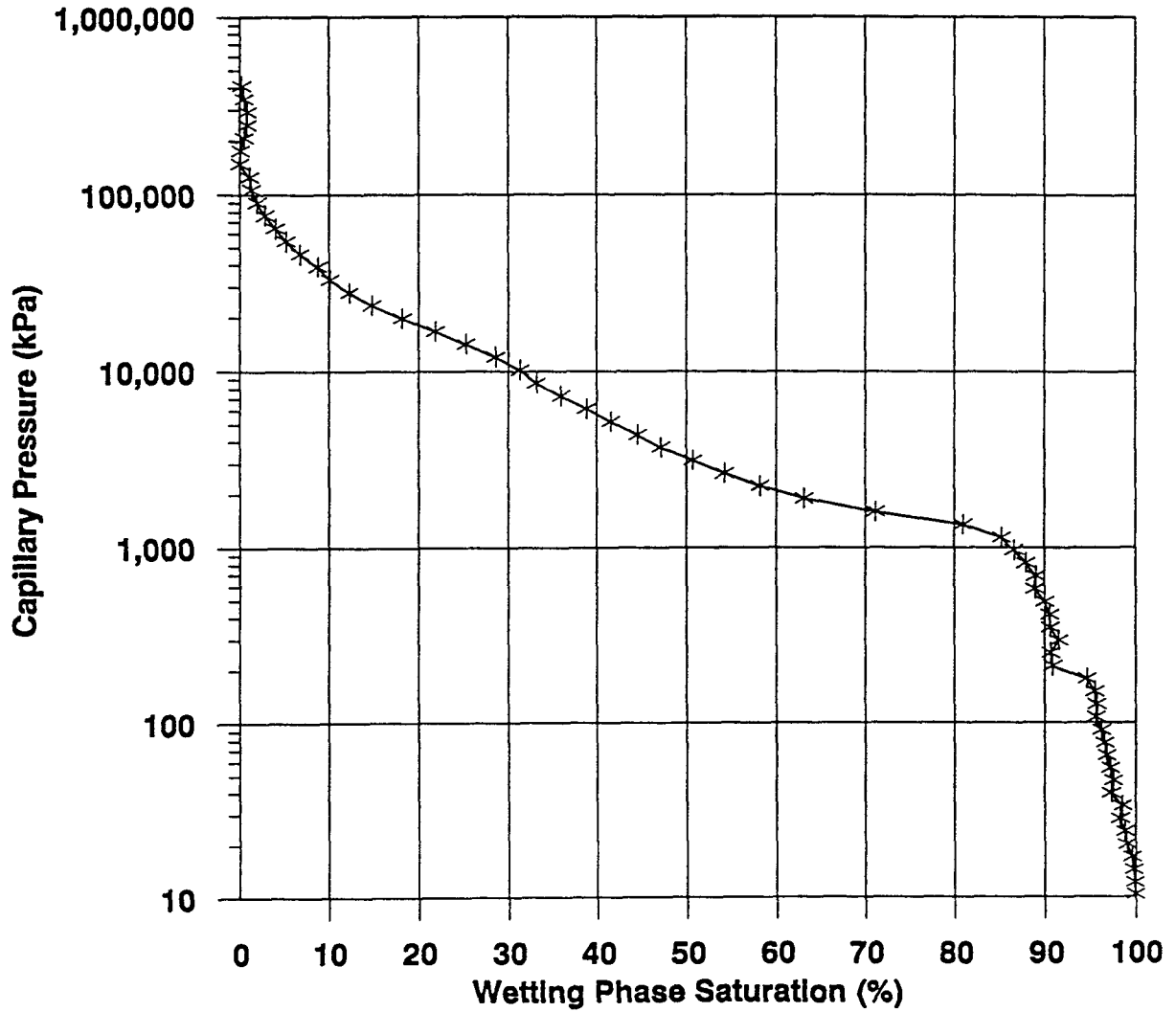


UPRC - STRATOS
SPECIAL CORE STUDY
CORE #7B

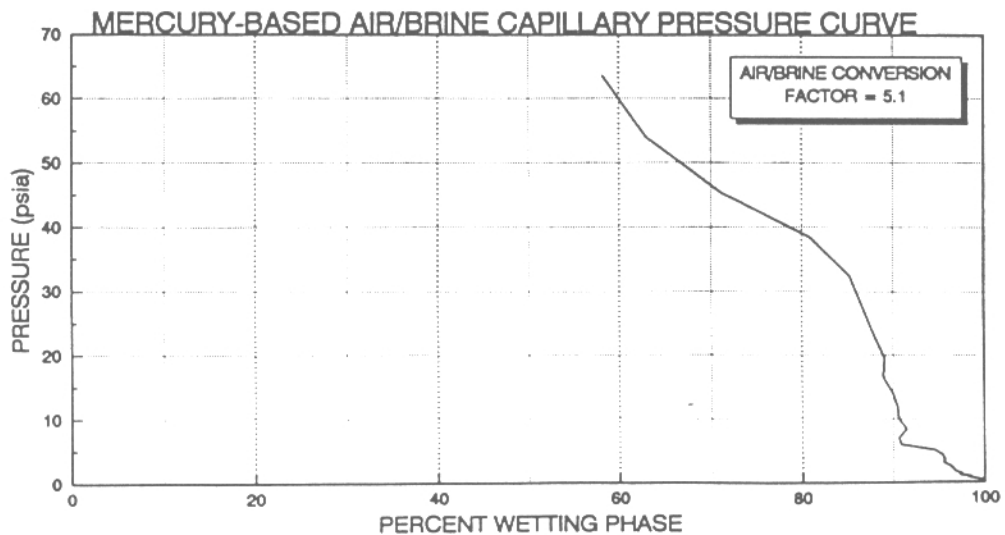
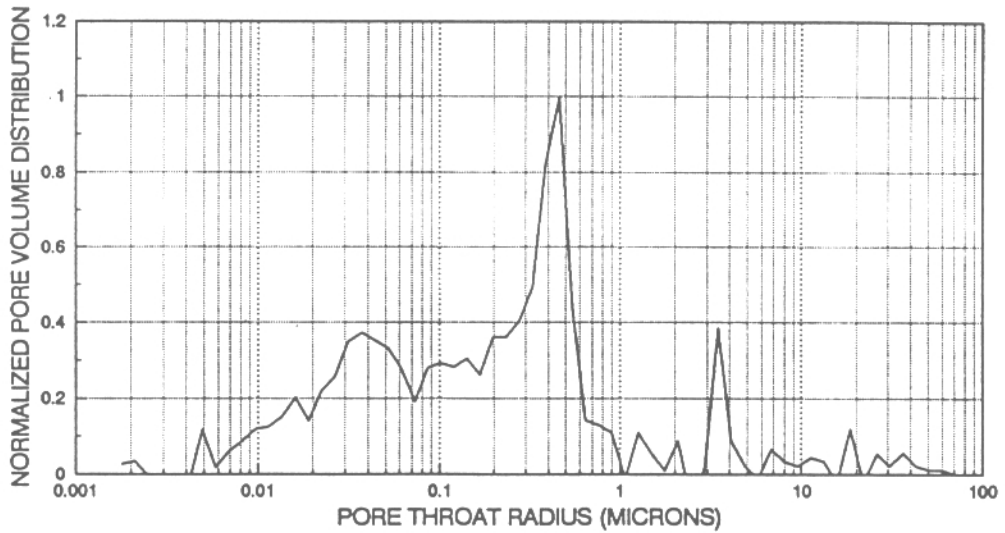
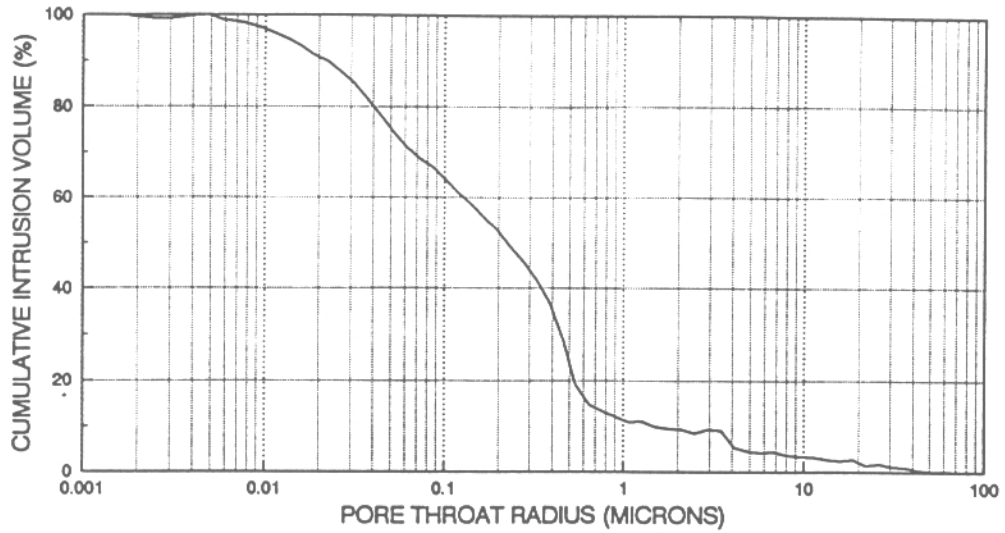


UPRC - STRATOS
SPECIAL CORE STUDY
CORE #7C

Mercury Injection Capillary Pressure
Standard Plot

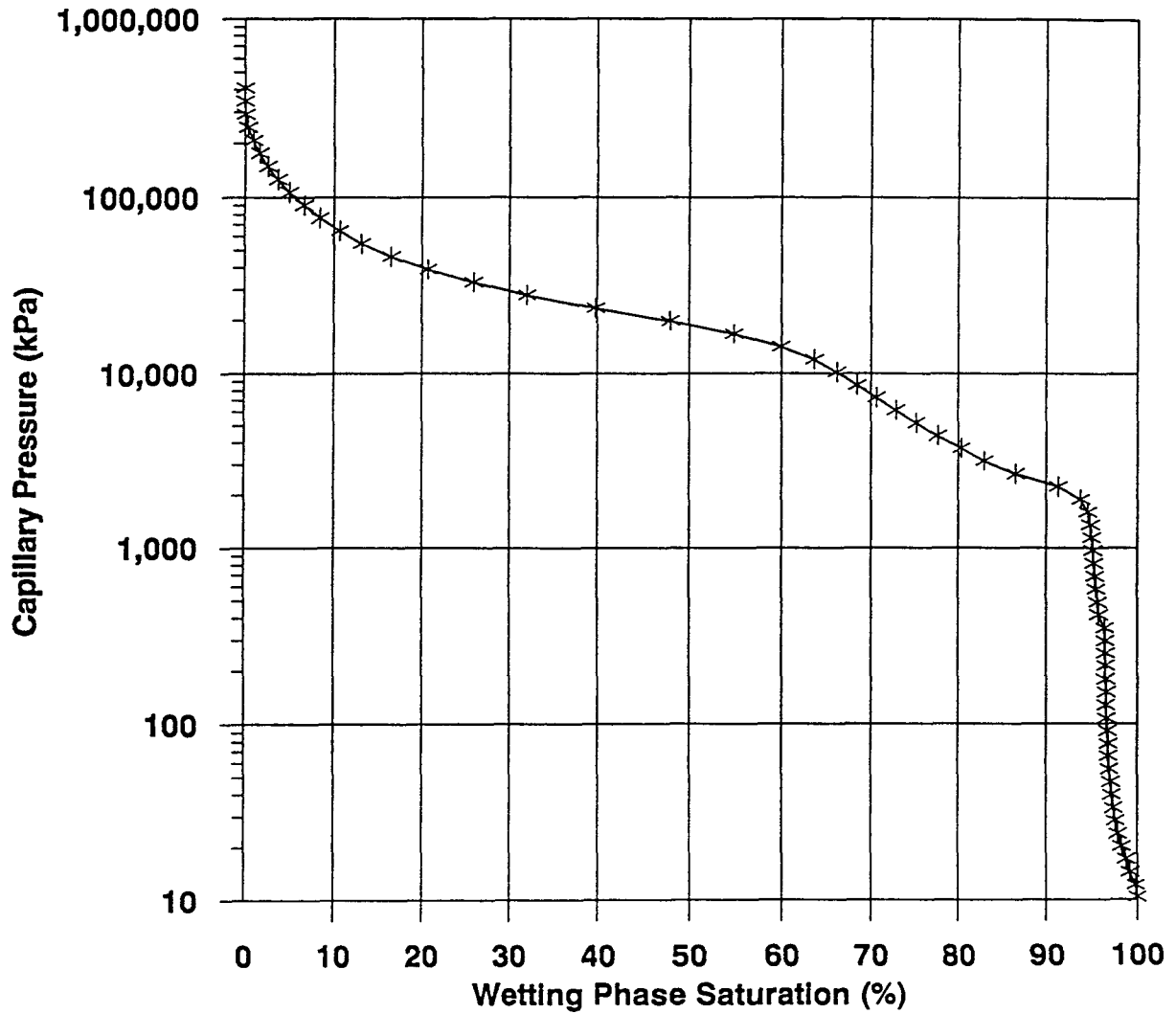


UPRC - STRATOS SPECIAL CORE STUDY CORE #7C

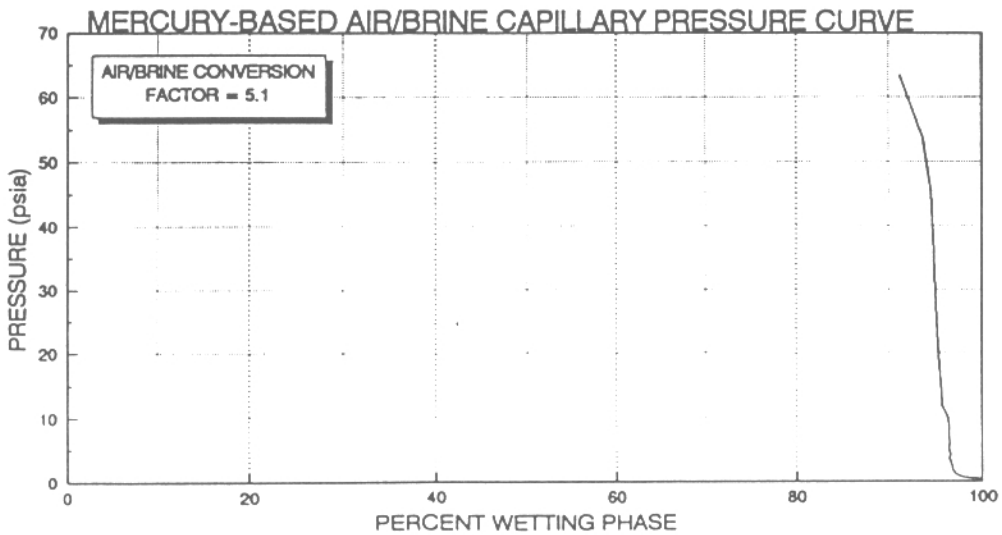
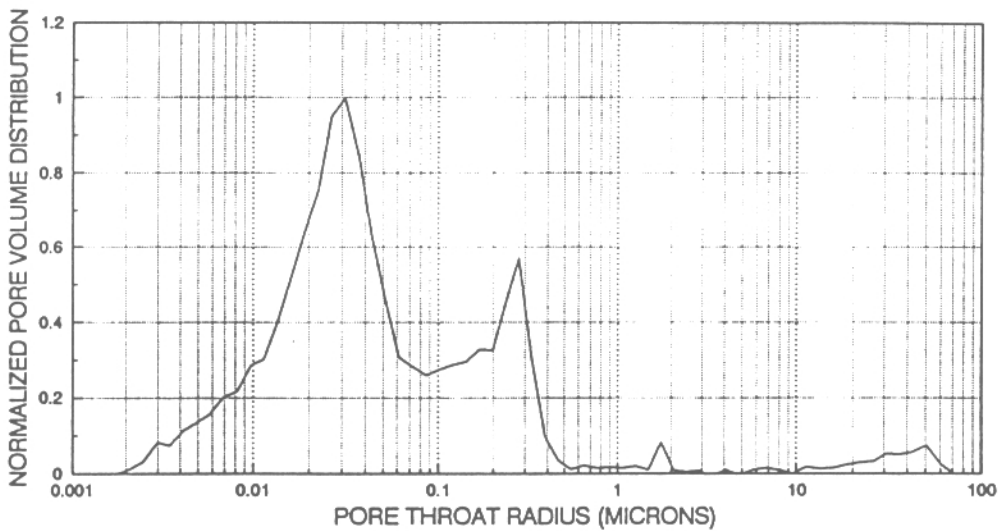
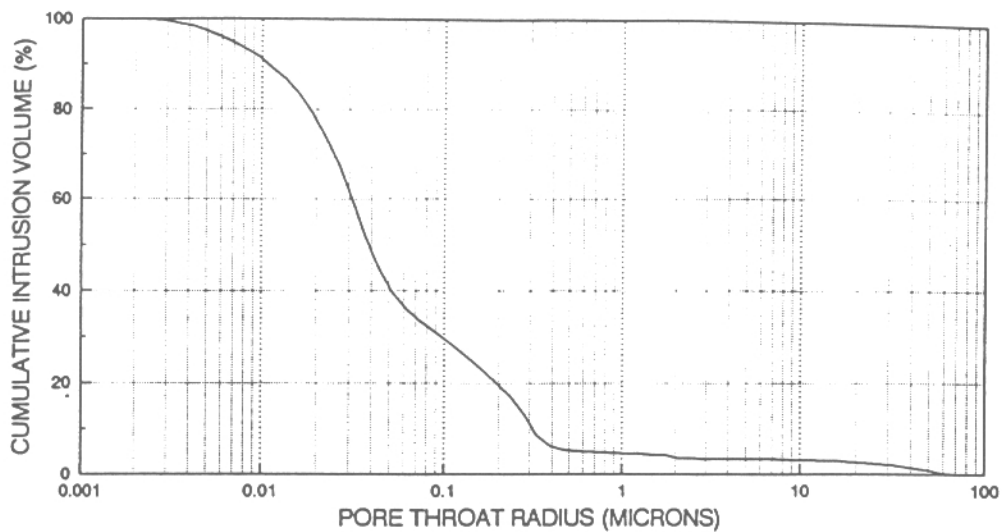


UPRC - STRATOS
SPECIAL CORE STUDY
CORE #30

Mercury Injection Capillary Pressure
Standard Plot

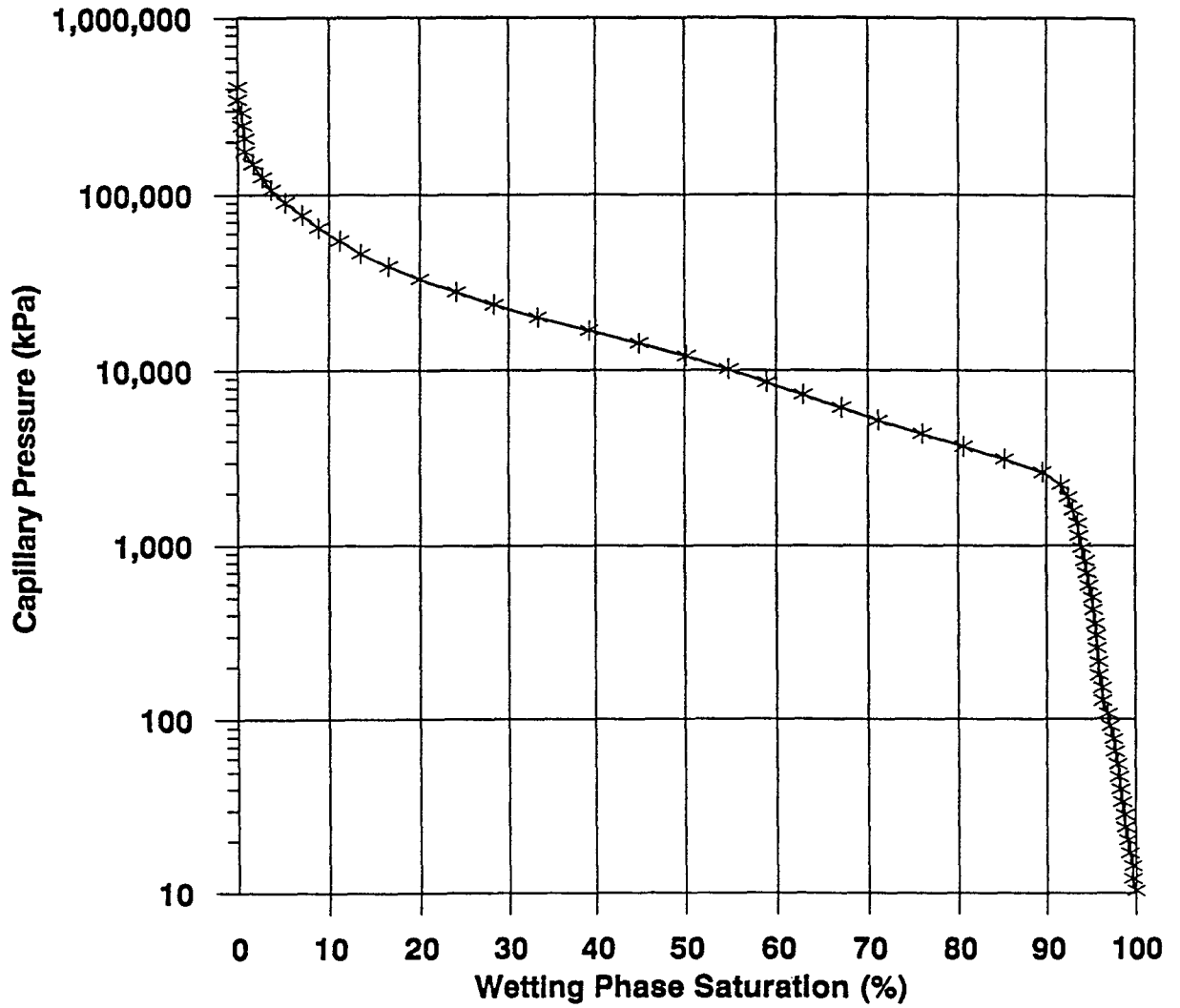


UPRC - STRATOS
SPECIAL CORE STUDY
CORE #30

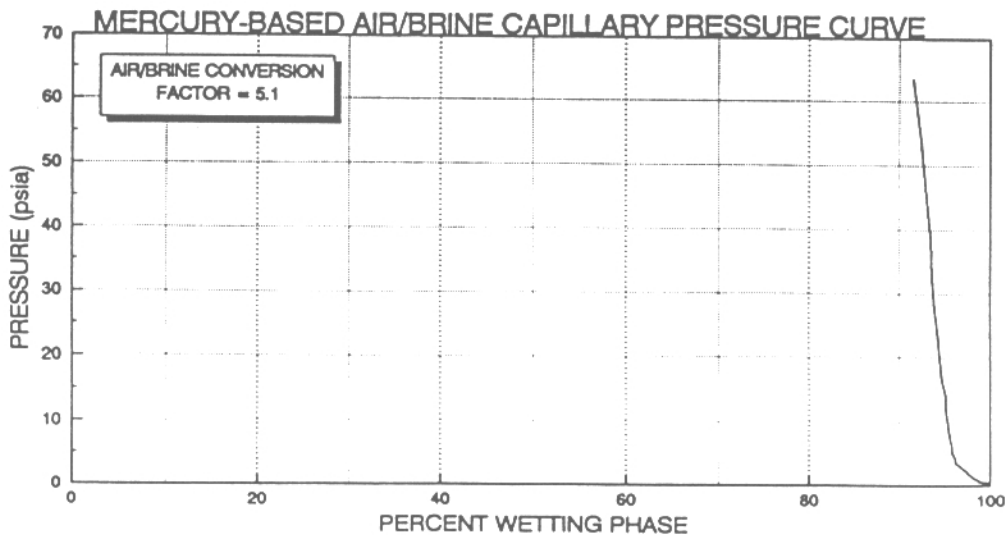
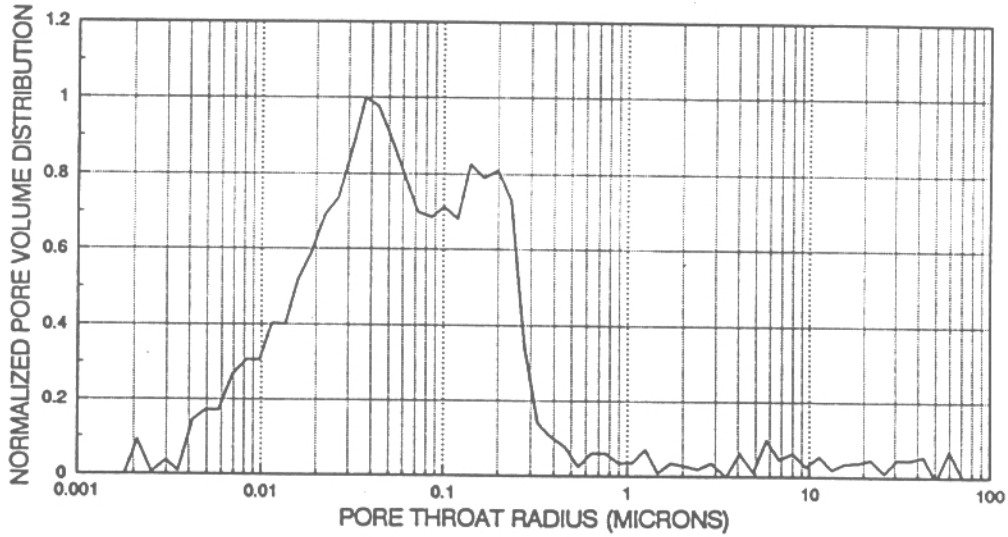
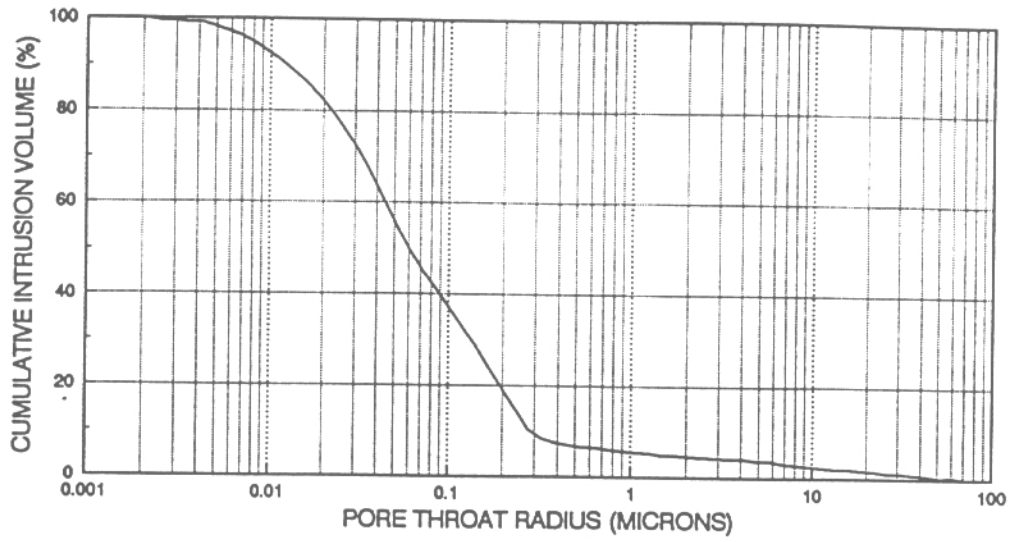


UPRC - STRATOS
SPECIAL CORE STUDY
CORE #48B

Mercury Injection Capillary Pressure
Standard Plot



UPRC - STRATOS
SPECIAL CORE STUDY
CORE #48B



Appendix B
Within Appendix C

**Petrology and Reservoir Quality Analysis
Sandstone
UPRC Fed #1
Union Pacific Resources Corporation.
GR-1519-96**

**Hycal Energy Research Laboratories Ltd
&
GR Petrology Consultants inc.
4605 - 12th Street N.E.
Calgary, Alberta T2E 4R3
Ph: (403)291-3420 Fax:(403)250-7212
April, 1996**

**Reservoir Quality Assessment of Sandstone
UPRC Stratos Fed #1**

Table of Contents

| | |
|---|---|
| Introduction and Summary | 1 |
| General Summary | 1 |
| Objectives | 1 |
| Method of Analysis | 1 |
| Documentation | 2 |
| Summary of Petrology | 3 |
| Mineralogy | 5 |
| Reservoir Quality Characteristics | 5 |
| Reservoir Quality Assessment | 7 |
| Paragenesis and Reservoir Evolution | 7 |
| Controls on Reservoir Quality | 7 |
| Reservoir Sensitivity | 8 |

**Reservoir Quality Assessment of Sandstone
UPRC Stratos Fed #1**

Introduction and Summary

General Summary

This report summarizes the results of the thin section petrology scanning electron microscopy and X-ray diffraction analysis of three (3) sandstone samples selected from the Stratos Fed #1 well

The main emphasis of the analysis centres on an assessment of the basic reservoir characteristics of the sandstone

The petrology shows that the sandstone reservoir, as represented by the three samples is of poor quality, consisting of moderately sorted, upper fine to lowermost medium grained, argillaceous to highly quartz cemented, variably feldspathic, quartzose sublitharenite to litharenite with fair porosity (6 to 11%) as determined by conventional core analysis and low (0.11 to 0.21md) permeability.

Primary intergranular porosity in all sandstones has been lowered either by the effects of compaction and by compacted illite clay matrix or by extensive quartz cement. In the interval represented by sample Hy-37 ferroan calcite also cements porosity. Some secondary porosity formed after the dissolution of scattered unstable rock fragments and feldspar grains. Microporous illite occludes porosity in all three sandstone samples.

The samples selected from the Fed #1 wells represent poor reservoir quality sandstones with a high relative micro-porosity component. The sandstones may not be capable of commercial hydrocarbon production.

Completion programs could call for fracture stimulation with an energized proppant carrying fluid and high strength proppant.

Objectives

The petrological evaluation centred on the basic rock characteristics and reservoir quality assessment of the sandstone represented by the three samples.

Method of Analysis

Three samples were selected that represent the general reservoir sandstones encountered by the Stratos Fed #1 well. Standard sized thin sections were prepared for each sample. The sections were then submitted for conventional, comprehensive thin section petrology that provided the compositional and textural data required for basic reservoir quality assessment.

Reservoir Quality Assessment of Sandstone UPRC Stratos Fed #1

and the interpretation of paragenesis and reservoir evolution. Textural and compositional data are based on a 300 point modal analysis of each slide. Grain size analysis is based on 300 long-axis measurements of competent grains. Scanning electron microscopy of each sample showed the distribution and morphology of the clay matrix and the degree of pore occlusion by cements and clays. X-ray diffraction analysis provided semi-quantitative bulk mineralogy and confirmed the presence of a swelling clay component.

Documentation

The following tables, figures and photomicrographs document the petrological summary

1. Table 1 - Petrographic Sample Summary.
2. Table 2 - Point Count Data and Lithological Summary.
3. Figure 1 - Ternary Sandstone Classification Diagram (QFR) with plutonic rock fragments at feldspar pole.
4. Figure 2 - Ternary Sandstone Classification Diagram (QFR) with plutonic rock fragments at rock fragment pole.
5. Figure 3 - Ternary Porosity Distribution Diagram.
6. Table 3 - Grain Size Analysis.
7. Figure H1 - Grain Size Distribution Histograms.
8. Table 4 - Petrophysical Summary.
9. Table 5a - Summary of X-ray Diffraction Bulk Analysis.
10. Table 5b - Summary of X-ray Diffraction Glycolated Clay Analysis.
11. Plates 01 to 12 - Thin Section and SEM Photomicrographs and Descriptions of Salient Sandstone Features.

Table 1: Petrographic Sample Summary

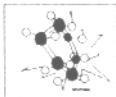
Company : Union Pacific Resources Corporation.

FILE: GR151996

Location : Stratos Area

| 1 Sample No. | 2 Well | 3 Depth (ft) | 4 Sample Type | 5 Ca Por (%) | 6 Ca Kmax (Md) | 7 TS Por (% Effec) | TYPE OF ANALYSIS | | | |
|-----------------|-----------|--------------------|---------------------|--------------------|----------------------|--------------------------|------------------|----------|-----------|-------------|
| | | | | | | | 8 TS | 9 XRD | 10 SEM | 11 OTHER |
| Hy-6a | Fed#1 | 16025.00 | CC | 6.2 | 0.20 | tr | X | X | X | GS |
| Hy-31a | Fed#1 | 16063.20 | CC | 7.7 | 0.11 | 1.0 | X | X | X | GS |
| Hy-37 | Fed#1 | 16069.20 | CC | 10.9 | 0.13 | 2.0 | X | X | X | GS |

| | |
|---|---|
| <p>1. Hycal. SAMPLE NUMBER</p> <p>2. WELL LOCATION</p> <p>3. DEPTH INTERVAL</p> <p>4. SAMPLE TYPE</p> <p>CC CONVENTIONAL CORE and PLUG ID</p> <p>DC DRILL CUTTINGS</p> <p>SWC SIDE WALL CORE</p> <p>5. CORE ANALYSIS POROSITY</p> <p>6. PERMEABILITY - millidarcies</p> | <p>7. THIN SECTION POROSITY - % Effective</p> <p>8. THIN SECTION GENERAL PETROLOGY</p> <p>9. XRD - X-RAY DIFFRACTION</p> <p>10. SEM - SCANNING ELECTRON MICROSCOPY</p> <p>11. OTHER</p> <p>GS - GRAIN SIZE ANALYSIS</p> <p>PC - POROSITY COUNT</p> <p>ov - cursory overview</p> |
|---|---|



COMPANY: Union Pacific Resource Corporation
 WELL NAME: Stratos Federal #1
 LOCATION: Stratos

FILE NAME: GR151996
 FORMATION: n/a
 DEPTH: 16025-70ft
 SAMPLES: 37
 POROSITY: Included
 COUNTS: 300

Table 2

POINT COUNT DATA AND LITHOLOGICAL SUMMARY

| MODAL ANALYSIS (%) - INCLUDES POROSITY | | | | | | | | | | | | | | | | | | | | | | | | | | | | | | | | | | | |
|--|-------------|--------------------------------|----|----|----|-----|-----|-----|-----|----|-------|----------------------------|-------|----|-------|----|-----------------|----|----|-------|----|---------|----|----|-----|----------|-------|----|----|-----------|--|-------|--|-----|-----|
| TS# | Total Por % | SILICICLASTIN FRAMEWORK GRAINS | | | | | | | | | | CARBONATE FRAMEWORK GRAINS | | | | | CLAY and Matrix | | | | | CEMENTS | | | | POROSITY | | | | | | | | | |
| | | MQ | PQ | FD | CT | SRF | IRF | MRF | RFU | OT | OTHER | | OTHER | | OTHER | | HC | DO | CA | OTHER | | MA | DM | KA | ILL | CHL | OTHER | | AQ | CARBONATE | | OTHER | | INT | MOL |
| | | 1 | 2 | 3 | 4 | 5 | 6 | 7 | 8 | 9 | 10 | 11 | 12 | 13 | 14 | 15 | 16 | 17 | 18 | 19 | 20 | 21 | 22 | 23 | 24 | 25 | 26 | 27 | 28 | 29 | | | | | |

| | | | | | | | | | | | | | | | | | | | | | | | | | | | | | | | | | | | |
|-----|-----|------|-----|-----|------|-----|-----|-----|-----|-----|----|---|-----|----|-----|---|---|---|---|---|------|----|---|-----|-----|---|---|-----|------|----|---|-----|---|-----|-----|
| 6a | tr | 44.7 | 1.7 | tr | 14.0 | 2.3 | 2.7 | 3.0 | 0.7 | - | tr | - | - | - | 0.3 | - | - | - | - | - | - | tr | - | - | 5.3 | - | - | - | 25.3 | - | - | tr | - | - | tr |
| 31a | 1.0 | 65.0 | tr | 1.3 | 5.3 | 0.7 | 4.0 | 1.0 | 1.0 | 1.3 | tr | - | - | tr | tr | - | - | - | - | - | 17.0 | - | - | 0.3 | - | - | - | 1.7 | 1.3 | tr | - | 0.3 | - | 0.3 | 0.7 |
| 37 | 2.0 | 47.3 | tr | 6.0 | 6.0 | 1.7 | 8.0 | 1.0 | 1.0 | 0.7 | tr | - | 0.3 | tr | 0.3 | - | - | - | - | - | 5.7 | - | - | 9.3 | - | - | - | 9.3 | 2.0 | tr | - | 0.3 | - | 1.3 | 0.7 |

| | | | | |
|---|---|--|--|--|
| MO - MONOCRYSTALLINE QUARTZ PQ - POLYCRYSTALLINE QUARTZ CT - CHERT FD - FELDSPAR SRF - SEDIMENTARY ROCK FRAGMENT F - METAMORPHIC ROCK FRAGMENT | IRF - IGNEOUS ROCK FRAGMENT RFU - UNDIFFERENTIATED FRAGMENT PY - PYRITE MI - MICA HC - HYDROCARBON BIO - BIOCLASTS | PR - PLANT REMAINS PHO - PHOSPHATES CAR - CARBONACEOUS KA - KAOLINITE IL - ILLITE CHL - CHLORITE DO - DOLOMITE | AQ - AUTHIGENIC SILICA SM - SILICA MATRIX HM - HEAVY MINERALS SID - SIDERITE LEU - LEUCOXENE CA - CALCITE | ANH - ANHYDRITE GL - GLAUCONITE MA - MATRIX INT - INTERGRANULAR POROSITY MOL - GRAIN MOLDIC POROSITY |
|---|---|--|--|--|



Figure 1
Ternary Classification Diagram
(Q,F,RF)
Stratos Fed #1 Sandstone
Plutonics Classified as Feldspar

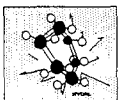
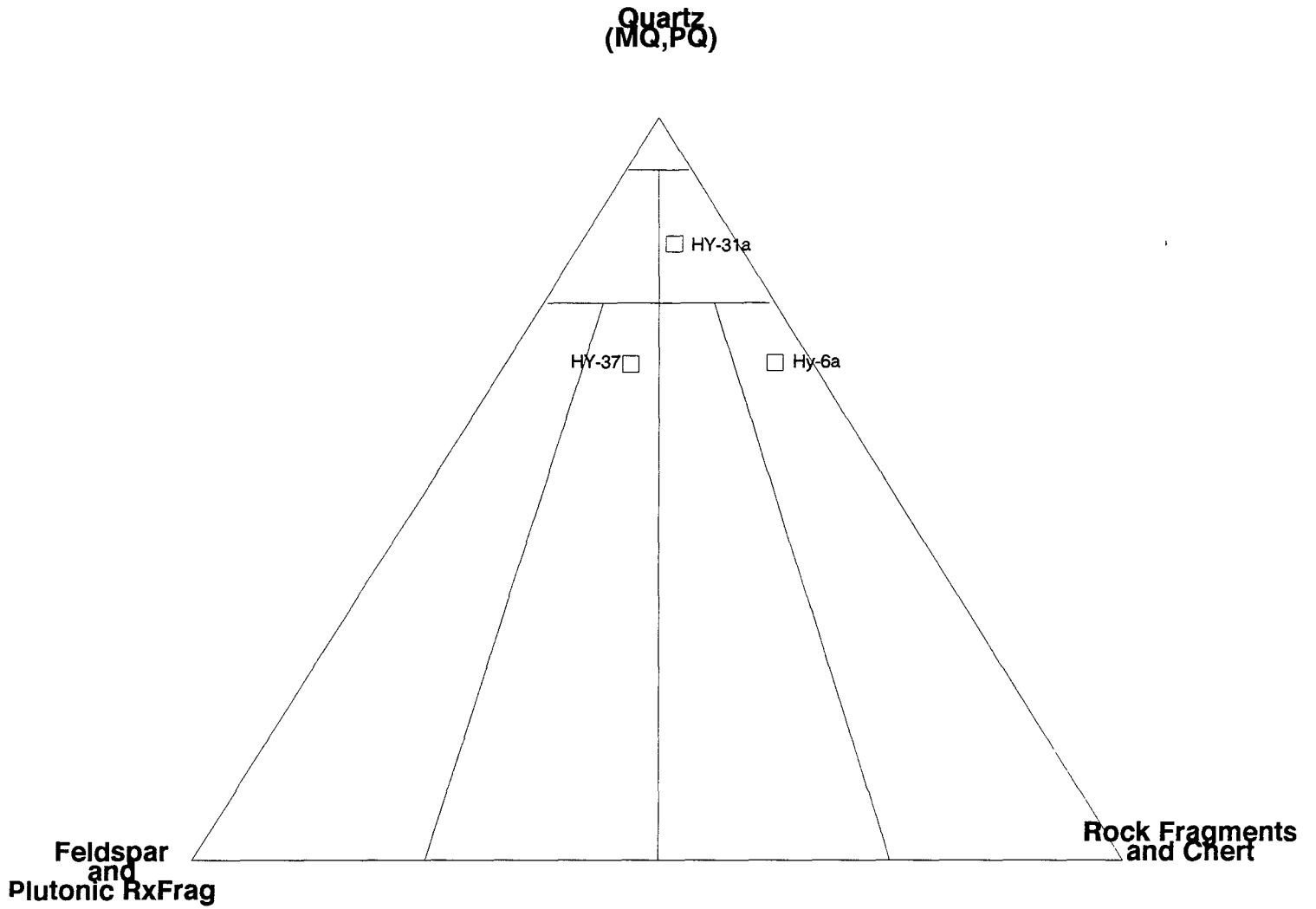
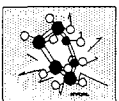
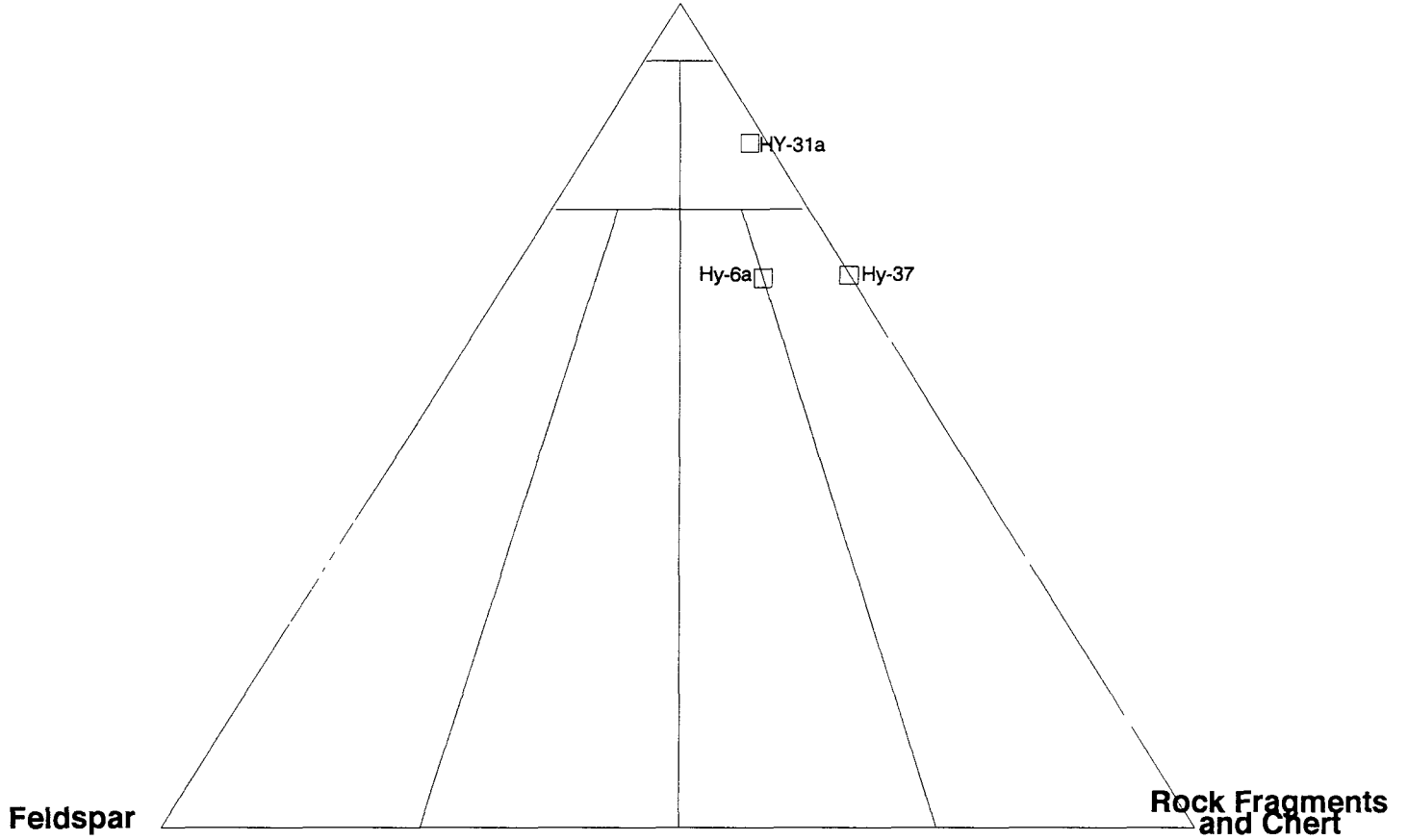
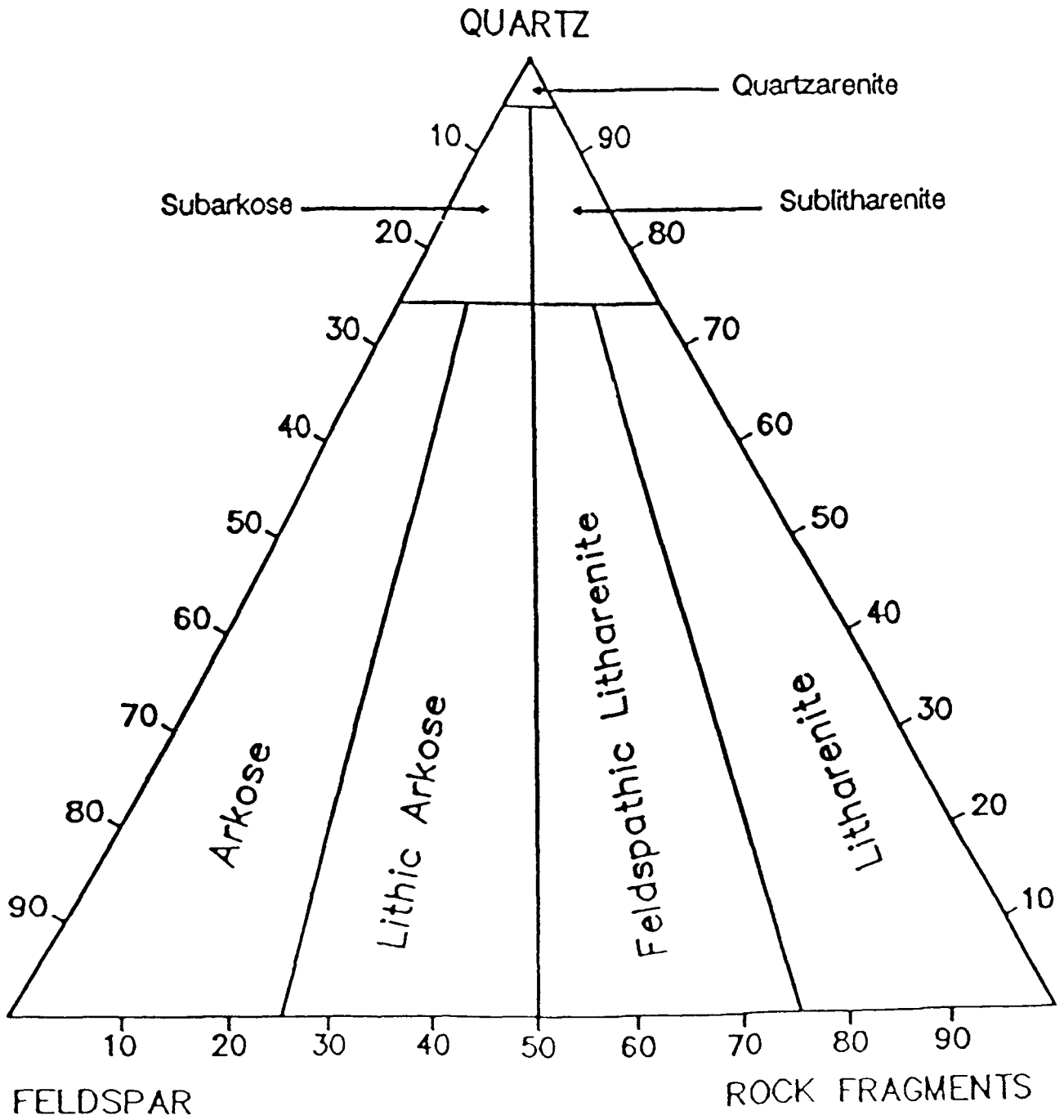


Figure 2
Ternary Classification Diagram
(Q,F,RF)
Stratos Fed #1 Sandstone
Plutonics Classified as Rock Fragments

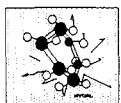
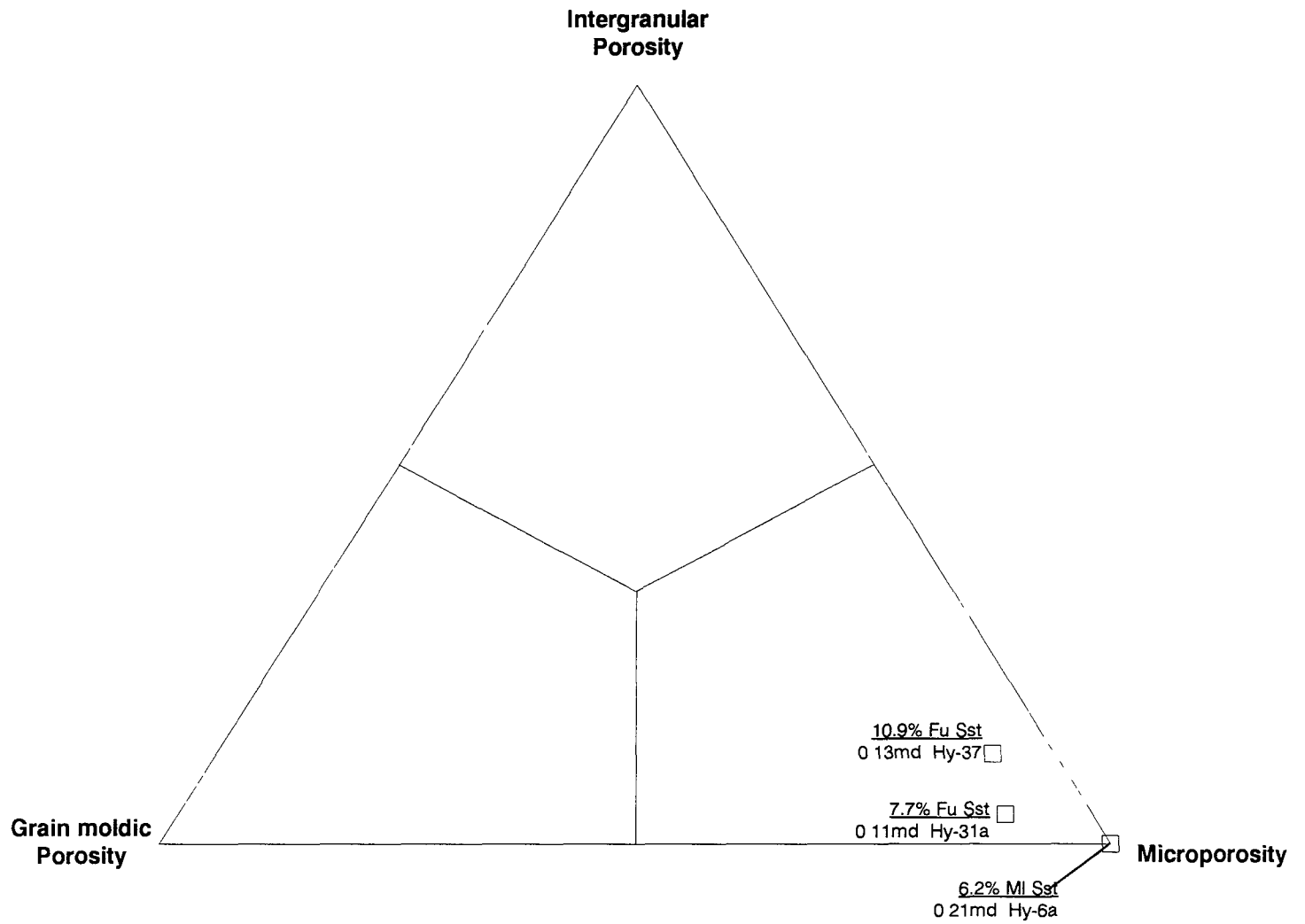
**Monocrystalline
Quartz
(MQ, PQ)**



Ternary Classification Diagram



**Figure 3: Porosity Distribution Ternary Diagram
Stratos Fed #1 Sandstone**



Porosity Relationships

Intergranular Porosity

Log and core porosity decrease
H₂O sat decrease
K increase
H₂O prod may increase
Fluid production increase
Reservoir quality increase



Log and core porosity may decrease
H₂O sat decrease
K decrease
H₂O prod may increase
Fluid production decrease
Reservoir quality decrease

Log and core porosity increase
H₂O sat increase
K decrease
H₂O prod decrease
Fluid production decrease
Reservoir quality decrease

Moldic Porosity

Microporosity

**Table 3: Grain Size Analysis
Fed #1**

| Sample No. | Depth (ft) | Unit | Mean (mm) | Max (mm) | Min (mm) | St dev (mm) |
|------------|------------|------|-----------|----------|----------|-------------|
| Hy-6a | 16,025.00 | n/a | 0.260 | 0.558 | 0.094 | 0.074 |
| Hy-31a | 16,063.20 | n/a | 0.219 | 0.515 | 0.033 | 0.082 |
| Hy-37 | 16,069.20 | n/a | 0.211 | 0.460 | 0.051 | 0.074 |
| | 1 | | | | | |

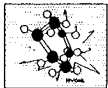
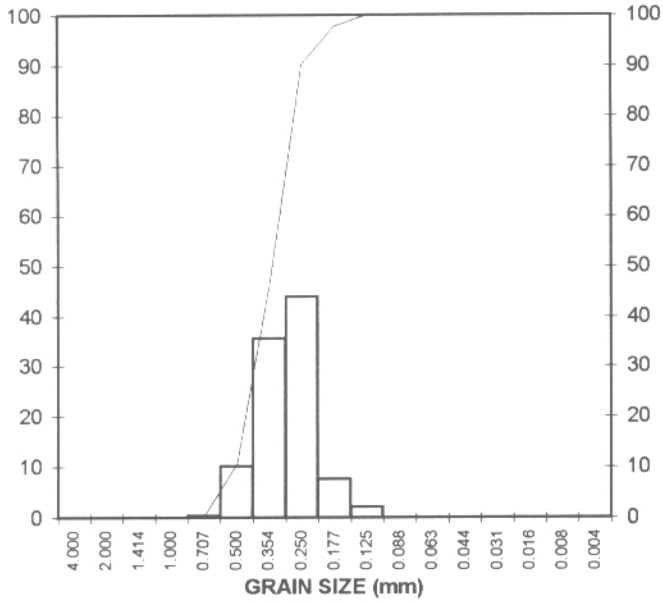
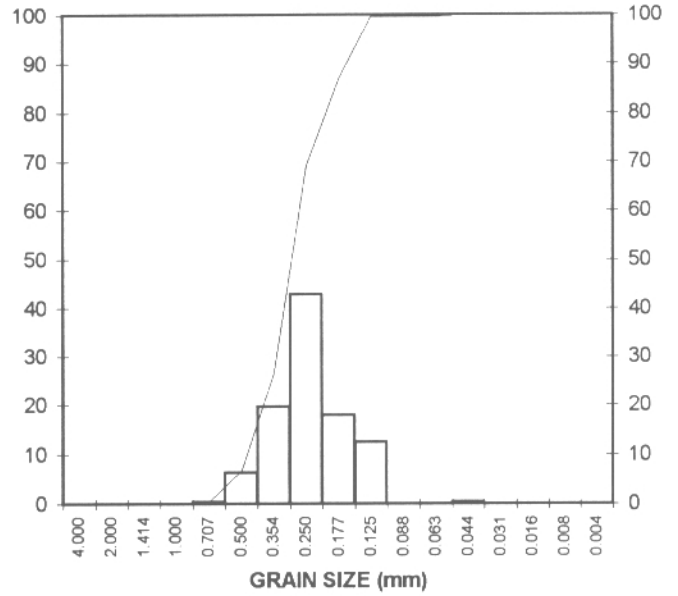


FIGURE H1: GRAIN SIZE HISTOGRAMS

A
Hy-6a (Stratos Fed #1) 16,025.0ft



B
Hy-31a (Stratos Fed #1) 16,063.20



C
Hy-37 (Stratos Fed #1) 16,069.20ft

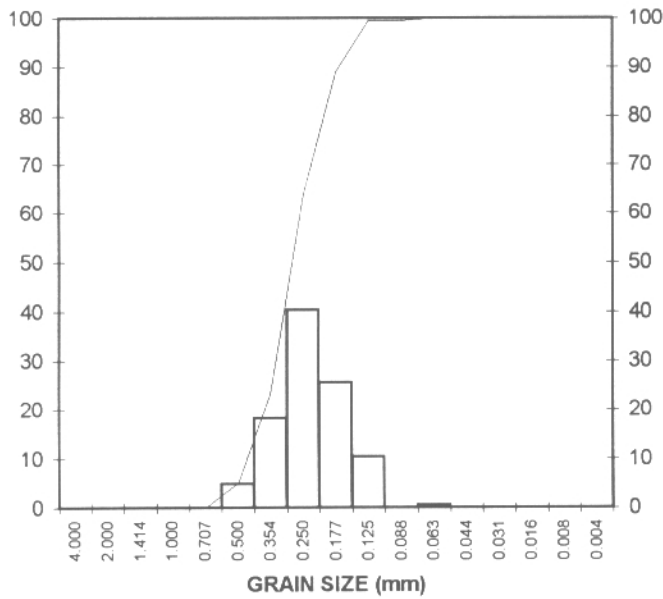


Table 4: Petrophysical Summary

| Form | Samples | Mean (mm) | MQ | Lith | Cem | Clay/Mtx | CAØ (%) | TSØ (%) | | | k _{max} (md) | Qual |
|------|---------|-----------|------|------|------|----------|---------|---------|-----|-----|-----------------------|------|
| | | | | | | | | INT | M | u | | |
| SST. | Hy-6a | 0.260 | 44.7 | 24.4 | 25.3 | 5.3 | 6.2 | tr | tr | 6.2 | 0.21 | Poor |
| SST | Hy-31a | 0.219 | 65.0 | 13.3 | 3.0 | 17.3 | 7.7 | 0.3 | 0.7 | 6.7 | 0.11 | Poor |
| SST | Hy-37 | 0.211 | 47.3 | 18.4 | 11.3 | 15.0 | 10.9 | 1.3 | 0.7 | 8.9 | 0.13 | Poor |

| | | |
|--|--|---|
| <p>MQ - Monocrystalline Quartz Lith - Lithic grains Mean - Mean grain size (mm) Cem - Authigenic Cements (Q, Cal, Py) Bit - Residual Hydrocarbon and Bitumen</p> | <p>TSØ - Point counted porosity INT - Intergranular M - Moldic u - Microporosity - Core porosity minus TS porosity</p> | <p>CAØ - Measured core porosity k_{max} - Core permeability Qual - Reservoir quality assessment</p> |
|--|--|---|



Table 5a
Summary of XRD Bulk Analysis
Stratos Fed #1 Sandstone

| Sample. | Depth (ft) | Qtz | K-Feld | Na-Feld | Cal | Dol | Sid | Hal | Pyr | Kaol | Ill | Chl | MI | Sm |
|---------|------------|------|--------|---------|-----|-----|-----|-----|-----|------|-----|-----|-----|----|
| Hy-6a | 16025.25 | 93.0 | tr | 3.0 | - | - | - | - | tr | 1.0 | 4.0 | tr | 1.0 | - |
| Hy-31a | 16063.20 | 75.0 | tr | 8.7 | 1.7 | tr | 1.3 | - | 1.3 | 3.3 | 7.0 | tr | 1.0 | - |
| Hy-37 | 16069.20 | 78.0 | tr | 6.0 | 5.0 | 1.0 | - | - | 1.0 | 1.0 | 6.0 | tr | 1.0 | - |

| | | |
|--|---|--|
| <p>Qtz - Quartz (SiO₂) K-Feld* - Potassic Feldspar Na-Feld* - Sodic Feldspar Cal - Calcite (CaCO₃) Dol - Dolomite ((Ca,Mg)CO₃) Sid - Siderite (FeCO₃)</p> | <p>Hal - Halite (NaCl) Pyr - Pyrite (FeS₂) Mack - Mackinawite (Fe₉S₈) Kaol* - Kaolinite Ill* - Illite (includes mica and clasts)</p> | <p>MI* - Mixed-Layer Clay Chl* - Chlorite Ot - Other Sm* - Smectite * - Complex Silicates P - Present</p> |
|--|---|--|

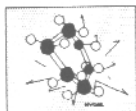
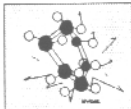


Table 5b
Summary of XRD Glycolated Clay Analysis
Stratos Fed #1 Sandstone

| Sample No. | Tot Clay | Kaol | Ill | MI | Chl | Sm |
|------------|----------|------|------|------|-----|----|
| Hy-6a | 6.0 | 40.0 | 46.0 | 22.0 | 4.0 | - |
| Hy-31a | 11.3 | 42.0 | 55.0 | 8.0 | 5.0 | - |
| Hy-37 | 8.0 | 17.0 | 69.0 | 8.0 | 6.0 | - |

| | |
|--|---|
| Ot - Other non clay grains or cements | Sm - Smectite |
| Kaol - Kaolinte | Tot Clay - Total clay in bulk sample |
| Ill- Illite | |
| Chl - Chlorite | |
| MI- Mixed Layer Clay | |



**Reservoir Quality Assessment of Sandstone
UPRC Stratos Fed #1**

Summary of Petrology

Thin section petrology, X-ray diffraction analysis and scanning electron microscopy of eight sandstone samples selected from Fed #1 well showed that:

1. The sandstone samples represent a sequence or sequences of slightly to moderately feldspathic, highly quartzose sublitharenite to litharenite with fair core measured porosity, low effective porosity and low permeability. Mean grain size of the sandstone ranges from 0.211mm in sample Hy-37 (16069.20ft) to 0.260mm in sample Hy-6a (16,025ft). Grain size distribution histograms (figure H1) show moderate sorting of the grains. Plates 1, 3A, 3B, 5, 7A, 7B, 9, 11A and 11B show the general texture, fabric and composition of the each of the sandstones

2. Subrounded to subangular monocrystalline quartz grains dominate the framework in all three sandstones as shown on plates 1B, 2B, 5B, 5D, 5B, 5D, 7B, 7D, 9B and 9D and on figures 1 and 2. Modal analysis indicates that monocrystalline quartz grains form from 45% to 47% of samples HY-6a and 37 to about 65% of sample Hy-31a. Chert grains are the next most abundant framework component, forming from 14% of 6a to 8% of 37 to 4% of 31a. In these sandstones, some chert grains have been leached or completely dissolved. Isolated grain molds are formed with dissolution of cherts. Micro-porosity is preserved in partly leached chert grains. Plates 1C, 2C, 8B and 9C show examples of non-leached, partly leached and dissolved cherts.

Plutonic rock fragments are moderately common in samples 31a and 37 where they form 4 and 8% of the sandstones respectively. In sample 6a, plutonic grains are less abundant at 2.7%

Polycrystalline quartz grains, highly scattered sedimentary rock fragments, and a few metamorphic rock fragments form from 4 to 10% of the rocks and are most abundant in sample 6a. Detrital feldspars occur in trace amounts in sample Hy-6a but are more common in samples Hy-31a and Hy-37. Sodic feldspars form from 1 to 2% of 31a by modal analysis and up to 6% of sample 37 X-ray diffraction bulk analysis shows up to 3% sodic feldspar in sample 6a, up to 9% feldspar in 31a and about 6% feldspar in sample 37. Some of the feldspars in the samples are included under plutonic rock fragments in the modal analysis. Other untwinned and unstained feldspars were counted as quartz.

3 Accessory minerals and grains occur in small amounts and include muscovite micas (trace to 0.3%), heavy minerals (trace) and glauconite (trace to 0.3%)

4 No authigenic kaolinite clay was detected in either the thin section petrology or scanning electron microscopy of sandstones. However, thin section petrology shows that fine illite clays bridge and partly occlude intergranular pores and that compacted matrix, composed of illite and kaolinite lowers reservoir quality

Reservoir Quality Assessment of Sandstone UPRC Stratos Fed #1

The scanning electron microscopy shows that residual amounts of grain moldic and intergranular porosity are occluded or partly occluded with authigenic illite. Plates 2D, 3C, 4B, 4C, 4D, 8A and 11D show authigenic illite clay that occurs as growths on underlying detrital illite or as a pore lining and pore bridging material. Modal analysis suggests the presence of 5% authigenic illite in sample 6a, less than 1% authigenic illite in sample 31a and up to 9% authigenic illite in sample 37. However, it is very difficult to differentiate micro-porous detrital illite and authigenic illite in thin section.

X-ray diffraction analysis suggests that illite is somewhat less common in the rocks than indicated by modal analysis. A micro-porosity component is preserved in illite clays.

5. Matrix and pseudo-matrix consisting of detrital illite, kaolinite and mixed layer illite-smectite clay and scattered compacted clay rich clasts occurs low (6a) to high (31a) volumes ranging up to 17% of the sandstones. Compacted between framework grains, matrix is considered one of the most significant permeability reducing phases in the interval represented by sample 31a and a moderate permeability reducing phase in the interval represented by sample 37. Plates 5A, 5C, 6, 7 and 8a show the extensive matrix in sample 31a. Plates 10B, 10C, 10D and 11B show the less extensive matrix in sample 37. Matrix clays preserve a micro-porosity component. Low permeability measured in samples Hy-31a and 37 can be attributed to matrix that isolates pores. In both samples 31a and 37 compacted matrix has inhibited quartz cementation.

6. Authigenic cements occlude intergranular pores and lower permeability, particularly in sample Hy-6a. Authigenic quartz (plates 1A, 1C, 2A, 2B, 2C, 3A, 3B, 3D), emplaced as overgrowths on quartz grains, occludes up to 25% intergranular porosity in sample 6a. Grain to grain contacts suggest quartz cementation occurred following incipient chemical compaction and prevented extensive grain suturing.

In the interval represented by sample Hy-31a abundant matrix inhibited quartz cementation. Quartz cement forms only 1 to 2% of 31a. Similarly matrix inhibited quartz cementation in the interval represented by sample 37. Quartz cement forms 9 to 10% of sample 37. Quartz cements, where not inhibited by clay occlude porosity and lower the sandstone reservoir quality.

Ferroan calcite cement occludes a small amount of porosity in sample 31a and replaces or partly replaces grains as shown on plates 5C and 10B. In this sandstone ferroan calcite forms 1 to 2%. In sample 37 ferroan calcite is more prevalent. In 37 calcite cements intergranular porosity and replaces grains, earlier cements and matrix to form about 2 to 3% of the rock. Plates 9C and 10A show the calcite. X-ray diffraction bulk analysis shows calcite forms 1.7% of sample 31a (an amount indicated by the modal analysis) and up to 5% of sample 37. We attribute the discrepancy between modal analysis calcite and XRD calcite in sample 37 to the heterogeneous distribution of the cement. In these sandstones there is no evidence to suggest calcite was dissolved to form secondary porosity.

Reservoir Quality Assessment of Sandstone UPRC Stratos Fed #1

Mineralogy

All three samples were submitted for bulk and clay X-ray diffraction analysis. The bulk analysis (Table 5a) shows that quartz dominates the sandstone mineralogy (75 to 93%). The amount of quartz detected by XRD analysis correlates well with the amount of quartz indicated by the modal analysis in sample 6a (90% XRD vs 93% modal). In sample 31a the modal analysis shows about 74% quartz which correlates well with the 75% quartz calculated from the XRD bulk analysis. Modal analysis quartz content of 66% in sample 37 does not correlate well with the 78% quartz as calculated from the XRD analysis. We assume additional quartz occurs in plutonic rock fragments and in matrix.

Feldspars form from 3 to 9% of the rocks by XRD bulk analysis. Feldspars calculate at higher amounts by XRD than by modal analysis in all three samples suggesting that some feldspars were included in the plutonic rock fragment and quartz grain categories on the modal analysis.

Calcite forms from 1.7 to 5% of samples 31a and 37 respectively. The heterogeneous distribution of calcite probably accounts for any discrepancy between modal and XRD analysis.

Clays form from 6 to 12% of the rocks by XRD analysis and consist of illite, kaolinite, mixed-layer illite-smectite and chlorite. The clay analysis (Table 5b) shows that illite dominates the clay fraction in all three sandstones (46 to 69% of the clay fractions). Kaolinite forms about 40% of the clay fractions in samples Hy-6a and 31a. In sample 37 kaolinite forms only 17% of the clay fraction. In these sandstones kaolinite occurs in detrital form in association with illite.

Mixed-layer illite-smectite clays form about 8% of the clay fraction in samples 31a and 37 and up to 22% of the clay fraction in sample 6a. The clays are susceptible to expansion in water. Any clay expansion would completely eliminate the already low sandstone permeability.

Small amounts of chlorite (4 to 6% of the clay fractions) are present.

Reservoir Quality Characteristics

The sandstone samples recovered from the Stratos Fed #1 exhibit the following reservoir quality characteristics as indicated on table 4:

- 1 Quartz dominated sandstone-faintly burrowed with poorly connected modified primary and secondary grain moldic porosity (trace to 2%).
- 2 Mean grain size of ranging from 0.211 to 0.260mm
- 3 Moderate to high volumes of clay and matrix (5 to 18%) that greatly lowers reservoir quality in the intervals represented by samples 31a and 37

Reservoir Quality Assessment of Sandstone UPRC Stratos Fed #1

4. Low to high volumes of pore fill cements (3 to 25%) that greatly lower the reservoir quality in the interval represented by sample 6a.

5 No pore occluding bitumen.

Permeability (0.11 to 0.21md) measured by conventional core analysis appears high compared with the texture and composition of the rocks as determined by thin section petrology. We expect that micro-fractures (Plate 8C) may have affected the core analysis results. The thin section petrology and scanning electron microscopy indicates these are very low reservoir quality sandstones.

Primary intergranular porosity in the interval represented by sample 6a was greatly reduced and modified by the effects of compaction and by intense cementation by quartz. In the interval represented by sample 31a primary porosity was destroyed by compaction, compacted and deformed matrix clays and by small amounts of quartz and calcite cement. In the interval represented by sample 37 reservoir quality was lowered by the effects of compaction, compacted and deformed matrix and pseudo-matrix, by authigenic quartz cement and by ferroan calcite cement. The dissolution of unstable grains has very slightly enhanced porosity and reservoir quality.

**Reservoir Quality Assessment of Sandstone
UPRC Stratos Fed #1**

Reservoir Quality Assessment

Paragenesis and Reservoir Evolution

Very low reservoir quality sandstone reservoirs cored by the Stratos Fed #1 well evolved through the following paragenesis.

- 1 Compaction and deformation of matrix, rare soft grains, (interval represented by samples 31a and 37) and reorientation and packing of quartz grains resulted in a moderate (6a) to high (31a, 37) loss of primary intergranular porosity. .
2. Incipient chemical compaction and precipitation of authigenic quartz cement as syntaxial overgrowths on monocrystalline quartz grains lowered primary porosity by as much as 25% in interval represented by the sample 6a. Clay matrix inhibited quartz cementation in samples 31a and 37
3. Emplacement of authigenic illite clays as overgrowths on detrital illite and as bridges across the remaining pores.
- 4 Emplacement of some calcite cement as pore fill and as a replacement mineral of matrix, quartz cement and quartz grains and rock fragments. Most of the residual porosity in samples 31a and 37 destroyed. No calcite emplaced to quartz cemented interval represented by sample 6a.
- 5 Dissolution of unstable grains very slightly enhanced effective porosity by trace to 1%.

Controls on Reservoir Quality

Reservoir quality in the sandstone drilled by the Stratos Fed #1 well is a function of the volume of porosity, the type and distribution of porosity, the volume and distribution of authigenic cements and the volume and distribution of matrix clays. Reservoir properties, early in the sandstone paragenesis, were strongly influenced by depositional parameters such as the sand grain size and the amounts of detrital mud matrix. Later diagenesis overprints the original depositional controls of reservoir quality.

In the intervals represented by samples 31a and 37 abundant detrital matrix lowered reservoir quality. With compaction that matrix was deformed between more competent quartz grains and reservoir quality declined even further.

Good primary intergranular porosity in coarser, cleaner sandstones as represented by sample 6a was destroyed by extensive quartz cementation.

Reservoir Quality Assessment of Sandstone UPRC Stratos Fed #1

Figure 3 also suggests the distribution and type of porosity exerts a controlling influence on reservoir quality. The diagram shows porosity types (intergranular, grain moldic, micro) on a triangular plot. All of the sandstones plot well within the area dominated by non-effective micro-porosity. In these rocks micro-porosity occurs in partly leached chert grains and in matrix clays. The diagram shows that most of the porosity as measured by core analysis is micro-porosity.

Reservoir Sensitivity

Petrology shows that the sandstones contain small to moderate amounts of illite clay small to high volumes of detrital illite, clay matrix and some mixed-layer illite-smectite expandable clay. We would suggest these sandstones are sensitive to water in terms of clay swelling and in terms of water entrapment in micro-pores. The sandstones should not be sensitive to HCl acid in mineralogical terms; however, would not benefit by HCl acid stimulation.

The rocks contain small amounts of leached grain remnants that could be susceptible to migration.

The rocks submitted for petrological analysis represent very low reservoir quality intervals with a maximum of 0.21md permeability as measured at ambient conditions. Given the depth of the reservoir (16,000 + ft) it may not be capable of commercial gas production unless there are fractured intervals or intervals characterized by solution enhanced intergranular porosity.

Completion programs could include:

1. Underbalanced perforation through clean KCl brine.
2. An HCl acid wash, only if required, to establish good communication with the sandstone reservoir. The rocks contain small amounts of acid soluble cements and grains and will not, themselves, benefit from an HCl acid stimulation. We do not expect the sandstones to be sensitive to HCl acid in terms of emulsion or sludge formation.
3. Fracture stimulation. Consider an energized fluid, as the sandstones are characterized by relatively high volumes of clay micro-porosity (see figure 3). A high strength proppant would be required.

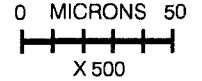
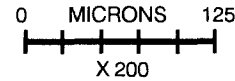
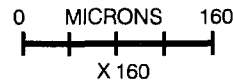
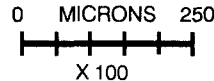
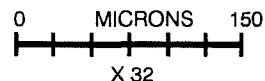
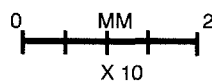
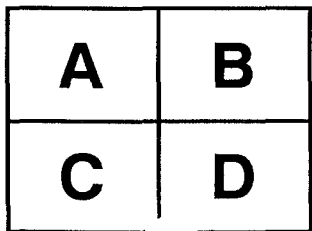
**Thin Section and SEM Photomicrographs
and
Descriptions**

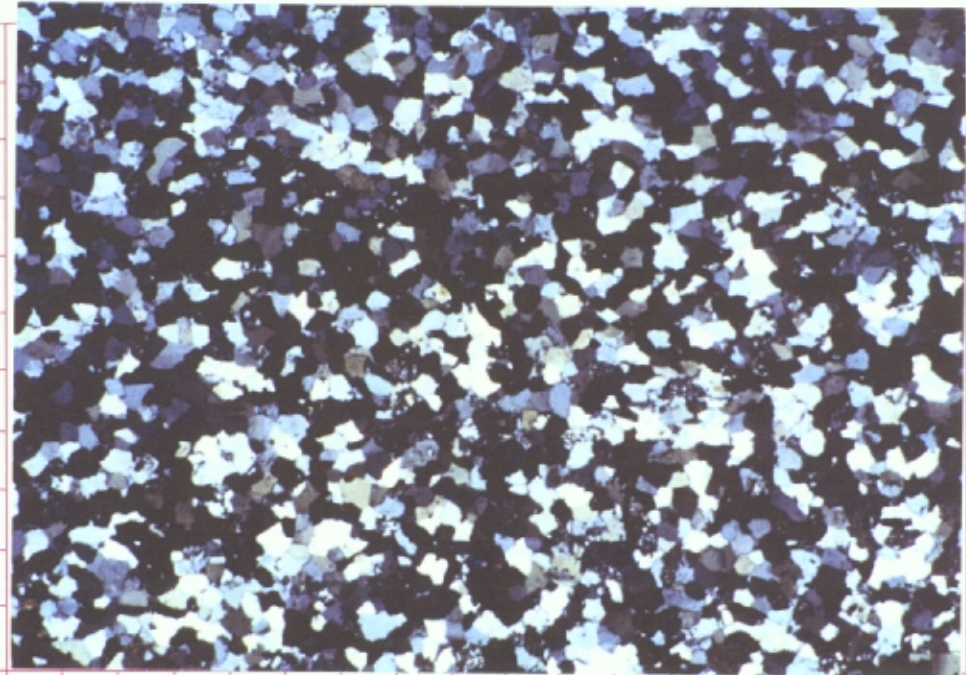
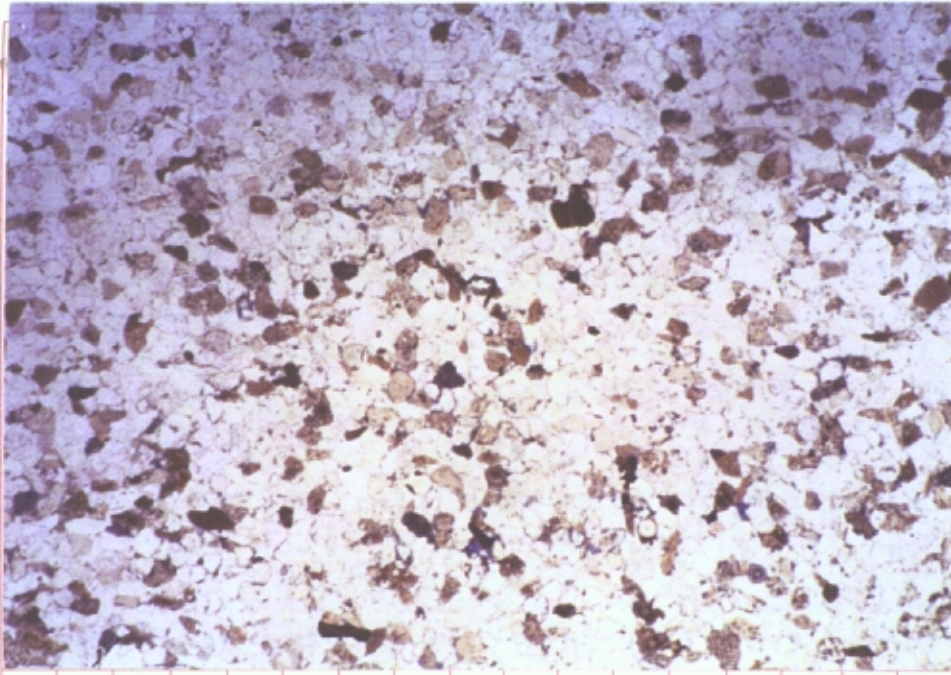
Thin Section Descriptions Plate 01
Stratos Fed #1
Cemented Litharenite
Porosity 6.2% (trace*) Permeability 0.21md

Sample No Hy-6a: 16,025.0ft

A-D Strongly quartz cemented, moderately sorted, lowermost medium grained, quartzose litharenite with low effective porosity and low permeability. The sandstone framework consists mainly of quartz overgrown monocrystalline quartz grains with lesser cherts (K-1, M-7, R-9 on C), scattered plutonic and metamorphic rock fragments and a few sedimentary clay clasts. Photomicrograph C suggests that extensive quartz cementation prevented strong chemical compaction of the sandstone. Isolated grain molds (J-6 on C) formed with the dissolution of some of the unstable rock fragments. Micro-porosity is preserved in grain rimming clays and in leached grains. **Photos A and B PPL,XP X10; Photos C and D PPL,XP X32**

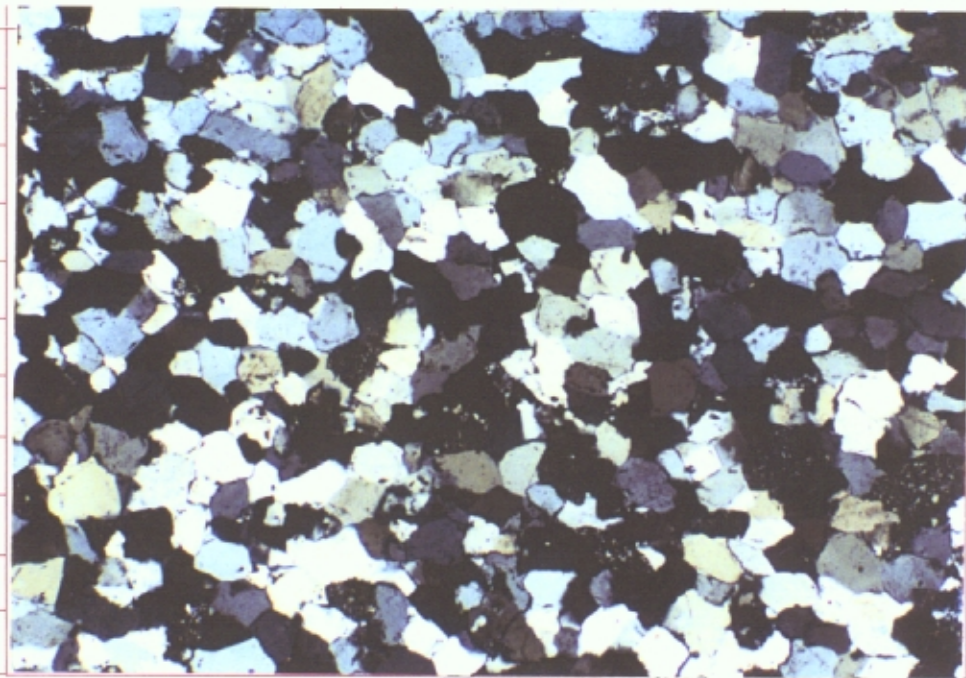
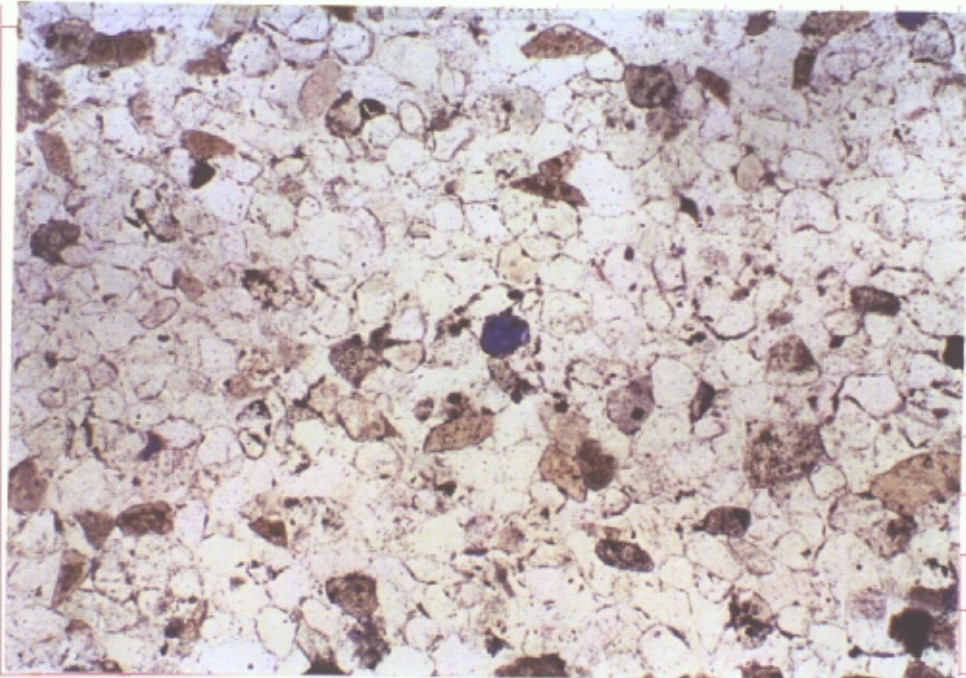
*** Thin Section Porosity**





A B C D E F G H I J K L M N O P Q R

A B C D E F G H I J K L M N O P Q R



A B C D

A B C D

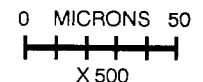
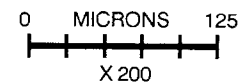
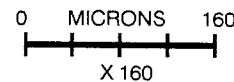
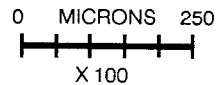
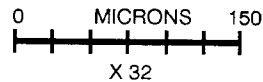
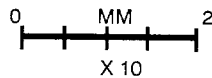
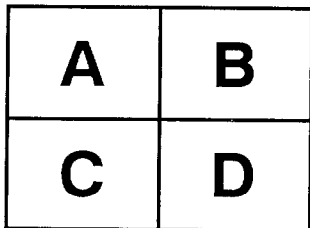
Plate 01- 600

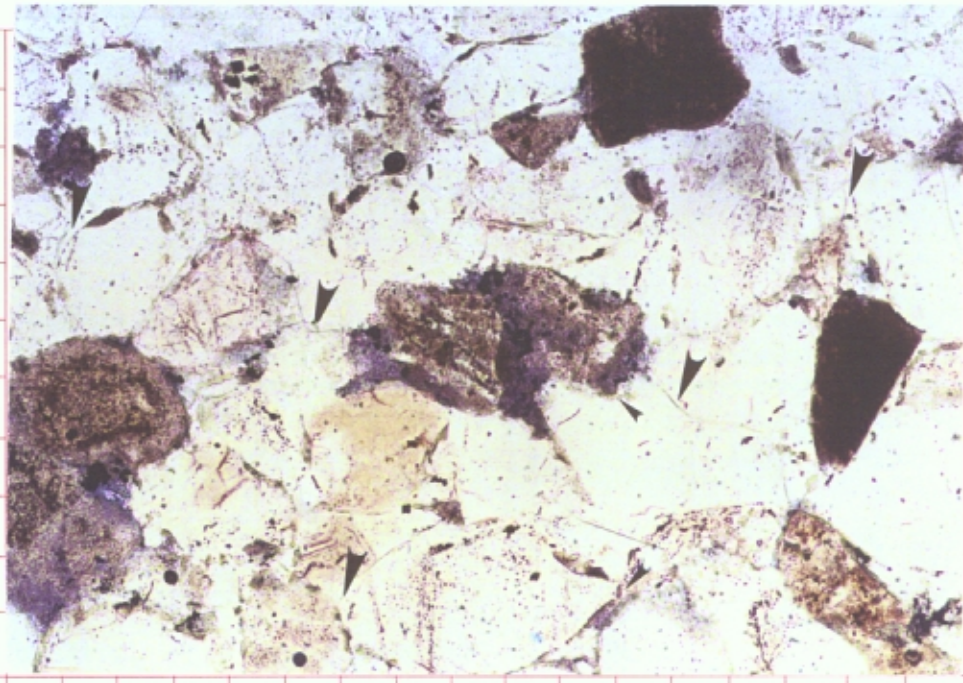
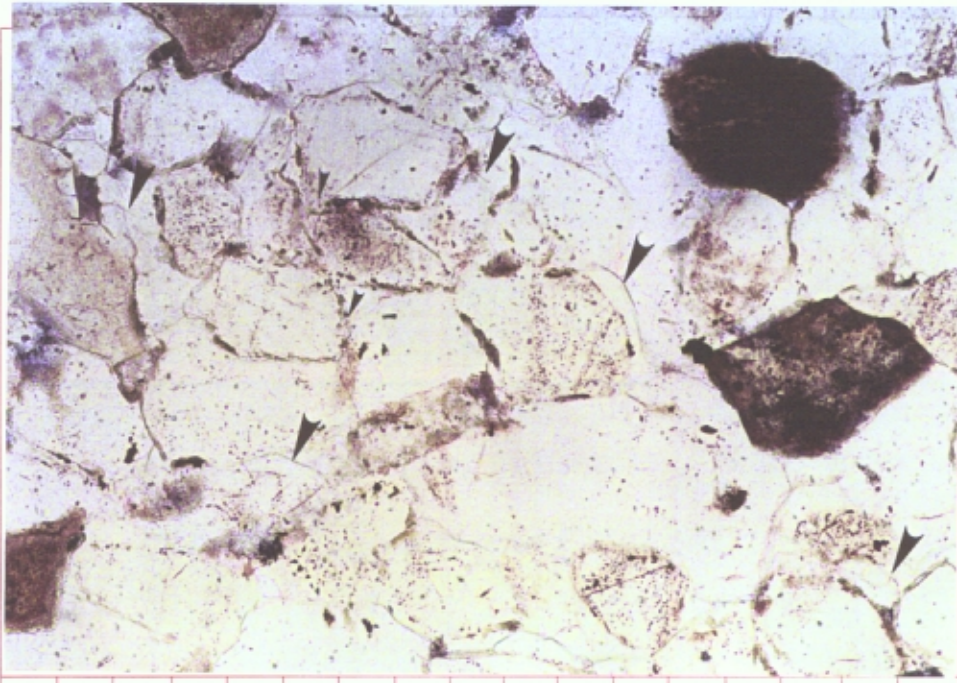
Thin Section Descriptions Plate 02
Stratos Fed #1
Cemented Litharenite
Porosity 6.2% (trace*) Permeability 0.21md

Sample No Hy-6a: 16,025.0ft

- A-B** Authigenic quartz (arrows), emplaced as syntaxial overgrowths on monocrystalline quartz grains, cements porosity and destroys the reservoir quality of the sandstone. There are a few interpenetrating grain contacts (small arrows); however, extensive quartz cementation has prevented extensive chemical compaction. Micro-porosity (B-10 on B) is preserved in partly leached chert grains. **Both Photos PPL X100**
- C** Shows micro-porosity (arrows) in a partly leached chert grain. The complete dissolution of these grains forms isolated grain molds. Note the micro-porous clay rims (small arrows) on some of the grains. **PPL X200**
- D** Intergranular porosity between chert grain (O-4) and surrounding quartz grains occluded with micro-porous illite clay (arrows). **PPL X500**

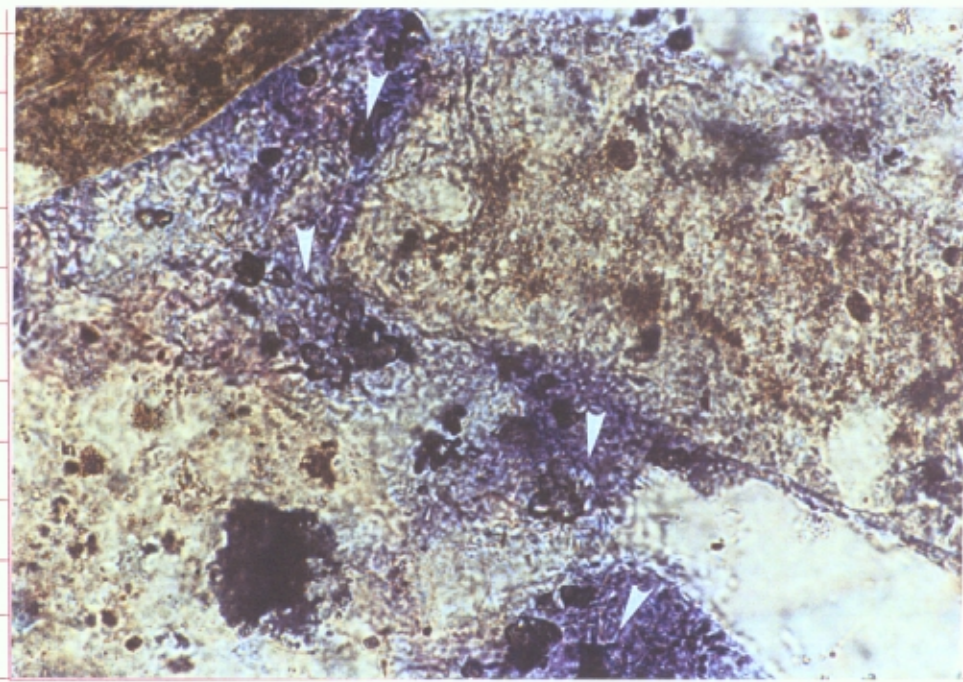
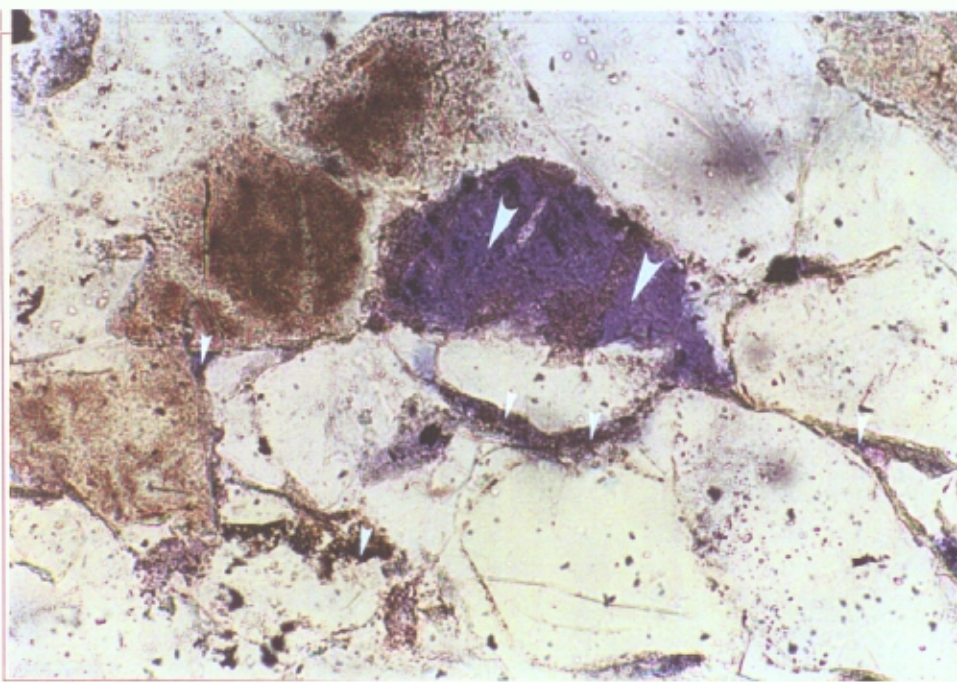
*** Thin Section Porosity**





A B C D E F G H I J K L M N O P Q R

A B C D E F G H I J K L M N O P Q R



A B C D E F G H I J K L M N O P Q R

A B C D E F G H I J K L M N O P Q R

Plate 02-6a



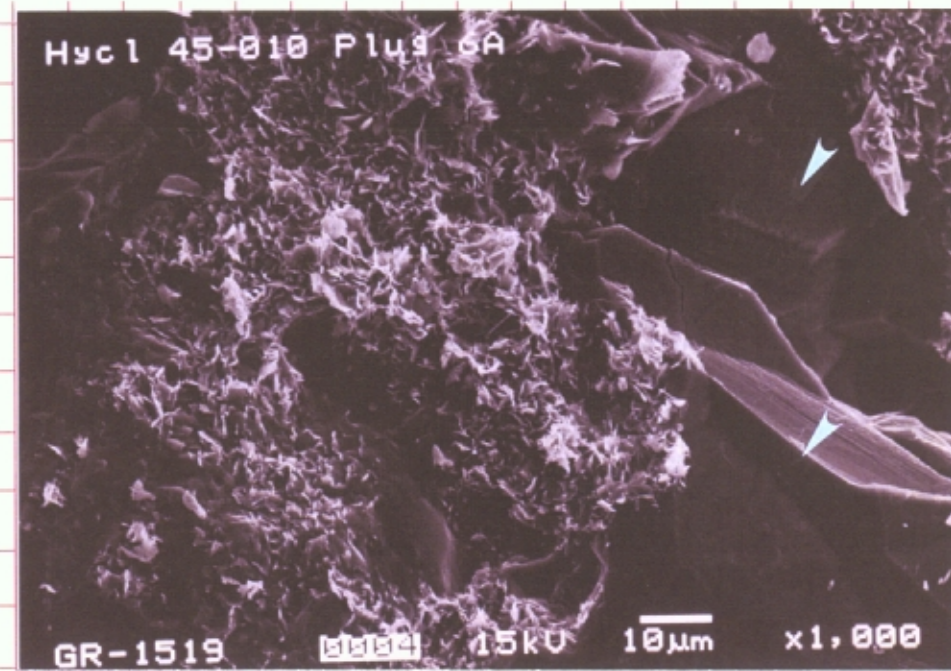
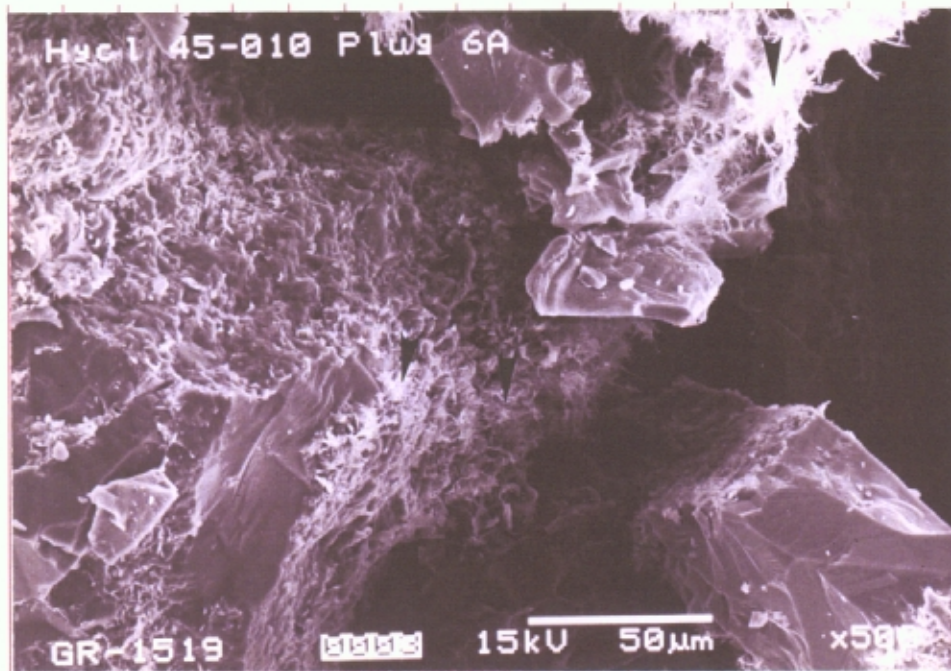
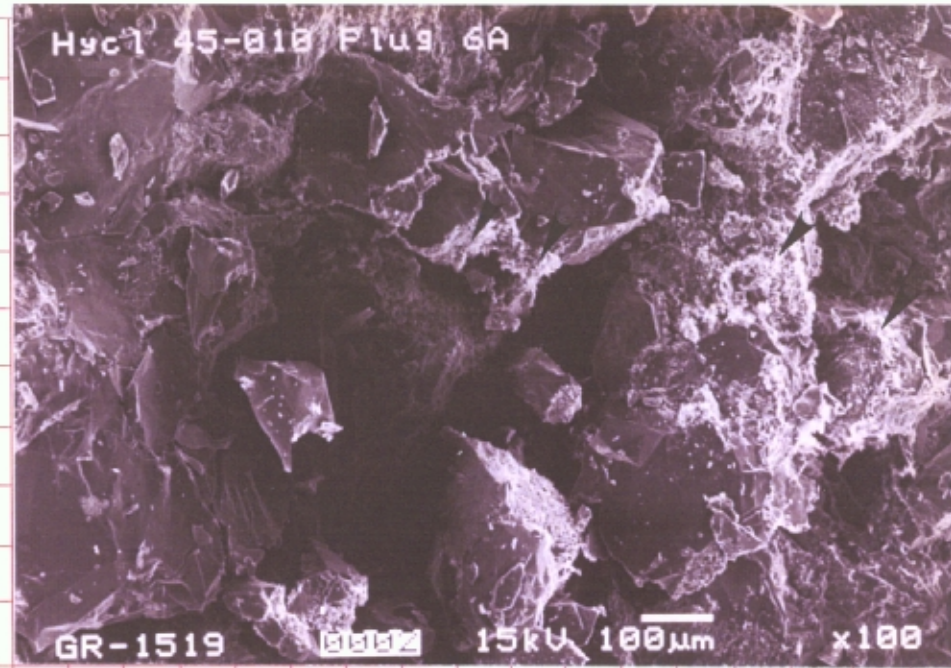
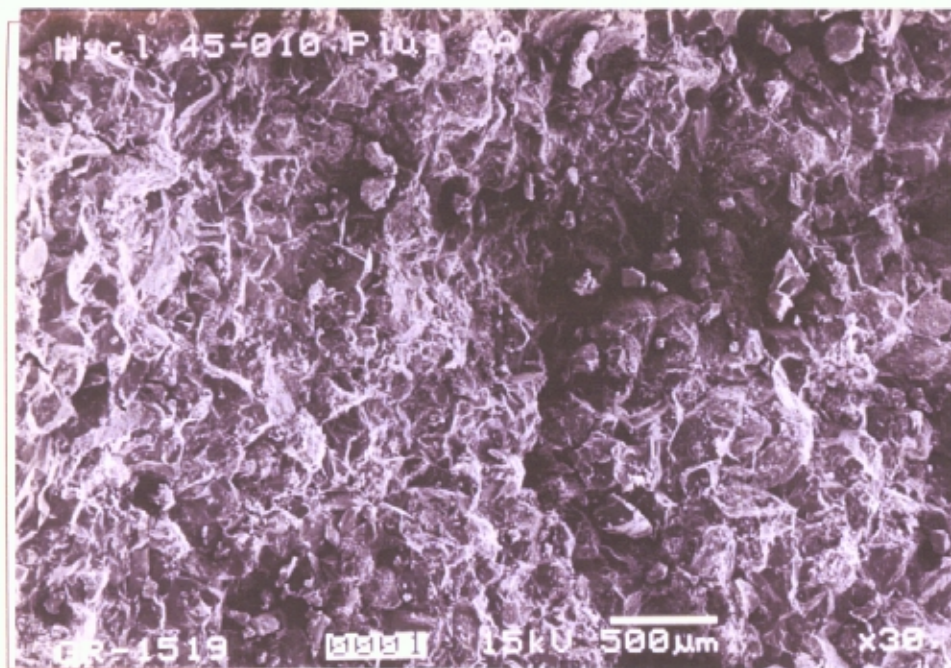
SEM Photomicrographs and Descriptions Plate 03
Stratos Fed #1
Cemented Litharenite
Porosity 6.2% (trace*) Permeability 0.21md

Sample No Hy-6a: 16,025.0ft

- A-B** Quartz cemented, moderately sorted, lowermost medium grained, quartzose litharenite with low effective porosity and low permeability. Scattered, modified intergranular pores (K-6 on B) are preserved in the vicinity of some of the lithic grains. However, extensive quartz cementation has greatly lowered the reservoir quality of the sandstone. Illite clays (arrows on B) line and occlude pores and isolated grain molds. **Photo A X30, Photo B X100**
- C** Illite clays (arrows) line and partly occlude the modified intergranular pore. These types of pores are isolated and contribute little to sandstone reservoir quality. Micro-porosity is preserved in the illite. **X500**
- D** Shows a compacted, micro-porous clay clast (H-4) and the quartz cement (arrows) that destroys the reservoir quality. A micro-porosity component is preserved in the clay. **X1000**

*** Thin Section Porosity**

| | |
|----------|----------|
| A | B |
| C | D |



A B C D E F G H I J K L M N O P Q R A B C D A B C D E F G H I J K L M N O P Q R

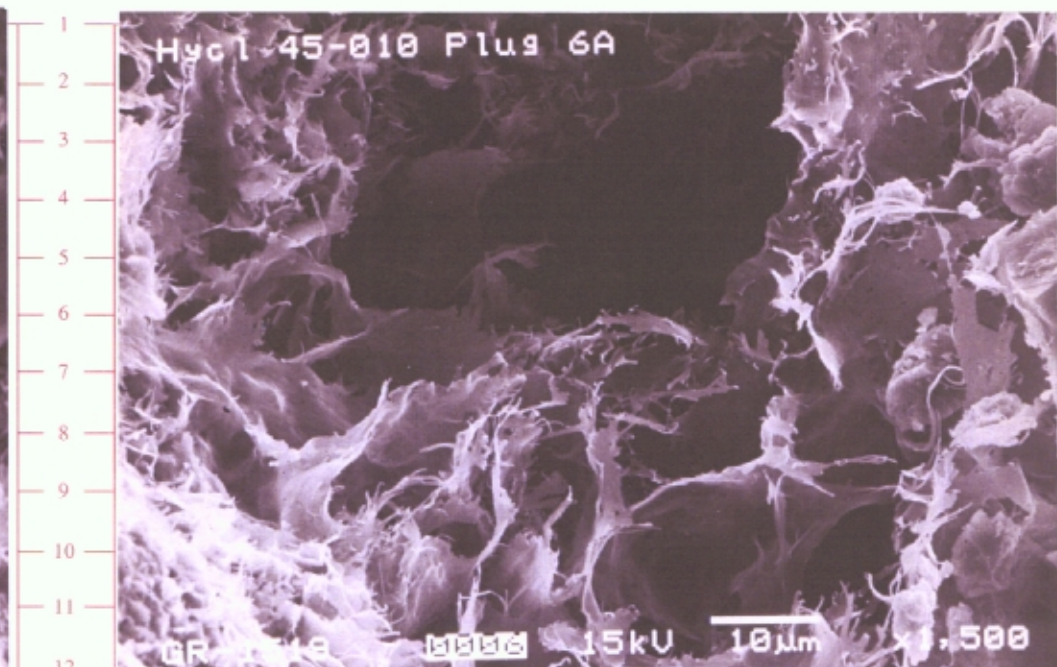
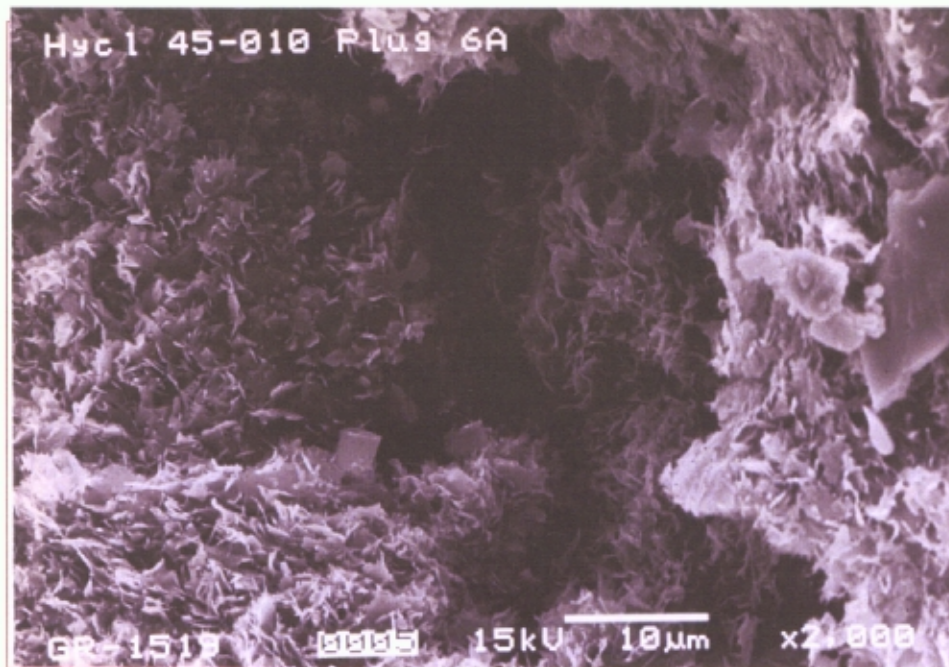
SEM Photomicrographs and Descriptions Plate 04
Stratos Fed #1
Cemented Litharenite
Porosity 6.2% (trace*) Permeability 0.21md

Sample No Hy-6a: 16,025.0ft

A-D All four scanning electron micrographs show illite clays that line or bridge intergranular or grain moldic pores. The occlusion or partial occlusion of the few pores that remained after extensive quartz cementation by illite, further lowers the sandstone reservoir quality. The pore shown on photo A is preserved between clay coated lithic grains. **Photo A X2000, Photo B X1500, Photo C X3000, Photo D X2000**

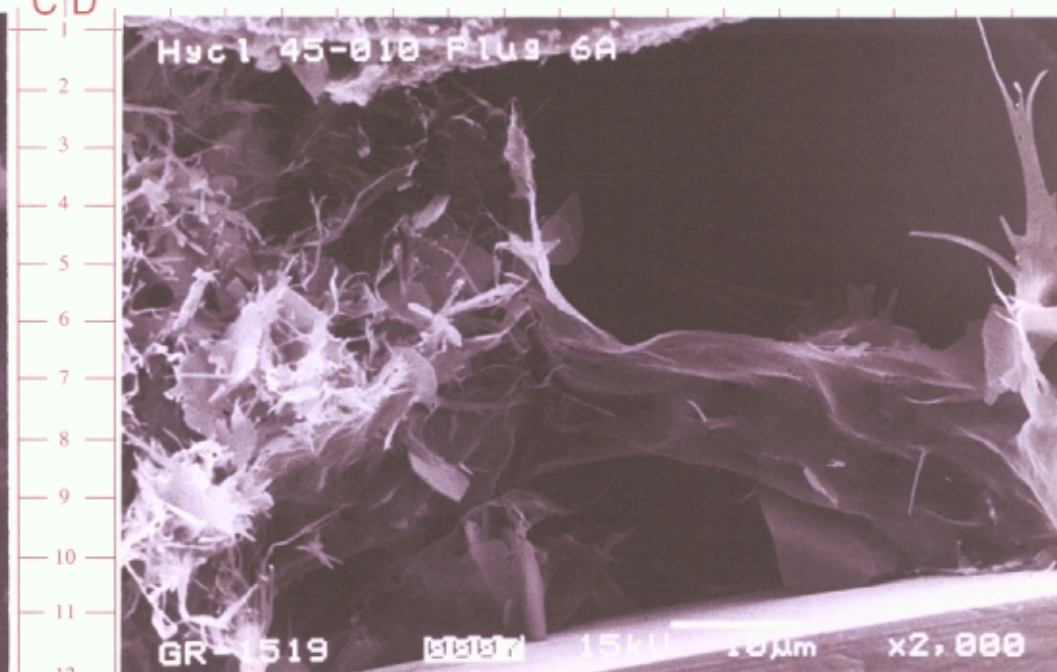
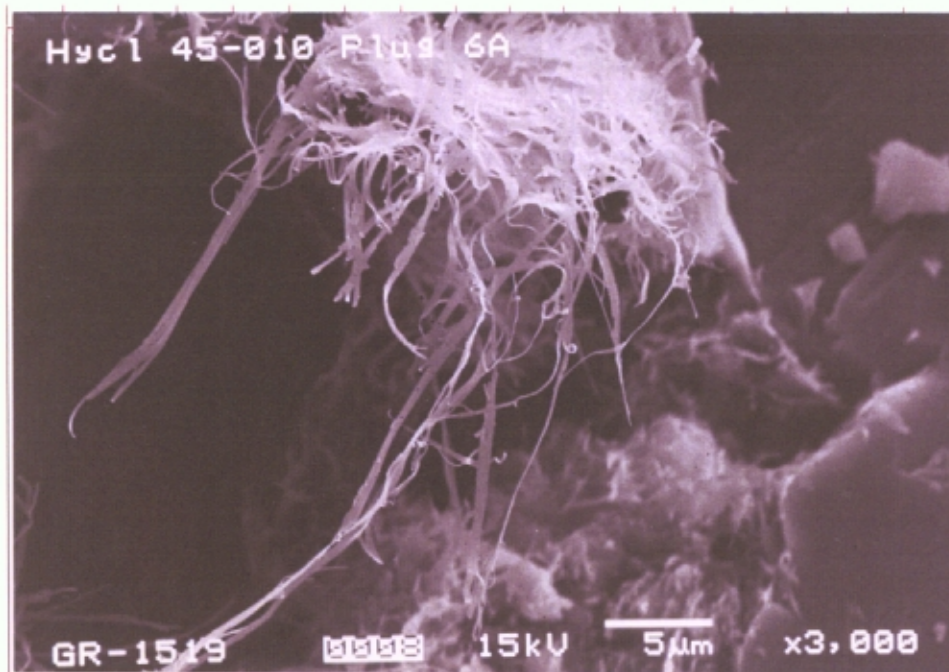
*** Thin Section Porosity**

| | |
|----------|----------|
| A | B |
| C | D |



A B C D E F G H I J K L M N O P Q R

A B C D E F G H I J K L M N O P Q R



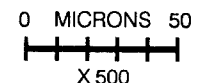
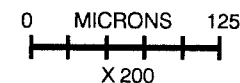
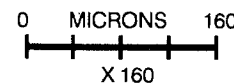
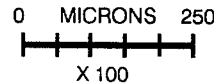
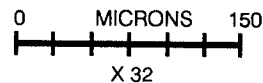
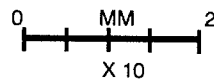
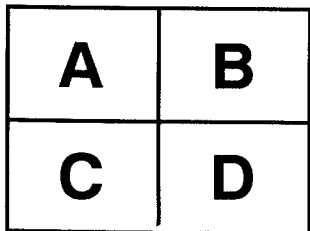
A B C D E F G H I J K L M N O P Q R

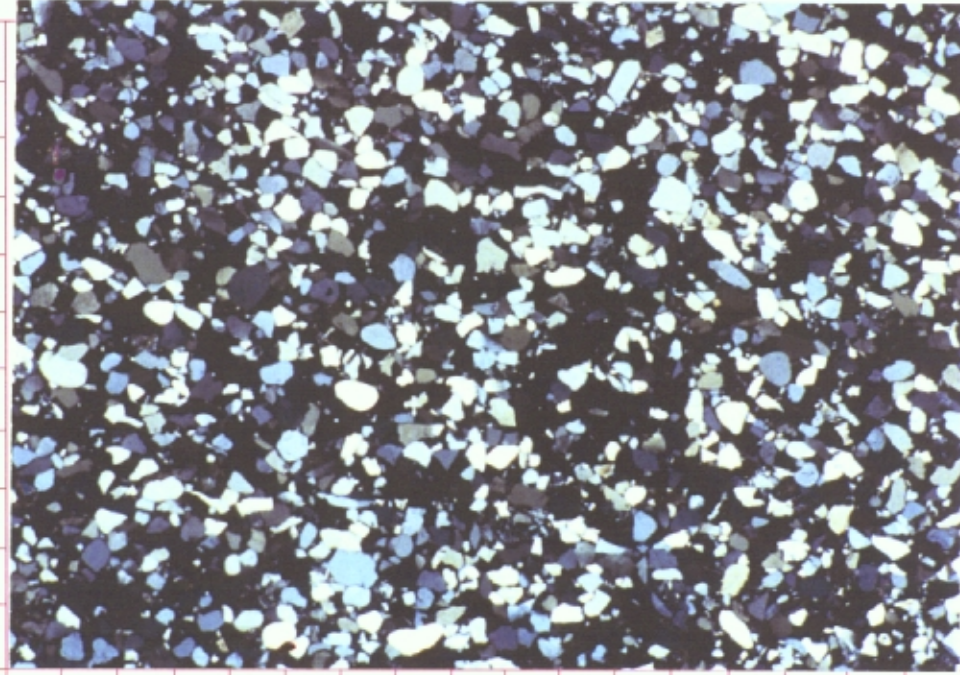
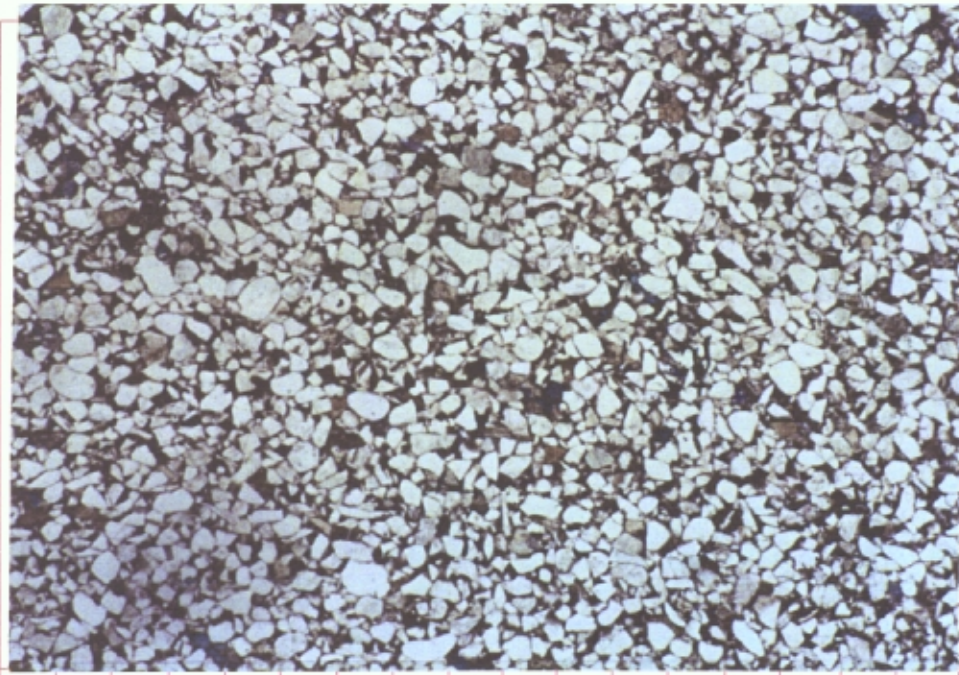
Thin Section Descriptions Plate 05
Stratos Fed #1
Argillaceous Sublitharenite
Porosity 7.7% (1.0%*) Permeability 0.11md

Sample No Hy-31a: 16,063.20ft

A-D Faintly burrowed, moderately sorted, upper fine grained, argillaceous, quartzose sublitharenite with low effective porosity and low permeability. The sandstone framework consists mainly of angular to subrounded monocrystalline quartz grains (grey and white on photos B and D). Ferroan calcite (C-5 on C) replaces some of the grains and cements a few pores. Illite clays (brown) compacted between quartz grains, inhibited quartz cementation and greatly lowered the sandstone reservoir quality. Isolated grain molds formed with the dissolution of a few unstable rock fragments, feldspar grains and chert grains. Micro-porosity is preserved in leached grains and in clay matrix. **Photos A and B PPL,XP X10; Photos C and D PPL,XP X32**

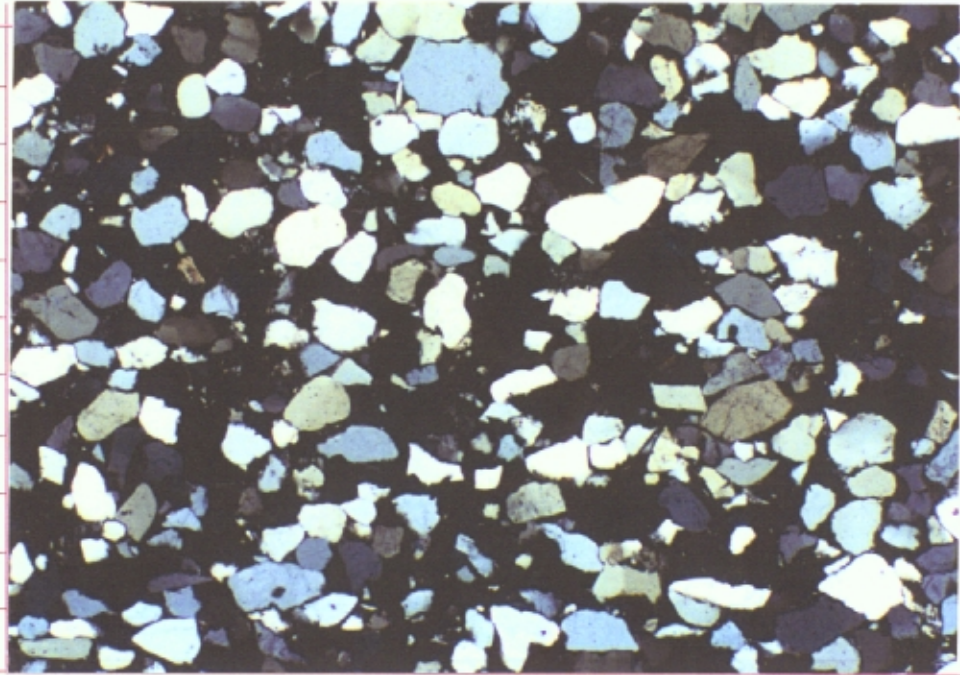
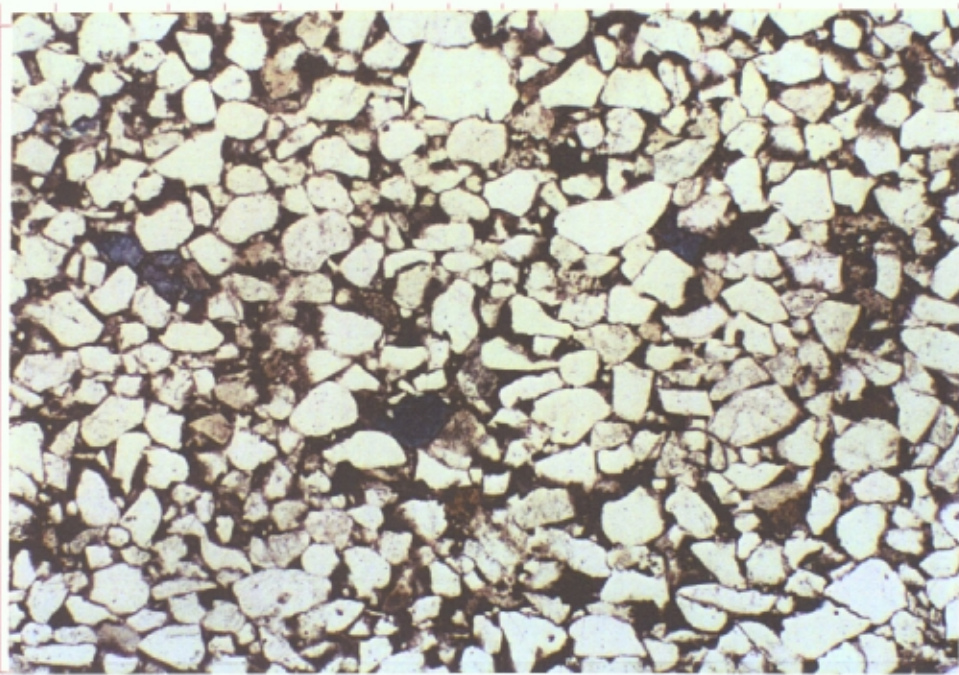
*** Thin Section Porosity**





A B C D E F G H I J K L M N O P Q R

A B C D E F G H I J K L M N O P Q R



A B C D

A B C D

Plate DS-31a

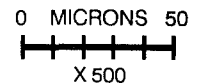
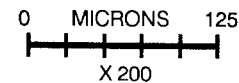
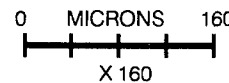
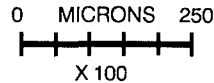
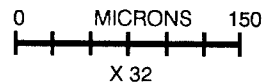
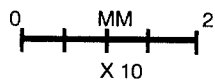
Thin Section Descriptions Plate 06
Stratos Fed #1
Argillaceous Sublitharenite
Porosity 7.7% (1.0%*) Permeability 0.11md

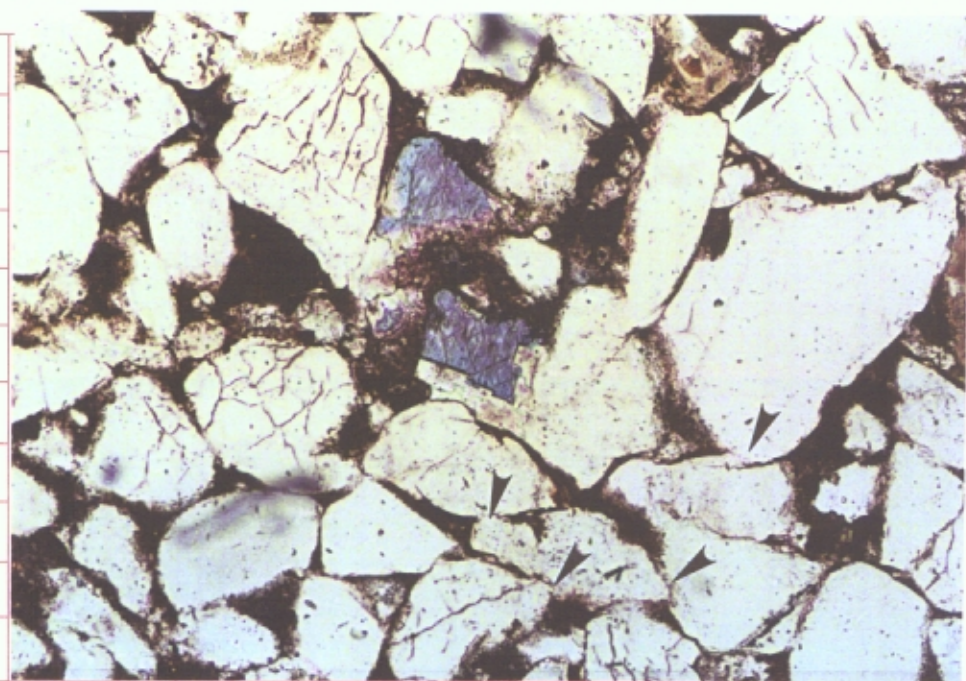
Sample No Hy-31a: 16,063.20ft

- A** Matrix illite clay (dark brown), compacted between grains greatly lowered the reservoir quality of the sandstone and inhibited the precipitation of quartz cement. **PPL X100**
- B** Shows a greater number of interpenetrating grain contacts (arrows) than in sample 6a and the compacted illite clay matrix (dark brown). Ferroan calcite (I-4, J-6) cements a few pores and partly replaces quartz grains. **PPL X100**
- C** Clay matrix (dark brown) destroys the reservoir quality of the sandstone. Micro-porosity is preserved in the compacted clay. **PPL X200**
- D** Detail of micro-porosity (small arrows) in matrix illite clay. **PPL X500**

*** Thin Section Porosity**

| | |
|----------|----------|
| A | B |
| C | D |





A B C D E F G H I J K L M N O P Q R

A/B
C/D

A B C D E F G H I J K L M N O P Q R

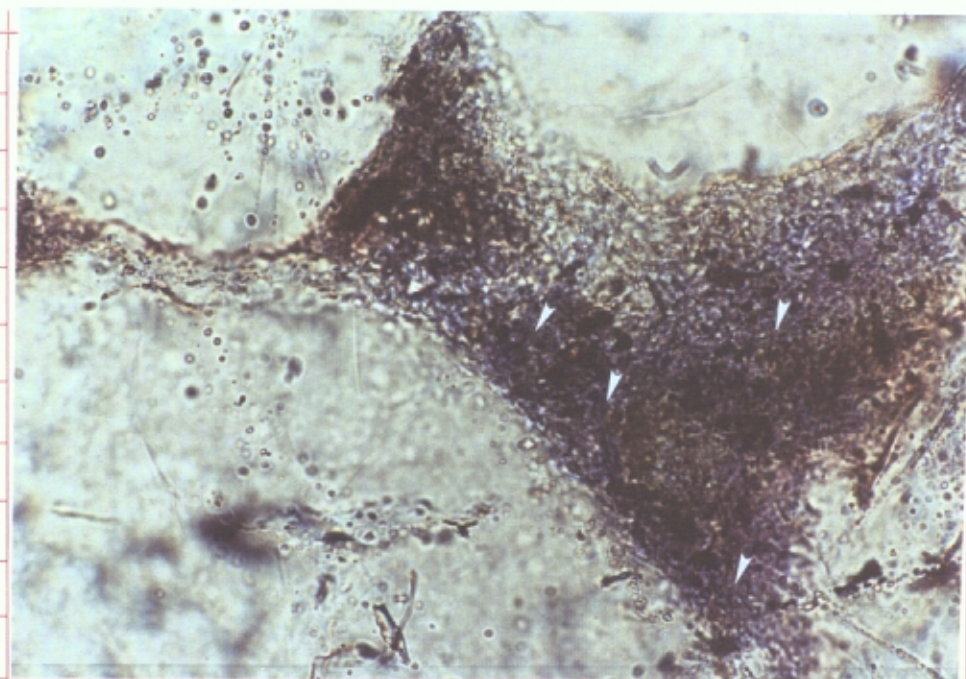


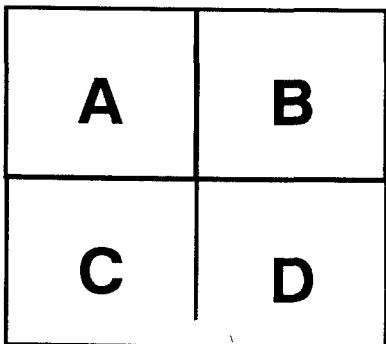
Plate 06-315

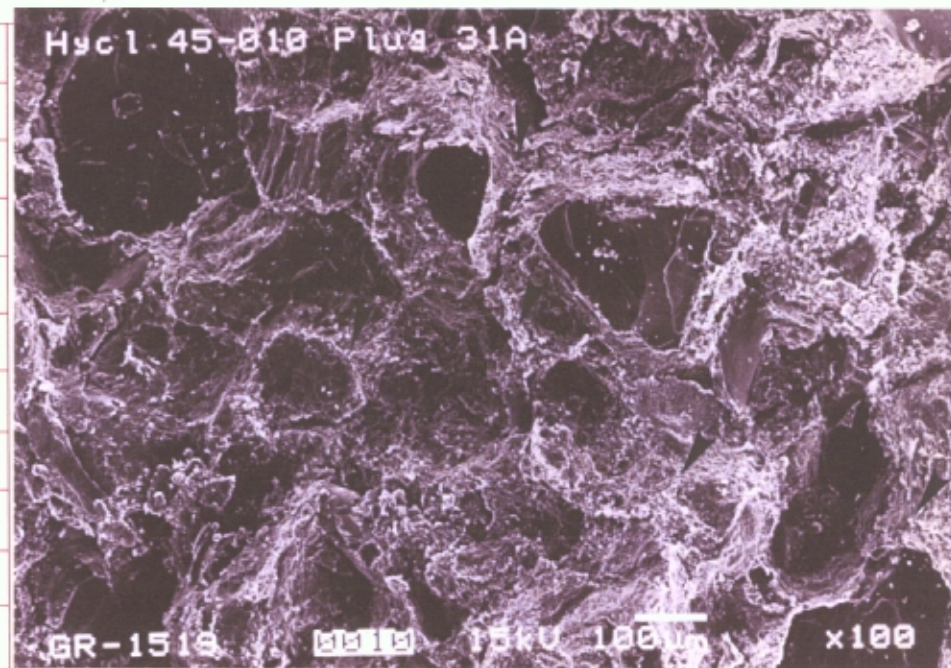
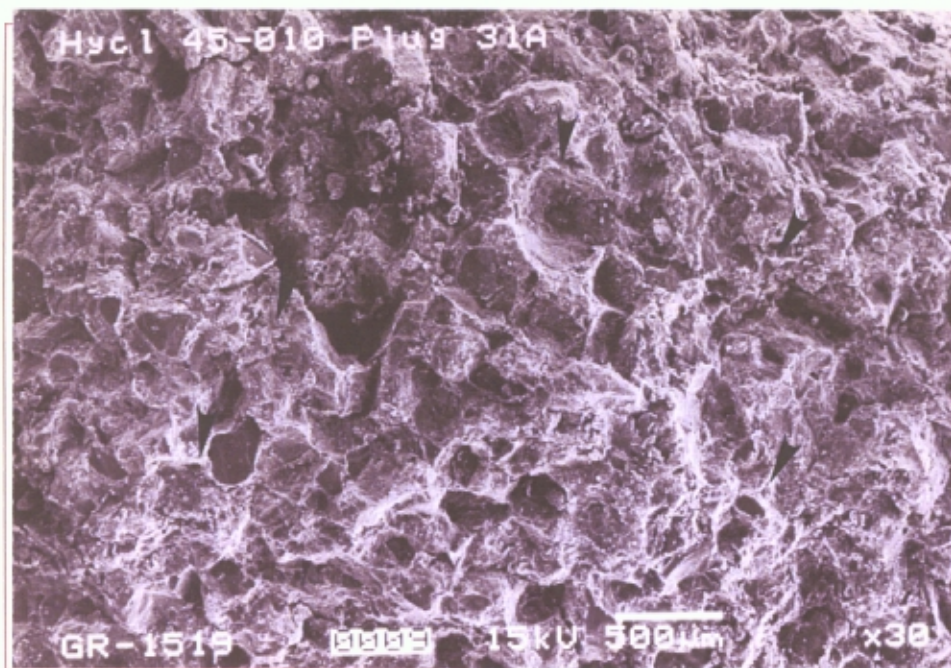
SEM Photomicrographs and Descriptions Plate 07
Stratos Fed #1
Argillaceous Sublitharenite
Porosity 7.7% (1.0%*) Permeability 0.11md

Sample No Hy-31a: 16,063.20ft

A-D Extensive, compacted illite clay matrix (arrows) greatly lowers the reservoir quality of this moderately sorted, upper fine grained, quartzose sublitharenite. Micro-porosity (small arrows) is preserved in the clay matrix. **Photo A X30, Photo B X100, Photo C X500 Photo D X1000**

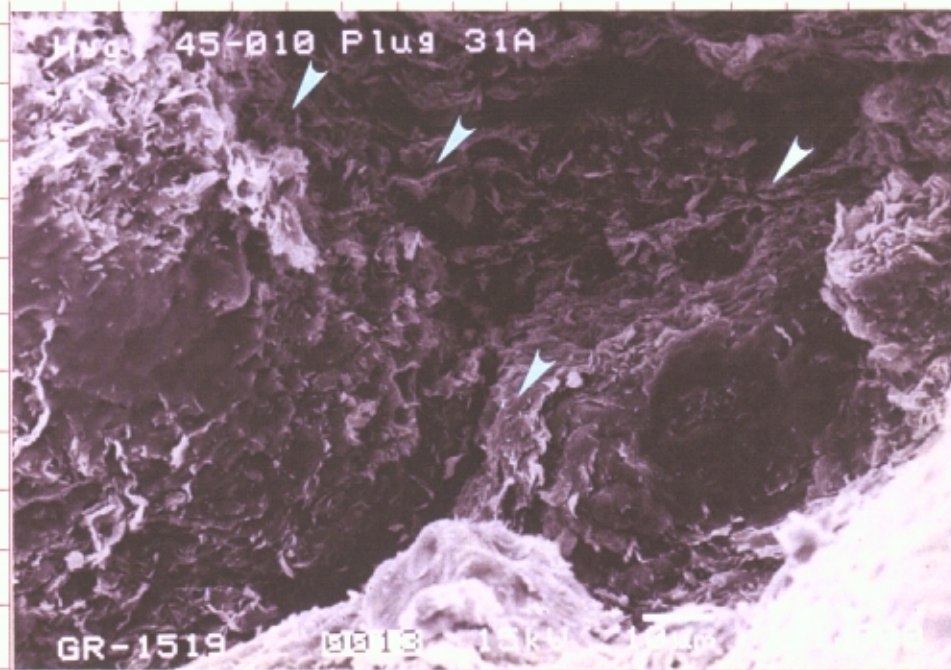
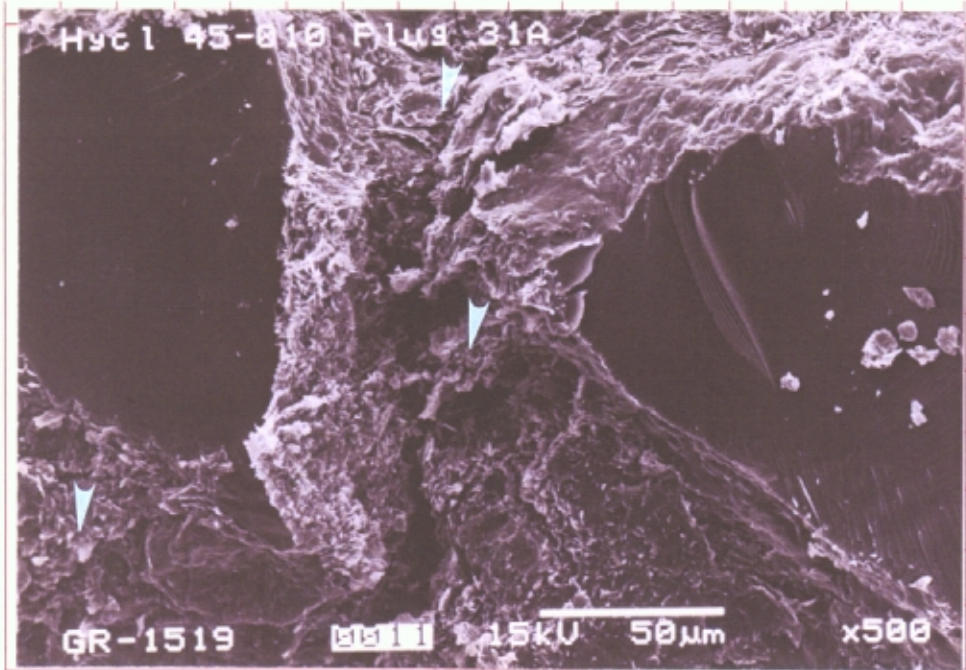
*** Thin Section Porosity**





A B C D E F G H I J K L M N O P Q R

A B C D E F G H I J K L M N O P Q R



A B C D
1
2
3
4
5
6
7
8
9
10
11
12

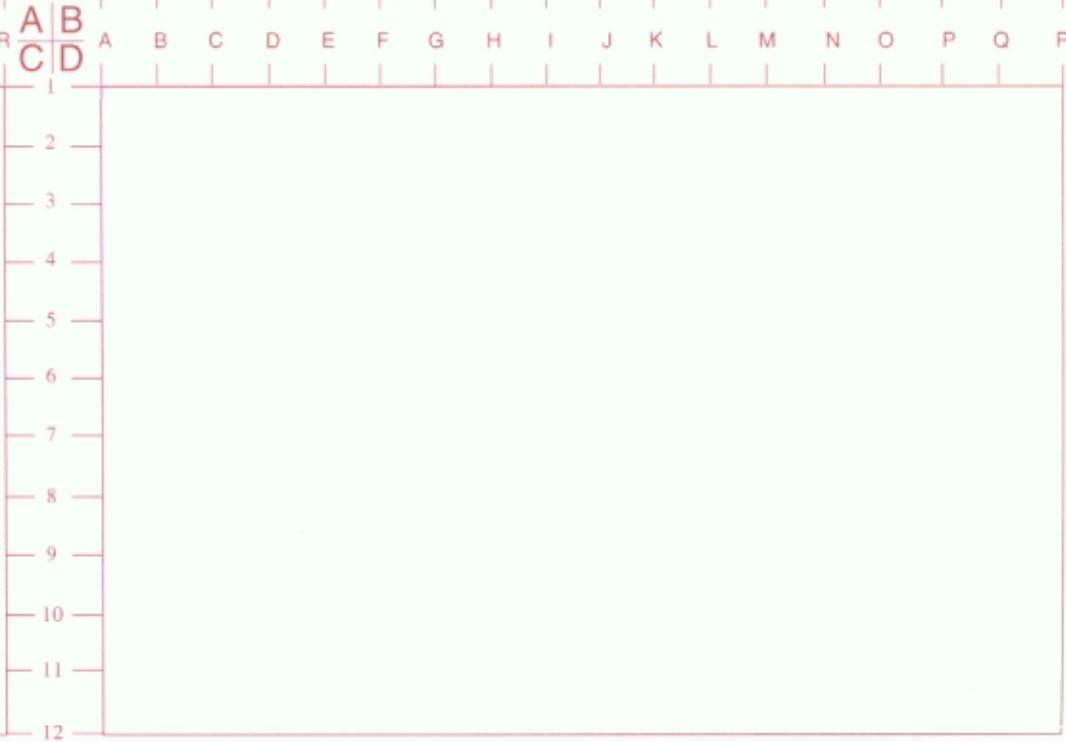
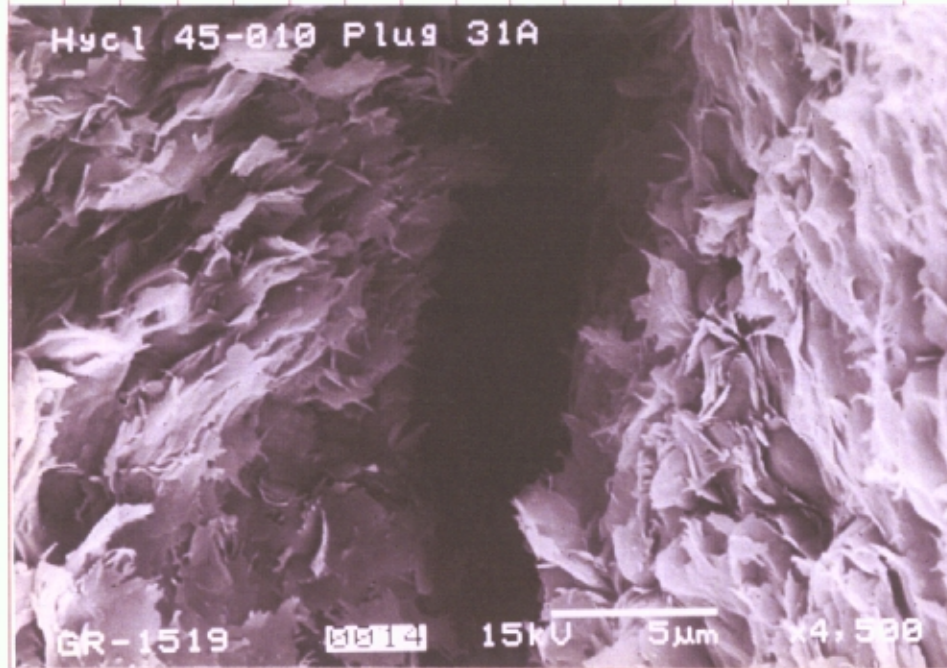
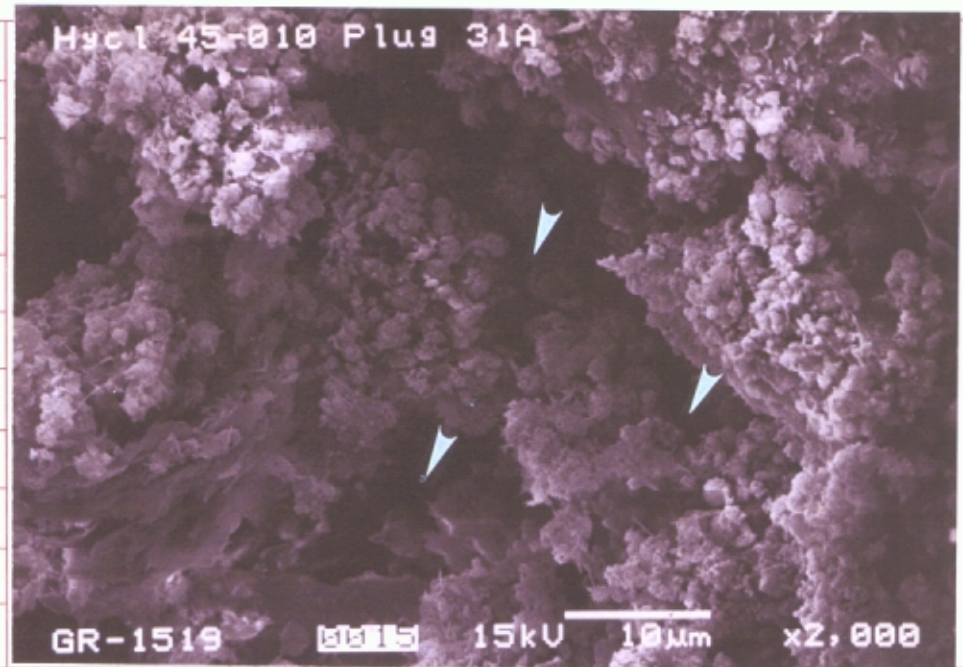
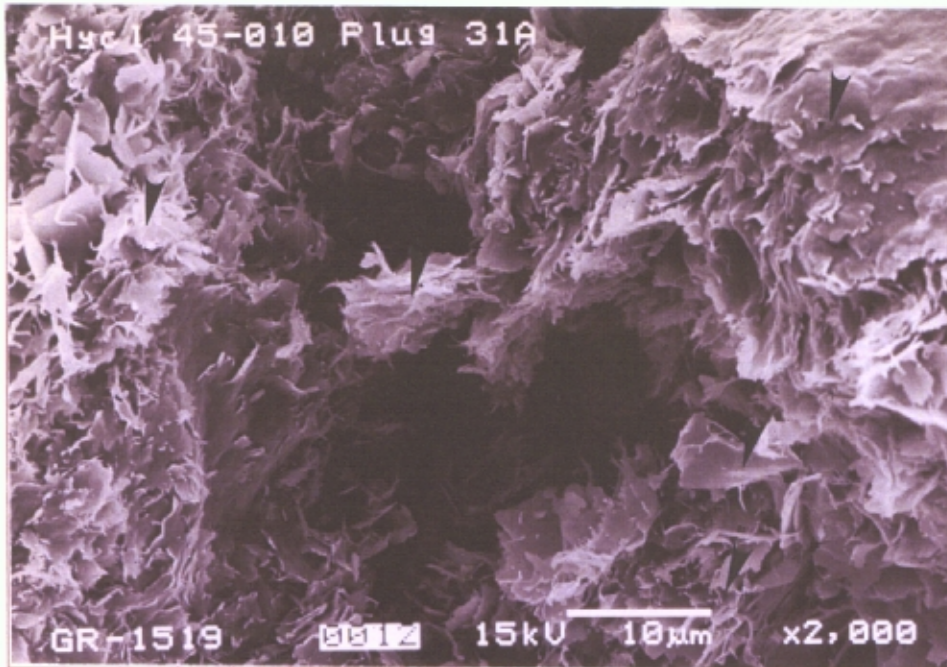
SEM Photomicrographs and Descriptions Plate 08
Stratos Fed #1
Argillaceous Sublitharenite
Porosity 7.7% (1.0%*) Permeability 0.11md

Sample No Hy-31a: 16,063.20ft

- A** Illite clays (arrows), coat the grains surrounding the pore (photo centre) and partly occlude the pore. Micro-porosity is preserved in the clay fabric. **X2000**
- B** Shows micro-porosity (arrows) preserved in a partly leached chert grain. **X2000**
- C** Micro-fractures (photo centre) are artificial but could have contributed the permeability as determined by conventional core analysis. Illite clays coat grains and occlude pores. **X4500**

*** Thin Section Porosity**

| | |
|----------|----------|
| A | B |
| C | D |

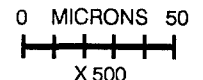
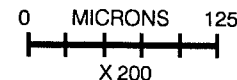
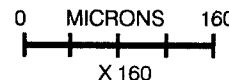
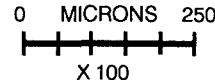
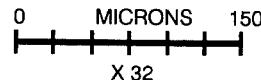
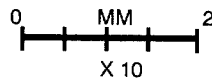
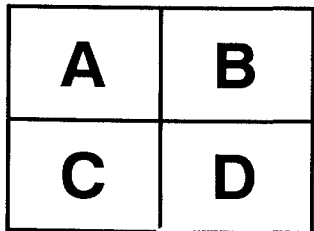


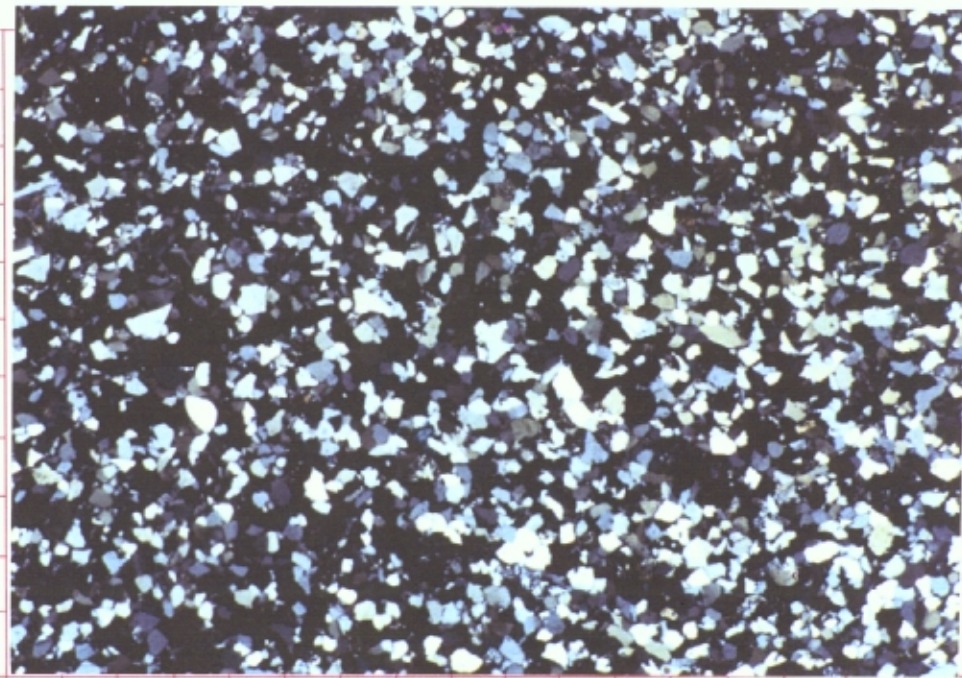
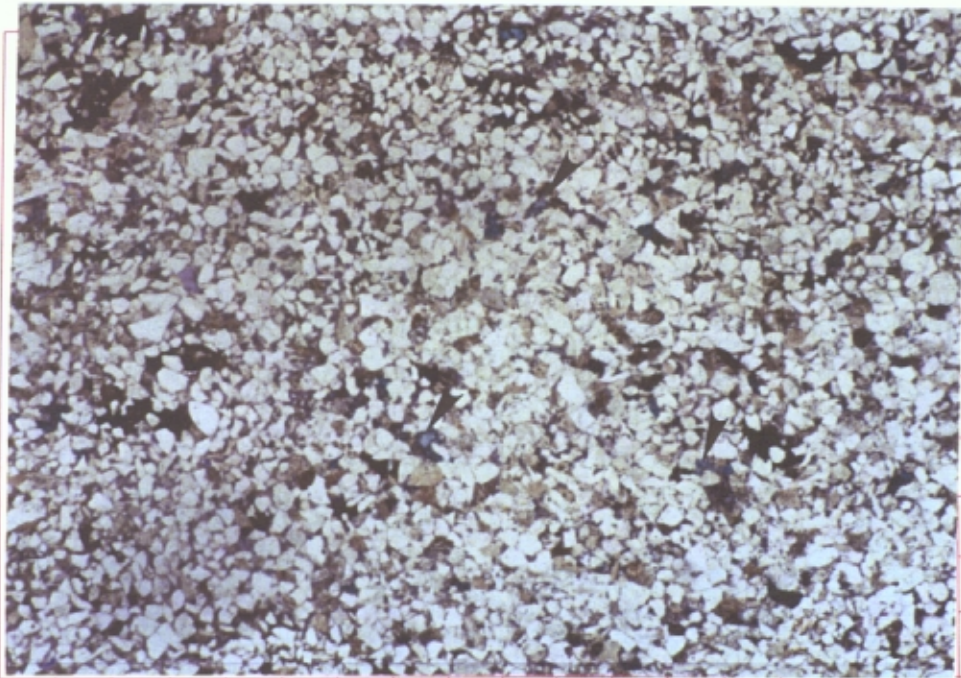
Thin Section Descriptions Plate 09
Stratos Fed #1
Argillaceous Sublitharenite
Porosity 10.9% (2.0%*) Permeability 0.13md

Sample No Hy-37: 16,069.20ft

A-D Moderately sorted, upper fine grained, quartzose sublitharenite with low effective porosity and low permeability. Irregularly distributed ferroan calcite (arrows) occludes a few pores and replaces or partly replaces grains, matrix and earlier quartz cements. Matrix illite clay (brown) compacted between grains lowers the reservoir quality. Micro-porosity is preserved in matrix clays and in scattered leached grains. The sandstone framework is dominated by angular to sub-rounded monocrystalline quartz grains (grey and white on B and D) and contains small volumes of chert, feldspar and plutonic rock fragments. **Photos A and B PPL,XP X10; Photos C and D PPL,XP X32**

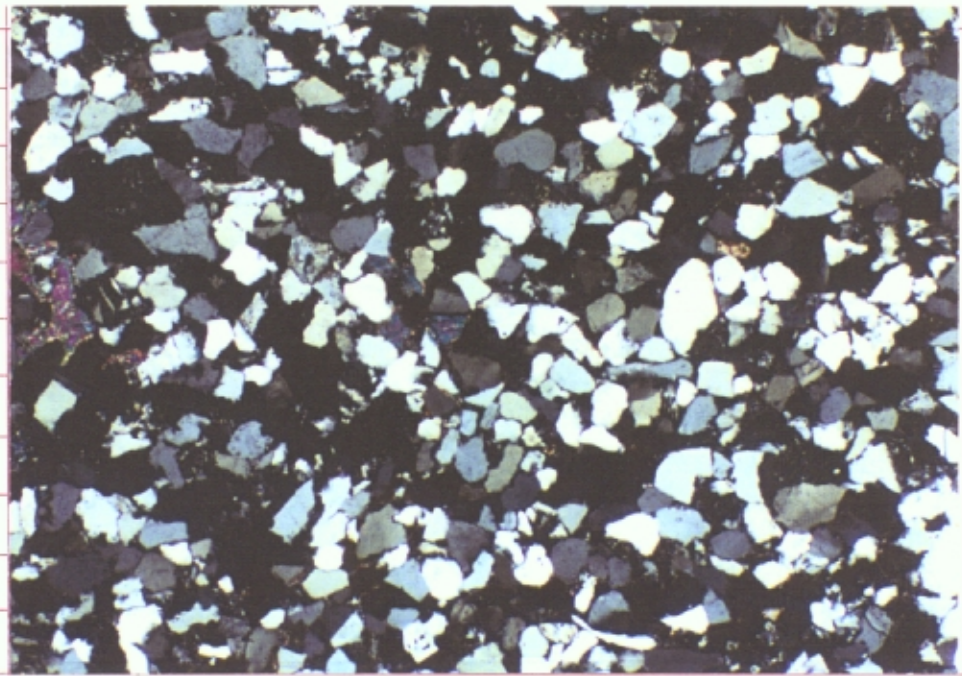
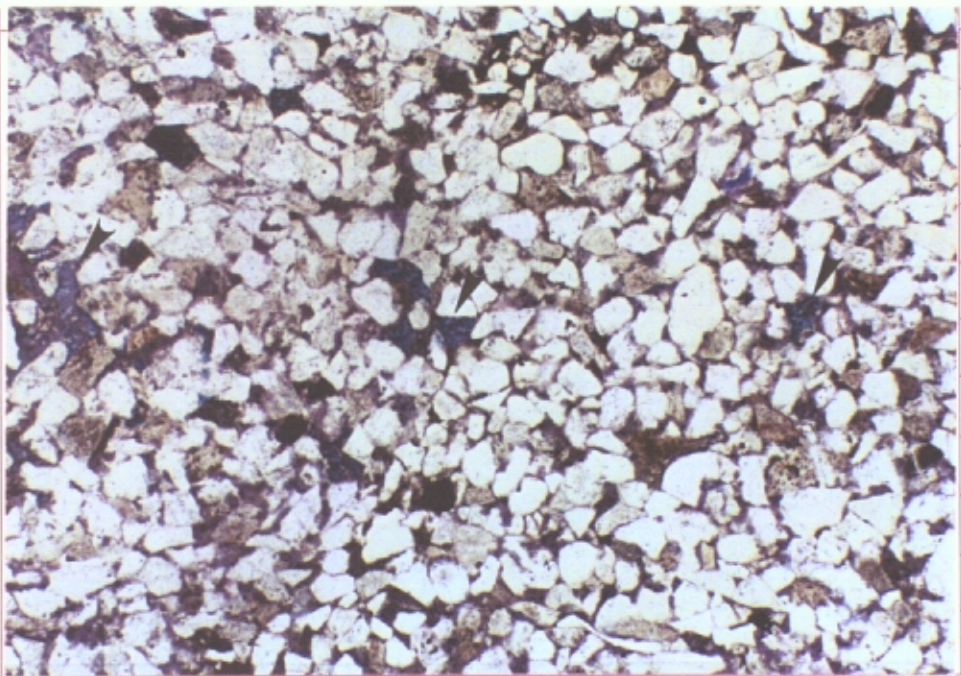
*** Thin Section Porosity**





A B C D E F G H I J K L M N O P Q R

A B C D E F G H I J K L M N O P Q R

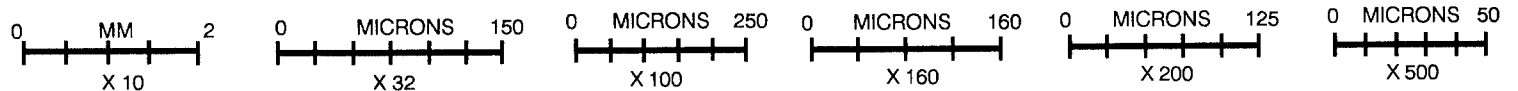
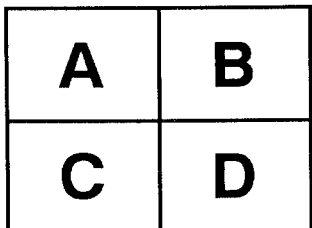


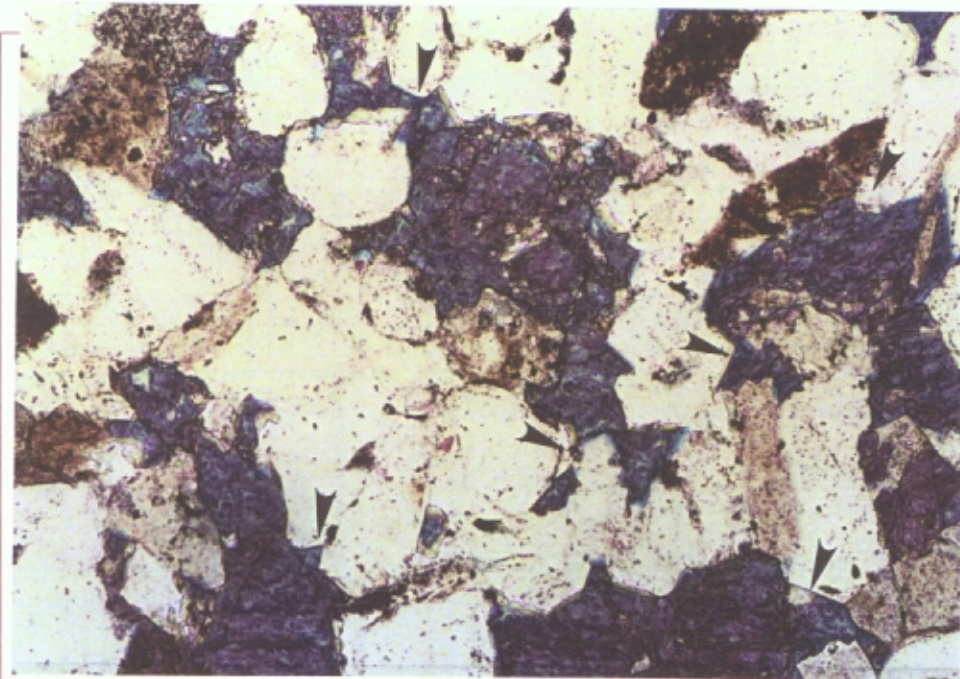
Thin Section Descriptions Plate 10
Stratos Fed #1
Argillaceous Sublitharenite
Porosity 10.9% (2.0%*) Permeability 0.13md

Sample No Hy-37: 16,069.20ft

- A** Ferroan calcite (stained blue), emplaced after cementation by authigenic quartz (arrows) cements porosity and replaces grains, matrix and earlier cements. If an equivalent sandstone were in a diagenetic regime where calcite could dissolve, good reservoir quality could form in these sandstones. Reservoir quality in this sandstone has been eliminated by the effects of compaction and cementation by quartz and calcite. **PPL X100**
- B** Shows compacted clays and clay clasts (arrows) that greatly lower the reservoir quality of the sandstone. A few isolated pores (large white arrow) are present. Micro-porosity is preserved in clay fabrics. **PPL X100**
- C-D** Show at moderate and high magnification micro-porosity (arrows) in matrix illite clay **Photo C PPL X200, Photo D PPL X500**

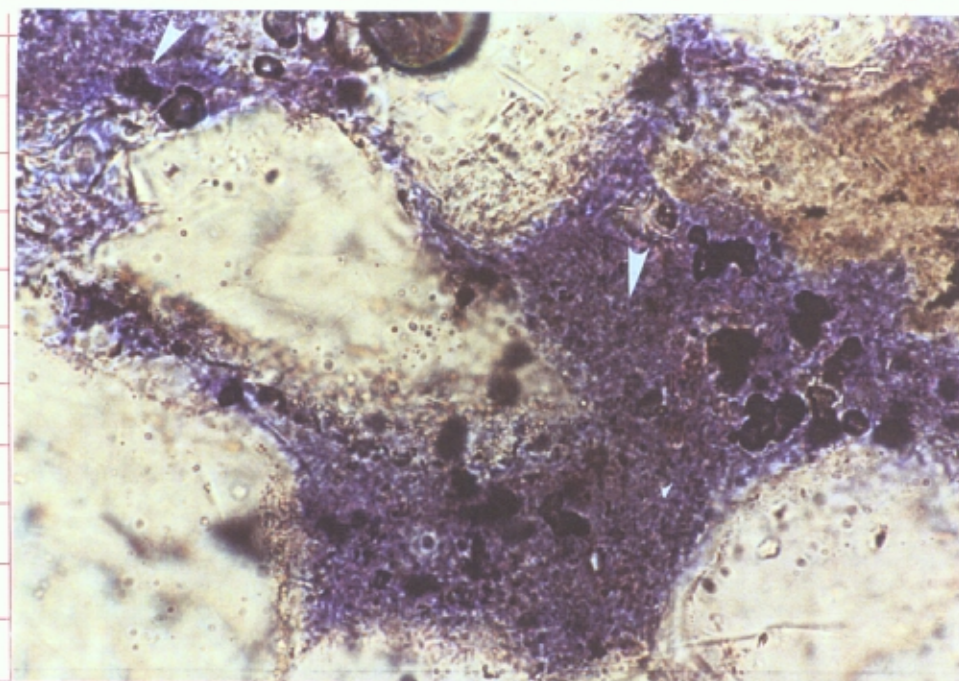
*** Thin Section Porosity**





A B C D E F G H I J K L M N O P Q R

A B C D E F G H I J K L M N O P Q R



A B C D

A B C D



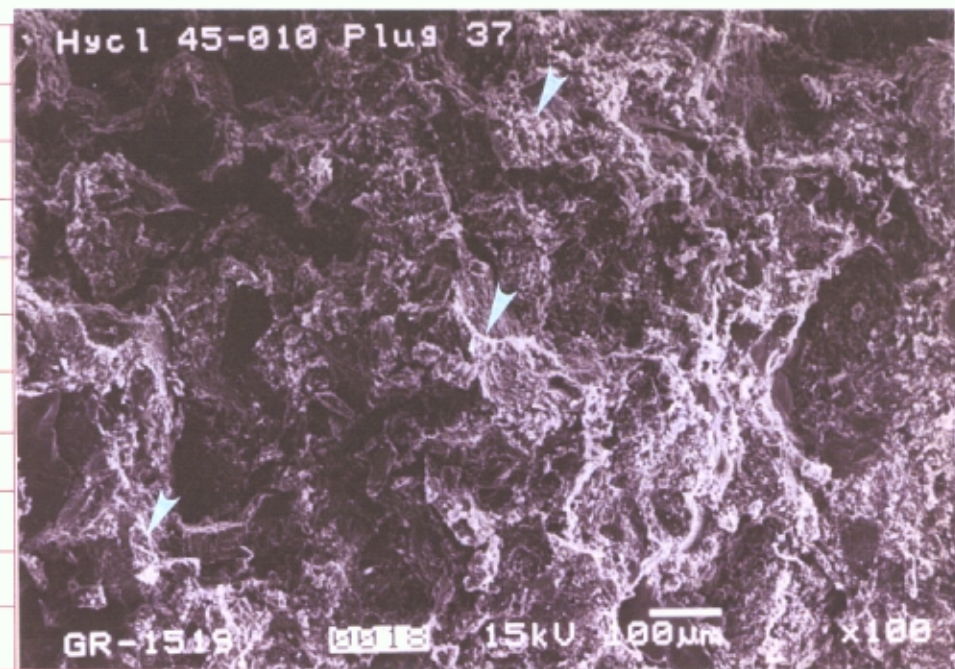
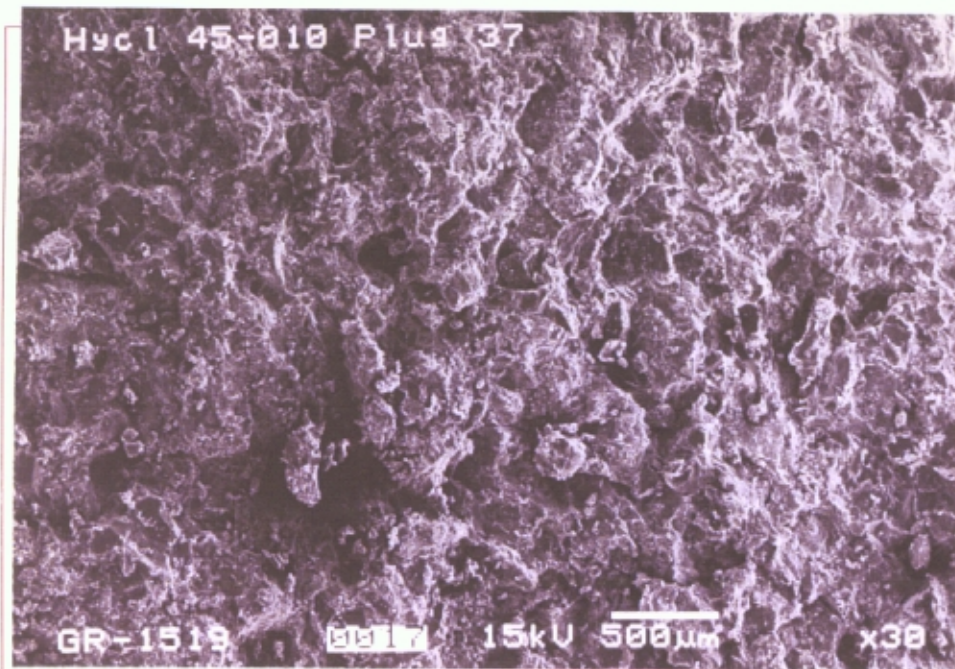
SEM Photomicrographs and Descriptions Plate 11
Stratos Fed #1
Argillaceous Sublitharenite
Porosity 10.9% (2.0%*) Permeability 0.13md

Sample No Hy-37: 16,069.20ft

A-D Variably argillaceous and partly ferroan calcite cemented, upper fine grained, quartzose litharenite with isolated modified intergranular and grain moldic pores that are lined and bridged with illite clays (arrows). Micro-porosity is preserved in the clay fabrics. **Photo A X30, Photo B X100, Photo C X500 Photo D X1500**

*** Thin Section Porosity**

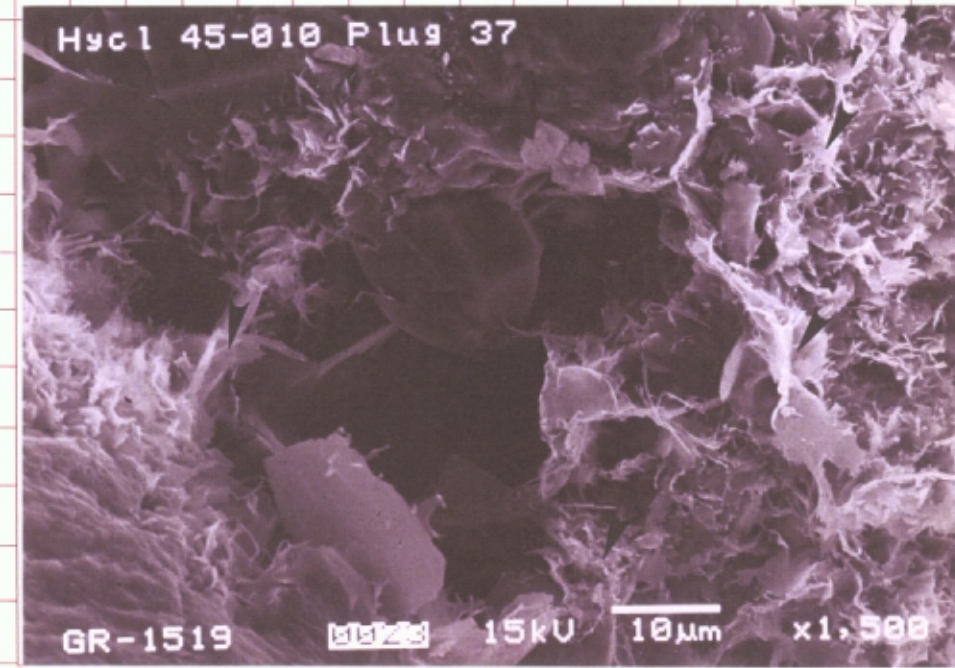
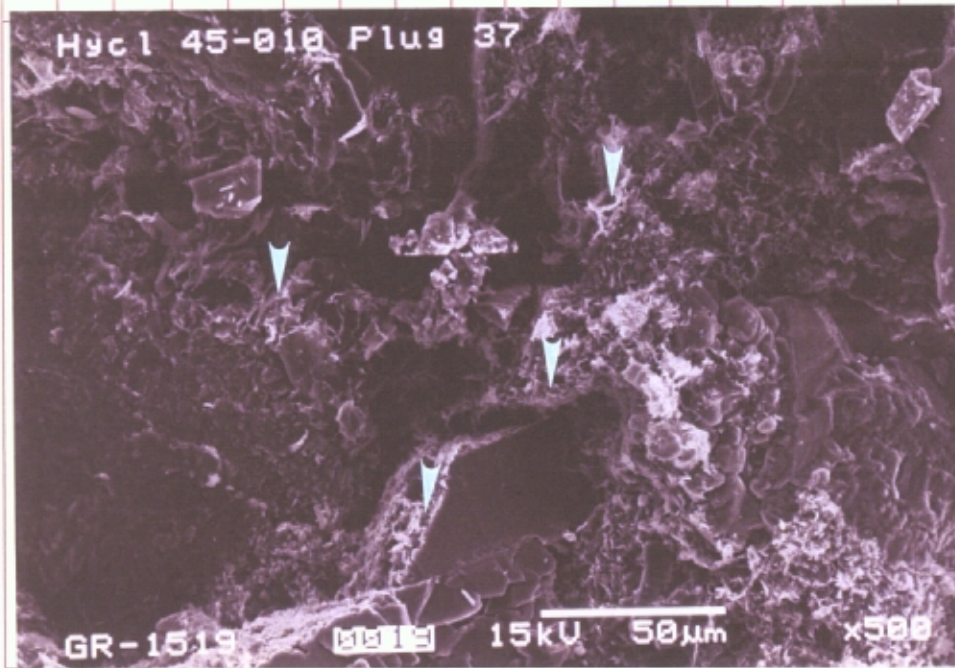
| | |
|----------|----------|
| A | B |
| C | D |



A B C D E F G H I J K L M N O P Q R

A B
C D

A B C D E F G H I J K L M N O P Q R



SEM Photomicrographs and Descriptions Plate 12
Stratos Fed #1
Argillaceous Sublitharenite
Porosity 10.9% (2.0%*) Permeability 0.13md

Sample No Hy-37: 16,069.20ft

A A modified intergranular pore (photo centre), preserved between a quartz grains and a lithic grain (left) is lined and partly occluded by micro-porous illite clays. **X2000**

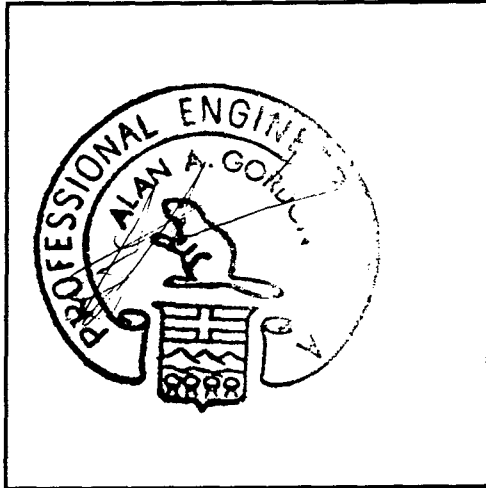
*** Thin Section Porosity**

| | |
|----------|----------|
| A | B |
| C | D |

Date: April 1996

Project: Petrology - (UPRC Fed #1)

Professional: A.A. Gordon, P.Eng.



| |
|--|
| <p>PERMIT TO PRACTICE GR Petrology Consulting Inc</p> <p>Signature <u>[Signature]</u></p> <p>Date <u>Apr 96</u></p> <p>PERMIT NUMBER: P 5829</p> <p>The Association of Professional Engineers Geologists and Geophysicists of Alberta</p> |
|--|

Appendix C
Within Appendix C

Reductions in the Productivity of Oil and Low Permeability Gas Reservoirs Due to Aqueous Phase Trapping

D B BENNION, R F BIETZ, F B THOMAS
 Hycal Energy Research Laboratories Ltd
 M P CIMOLAI
 Canadian Hunter Exploration Limited

Abstract

Many hydrocarbon bearing reservoirs exhibit the potential for significant productivity reductions due to adverse relative permeability effects associated with the retention of invaded aqueous fluids. These fluids could include water-based drilling mud filtrates, completion fluids, fracture fluids, workover fluids, kill fluids or stimulation fluids (including spent acid).

This paper identifies potential mechanisms behind phase trapping and identifies particular reservoir types which tend to be susceptible to this type of formation damage, most notably low initial water saturation gas reservoirs and strongly oil-wet oil reservoirs. Laboratory techniques to investigate the severity of aqueous trapping and various remedial techniques are described, and two field case studies illustrating the potential for permeability impairment due to invasive aqueous trapping are presented. One case study describes a series of wells completed in the Paddy formation and the second in the Cadomin formation in the Deep Basin area of central Alberta (both gas producing zones). Laboratory case studies documenting the phenomenon of aqueous phase trapping in strongly oil-wet porous media are also presented.

Introduction

Oil and gas bearing formations are potentially susceptible to many different types of formation damage.¹⁻⁶ In this paper we are exclusively concerned with damage associated with aqueous phase trapping (or water trapping or blocking as it is often referred to). To understand the concept of aqueous phase trapping, it is essential to differentiate between the concept of initial (often referred to as connate) aqueous phase saturation ($S_{w,i}$) and irreducible aqueous phase saturation ($S_{w,irr}$).

- Initial aqueous phase saturation is the initial average fractional portion of the pore space which is occupied by water. The value of the initial aqueous phase saturation is controlled by numerous factors, including reservoir geology, depositional history, temperature, wettability, height above free water contact and pore size distribution. The key point to differentiate in this area is that the initial aqueous phase saturation is not necessarily, and often is not, equal to the irreducible aqueous phase saturation and can be either higher or lower than the irreducible saturation. It is in the second case, where the $S_{w,i}$ is less than $S_{w,irr}$, where productivity

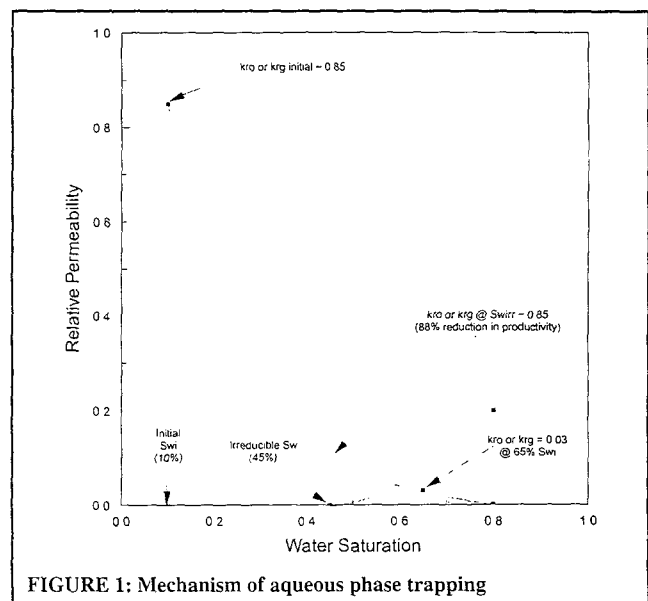


FIGURE 1: Mechanism of aqueous phase trapping

reductions due to phase trapping can occur

- Irreducible aqueous saturation represents that saturation which is forced to exist in the reservoir by capillary mechanics. Once again, the value of the $S_{w,irr}$ is determined by parameters such as the reservoir morphology, pore size distribution, pore throat size distribution, wettability, surface roughness, etc. We often obtain estimates of $S_{w,irr}$ through the use of air-brine or air-mercury capillary pressure tests. Although these values often provide good approximations to $S_{w,irr}$, they may be poor indications of actual $S_{w,i}$.

Mechanism of Aqueous Phase Trapping

Figure 1 provides an illustrative example of a set of relative permeability curves. The diagram is applicable to either an oil or a gas reservoir. Examination of Figure 1 indicates that, if the zone of interest is at some aqueous saturation greater than the irreducible value of 45%, aqueous trapping will not be a severe problem because the reservoir is already initially highly saturated with water and may even be producing free mobile brine. We can see that if this is the case, the initial productivity of the reservoir will already have been substantially reduced due to an unavoidable, pre-existing, high aqueous phase saturation.

TABLE 1: Water carrying capacity of dry natural gas at selected temperatures and pressures⁽⁹⁾.

| Temperature (°C) | kg-H ₂ O/10 ³ m ³ gas at T & P | | | |
|---------------------|---|-------|-------|--------|
| | Pressure (kPag) | | | |
| | 101.3 | 1380 | 10340 | 27570 |
| 15.6 | 14.0 | 16.3 | 23.5 | 46.2 |
| 40 | 51.5 | 56.3 | 84.6 | 125.4 |
| 60 | 139.2 | 141.6 | 194.4 | 282.0 |
| 80 | 328.0 | 310.8 | 400.3 | 578.2 |
| 100 | 539.0 | 609.0 | 789.0 | 1136.7 |

One factor which characterizes some gas reservoirs and most strongly oil-wet reservoirs is the fact that they exhibit abnormally low initial water saturations. It is not at all unusual for strongly oil-wet carbonate or sandstone formations to exhibit initial water saturations of less than 5%, and these saturations are, in general, fairly independent of the permeability distribution which exists in the reservoir. Gas reservoir aqueous saturations vary with some instances of near zero initial water saturation being observed in numerous Michigan reef gas reservoirs⁽⁷⁾, although in most situations a finite but low (e.g., 10-25%) initial aqueous saturation exists.

The phase trap occurs when the formation is invaded by the aqueous phase. Examination of Figure 1 illustrates that the formation basically "springs" back to its true irreducible water saturation once exposed to aqueous fluid. The formation initially absorbs water in a spongelike fashion until the irreducible water saturation is achieved and the aqueous phase achieves a finite relative permeability value and hence becomes mobile and begins to flow in the pore system.

It is obvious from Figure 1 that the severity of the reduction in productivity due to an aqueous phase trap will depend on

- The difference between the "initial" S_{wi} and the true "irreducible" S_{wirr} . The larger the difference, the greater the potential permeability reduction (e.g., if S_{wirr} had been 65% instead of 45% in our example in Figure 1, one can see that the Kro or Krg would have been further reduced to only 0.03).
- The configuration of the gas or oil phase relative permeability curve in the region between S_{wi} and S_{wirr} . Obviously, if this curve is relatively linear (as shown by the dashed line in Figure 1), the damage would be much less than for the presented example of a typical convex set of gas-liquid or water-oil relative permeability curves. Conventional relative permeability measurements are usually conducted above S_{wirr} and thus provide little information on this phenomenon.
- Saturation hysteresis effects altering the location of S_{wirr} . In some cases, experimental evidence⁽⁸⁾ indicates that the actual value of the irreducible liquid saturation can be altered by contact angle hysteresis effects induced by cyclic saturation changes. This phenomenon will be discussed in greater detail in the following sections.
- Depth of invasion of the aqueous phase into the reservoir.

Origin of Abnormally Low S_{wi}

A major question which always arises in the discussion of water-trapping phenomenon is not so much the existence of the water block, but how the reservoir matrix attained this abnormally low initial water saturation in the first place. Theoretically speaking, given the constraint imposed by Figure 1, if an oil or gas

reservoir was initially 100% saturated with brine prior to oil or gas influx, there should be no way that the saturation could have been reduced below S_{wirr} as the aqueous phase has no mobility at saturations below that level.

There are several hypotheses as to why this may occur; in fact the phenomenon may be related to a combination of these hypotheses (or possibly to phenomenon not yet defined).

- Vapourization (gas reservoirs) – Due to the fact that the reservoir is created over geologic time, it is possible that, early in the history of the reservoir, both temperature and pressure were much less when initial gas invasion occurred. Table 1 illustrates the water carrying capacity of natural gas⁽⁹⁾. One can see that dry gas at 27570 kPag and 100°C is capable of vapourizing and holding 1,136.7 kg/10³m³ of water vs only 14.0 kg/10³m³ at 101.3 kPag and 15.6°C. Therefore, it can be seen that a desiccation effect could occur. If one goes through the calculations, one finds that gas throughput would have had to be quite large for a significant reduction in S_{wi} to occur due to this mechanism, but over geologic time such a large, regional migration of gas is certainly possible. Localized tectonic activity after deposition, creating high geothermal gradients may also have been a contributing factor in water vapourization in some instances.
- Changes in pore geometry (due to overburden compression and diagenesis) – The original depositional environment of the reservoir likely exhibited higher porosity and permeability characteristics during initial migration of hydrocarbons into place. This higher reservoir quality may have resulted in a much lower initial irreducible water saturation. Over geologic time, overburden pressure increased causing compaction and a reduction in porosity and pore size distribution. Reservoir diagenesis processes contribute to the potential formation of high surface area clays and other authigenic materials containing microporosity resulting in an overall reservoir quality reduction and less favourable capillary pressure characteristics. This would result in a much higher S_{wirr} value, but, if no additional water influx occurred, the reservoir water saturation would remain at its original lower value, now at some value less than S_{wirr} .
- Adsorption – It is known that most clays and many reservoir minerals (e.g., Anhydride) will react with water to form hydrated complexes⁽⁷⁾. This physical adsorption process would result in a portion of the effective water being potentially removed from the pore space and hydrated into the clays (if the clays are formed authigenically).
- Irreducible saturation hysteresis effects – Various authors⁽¹⁰⁾ have documented that the presence of an initial wetting phase saturation tends to enhance the spontaneous imbibition of that fluid (i.e., tends to make it even more strongly wetting). This being the case, one would expect that there

TABLE 3: Conditions causing potential aqueous trapping phenomenon.

| Increasing Severity of Water Trap Potential | Decreasing Severity of Water Trap Potential |
|---|--|
| 1 Strongly oil-wet reservoir with very low (<10%) S_{wi} . Severity appears related to reducing reservoir quality in many cases | 1 Neutral to water-wet oil reservoirs with typical water saturations for the permeability range under consideration (i.e. $S_{wi} \geq S_{wirr}$) |
| 2 Gas reservoir (any permeability) exhibiting unusually low S_{wi} (generally <20%) | 2 Gas reservoir (any permeability) with $S_{wi} \geq S_{wirr}$ |
| 3 Low permeability gas reservoirs exhibiting higher S_{wi} s, but at values still less than S_{wirr} . | 3 Low permeability gas reservoir exhibiting high $S_{wi} \geq S_{wirr}$ |
| 4 High rates of uncontrolled aqueous fluid loss to the formation due to poor fluid loss control or extremely overbalanced treatment operations (i.e. overbalanced drilling, fracturing, etc.) | 4 Wells with low or zero fluid loss to the formation due to superior fluid loss control (artificial bridging agents, etc.) |
| 5 Multiple cycles of aqueous fluid invasion in a given zone | 5 Eliminating or minimizing cycles of aqueous invasion |

er retained water saturation. The trapped location of these globules of water in the central portion of the pore space will have a greater reducing effect on oil phase permeability than in the initial low S_{wi} state observed at the conclusion of Phase 2.

Laboratory Verification of Aqueous Phase Trapping in Strongly Oil-wet Porous Media

Table 2 summarizes the results of three reservoir condition coreflow tests conducted on preserved state strongly oil-wet sandstone core samples. The cores utilized in these tests had never been previously contacted with water, being exclusively drilled and cored with hydrocarbon based fluids. Examination of the initial water saturations of the three preserved samples indicated very low initial values ranging from 2.5 to 4.5%, consistent with the strongly oil-wet nature of the rock. Initial permeability of the samples to oil at the initial S_{wi} varied from 51.8 to 156.6 mD. Each sample was then flushed with a non-damaging equilibrium formation brine, and then reflushed to irreducible water saturation at field realistic drawdown pressure gradients of 4,000 kPa per metre. Examination of the data indicates that the irreducible saturation increased from less than 5% in all cores to the range of 20% to 34%. This resulted in a 93%-96% reduction in effective oil permeability, clearly illustrating the reducing effect of the establishment of an aqueous block on oil phase permeability.

Reservoir Processes Which Can Cause a Water Trap and Reservoir Types Susceptible to Damage

The potential for aqueous phase trapping occurs anytime an aqueous fluid invades an abnormally low initial water saturation reservoir. These fluids could include:

- Water based drilling fluid filtrates
- Cement filtrates
- Water based completion fluids
- Water based workover fluids
- Water based kill fluids
- Water based stimulation fluids

Table 3 provides a comparative summary of conditions which tend to increase or decrease the potential severity for aqueous trapping in selected situations. These guidelines are based upon general experience and should not be taken as indicative of all potential reservoir scenarios.

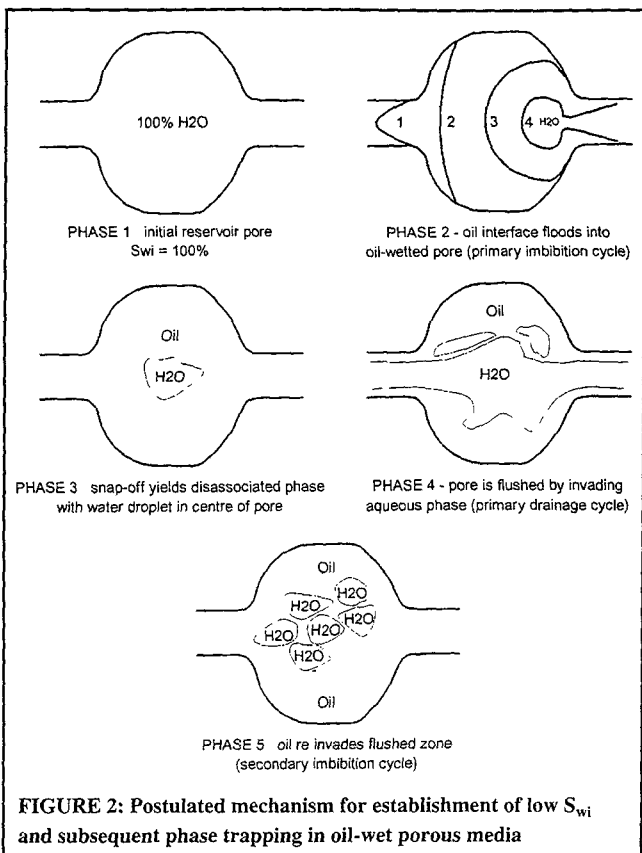


FIGURE 2: Postulated mechanism for establishment of low S_{wi} and subsequent phase trapping in oil-wet porous media

TABLE 2: Illustration of Aqueous phase trapping in strongly oil-wet porous media

| Core # | Initial S_w | Koif (mD) | Post-Water Flush S_w | Koif (mD) | % Reduction in Oil Permeability |
|--------|---------------|-----------|------------------------|-----------|---------------------------------|
| 1 | 0.0395 | 156.6 | 0.2255 | 5.83 | 96.3% |
| 2 | 0.0259 | 51.8 | 0.2057 | 3.42 | 93.4% |
| 3 | 0.0453 | 132.3 | 0.3411 | 5.83 | -95.6% |

could be differences in the irreducible saturation obtained if multiple cycles of drainage and imbibition of water were conducted versus only a single primary cycle. This phenomenon for a strongly oil-wetted system is illustrated in Figure 2(11). The specific mechanisms presented in Figure 2 are detailed in the following paragraphs.

Initially (Phase 1), the porous media is 100% saturated with the non-wetting phase (water). Phase 2 (steps 1-4) shows various positions of the oil-water interface, as a function of time, as oil invades the pore and wets the rock with a relatively high contact angle (about 160° in this example). This results in a very efficient displacement of water from the pore except for a small discontinuous globule (Phase 3) which is created by snap-off phenomenon. The magnitude of the initial water saturation created by this phenomenon will be influenced by the ratio of pore throat to pore diameter.

Subsequent invasion by an aqueous fluid (Phase 4) results in a preferential channelling of the aqueous phase through the central portion of the pore. As the invaded water contacts the initial water present in the centre of the pore, the potential for the establishment of droplets of encapsulated water, separated by thin films of oil, exists (depending on interfacial tension, oil and water properties and pore geometry).

Subsequent re-invasion of the oil phase (Phase 5) results in the phenomenon of the advancing oil interface now contacting a variety of irregular potential oil-water interfaces instead of the initial uniform displacement (illustrated in Phase 2). This results in the potential for the generation of multiple stable oil-water interfaces and a potential for a large-

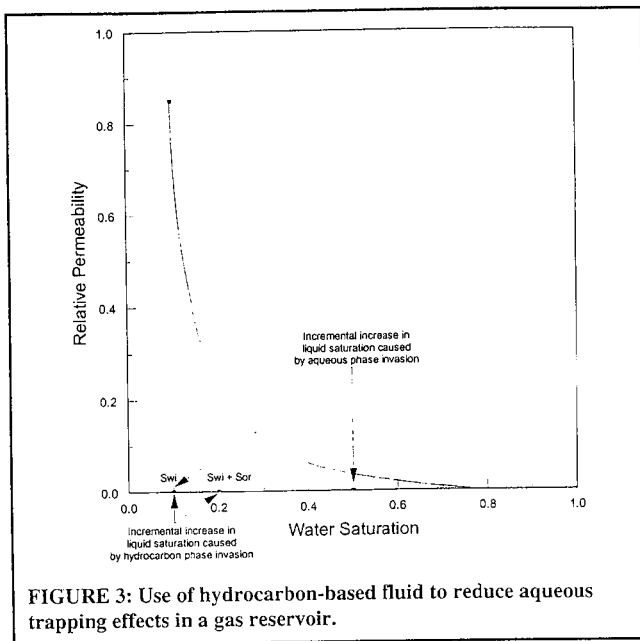


FIGURE 3: Use of hydrocarbon-based fluid to reduce aqueous trapping effects in a gas reservoir.

Minimizing Potential for Aqueous Trapping in the Field

If productivity reductions due to aqueous phase trapping are identified as a potential problem source for a given reservoir, the following options should be considered:

- a) Avoid the use of water based drilling, completion or stimulation fluids in the reservoir, if economically and technically feasible. It is obvious that use of a hydrocarbon fluid which will be miscible with the reservoir crude oil is an advantage in an oil system as this eliminates the potential for any type of an aqueous trap. This, of course, assumes that the introduced fluid itself does not cause any deleterious incompatibility effects (e.g., asphaltene precipitation, sludges).

Hydrocarbon fluids may also have particular application in gas reservoirs where water trapping occurs. It is obvious that, if we introduce a hydrocarbon based fluid into a reservoir initially containing only gas and water, we will establish a trapped hydrocarbon saturation. Since the vast majority of dry gas reservoirs exhib-

it strongly water-wet behaviour (unless there is some immobile initial liquid hydrocarbon saturation present in the pore space which could cause an oil-wetted state), the entrained hydrocarbon saturation will be encapsulated in the central portion of the pore and will often be much less in its total magnitude than the additional liquid saturation which may have been entrapped had an aqueous fluid been introduced into the system. This phenomenon is further detailed in Figures 3 and 4 and two field case histories follow illustrating this type of reservoir behaviour.

The use of a hydrocarbon fluid in a gas reservoir situation could be contraindicated in situations where:

- i) Permeability is very low causing a greater capillary retention of hydrocarbons.
- ii) An initial and potentially wetting immobile or mobile liquid hydrocarbon saturation is present.
- iii) The reservoir contains potential minerals which may be naturally oil-wet (i.e., pyrobitumen, graphite, talc, coal, sulphur, sulfides, etc.).

If a potential for oil-wetting in a gas reservoir is apparent, the reservoir may retain an undesirably high oil saturation, increasing the relative apparent damage (comparable or worse than that induced by the use of water-based fluids).

If aqueous fluids must be utilized due to economic or technical considerations, minimizing the depth of the flushed zone is crucial in minimizing damage. This would include consideration of low fluid loss systems, artificial bridging agents, balanced or underbalanced drilling operations, use of air drilling or gaseous based frac fluids, etc.

Methodologies for Removing Existing Aqueous Traps

Various methodologies have been attempted by different operators to attempt to stimulate reservoirs damaged by aqueous phase trapping phenomenon. A major problem in most cases is ensuring that the injected treatment fluids come into contact with the affected zone. This may require several cyclic type treatments of gradually increasing radius in certain situations. Common stimulation treatments include:

- a) Injection of CO₂ gas (dissolves in trapped water, increases available blowdown energy to produce water, can lower gas-liquid interfacial tension).
- b) Injection of a mutual solvent (usually methanol), sometimes

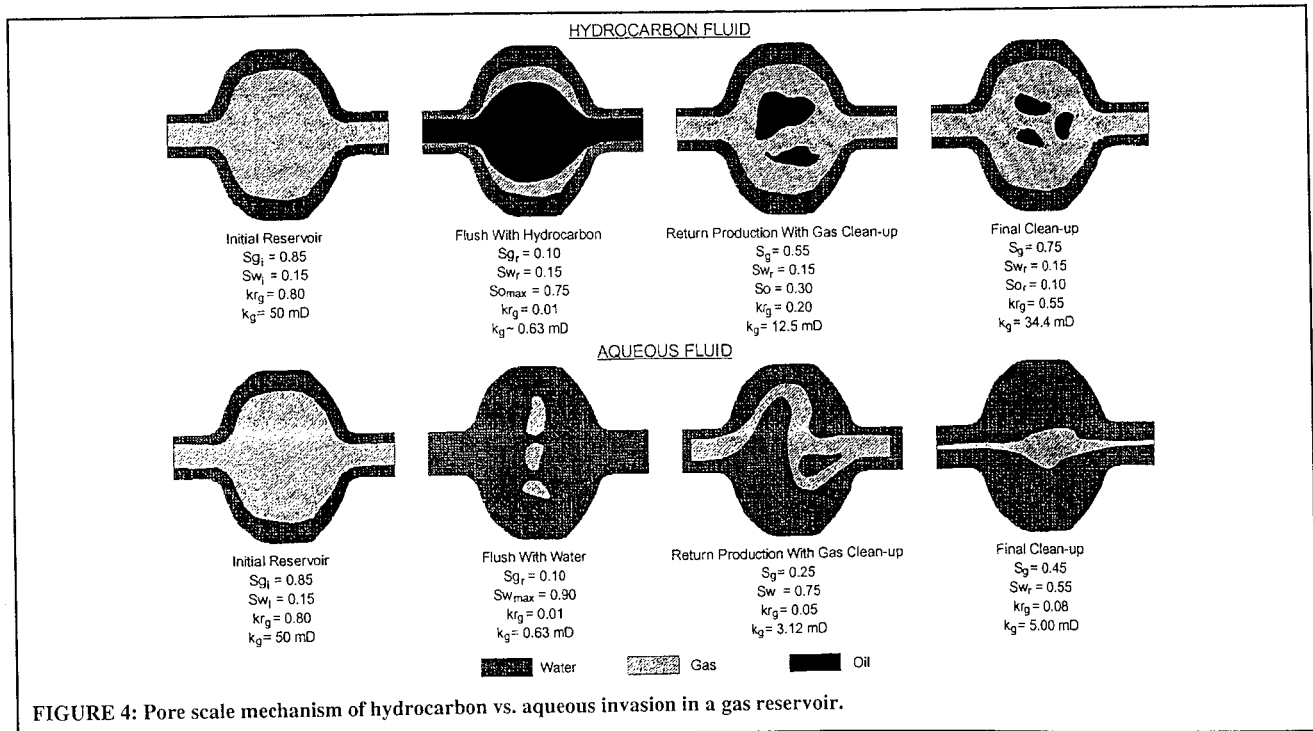


FIGURE 4: Pore scale mechanism of hydrocarbon vs. aqueous invasion in a gas reservoir.

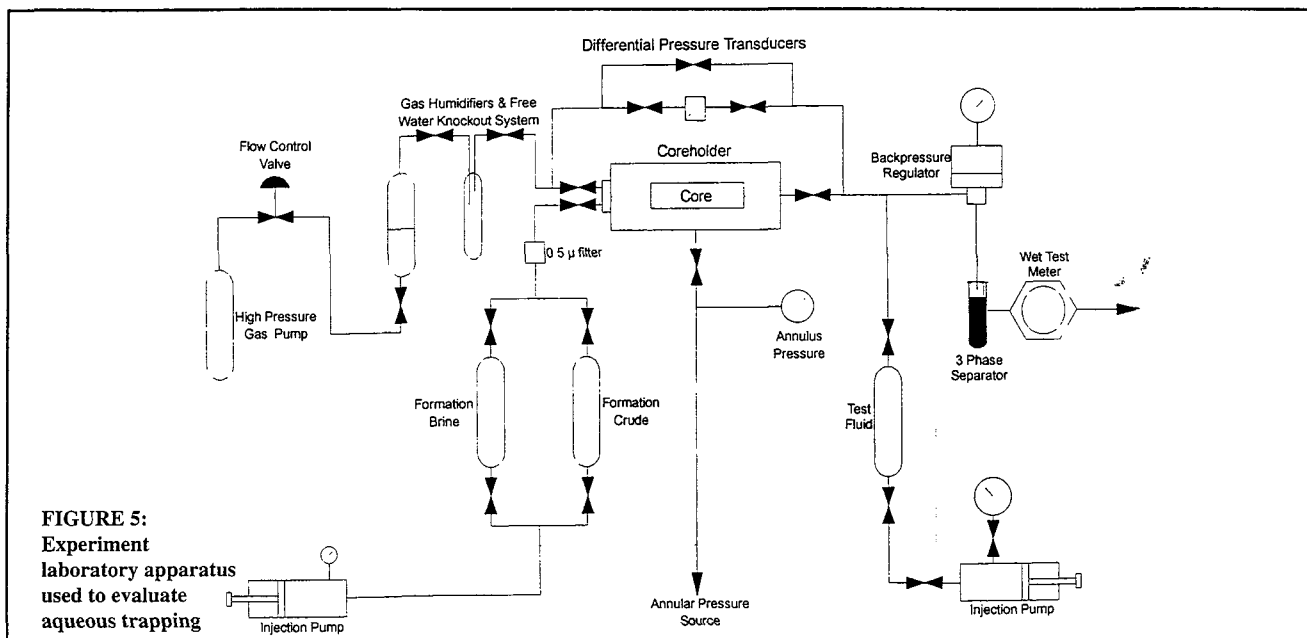


FIGURE 5:
Experiment
laboratory apparatus
used to evaluate
aqueous trapping

- in conjunction with CO₂. This type of treatment has experienced the most success in field experimentation with gas reservoirs. Heavier alcohols are often used for oil reservoir applications (i.e., isopropanol, butanol)
- Evaporation of the water in the trapped zone by extended duration dry (desiccated) gas injection
 - Hydraulic fracturing beyond the trapped zone (providing a suitable fracture fluid which does not aggravate existing damage problems can be formulated)

Laboratory Techniques to Evaluate the Potential for Water Trapping Phenomenon

Recent developments in laboratory special core analytical techniques have made it possible to ascertain formation sensitivity to aqueous trapping and to evaluate and optimize potential fluid systems for use in the field. Ideally, laboratory tests should duplicate reservoir conditions of temperature, pressure and overburden pressure as closely as possible. Aqueous trapping tests can follow a number of different types of procedures, but the most common is as follows:

- Obtain samples of representative reservoir core material. Full diameter samples may be required if the formation is particularly heterogeneous. Preserved state core samples (at the correct S_{wi}) or restored state core samples at correct initial oil and water saturations must be utilized for oil reservoirs and core material at the correct initial S_{wi} (or S_{wi} and S_{oi} if liquid hydrocarbons are present) must be utilized for gas reservoirs. Specialized handling and restoration techniques must be utilized to obtain the correct initial sub-irreducible saturations which are important in quantifying aqueous trapping effects.
- Aqueous phase saturation is gradually introduced by precisely metering and dispersing fluid throughout the sample. Permeability measurements to humidified equilibrium gas or oil are measured at specified saturation levels to note how increasing water saturation reduces relative permeability.
- Once the irreducible water saturation is exceeded, mobile water begins to be produced from the core. This allows us to ascertain the difference between the initial permeability at S_{wi} vs the apparent permeability which will result at S_{wirr} if the reservoir is contacted by an aqueous phase.

Using this type of methodology, a figure similar to Figure 1 can be generated for any particular system. This will provide an indication of the severity of the effects which may potentially be expected due to an aqueous phase trap and the value of the true S_{wirr} in comparison to the initial S_{wi} . Good initial S_{wi} data are cru-

cial and are best obtained from analysis of oil based core or log data where a combination of deep/shallow induction logs indicate that near wellbore flushing effects have not affected the values of the log measured water saturations. Data from water based cores and wells which have experienced extensive and deep fluid invasion or data from conventional relative permeability or capillary pressure tests may yield artificially high estimates of S_{wi} in some cases and should be utilized with caution.

Once an aqueous phase trap is established, additional laboratory tests can be conducted to simulate various types of stimulation treatments (i.e., mutual solvent and CO₂ flood) which may be attempted on a damaged zone to ascertain the effectiveness of these techniques prior to the expense and risk of their implementation in the field.

Figure 5 provides a schematic of the typical lab apparatus utilized for these types of experimental studies.

Field Case Studies

Case #1 – Paddy Formation

a) Reservoir Description – The Paddy “A” gas reservoir, Figure 6, in the Deep Basin area of west central Alberta, has a history of extensive formation damage among the most prolific wells in the zone. While undoubtedly many factors contribute to this problem, only recently has the importance of aqueous entrapment to formation damage in the Paddy been identified.

Discovered at a depth of 1,700 m in the late 1970’s, the pool has been on production since 1980 and has produced in excess of $4,200 \times 10^6 \text{ m}^3$ of gas to date. Characteristic of the Deep Basin, the zone was initially under pressured at an original reservoir pressure of 12,500 kPag. The formation reaches thicknesses of 25 m with an average porosity of 15%, water saturation ranges from 10 - 25%, and in situ permeabilities have values up to 800 mD. Production is sweet gas with an average methane content of 85%. A typical log profile of a well in the zone is presented in Figure 7.

In its geologic setting, the Paddy formation comprises a number of stacked, tidal and fluvial channel-fill deposits within an estuarine bay complex. The Paddy “A” pool consists of a thick accumulation of clean, uniform, well sorted medium-to-coarse-grained sands deposited under a characteristic high energy environment. The sands consist of over 90% quartz with associated cherts, calcite and minor amounts of diverse clays.

b) Previous Field Experience – During 1980, Canadian Hunter drilled four wells in the main pool with a fresh water gel chem system. Drill stem tests across two of the wells (10-6-72-11 W6

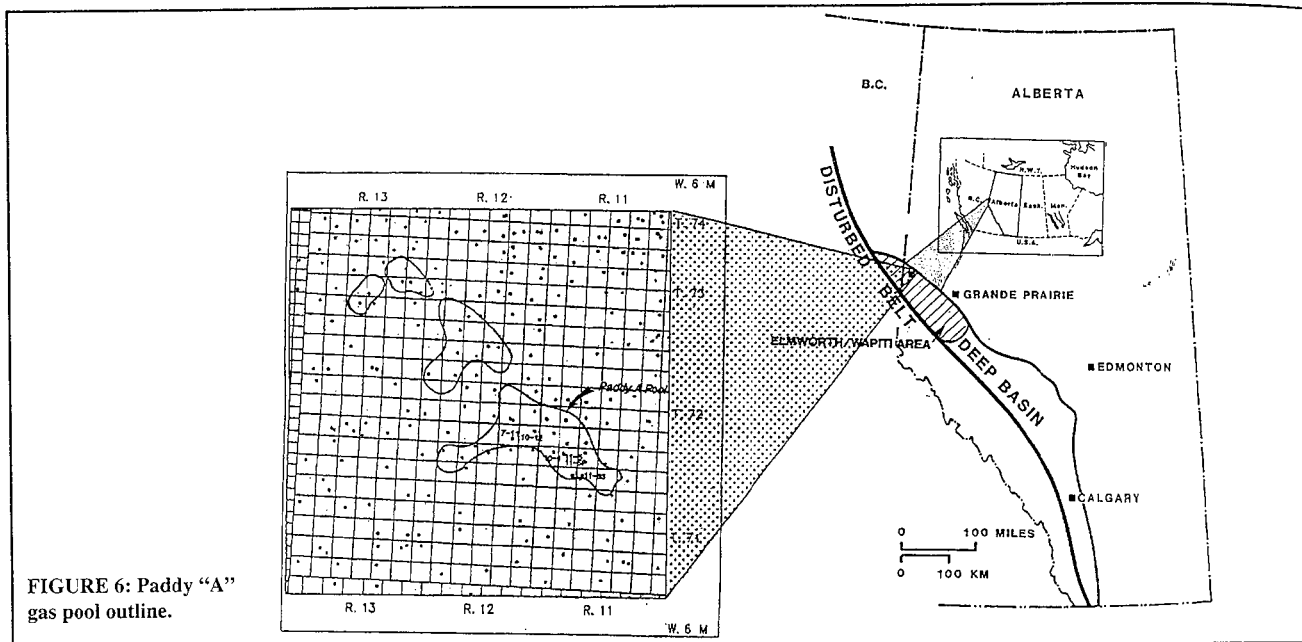


FIGURE 6: Paddy "A" gas pool outline.

and 10-12-72-12 W6) indicated little significant damage to the zone while a third well (11-5-72-11 W6) showed substantial damage with a calculated skin value of +28. Notably, the 11-5 well demonstrated considerable cleanup and had not achieved a stabilized rate over the two hour main flow. The fourth well (7-11-72-12 W6) encountered a mechanical problem during the drill stem test and could not be analysed. However, significant damage would not have been expected as the well DST'd a stable $155 \times 10^3 \text{ m}^3/\text{d}$ at an 800 kPag drawdown with no fluid recovery.

Subsequently on completion, the four wells were hydraulically fractured with 23 tonne treatments using a gelled KCl water system. Post frac production testing revealed consistently high induced formation damage across the fractures, with calculated apparent skin factors ranging as high as +51 in the 7-11 well. Multiple rate testing across the 7-11 and 10-12 wells revealed that only a minor portion of the skin effect was due to turbulence. For the 7-11 well, in particular, the calculated skin was effectively the true skin.

The wells were subsequently placed on production and further workover attempts were limited to reperforating with marginal success. By the fall of 1985, a redrill of the 11-5 location was approved and the twin 11-5 well was air drilled to the base of the zone. Upon production testing, the redrill had again been damaged through the Paddy, calculating an apparent +30 skin from buildup analysis. By contrast to the previous wells, however, the skin effect was determined to be dominated by turbulent flow with a true skin of +4. The damage induced by air drilling consequently appeared to be related to an effect of fines plugging within the formation as contrasted to the previous fluid entrapment phenomenon.

The following year in early 1986, a sixth well (11-33-71-11 W6) drilling an uphole target was extended to the Paddy off the southeastern flank of the established pool. The well encountered a prolific sand in a new lobe 800 kPag below the original pool pressure but still 5,200 kPag above the average pool pressure to the northwest. Again drilled with an aqueous gel chem system, a DST upon penetration demonstrated a moderate skin effect of +6.5 which may likely have been dominated by turbulence at the test flow rate of $350 \times 10^3 \text{ m}^3/\text{d}$. In an attempt to minimize further invasive damage, casing was run to depth but cemented above the Paddy leaving the zone open hole behind pipe. The casing was subsequently perforated underbalanced through tubing and tested at a rate of $460 \times 10^3 \text{ m}^3/\text{d}$ with a true skin of -3.3. This experience with the 11-33 well dramatically demonstrated the sensitivity of the Paddy to aqueous fluid invasion.

c) Laboratory Design Program – Recognizing the broader significance of fluid entrapment problem (in particular with respect

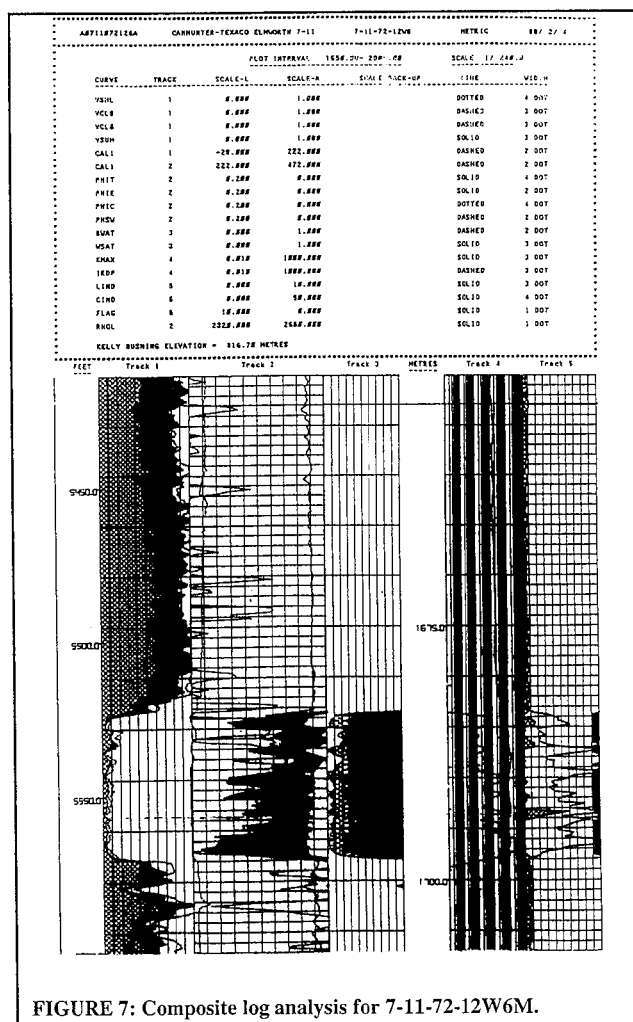


FIGURE 7: Composite log analysis for 7-11-72-12W6M.

to the water blocking effect in the deeper Cadomin formation within the Deep Basin), a program of laboratory studies was initiated in 1990 to further research this phenomenon and develop appropriate solutions. A pure hydrocarbon based drilling fluid was developed with the dual objectives of minimizing overbalance to limit fluid invasion while drilling and eliminating water from the system.

Coreflood studies were subsequently extended to the Paddy

TABLE 4: Paddy coreflood permeability summary.

| Test Phase | S _w | S _o | S _g | Measured Permeability | |
|--|----------------|----------------|----------------|--------------------------------------|-------|
| | | | | (μm) ² x 10 ⁻³ | (mD) |
| Initial Bench Air Permeability (S _w = 0.0) | 0.000 | 0.000 | 1.000 | 103.0 | 104.0 |
| Initial Brine Permeability (S _w = 1.000) | 1.000 | 0.000 | 0.000 | 45.0 | 45.6 |
| Gasflood Terminal Permeability (at initial S _{wr}) | 0.447 | 0.000 | 0.553 | 13.3 | 13.5 |
| Internal Pore Depressurization (to reduce S _{wr}) | 0.431 | 0.000 | 0.569 | - | - |
| Gas Permeability (at new S _{wr}) | 0.431 | 0.000 | 0.569 | 17.6 | 17.8 |
| Fracture Oil Displacement | 0.431 | 0.521 | 0.048 | - | - |
| Gasflood Terminal Permeability | 0.431 | 0.085 | 0.484 | 15.3 | 15.5 |

Note: all gas/fluid permeabilities reported were conducted at full reservoir conditions of 9950 kPa and 55°C

formation in which core samples, restored to conditions of original reservoir pressure and temperature, were flooded with formation brine and reverse flooded with humidified nitrogen gas to measure entrainment effects. Following this, a light condensate was used in place of brine repeating the cycle to evaluate the effects of potential hydrocarbon invasion in the zone.

The results of an example run are tabulated in Table 4. Initial bench permeability of the core sample to air was 104 mD. At restored reservoir conditions, single phase permeability of the core sample to brine measured 45.6 mD (which equates to the single phase gas permeability at reservoir conditions). Upon reverse gasflood to equilibrium, the relative permeability of the sample to gas is reduced to 13.5 mD with an accompanying residual water saturation of 44.7%.

In a further attempt to reduce the entrained water saturation, the core was subsequently pressure pulsed (rapidly depressurized to 0 kPag and then repressurized). The endpoint water saturation showed only a marginal reduction to 43.1% and a slight permeability increase to 17.8 mD.

Originally, from DST and log analysis of the cored well, formation water saturation was evaluated to average 10% while near wellbore in situ permeability calculated to 39 mD. Consequently, the effect of induced water invasion would appear to create in the order of a four and one half fold increase in connate water saturation held by the core with a corresponding two-thirds reduction in relative gas permeability. The substantial magnitude of this effect is, similarly, in proportion to the reduced flow efficiency observed in the original four post-fractured wells.

At the higher residual water saturations established in the core sample above, further flooding with the light hydrocarbon resulted in a reverse gasflood condensate saturation of 8.5% with a corresponding 13% permeability reduction to 15.5 mD. This relatively benign effect of the hydrocarbon phase on the return permeability was consistent with earlier results in developing the previously mentioned non-aqueous drilling system.

d) Field Application – In ensuing development within the Paddy formation, this oil based drilling fluid was utilized. Each well was drilled to the base of the zone with the oil based mud and terminated as an open hole completion removing any contact to the formation with water. The first three wells drilled in the program encountered reservoir with formation permeabilities of 46, 169 and 167 mD and respective flow capacities of 410, 680 and 1100 mD-m. Corresponding skin values of +4.5, -1.1 and +8.9 at flowrates of 340 x 10³, 350 x 10³ and 420 x 10³ m³/d respectively were again likely dominated by turbulence.

Within the same time period, a fourth well in the area was drilled through the formation with a flocculated water, gel chem system to a deeper target. From an initial DST, the reservoir displayed a permeability of 40 mD, 350 mD-m flow capacity and an apparent skin of +12.2. The zone was subsequently cased, perfo-

rated under a water column, flow tested and it was determined that a remedial cement squeeze would be required to isolate an adjacent water bearing zone.

The pay interval was then completed using an innovative penetrator tool drilling eight radial laterals with the hydrocarbon system. Both post cleanup flow rates, prior to and after the penetrator workover, were identical. However, from further post completion flow testing, comparable reservoir parameters of 53 mD and 420 mD-m for the formation were again masked by invasive damage calculating in excess of a +50 skin value.

The above field experience with the Paddy formation has contrasted several examples where aqueous invasion of the zone has been a dominant factor in the final productivity analysis. Where an aqueous drilling system has been used, initial DST results have shown a range from essentially none to smaller amounts of invasive damage. This might be attributed to the filter cake building properties of the mud system designed to minimize fluid loss.

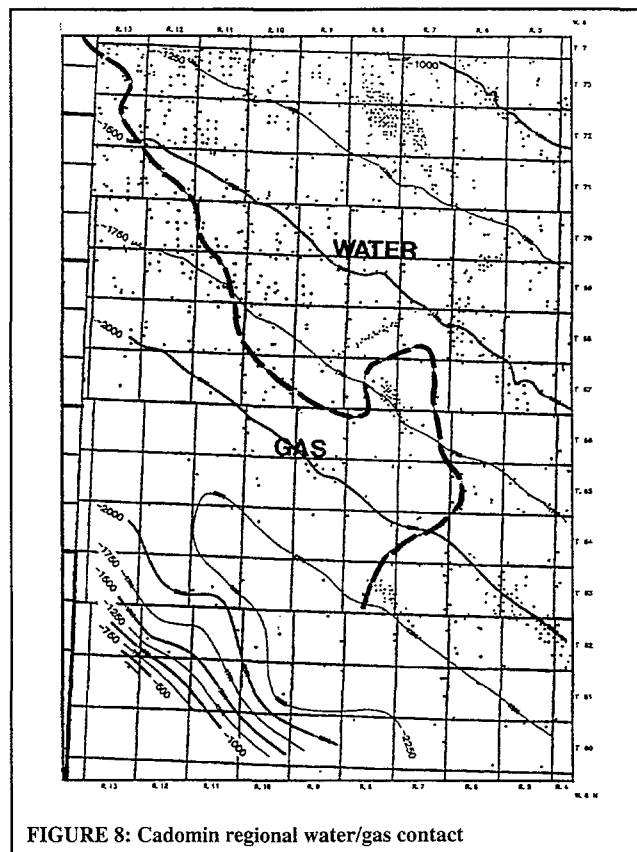


FIGURE 8: Cadomin regional water/gas contact

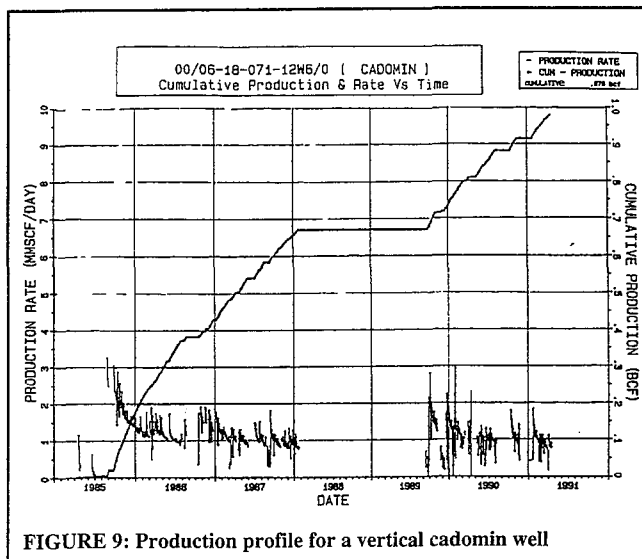


FIGURE 9: Production profile for a vertical cadomin well

Alternately, where an exposed aqueous system has been otherwise employed (i.e., highly invasive hydraulic fracturing treatments), it would appear the damaging effects are pronounced

Case #2 - Cadomin Formation

a) Reservoir Description – The Cadomin formation in the Deep Basin area of west central Alberta is unusual in that up dip, regionally pressured, water overlies down dip, under pressured gas (Figure 8). The zone is a regionally extensive, highly heterogeneous, sandy conglomerate deposited from multiple alluvial fans originating from the mountains to the west and later reworked by a crosscutting braided stream sourcing additional material from the southeast. In contrast to the Paddy formation discussed previously, the Cadomin presents a case study for a markedly lower permeability reservoir displaying similar, pronounced aqueous entrapment effects.

Currently, in excess of $100 \times 10^9 \text{ m}^3$ of gas in place have been delineated by vertical penetrations demonstrating matrix permeabilities in the micro to 10 millidarcy range overlain with a natural fracture system. The zone is comparatively thin, averaging 6 m in thickness with a corresponding 5-6% porosity, 20% water saturation and 20,000 kPag reservoir pressure at an average depth of 2,450 m.

The gas accumulation is believed to have been generated during a period of deep burial from southeastern coals that may have released in excess of $8 \times 10^{12} \text{ m}^3$ of gas. Over time, this volume subsequently migrated hundreds of kilometers to northwestern outcrops displacing water updip to the water/gas transition and concurrently desiccating the formation below an equilibrium connate water saturation. With following uplift, erosion and cooling, the zone is presently both undersaturated and underpressured. In addition, a variation of decreasing pressure at datum is demonstrated ranging from the southern area of source coals to the northwestern outcrop indicating the system remains in a dynamic state of gas migration⁽¹²⁾.

b) Previous Field Experience – Experience with a number of vertical wells brought onstream in the early 1980's typified the production characteristics for the zone as illustrated by the daily production history for an example well of Figure 9. In general, production rapidly declines from an initial rate ranging from $30 - 180 \times 10^3 \text{ m}^3/\text{d}$ to within 20 - 35% of this initial rate within several months.

While pressure readings within the first few months of shut-in indicate single well reserves between $15 - 70 \times 10^6 \text{ m}^3$ from material balance evaluation, pressure buildup data across several years can often be extrapolated to original reservoir pressure supporting the extensive, lower permeability deposit as mapped. The drainage volume accessed on the shorter time scale, however, often averaged significantly less than the mean $110 \times 10^6 \text{ m}^3$ volume mapped across a single section spacing unit indicating tighter

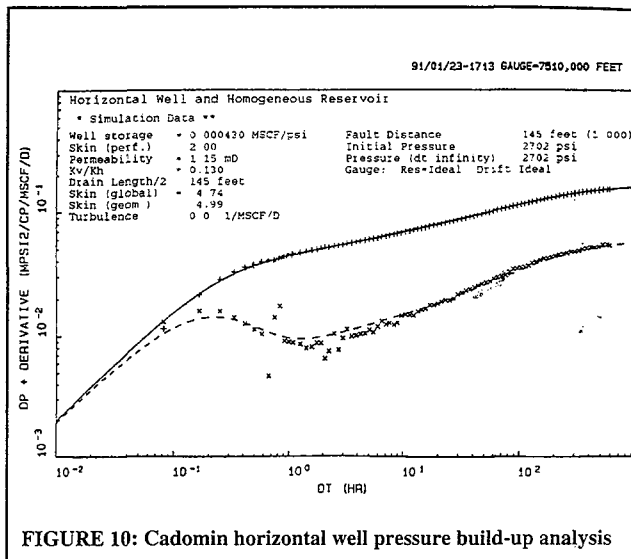


FIGURE 10: Cadomin horizontal well pressure build-up analysis

vertical well control would be required to adequately drain the formation.

Confirming earlier petrographic and geological studies, the wide variability in rate and pressure buildup response among the vertical wells in the zone suggested an extremely heterogeneous reservoir environment across a scale as small as several tens of metres. Rationalizing the production profile observed a vertical penetration in the zone might rapidly drain a localized pod of higher permeability reservoir with the surrounding tighter matrix controlling the longer term inflow (dual porosity response) complicated by variations in reservoir geometry. What would be required to more effectively drain the formation would be some form of a highly conductive, deeply penetrating completion.

Traditionally, the majority of completions across the Cadomin were limited to multistage, balled acid treatments often taken to near the 42 MPa breakdown pressure of the formation. From experience, this stimulation generally achieved comparable results to propped hydraulic fractures which suffered from a number of anomalous problems. Of the numerous hydraulic fracture designs attempted, roughly half prematurely reached casing strength pressure limitations in the range of 65 MPa while almost all showed very poor conductivity irrespective of the proppant volumes placed. The greater majority of these fractures were run with an aqueous frac fluid, most often a gelled water/methanol system.

Given the history of associated problems and limitations with hydraulic fracturing in the Cadomin, in 1989 Canadian Hunter experimented with the drilling of a 285 m horizontal well in the zone. In addition to the advantage of providing extended access to the reservoir, horizontally drilling through the formation added the dual advantages of providing control over the orientation of the well (perpendicular to the direction of induced and potential natural fractures governed by the regional stress environment) and obtaining direct data on the properties of the penetrated formation.

The well was drilled with an aqueous mud system utilizing calcium carbonate as a bridging agent to offset the 5,500 kPag overbalance of the static mud column, and completed open hole with an uncemented liner over the horizontal zone. The well encountered 210 m of horizontal pay interval from log analysis. The presence of natural fractures perpendicular to the well trajectory was also confirmed from the interpretation of both a formation microscanner log and production testing.

Subsequent to rig release, the well was acidized and flowed to cleanup at an initial rate of $110 \times 10^3 \text{ m}^3/\text{d}$, comparable to the performance of an immediately offsetting vertical well within the spacing unit and consequently considerably below expectations. In ensuing operations on the well to identify the basis of this apparent anomaly, it became evident that significant fluid losses to the formation were experienced, particularly in kill operations using KCl water prior to reconfiguring downhole tubulars. The reservoir displayed a marked tendency to imbibe water resulting

TABLE 5: Cadomin coreflood permeability summary.

| Displacement Phase | Saturation | | | Permeability | | Relative Permeability |
|---------------------------|----------------|----------------|----------------|--------------------------------------|-------|-----------------------|
| | S _o | S _w | S _g | (μm) ² x 10 ⁻³ | (mD) | |
| Air @ 20°C, 1,380 kPag | 0.000 | 0.000 | 1.000 | 3.8 | 3.9 | - |
| Air @ 82°C, 27,580 kPag | 0.000 | 0.000 | 1.000 | 0.16 | 0.16 | - |
| Brine | 0.000 | 1.000 | 0.000 | 0.175 | 0.177 | 1.000 |
| Reverse Gas | 0.000 | 0.520 | 0.480 | 0.054 | 0.055 | 0.310 |
| Raw Escaid-90 @ 2,760 kPa | 0.721 | 0.210 | 0.069 | - | - | - |
| Raw Escaid-90 @ 4,140 kPa | 0.753 | 0.180 | 0.067 | - | - | - |
| Raw Escaid-90 @ 5,520 kPa | 0.774 | 0.160 | 0.066 | - | - | - |
| Raw Escaid-90 @ 6,890 kPa | 0.784 | 0.150 | 0.066 | - | - | - |
| Reverse Gas | 0.090 | 0.150 | 0.760 | 0.142 | 0.144 | 0.814 |

in a significant reduction in the permeability to gas

c) Laboratory Design Program – In order to further investigate this behaviour, a program of laboratory coreflood studies was undertaken at reservoir conditions in an attempt to simulate the downhole processes. The coreflood testing immediately revealed a significant water entrapment behaviour in the Cadomin. From leakoff tests conducted on full diameter core mounted to measure vertical permeability across the zone (Table 5), bench Kv to air was 3.9 mD (Kv measured was approximately 0.5 K_{h,max}). At restored reservoir conditions, the in situ single phase core permeability to either air or formation brine decreased to 0.17 mD. However, upon reverse gas flooding the brine saturated core, entrained water saturations in excess of 50% were observed after stabilized flow periods, reducing the core permeability by two-thirds to 0.055 mD. By contrast, this residual water saturation is a 2.5 fold multiple of the formation water saturation established from logs. The magnitude of this effect on the relative permeability to gas across a 0.3 m core sample provided a profound insight into the potential aqueous phase trap problem observed in the horizontal well.

In order to mitigate this entrapment effect, further lab studies were conducted to evaluate the invasive characteristics of several non-aqueous fluids. Table 5 presents the results of pursuant leakoff testing on the above core sample with a commercially refined C₁₀-C₁₁ component mixture. It was observed that at increasing pressure differentials through the core, entrained water was remobilized reducing the residual water saturation in the core to in situ levels while introducing up to a 9% residual hydrocarbon saturation. Of consequence, however, the return permeability of gas in the core increased to 0.144 md, within 80% of the original single phase gas permeability. This behaviour indicated the potential for the development of a drilling fluid based on a non-polar medium which would provide relatively benign invasive properties. In addition, the use of a water free, hydrocarbon based fluid in well operations would provide an essentially near balanced hydrostatic liquid column which would act to further minimize invasion into the formation.

d) Field Application – Upon the design and lab testing of an appropriate drilling system for this application, Canadian Hunter drilled a followup 600 m horizontal well in the Cadomin in 1991. Despite encountering an overall comparatively poorer reservoir, this well penetrated an equivalent length of thinner net pay interval to the first well and was rig released as an unlined open hole. Upon production testing, the well immediately flowed at similar rates to the first horizontal with no further stimulation efforts.

Pressure buildup analysis of this well later indicated only a nominal skin damage of +2 (Figure 10) which could be expected from ancillary effects such as damage from drilling fines invasion as one example. Irrespectively, it would appear that the severe permeability reductions associated with aqueous entrapment observed in the laboratory were not evidently manifest in this second well.

The Cadomin case study has served to significantly impact the approach to field operations within Canadian Hunter from two major aspects. Primarily, attention has now been focussed on the relative importance of the aqueous entrapment effect to productivity restrictions. Secondly, the broader applicability of hydrocarbon fluid systems has become recognized in the design of various well programs, with particular emphasis on the unique characteristics of horizontal wells.

Conclusions

The laboratory and field results indicate that

1. Aqueous phase trapping has the potential for severe productivity reductions in both oil and gas reservoirs. The magnitude of the reduction appears to be a function of:
 - a) The difference between initial and true irreducible water saturation
 - b) Wettability of the porous media (oil-wet porous media generally exhibit much lower initial water saturations)
 - c) Cyclic hysteresis effects caused by multiple invasion and drainage cycles of an aqueous phase
 - d) Depth of the invaded zone
2. Case studies indicate that the use of hydrocarbon based fluids may be advantageous in certain situations where the potential for a water trap exists. However, hydrocarbon fluids may also be significantly damaging to reservoirs in situations where
 - a) Incompatibility between the invading hydrocarbon phase and formation crude oil or brine exists
 - b) Very low permeability zones are present (<0.01 mD) causing high capillary retention of either oil or water
 - c) Presence of an initial and potentially wetting liquid hydrocarbon phase (in a gas reservoir)
 - d) Presence of naturally oil-wetted minerals (in a gas reservoir)
3. Properly conducted laboratory studies can provide insight into the severity of potential aqueous trapping problems and allow design and evaluation of effective drilling, completion and

stimulation fluid systems to maximize production rates and minimize costs associated with expensive and often unsuccessful stimulation treatments

Acknowledgement

The authors express appreciation to the management of Canadian Hunter Exploration Limited for permission to publish this data

REFERENCES

- 1 BENNION, D B , THOMAS, F B , BENNION, D W , *Effective Laboratory Coreflood Tests to Evaluate and Minimize Formation Damage in Horizontal Wells; presented at the Third International Conference on Horizontal Well Technology, Houston, Texas, Nov 12-14, 1991*
- 2 BENNION, D B , SCOTT, J A , BENNION, D W , *Detailed Laboratory Studies of Chemically and Biologically Induced Formation Damage in the East Wilmington Field; Paper CIM 92-44, presented at the CIM Annual Technical Conference, Calgary, Alberta June 7-10, 1992*
- 3 BEATTY, T , BENNION, D B , HEBNER, B , HISCOCK, R , *Minimizing Formation Damage in Horizontal Wells: Laboratory and Field Case Studies; presented at the CIM Annual Technical Conference, Calgary, Alberta, May 10-12, 1993*
- 4 ENG, J H , BENNION, D B , STRONG, J B , *Velocity Profiles in Perforated Completions; Paper CIM/AOSTRA 91-50; presented at the CIM/AOSTRA 1991 Technical Conference, Banff, Alberta, April 21-24, 1991*
- 5 BENNION, D B , CHAN, M , SARIOGLU, G , COURTNAGE, D , WANSLEEBEN, J AND HIRATA, T , *The In Situ Formation of Bitumen-Water Stable Emulsions in Porous Media During Thermal Stimulation; SPE 25802, presented at the 1993 SPE Thermal Operations Symposium, Bakersfield, California, Feb 8-10, 1993*
- 6 Bennion, D B , Thomas, F B and Sheppard, D A , *Formation Damage Due to Mineral Alterations and Wettability Changes During Hot Water and Steam Injection in Clay Bearing Sandstone Reservoirs; SPE 23783, presented at the 1992 SPE Symposium on Formation Damage Control, Lafayette, LA, Feb 26-27 1992*
- 7 KATZ, D L AND LUNDY, C L , *Absence of Connate Water in Michigan Reef Gas Reservoirs - An Analysis; AAPG Bulletin, Vol 66, No 1 (January 1982), pp 91-98*
- 8 BIETZ, R F , BENNION, D B , PATTERSON, J P , *Gas Storage Reservoir Performance Optimization Through The Application of Drainage and Imbibition Relative Permeability Data; Paper CIM 92-75, presented at the CIM Conference Calgary, Alberta, June 7-10, 1992*
- 9 McKETTA AND WEHE *Dew Point of Natural Gas; Hydrocarbon Processing; August, 1958*
- 10 McCAFFERY, F G , *The Effect of Wettability on Relative Permeability and Imbibition in Porous Media; Ph D Thesis, University of Calgary, September, 1973*
- 11 WARDLAW, N C , *The Effects of Geometry, Wettability, Viscosity and Interfacial Tension on Trapping in Single Pore Pairs; JCPT, May-June 1982*
- 12 MASTERS, J A , *Elmworth - Case Study of a Deep Basin Gas Field; AAPG Memoir 38 1984*

Provenance - Original Petroleum Society of CIM manuscript, **Reductions in the Productivity of Oil and Gas Reservoirs Due to Aqueous Phase Trapping** (93-24), first presented at The Petroleum Society of CIM 44th Annual Technical Conference in Calgary, Alberta, May 9-12, 1993 Abstract submitted for review November 5, 1992; editorial comments sent to the author(s) November 8, 1993; revised manuscript received December 3, 1993; paper approved for publication January 31, 1994 ¶

Authors' Biographies



Brant Bennion is currently president of Hycal Energy Research Laboratories Ltd of Calgary, Alberta He is involved in research in multi-phase flow in porous media, formation damage studies, miscible and thermal EOR Brant received a B Sc in Chemical Engineering from the University of Calgary in 1984, has authored over 40 technical papers and has lectured worldwide He is a member of APEGGA and a Board member of the Calgary Section of The Petroleum Society of CIM



Ronald Bietz is the manager of Engineering at Hycal Energy Research Laboratories Ltd Ron graduated from the University of Wyoming in 1987 with a B Sc in Petroleum Engineering Ron's interests include formation damage and multiphase flow in porous media Ron has authored/co-authored five technical papers



Brent Thomas holds a doctorate in Chemical Engineering He has worked on Enhanced Oil Recovery applications for the last ten years, including gas injection, chemical flooding, solids precipitation and thermal applications He is presently vice president of Hycal Energy Research Laboratories Ltd



Mauro Cimolai is a reservoir engineer with Canadian Hunter Exploration Ltd and has been involved in studies in drilling completion and production design in the deep basin area of Alberta for the last eight years His interests include the reservoir engineering aspects of horizontal drilling and formation damage Mauro is a graduate of the University of Alberta, a professional engineer and a member of APEGGA and The Petroleum Society of CIM

THIS IS A PREPRINT - SUBJECT TO CORRECTION

REMEDICATION OF WATER AND HYDROCARBON PHASE TRAPPING PROBLEMS IN LOW PERMEABILITY GAS RESERVOIRS

D Brant Bennion, F Brent Thomas, Ronald F Bietz, Douglas W Bennion
Hycal Energy Research Laboratories Ltd

PUBLICATION RIGHTS RESERVED

THIS PAPER IS TO BE PRESENTED AT THE 47TH ANNUAL TECHNICAL MEETING OF THE PETROLEUM SOCIETY OF CIM IN CALGARY, ALBERTA, JUNE 10-12, 1996 DISCUSSION OF THIS PAPER IS INVITED SUCH DISCUSSION MAY BE PRESENTED AT THE TECHNICAL MEETING AND WILL BE CONSIDERED FOR PUBLICATION IN CIM JOURNALS IF FILED IN WRITING WITH THE TECHNICAL PROGRAM CHAIRMAN PRIOR TO THE CONCLUSION OF THE MEETING

ABSTRACT

Aqueous and hydrocarbon phase traps can occur in porous media when water- or oil-based fluids come into contact with a formation which exhibits a "subirreducible" initial liquid saturation of the phase of interest. This commonly occurs with water-based fluids in many low permeability desiccated gas bearing formations and in depleted conditions in rich gas retrograde condensate reservoirs. This paper documents how phase traps are induced by direct displacement, countercurrent imbibition or depletion effects, and presents techniques for diagnosing whether a reservoir is a candidate for an aqueous phase trapping problem. Techniques to minimize problems with aqueous and hydrocarbon phase trapping are reviewed, followed by discussion of methods to reduce or remove the effect of existing phase traps, such as increased drawdown, alteration of IFT, alteration of pore geometry or direct removal methods. A brief discussion of laboratory techniques used to screen the optimum process for selection are also presented.

INTRODUCTION

The phenomena of permanent entrainment of extraneous or insitu generated aqueous or hydrocarbon based liquids in porous media has been documented in the literature as a mechanism for significant permeability impairment in low permeability intercrystalline sandstone and carbonate formations¹⁻⁵

Phase traps normally occur when a water or hydrocarbon based fluid is either forced or imbibed into porous media with a subirreducible water or hydrocarbon saturation (ie at a saturation less than the irreducible liquid saturation given the geometry, wettability and capillary mechanics of the system under consideration). Subirreducible hydrocarbon saturations are common in rich gas retrograde systems existing in a sub-dewpoint condition, or in mature gas fields which may have migrated into previously oil-saturated strata. Subirreducible water saturations in low permeability gas reservoirs are also quite common. The mechanism for the establishment of a sub-irreducible water saturation in a low permeability gas-bearing reservoir is the

subject of some controversy. The dominant mechanism is thought to be desiccation motivated by a large regional migration of gas under conditions of increasing temperature and pressure through a given reservoir area over a long period of geological time. The basic mechanism of a phase trap is created by the relative permeability effect associated with an increase in the immobile water or hydrocarbon saturation. This phenomena is illustrated on a pore scale in Figure 1 and from a mechanistic point of view as Figure 2

The severity of the phase trap is strongly influenced by

The magnitude of the difference between the "initial" and final trapped "irreducible" liquid saturation which exists in the porous media The greater this difference, the larger the adverse relative permeability effect and the greater the potential reduction in permeability

The configuration of the gas or oil phase relative permeability curves at low liquid saturation levels The more adverse the configuration of these curves (ie the more convex the relative permeability curve), the more significant the reduction in permeability for a given increase in trapped liquid saturation

The depth of invasion of the trapped phase The greater the volume of fluid lost and deeper the invasion, the more difficult and slow the mobilization of this fluid becomes. This is due to dispersion of the available drawdown gradient over a much larger distance resulting in a reduced effective drawdown gradient per unit reservoir length. This is pictorially illustrated in Figure 3

The available reservoir drawdown pressure Since residual liquid saturation is a direct function of the capillary gradient applied to the system, it can be seen that the greater the available pressure for drawdown, the higher the capillary gradient which can be applied and, therefore, the lower the resulting ultimate residual liquid saturation which can be obtained. This phenomena is also illustrated as a portion of Figure 3

HOW ARE AQUEOUS AND HYDROCARBON PHASE TRAPS ESTABLISHED

The potential for a phase trap obviously exists any time a water or hydrocarbon based fluid (or in some cases pure

gas) is introduced into a formation in excess of the "irreducible" saturation value of that particular phase given the current conditions of pore geometry, wettability, IFI and drawdown. Common processes in which these fluids may be introduced into the formation would include:

Physical displacement of hydrocarbon, aqueous or gaseous media into the formation during overbalanced drilling, completion, stimulation, workover or kill operations In any overbalanced operation some fluid losses to the formation are inevitable. The significance of the damage will often be determined by the actual volume of fluid lost and the ultimate completion program for the well. For example, very shallow invasion of drilling mud filtrate in a well which will be cemented, cased and subsequently perforated may be inconsequential as the perforating charge will penetrate well beyond the range of the mud filtrate invasion. Compare this to a barefoot or open hole completion where the effect of even shallow fluid invasion may be significant.

Imbibition and countercurrent imbibition This mechanism of imbibition of aqueous (in water-wet porous media) and hydrocarbon (in oil-wet porous media) filtrates has been discussed in the literature^{1,3,4,6,7}. These phenomena can readily occur during both overbalanced and underbalanced operations in subirreducibly saturated formations.

Crossflow from wet zones In multiply completed zones, crossflow of produced water/oil from lower wet intervals may invade/imbibe into upper sub-irreducibly saturated zones establishing phase traps.

Hydrocarbon phase traps are commonly established by the production of rich gas condensate formations at bottomhole pressures less than the system dewpoint This may occur during normal well production operations or, in some cases, during an underbalanced drilling operation where the circulating bottomhole pressure is less than the effective system dewpoint pressure. This results in the accumulation of a trapped liquid condensate saturation, sometimes of an appreciable value, in the region directly adjacent to the wellbore or fracture face which can significantly impair productivity. This process is schematically illustrated as Figure 4

Hydrocarbon phase traps may also be created in gas injection wells due to the entrainment of compressor lubricants in the injected gas. Once again, the entrapment of this immiscible hydrocarbon phase may cause a reduction in gas injectivity.

Hydrocarbon phase traps may also be established by the entrainment of skim or slug oil when injecting water into aquifer zones (zones that are initially 100% saturated with water). Capillary pressure forces trap this residual oil saturation in the near injection well region. Since the majority of these injection wells exhibit water-wet behaviour (due to the fact that no pre-existing hydrocarbon saturation was present to establish an oil wetting condition), even a relatively small trapped oil saturation can have a large reducing effect on water injectivity. This phenomena is discussed in further detail in the literature⁸ and has been schematically illustrated as Figure 5.

Gas phase traps are created in water source wells or producing oil wells when immiscible gas either is inadvertently injected into the formation such as during a poorly executed underbalanced drilling operation or an overbalanced completion or workover operation operating under a gas cushion. This can also occur when gas is liberated from the formation fluid by drawdown below the bubble point resulting in physical liberation of a free gas saturation. This phenomena can also occur during an underbalanced drilling operation if the circulating mud pressure is lower than the fluid bubblepoint. Due to the fact that no previous free gas saturation exists in the producing zone (assuming that the reservoir is in a undersaturated condition), a large reduction in oil or water permeability may be induced by the creation of a critical trapped gas saturation. This phenomena is schematically illustrated as Figure 6. This phenomena may be more or less inevitable in many oil producing formations simply because logistically it is impossible to economically produce the wells indefinitely at bottomhole pressures above the saturation pressure. Significant gas phase traps can also be created in water injection wells if non-condensable gas (usually air) is inadvertently injected into the wells due to pump suction, operation or cavitation problems.

DIAGNOSING THE POTENTIAL FOR PROBLEMS WITH AQUEOUS OR HYDROCARBON PHASE TRAPS

A knowledge of the permeability and initial fluid saturation characteristics of the formation under consideration is essential in order to properly evaluate the risk for a phase trap. Log or conventional core-based evaluations are commonly used to determine initial fluid saturations, but experience has indicated that these methods often overestimate insitu fluid saturations which can lead to a significant underestimation of both reserves in place and the potential for the establishment of phase traps.

Water saturations estimated from both log and core-based techniques may be influenced by flushing of the core and near wellbore region by mud filtrate. Subirreducibly saturated formations also do not produce any free water since the initial water saturation is less than the mobile value. Therefore, obtaining insitu fluid samples for an accurate evaluation of resistivity, which is essential for effective log saturation evaluations, is virtually impossible.

Recently, considerable work in the use of low invasion coring techniques, coupled with chemically or radioactively traced aqueous mud systems or hydrocarbon based coring fluids have been used to obtain an more accurate evaluation of initial water saturation in subirreducibly saturated systems. A combination of traced water based mud systems and sponge coring has been used to determine initial saturations in situations where both unknown, but potentially mobile, oil and water saturations are present. Gas coring has also been postulated as a technique for obtaining representative initial water saturations, but experience has indicated that high temperatures and desiccation effects associated with gas coring may lead to an artificially induced reduction in the measured water saturation of preserved cores obtained in this fashion.

The potential exists for a phase trap if the measured initial oil or water saturation is less than what would be considered to be the irreducible value at the capillary gradient available for the system. This irreducible saturation number is commonly obtained from conventional restored state or air-mercury capillary pressure measurements. A variety of sophisticated special core analysis techniques are also available to diagnose the severity of a phase trap.

problems once the initial saturation conditions have been definitively established

Bennion et al² developed a regression based correlation to predict the potential for aqueous phase trapping for both oil and gas reservoirs. The aqueous phase trap index (APT_i) is based on simple reservoir parameters obtained from an average routine core analysis. It is calculated from the uncorrected absolute gas permeability and a measured correct initial (not irreducible) water saturation using the equation

$$APT_i = 0.25[\log_{10}(k_{air})] + 2.2(S_{wi}) \quad (1)$$

where

- APT_i = Aqueous phase trap index
- k_{air} = Average formation absolute routine core analysis air permeability (mD)
- S_{wi} = Measured initial (not irreducible) water saturation (fraction)

The evaluation of the correlation indicates that values of APT_i

APT_i > 1.0 - Generally no problem with permanent aqueous phase trapping

1.00 > APT_i > 0.80 - Potential problem with permanent aqueous phase trapping

APT_i < 0.80 - Generally significant problems with permanent aqueous phase trapping

The lower the value of the APT_i index, the greater the severity of the potential phase trap. Figure 7 provides a graphical representation of the correlation given by Equation 1.

The database on trapped oil saturations is still too small to build a comparable correlation for hydrocarbon phase traps with a similar degree of confidence. There is no pre-existing oil saturation in most cases where hydrocarbon phase traps are problematic. In this situation, the introduction of any free liquid hydrocarbon saturation will likely cause damage.

HOW SIGNIFICANT WILL THE PHASE TRAP PROBLEM BE?

Phase trapping problems are significant only if the ultimate path of the production will be through the entrained fluid. As mentioned previously, very localized fluid losses in cased hole completions (or open hole completions which are subsequently perforated, under-reamed or fractured) may not be significant provided that the ultimate penetration depth of the completion or stimulation extends well beyond the radius of the invaded fluid.

Hydraulic and acid fracture treatments are often considered to be impervious to fracture face damage effects. In general, it is true that the productivity of most fracture treatments tends to be dominated by fracture conductivity rather than fracture face permeability. It is also generally true that the larger the effective fracture length the greater the amount of damage which can be tolerated. For example, very large fracture treatments can tolerate in excess of 95% reduction in permeability on the fracture face before productivity begins to drop. However, a near 100% reduction in permeability on the fracture face will obviously reduce the productivity of any size of fracture treatment. Therefore, appropriate fracture fluid design and identification of reservoirs that are susceptible to phase trapping, should be the focus of significant concern since phase trapping is one of the few formation damage mechanisms which is readily capable of causing near 100% reductions in permeability. This is particularly true in situations where significant invasion and low drawdown pressures may occur in depleted formations.

HOW CAN PHASE TRAP PROBLEMS BE MINIMIZED OR PREVENTED?

If the potential for a phase trap is present, the approach should be to

- Avoid introducing the fluid with phase trap potential into the formation if possible. For example, if the potential for a water trap in a gas reservoir exists, air or pure nitrogen may be considered as fluids. If it is an oil reservoir the an appropriate compatible hydrocarbon-based fluid should possibly be considered.

- If, due to technical or economic constraints, the base fluid used must be a fluid which has trapping potential, consideration should be given to attempting to reduce the fluid loss of the potentially damaging filtrate into the formation to as low as level as possible. This would include using appropriate rheology and fluid loss additives and using bridging agents or mud solids to reduce fluid and solids invasion into the formation. Cross-linked gels with brakers may be considered for fracture fluids to prevent significant invasion.
- If it is thought an unavoidable fluid invasion will occur, modify the fluid properties to reduce IFT, to reduce the amount of fluid present per unit volume of fluid lost, or to add inherent charge energy to aid in the mobilization of the fluid back out of the formation on formation blowdown. This may include the use of IFT reducing agents in the water or oil-based fluid (surfactants, mutual solvents, etc.) or the concurrent injection of a soluble gas, such as CO₂, to both swell the fluid (ie reduce the actual volume of fluid entering the formation) and to provide localized charge energy to create a steep pressure gradient to assist in the recovery of the fluid upon blowdown.
- The appropriate choice of the base fluid for an operation can often minimize the potential for an aqueous or hydrocarbon phase trap. For example, if water imbibition and trapping is thought to be a problem in an underbalanced drilling operation in a water-wet subirreducibly saturated gas reservoir using a water-nitrogen system, the use of a hydrocarbon based drilling fluid with the nitrogen would be a wise choice as there will be no motivation for countercurrent imbibition of the non-wetting phase. As long as the underbalanced condition is maintained, no fluid invasion or trapping should occur. In some situations, where aqueous phase trapping is known to be problematic (ie low S_{wi} gas reservoirs), the use of hydrocarbon fluids may be superior to water-based fluids simply because it traps the least. If the formation is water wet, an invading non-wetting hydrocarbon phase will be retained in the central portion of the pore system and may be mobilized easier and result in a lower overall incremental increase in trapped fluid saturation than if a water-

based fluid, which will be attracted directly to the pore walls, was used in the same situation. Figure 8 provides an illustration of this mechanism. Experimental evaluation is generally recommended to verify this supposition prior to testing in the field. A case study of this type is supplied in the literature¹.

- Underbalanced drilling and completion operations may be considered as techniques to avoid phase trapping. Care should be taken in this area as severe damage can occur if the underbalanced condition is comprised as no protective filter cake is formed on the surface of the formation to act as a barrier to fluid invasion. The absence of this cake also increases the potential for countercurrent imbibition if the inappropriate fluid base (as discussed previously) is used. A conventional overbalanced completion following underbalanced drilling may also be disastrous if a trapping fluid is used as a completion fluid since in the absence of a protective filter cake, massive fluid losses to the formation may occur.

REMEDICATION OF EXISTING AQUEOUS OR HYDROCARBON PHASE TRAPS

In many cases where the damage has already been done and a verified phase trap has been confirmed to exist, the problem is to stimulate the existing damaged well to attempt to restore all or a portion of the lost production. Techniques in this area generally fall into two categories:

- 1 Penetration of the phase trapped region to enter virgin undamaged reservoir.
- 2 Removal of the phase trap insitu to attempt to restore permeability in the damaged region.

Direct Penetration Techniques

These techniques are often considered if the phase trap is considered to be of large extent in a relatively small, well defined interval. The most common technique would be hydraulic or acid fracturing. Care must be taken in this situation to ensure that the phase trap problem is not further propagated during the "stimulation" treatment. In many cases where zonal fracture containment or multiple zones are an issue, or if the completion in question is a horizontal well in which multiple expensive and extensive

selectively isolated fracture treatments would be required, this may not be a viable option

Other direct penetration techniques for very localized phase traps would include re-perforation, open hole perforating, lance penetrators and explosi-fracs

Removal Techniques

These techniques are generally more exotic and situation specific and centre about the removal or reduction of the amount of extraneous trapped liquid which is present in the system. Different approaches are present for hydrocarbon and water based traps but they center about the same four basic areas of approach:

- 1 Increase in drawdown pressure
- 2 Reduction in intrafluid IFT
- 3 Alteration in pore geometry
- 4 Direct removal/replacement of the trapped fluid

Increase in Drawdown Pressure

It has already been illustrated that irreducible saturation is a function of the magnitude of the capillary gradient which can be applied to the system. Therefore, the higher the drawdown gradient which can be placed across the affected zone, the lower the ultimate residual trapped saturation which will be obtained. Unfortunately, due to the asymptotic nature of most capillary pressure curves near the "irreducible" saturation level, huge capillary pressure gradients are required to achieve even a small reduction in the trapped fluid saturation. Since large capillary pressure gradients are not normally attainable at most normal reservoir drawdown gradients, particularly in pressure depleted formations, this greatly reduces the widespread utility of this technique

Reduction in Intrafluid IFT

The equation governing capillary pressure, which controls fluid retention and residual saturations, is given by the relation

$$P_c = P_{nw} - P_w = (IFT)(1/R_1 + 1/R_2) \quad (2)$$

Figure 9 provides a schematic illustration of the radii of

curvature as mentioned in Equation 2. Figure 10 illustrates this phenomena in porous media and why lower permeability, finer grained porous media tend to exhibit higher capillary pressures and irreducible liquid saturations than their higher permeability counterparts

It can be seen that the capillary pressure is a direct linear function of the interfacial tension which exists between the trapped phase and the bulk producing (oil or gas) phase that exists in the formation. If some means of reducing the IFT can be found then it may become possible to mobilize the trapped fluid at the available drawdown pressure present in the reservoir.

For water-based phase traps in gas reservoirs, mutual solvents, such as methanol, have commonly been used for this purpose. A variety of chemical surfactants have also been used but with only limited success. It is difficult to create large reductions in gas-liquid IFT with chemical surfactants due to the disparate molecular nature of gas the liquid phases and the difficulty of a chemical surfactant to efficiently partition across the phase boundary. Chemical adsorption of the surfactant on reactive clays in sandstones and poor reaction with divalent cations common in connate waters in carbonate formations may also be limiting factors in this area.

For water traps in oil reservoirs, chemical surfactants have been more successful due to the ability to generate near zero oil-water IFT's with some chemical surfactant systems. Once again, surfactant consumption and compatibility issues may be problematic in certain formations. Mutual solvents have also been successful in these situations, but care must be taken with light alcohols such as methanol which are virtually immiscible with most liquid hydrocarbons and have significant sludge or emulsion potential. Higher molecular weight alcohols such as propanol or butanol may be more appropriate as mutual solvents in such situations.

Gaseous IFT reducing agents such as CO₂ for water traps in both oil and gas reservoirs, have also been used successfully in some situations. Carbon dioxide is often combined with a mutual solvent to obtain a synergistic effect and also add localized charge energy to increase the recovery of the trapped phases from low permeability formations.

Alteration in Pore Geometry

As described previously in Equation 2, the capillary pressure can also be reduced by increasing the radii of curvature which exist in the porous media in which the phase trap has occurred. This can normally only be affected by the appropriate use of acid to enlarge the size of the pore. The process is obviously better suited to carbonates which can have high inherent solubility in acid, but may also be applied to sandstones using appropriately designed HF acid treatments. The major risk created in this situation is that the spent acid becomes additional water present in the system which may exacerbate the problem with phase trapping. Therefore, high acid strengths are recommended to ensure that the acid penetrates the zone of effective invasion before spending.

Direct Removal Techniques

There are a variety of techniques for the removal of aqueous or hydrocarbon phase traps which would fall under the classification of direct removal techniques, these would include the following:

Dry Gas Injection

A common misconception is that, if an aqueous phase trap is established, long-term flow of the formation gas past the phase trapped region by producing the well will result in the evaporative removal of the trapped water. Since the reservoir gas, in virtually all cases, is in thermodynamic equilibrium with the connate water saturation which is initially present in the porous media, it is already effectively saturated with water vapour at reservoir temperature and pressure conditions and cannot, therefore, absorb any additional water vapour. This means that this technique will not be efficient at removing any of the trapped saturation by direct desiccation.

However, the injection of dehydrated gas such as tanked liquid nitrogen or pipeline spec dehydrated natural gas could have a significant desiccative effect on the formation and may reduce the trapped liquid saturation while establishing conduits of high gas saturation back to the undamaged bulk section of the reservoir. This process is schematically illustrated and appears as Figure 11. This has long been a documented process in increases in injectivity

in injection wells in gas storage reservoirs

Care must be taken if the trapped brine contains a high concentration of soluble ions. As this brine desiccates, these soluble ions will be precipitated from solution and may collect and plug the pore system. This is particularly true in the case of spent acid where very high calcium or magnesium concentrations may be present. Adequate lab screening to evaluate the technique is recommended prior to implementation to ensure that it is the best solution for the particular reservoir situation under consideration.

Formation Heat Treatment

This unique treatment is illustrated in Figure 12. Formation heat treatment (FHT) is documented in the literature⁵ as a technique for removing both water-based phase traps and water reactive clay-induced damage in gas bearing strata with limited pay extent. The technique involves the use of a special downhole tubing conveyed heating tool. Gas is injected through the tubing and heated downhole directly adjacent to the zone desired for treatment, and injected into the formation. The zone to be treated is generally about 2 meters in height by 1.5 to 2 meters in radial depth, with the objective being to elevate the temperature in the near wellbore region to over 500°C. Temperatures in this range result in both the supercritical extraction of any trapped water, plus the thermal decomposition and desensitization of any expanded reactive clay which may be present in the region. The technique holds promise for lower quality shallow gas strata which may be secondary target zones damaged by conventional fresh water based drilling and completion fluids.

Time

The old adage, "all things come to he (or she) who waits" has application in the field of aqueous phase trapping. Nature abhors steep gradients and when any bank of water based fluid is injected into a formation, there will be a natural capillary action over time which will tend to imbibe a portion of that saturation out into the reservoir to create a smooth capillary transition zone. This process is schematically illustrated as Figure 13.

It can be seen, particularly if the well is shut in and the

capillary action does not have to counteract a flowing pressure gradient, that the portion of the trapped fluid saturation above the "irreducible" saturation value may gradually be imbibed away from the near wellbore region and dispersed further into the formation. Many case studies exist where wells initially tested at uneconomic rates, were subsequently shut in for many years (and in many cases sold at bargain basement prices) and when re-tested, produced a significantly higher rates than in the initial evaluations. It must be remembered, though, that natural capillary action will only take the flushed zone down to the irreducible saturation, not the initial saturation. This means that, although capillary action may assist in the removal of a portion of the aqueous phase blocking effect, it cannot eliminate the basic aqueous phase trap established by the difference between the initial and irreducible saturations which exist in the system.

Repressurization

This is a technique often postulated for the removal of trapped retrograde condensate from a depleted region in the near wellbore area of a rich gas reservoir. Simple examination of a basic rich gas phase envelope (Figure 14) would appear to indicate that, if reservoir pressure is still above the dewpoint value, simply shutting the production well in and allowing the depleted near wellbore region to repressurize should result in the re-vaporisation of the trapped condensate and restoration of the initial permeability. This, however, is unfortunately a misnomer because the trapped condensate has been precipitated out of a large volume of gas which previously was produced. Since the insitu gas still contains a high concentration of heavy ends, there is a limited physical volume of trapped condensate which it can revaporize. Also, since the near wellbore region is in basically a static mode during the repressurization phase, the vaporization process also becomes very mass transfer limited due to the small interfacial area available for revaporization to occur across. Therefore, this is not a recommended technique for the effective removal of a trapped condensate saturation.

Lean Gas Injection

More effective for trapped condensate removal (as well as the potential removal of trapped water) is dry lean gas injection. If sufficient bottomhole injection pressures can be

attained (generally above 35,000 kPa) vaporizing miscibility can be obtained between conventional dry natural gas or nitrogen and many light volatile condensates. Since the gas being injected is lean and contains no heavy ends, it has the ability to vaporize a considerable fraction of the trapped liquid hydrocarbons. Also, operating in an injection mode facilitates a greater degree of mass transfer and rapid vaporization between the injected gas and the trapped liquid hydrocarbon phase. This technique is often used on a rotating basis in gas cycling operations as a means of stimulating condensate ring damaged production wells.

Rich Gas Injection

If injection pressures are too low to facilitate vaporizing miscibility with lean gas, richer gases such as liquid CO₂ or ethane have been used to obtain a similar effect at much lower pressures. While compression cost issues may be more significant in these cases, often conventional pumping rather than high pressure compression can be used when these gases are injected as supercritical liquids. Care must also be taken to ensure that the rich gas is compatible with the condensate and will not cause the undesirable precipitation of asphaltenes or other potentially damaging solids.

For even lower pressures, richer solvents such as propane and butane have also been used to remove condensate traps. Difficulties and safety concerns with the pumping of these highly flammable liquids have been the major restriction in their utility to date.

Localized Combustion

This is a technique which has been suggested (in theory) as a means of removing condensate traps in deeper low permeability rich gas reservoirs. The technique involves the injection of air into the damaged well. If the downhole temperature is sufficient (usually over 95°C), spontaneous ignition will occur resulting in the propagation of a small fireflood which consumes the trapped liquid condensate as a fuel source. The objective is to remove the trapped liquid hydrocarbon with the potential side benefit of removal of trapped connate water and clays due to the high temperature in a concurrent fashion. Major drawbacks include high temperature effects on downhole casing and

equipment, corrosion issues and well flashback (explosion) concerns when the wells are placed back in a producing mode.

Water Injection

This is a technique which has been used to displace trapped condensate in some very high permeability formations. The basic technique involves the injection of compatible water to displace the trapped condensate ring back a considerable distance from the wellbore. This is followed by inert gas injection to displace the water and reestablish conductive channels of high gas saturation to the reservoir. The technique is not recommended for lower permeability formations (less than 1000-2000 mD) due to phase trapping and hysteretic relative permeability issues associated with the cyclic introduction of water into the system.

Replacement with Solvent

Another technique for trapped condensate removal centres about hydrocarbon solvent injection to dilute and displace the trapped condensate. Since the solvents used are generally miscible with the trapped oil, they often simply displace the trapped condensate and replace it in an equivalent saturation which may result in no effective increase in permeability to gas. If a solvent has a lower IFT than the original condensate it is replacing, this type of treatment may be efficient. Solvents may also be useful in dissolving wax or asphaltene plugs which may have been created by extended production operations of paraffinic or asphaltic condensate systems.

Importance of Uniform Contact

The success of virtually all of the previously mentioned techniques centres about the effective contact with the trapped water or hydrocarbon phase. Since fluids naturally tend to follow the path of least resistance, this means that in many cases zonal isolation is required in order to attempt to direct the stimulation treatment to the area most required. This is particularly true for open hole completions and horizontal wells where large exposed surface areas may be available for stimulation.

Lab Screening Techniques

Most of the stimulation techniques described previously can be evaluated in the laboratory on appropriately selected and conditioned core material. Figure 15 provides a schematic illustration of a typical laboratory coreflow apparatus for evaluating reservoir condition fluid sensitivity. The objective of laboratory screening tests is to quantify the type and significance of the damage established by an initial phase trap and then to quantify the best stimulation technique to remove the damage and determine operation techniques to avoid inducing the damage.

Specialized core displacement tests can be conducted to quantify the severity of condensate, hydrocarbon or aqueous phase trapping, followed by a wide variety of documented laboratory procedures to evaluate treatments such as increased drawdown, application of IFT reducing agents, acidization, lean or rich gas injection, dry gas injection, solvent injection, formation heat treatment, capillary imbibition, etc to determine the optimal stimulation technique.

CONCLUSIONS

Aqueous and hydrocarbon phase trapping has been well documented to be a cause of significant permeability reduction in many lower permeability oil and gas producing formations. A variety of techniques have been presented to diagnose potential problem reservoirs which may be susceptible to phase trapping problems, as well as various operational techniques to avoid or mitigate phase trapping problems once they have occurred. Laboratory analysis is recommended as a portion of a methodical approach to diagnose the actual severity and type of the phase trap problem and design the best possible stimulation technique to remediate it.

ACKNOWLEDGEMENTS

The authors wish to express appreciation to Maggie Irwin and Vivian Whiting for their assistance in preparing the figures and text of the paper.

REFERENCES

- 1 Bennion, D B , et al, "Reductions in the Productivity of Low Permeability Oil and Gas Reservoirs Due to Aqueous Phase Trapping", *JCPT*, November, 1994, 45
- 2 Bennion, D B , et al , " Water and Hydrocarbon Phase Trapping in Porous Media, Diagnosis, Prevention and Treatment", to be published in the *Journal of Canadian Petroleum Technology*, June, 1996
- 3 Bennion, D B and Cimoli, M, "Aqueous Phase Trapping in Low Permeability Porous Media", SPE Gas Symposium, Calgary, 1993
- 4 Bennion, D B , et al , "Low Permeability Gas Reservoirs, Challenges and Opportunities", SPE Gas Symposium, April 1996, Calgary, Canada
- 5 Jamaludden, A K M , VanDamme, L M , Mann, B K and Bennion, D B., "Formation Heat Treatment (FHT) A State of the Art Technology for Near Wellbore Formation Damage Treatment", paper CIM 95-67 presented at the Petroleum Society of CIM 45th ATM, May 14-17, Banff, Canada
- 6 Bennion, D B , "Underbalanced Drilling Offers Pluses and Minuses", *Oil & Gas Journal*, January 2, 1996
- 7 Bennion, D B , et al, "Underbalanced Drilling, Does it Really Reduce Formation Damage?", *JCPT*, November, 1995
- 8 Bennion, D B , et al, "Injection Water Quality, A Key Factor to Successful Waterflooding", presented at the Annual Meeting of the Petroleum Society of CIM, June, 1994

FIGURE 1
PORE SCALE MECHANISM OF AQUEOUS PHASE TRAPPING IN A GAS RESERVOIR

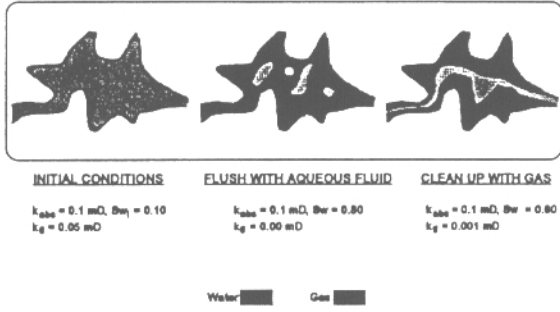


FIGURE 2
MECHANISM OF PHASE TRAPPING

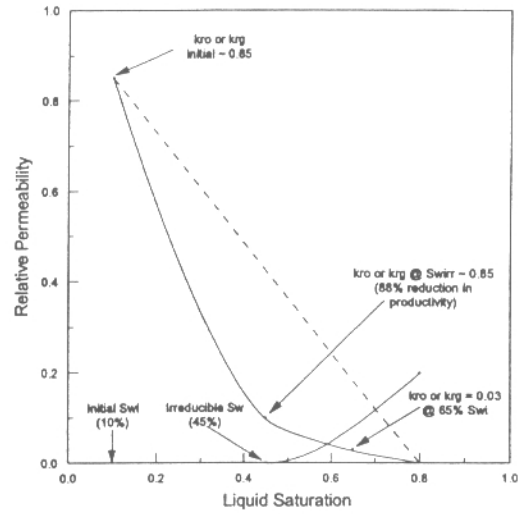


FIGURE 3
ILLUSTRATION OF EFFECT OF INVASION DEPTH AND DRAWDOWN GRADIENT ON PHASE TRAPPING

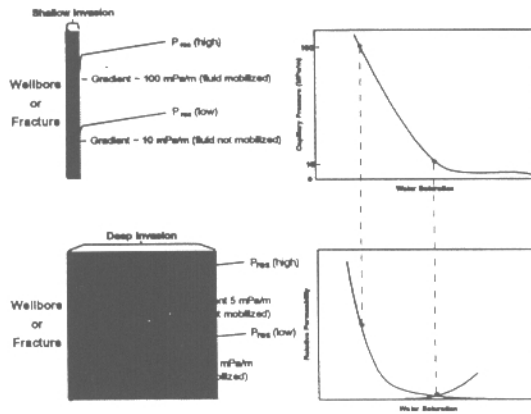


FIGURE 4
CONDENSATE TRAPPING AND VAPORIZATION MECHANISMS

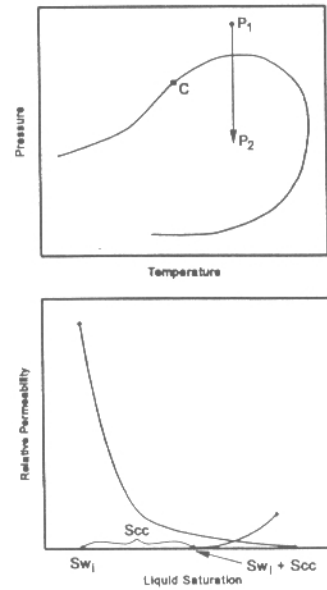


FIGURE 5
EFFECT OF SKIM OIL CONTENT ON NEAR WELLBORE INJECTIVITY

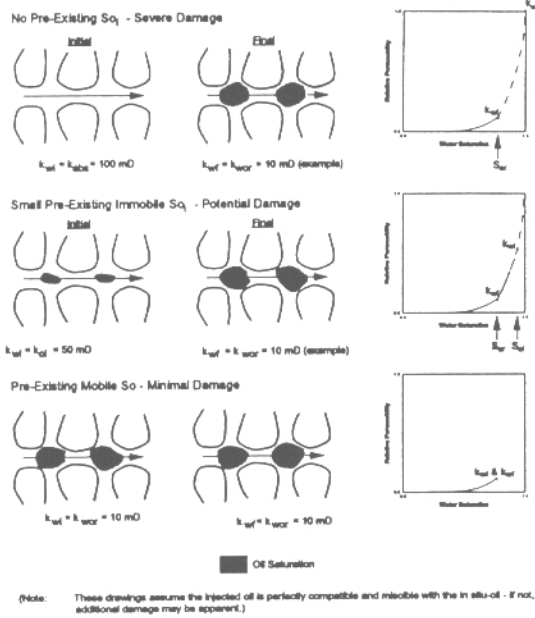


FIGURE 6
ILLUSTRATION OF RELATIVE PERMEABILITY EFFECTS ASSOCIATED WITH SKIM OIL OR FREE GAS ENTRAINMENT

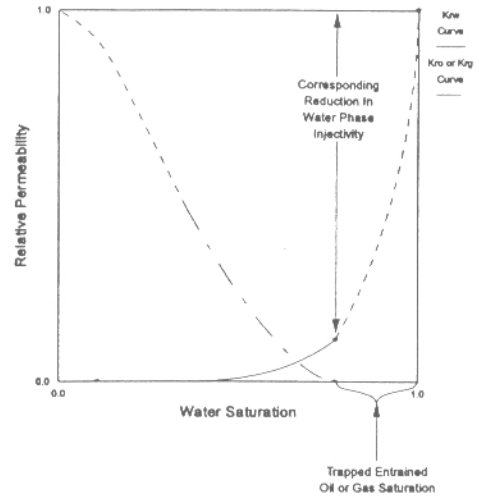


FIGURE 7
ILLUSTRATION OF APT CORRELATION FOR PRELIMINARY DIAGNOSIS OF AQUEOUS PHASE TRAP PROBLEMS

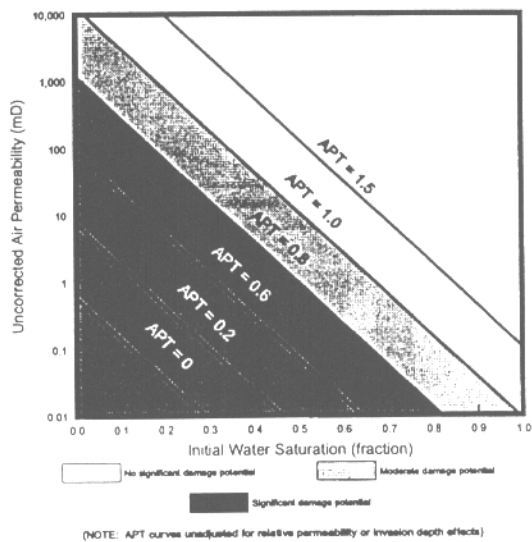


FIGURE 8
WATER vs OIL-BASED FLUID TRAPPING IN A WATER-WET SYSTEM

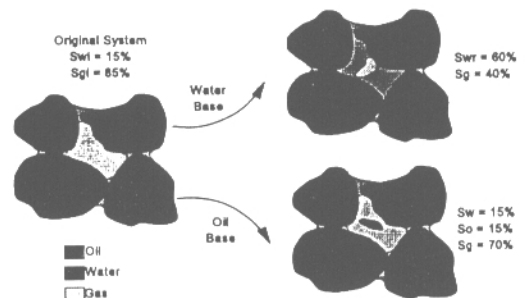


FIGURE 9
RADI OF CURVATURE
IN POROUS MEDIA

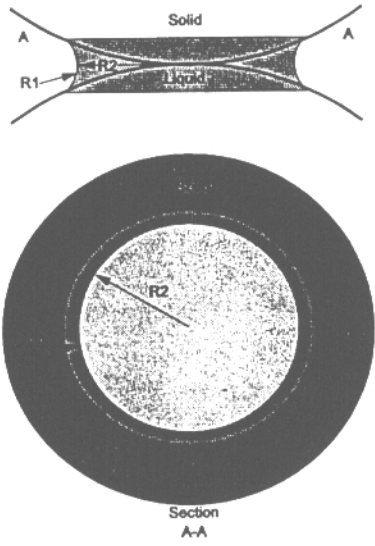


FIGURE 10
ILLUSTRATION OF CAPILLARY EFFECTS IN POROUS MEDIA

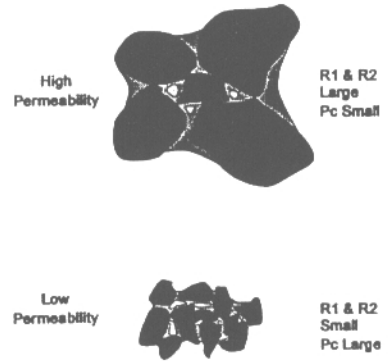


FIGURE 11
DRY GAS INJECTION PROCEDURE

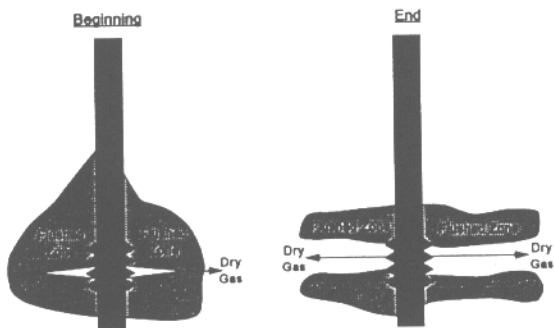


FIGURE 12
FORMATION HEAT TREATMENT PROCEDURE (FHT)

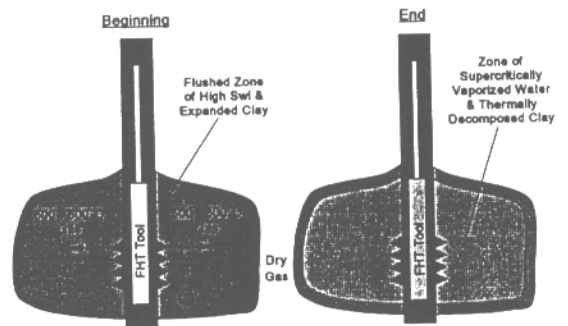
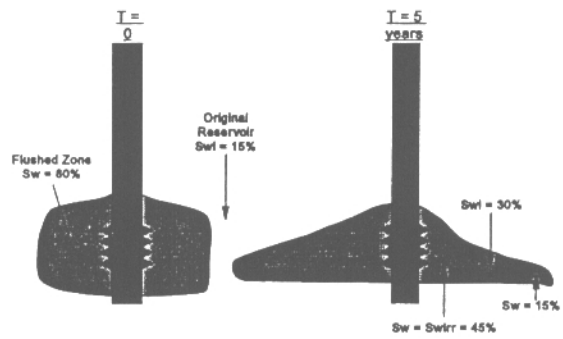


FIGURE 13
ILLUSTRATION OF CAPILLARY IMBIBITION vs TIME





SPE 35577

Low Permeability Gas Reservoirs: Problems, Opportunities and Solutions for Drilling, Completion, Stimulation and Production

D. B. Bennion, F B Thomas, R F Bietz, Hycal Energy Research Laboratories Ltd

Copyright 1996, Society of Petroleum Engineers, Inc

This paper was prepared for presentation at the Gas Technology Conference held in Calgary, Alberta, Canada, 28 April - 1 May 1996

This paper was selected for presentation by an SPE Program Committee following review of information contained in an abstract submitted by the author(s). Contents of the paper, as presented, have not been reviewed by the Society of Petroleum Engineers and are subjected to correction by the author(s). The material, as presented does not necessarily reflect any position of the Society of Petroleum Engineers, its officers, or members. Papers presented at SPE meetings are subject to publication review by Editorial Committees of the Society of Petroleum Engineers. Permission to copy is restricted to an abstract of not more than 300 words. Illustrations may not be copied. The abstract should contain conspicuous acknowledgement of where and by whom the paper was presented. Write Librarian, SPE, P O Box 833836 Richardson TX 75083 3836 U S A, Fax 01-214-952 9435

Abstract

As the industry seeks to increasingly exploit reserves of natural gas contained in low permeability intercrystalline sandstone and carbonate formations (<20 mD in permeability) many questions have arisen as to the optimum practices to drill and complete horizontal and vertical wells in these systems as well as the best techniques to hydraulic or acid fracture these formations to obtain economic production rates.

This paper provides a summary of recent work which has been conducted in the diagnosis and remediation of problems associated with tight gas reservoirs. Information on the importance of reservoir quality assessment and initial saturation determination is presented as well as a detailed discussion of common damage mechanisms which can affect the productivity of tight gas formations. These include fluid retention problems, adverse rock-fluid and fluid-fluid interactions, counter-current imbibition effects during underbalanced drilling, glazing and mashing, condensate dropout and entrainment from rich gases, fines mobilization and solids precipitation. The impact of these problems during drilling, completion, workover and kill operations is reviewed and suggestions presented for the prevention and potential remediation of these problems.

Specific examples of where these problems have been observed in 23 different common Western Canadian lower permeability gas horizons are presented in a summary format

for informative purposes

Introduction

Vast reserves of valuable natural gas and associated liquids exist trapped in low permeability intercrystalline and microfractured carbonate and sandstone formations throughout the world. Due to the low inherent viscosity of gas, conditions can be such that these reserves can be recovered from these low permeability strata in situations where the economic recovery of conventional liquid hydrocarbons would be impossible. This paper describes various mechanisms which can influence the effective recovery of gas from low permeability formations and presents a variety of drilling, completion, production and remediation techniques that have proven useful recently in optimizing the recovery of gas from formations of this type.

The definition of a "low" permeability reservoir is somewhat arbitrary, but for the purposes of this paper would be considered to be formations which have a surface routine average air absolute permeability of less than 20 mD. In-situ reservoir condition permeabilities in these types of reservoirs are generally less than 1 mD and can range down into the microDarcy range (10^{-6} D) in many situations.

Although the emphasis in this paper is specifically on low permeability gas reservoirs, much of the information presented is also applicable to higher permeability gas bearing formations.

What is the Challenge?

If we consider what could cause uneconomic production rates from a low permeability gas bearing formation, the options generally will fall into six categories, these being,

- 1 Poor reservoir quality - period!
- 2 Adverse initial saturation conditions
- 3 Damage induced during drilling and completion
- 4 Damage induced during hydraulic or acid fracturing
- 5 Damage induced during kill or workover treatments
- 6 Damage induced during production operations

Each of these categories will now be reviewed in more detail.

1. Poor Reservoir Quality - Period! The saying "You cannot make a silk purse out of a sow's ear" has definite applicability to the field of tight gas exploitation. Through the use of appropriate drilling, completion and in some cases large scale fracturing techniques, some operators have been amazingly successful in obtaining economic production rates from formations exhibiting in-situ matrix permeabilities of as low as 10^{-6} D. Some reservoir applications, however, are doomed to failure by the simple virtue of the fact that, no matter how successful and low damaging our drilling and completion operations, sufficient in-situ permeability, pressure, reserves or all of the above are not present to obtain economically viable wells. The prime objective of this paper is to identify candidates of this type, in comparison to those where the judicious application of the appropriate technology can obtain economic wells. In general, no documented evidence exists of economic production from formations having an interconnective matrix permeability of less than 10^{-6} D (even in the presence of successful large scale fracturing treatments). If an extensive micro or macrofracture system exists and the well can be completed without impairing the conductivity of the natural fractures, then documented cases exist where viable production has been obtained from source matrix of lower permeability values than 10^{-6} D. Penetration of a less extensive microfracture system by a conventional hydraulic or acid fracturing treatment, to augment inflow, has also been successful in some sub microDarcy reservoir applications. Well successes in these situations have been highly dependent on geological control and being able to effectively predict the location of and penetrate the pre-existing natural fractures with the wells or fracture treatments. Where such penetration has not occurred, the wells have generally been non viable.

2. Adverse initial saturation conditions. In many cases, gas exists in low permeability formations of "acceptable" permeability according to the previous criterion, but, due to adverse capillary forces, high in-situ saturations of trapped water, and in some cases, liquid hydrocarbons are present. If these saturations are too high, economic production of gas from the zone is often difficult due to:

- Limited reserves available for production due to the majority of the pore space being occupied by an immobile trapped fluid.
- Adverse relative permeability effects caused by the presence of high immobile fluid saturations rendering economic production rates impossible.

One of the first steps in ascertaining if gas is economically producible from a low permeability formation is the accurate determination of initial fluid saturations. This process is often difficult due to the fact that:

- Water saturations calculated from logs are often inaccurate due to limited availability of accurate "a", "m" and "n" electrical property data to calibrate field resistivity logs.

- Accurate R_w data is often unavailable for these formations, due to high capillary trapping effects, many of these zones do not produce mobile free water to facilitate accurate compositional and R_w measurements.

- Water saturations evaluated from cores drilled with water based fluids are often elevated due to core flushing and spontaneous imbibition effects. Water saturations obtained using air or nitrogen as coring fluids are often lower than true in-situ values due to localized heating during the coring process and core desiccation. Oil-based coring fluids can result in good water saturation determinations, but flushing can affect the accuracy of the measurement of the magnitude of any trapped initial liquid hydrocarbon saturation which may be present in the reservoir.

A variety of techniques are available to measure in-situ water and oil saturations, the best and most reliable being speciality coring programs in the producing zone of interest. In zones containing only an initial water saturation, radioactively traced (deuterium or tritium) coring fluids can provide an accurate evaluation of initial water saturation when coupled with low invasion coring technology (Ref. 1). When both an initial oil and water saturation are present and we desire to evaluate the true magnitude of the "free" gas saturation available for reserves evaluation and recovery, sponge coring, when coupled with a radioactively traced water based coring system and a low invasion coring tool can give good results, as illustrated in Fig. 1. It can be seen from Fig. 1 that with this data (after the oil volume is adjusted for gas solubility and swelling effects) one can accurately evaluate the free gas saturation and determine if sufficient reserves and relative permeability exist to obtain a viable and exploitable play. These techniques have been used in the past to ascertain initial saturations in formations such as the Montney, Gething, Rock Creek, Ostracod, Viking, Cardium and Jean Marie in Canada and in a number of low permeability Permian Basin gas fields in the United States. Although highly related to reservoir quality, if a free gas saturation of lower than 25-30% exists in the media this reduces both reserves and effective gas permeability below what would typically be quantified as economically producible values.

3. Formation Damage During Drilling and Completion.

Tight gas reservoirs are very susceptible to formation damage. This is due to the generally unforgiving nature of low permeability rock in that we can tolerate only a minimal amount of damage, due to the already inherently low permeability, and to the fact that low permeability formations generally experience much more severe damage than their higher permeability counterparts due to a high degree of sensitivity to capillary retentive effects, rock-fluid and fluid-fluid compatibility concerns.

In general, the degree of significance of formation damage associated with a tight gas reservoir during the drilling process will be related to the nature of the final completion

contemplated. Due to the low permeability nature of the matrix, unless huge losses of clear fluid to the matrix occur, due to poor fluid rheology and high hydrostatic overbalance pressures, the zone of extreme permeability impairment is generally contained in a fairly localized region adjacent to the wellbore. If hydraulic fracturing is the contemplated final completion technique, which is often the case in many low perm vertical gas wells, shallow invasive damage induced by drilling, cementing and perforating may not be significant as a well propagated and placed frac will penetrate far beyond the zone of drilling induced invasion and damage during the fracturing treatment will become the major issue of importance (to be discussed later). Exceptions would include failed or small frac treatments where short fracture half length does not effectively penetrate the zone of drilling induced damage, a high concentration of invaded fines which may subsequently be produced into and plug the high conductivity fracture directly adjacent to the wellbore, or simple mechanical problems initially propagating the frac due to high near wellbore tortuosity induced by formation damage (a problem often addressed with a small pre-frac HCl or HCl/HF acid squeeze to reduce tortuosity).

Drilling induced formation damage becomes more of an issue when open hole non-fractured completions are contemplated. When considering low permeability gas reservoirs, these types of completions are generally only successful if a large surface area of the formation can be accessed, such as in a horizontal well, a large vertical pay zone with a conventional well, or an openhole completion in a shorter but naturally micro/macros fractured zone of the formation.

Fluid Retention Effects. The single greatest enemy of tight gas, whether during drilling, completion, fracturing or workover operations, is fluid retention effects. These can consist of the permanent retention of both water or hydrocarbon based fluids or the trapping of hydrocarbon fluids retrograded in the formation during the production of the gas itself. This phenomena is commonly referred to as aqueous or hydrocarbon phase trapping and has been discussed in detail in the literature (Ref 2&3). Capillary pressure forces which exist in the porous media are the dominating factor behind fluid retention.

Capillary pressure forces, are defined as the difference in pressure between the wetting (generally water in most gas reservoirs) and non-wetting (gas) phases that exist in the porous media. This capillary pressure can be expressed by the following equation

$$P_c = P_{nw} - P_w \\ = (\text{Interfacial Tension})_{o-g \text{ or } g-w} (1/R_1 + 1/R_2) \quad (1)$$

This mechanism is pictorially illustrated in Fig 2. Fig. 3 illustrates how this mechanism is operative in low and high quality porous media and why capillary pressure and retention effects are more significant in low vs high permeability formations.

A large number of tight gas bearing formations are susceptible to phase trapping and fluid retention effects due to the fact that many of the economically producible formations would be considered to be "subirreducibly saturated" where the initial water saturation is at some value considerably less than what would be considered to be the "irreducible" liquid saturation. This, in fact, is the major reason why many tight gas reservoirs are exploitation candidates as this subirreducible saturation condition creates significant in-situ reserves and reduces the adverse relative permeability effects present in the system, thereby significantly increasing the productivity of the wells if they can be completed in a non damaging fashion. Most gas reservoirs of this type exhibit high log resistivities, produce no free water (other than fresh water of condensation from the produced gas), are not in direct communication with active aquifers or high water saturation zones and have a distinct propensity to retain the majority of any introduced water based fluid, much like a very large sponge. The basic mechanism of an aqueous phase trap is illustrated in Fig. 4. Fig. 5 illustrates the interplay of invasion depth and pressure with the severity of aqueous phase trapping. Equation 2 (Ref 3) is used as a predictive tool to provide an estimate of the significance of potential problems associated with aqueous phase trapping,

$$APT_i = 0.25[\log_{10}(k_{air} \text{ in mD})] \\ + 2.2(Sw_{i-\text{initial fraction}}) \quad (2)$$

Fig. 6 provides a pictorial representation of Equation 2. A value of the aqueous phase trap index (APT_i) of greater than 1.0 is generally an indication that significant problems with permanent aqueous phase trapping in the formation should not be apparent [although non permanent invasion and transient permeability impairment or aqueous phase loading (APL) may still occur (Ref 3)]. Values of APT_i between 0.8 and 1.0 indicate potential sensitivity to aqueous phase trapping, and values less than 0.8 generally indicate significant potential for damage due to permanent fluid retention if water based fluids are displaced or imbibed into the formation. The smaller the value of the APT_i index, the more significant the potential for a serious aqueous phase trapping problem. Examination of Figure 6 indicates that the permeability and initial saturation conditions in which many tight gas reservoirs exist render them prime candidates for aqueous phase trapping.

Countercurrent Imbibition. Underbalanced drilling, while touted as a means of minimizing formation damage (Ref 4&5), may actually increase the severity of near wellbore aqueous phase trap problems when it is used with water based fluids in horizontal wells which will be completed open hole in tight gas formations. Fig. 7 provides a schematic illustration of the mechanism of countercurrent imbibition which can occur during an underbalanced operation in a subirreducibly water saturated formation. Due to the discrepancy between the "initial" and "irreducible" saturations, one can see that there is a tremendous capillary force that exists between the initial water saturation level and the

irreducible saturation level (where the capillary pressure curve becomes vertically asymptotic). In a properly designed overbalanced operation the use of appropriate bridging and filter cake building agents can establish a near zero permeability filter cake on the face of the formation which may impede spontaneous imbibition effects. In an underbalanced drilling operation, if any free water saturation is present in the circulating fluid system, this is similar to establishing a gas-water contact directly adjacent to the wellbore face and continuous countercurrent imbibition effects into the formation can occur, even when a continuously underbalanced condition is maintained. The problem with aqueous invasion is attenuated if the underbalanced condition is lost or periodically compromised, or if a well drilled underbalanced is hydrostatically killed for completion, due to the fact that there is no protective filter cake to impede the large scale invasion of fluids into the formation in an overbalanced condition. Laboratory studies describing this phenomena are presented in detail in Ref. 4.

Mud Solids Invasion. The physical invasion of natural and artificial solids may occur during drilling, completion, workover or kill treatments if operating in hydrostatically overbalanced conditions. Due to the very small pore throats normally associated with low permeability gas reservoirs, any significant depth of invasion of mud solids into the rock is not normally observed (unless fractures or extremely small solids, which can sometimes be generated by PDC bits, are present). Once again, this is usually only a concern in situations where open hole completions are contemplated due to the shallow nature of the damage.

Glazing. Glazing, mashing or wellbore polishing can be a problem in some open hole tight gas completions, particularly if pure gas is used as the drilling media. Due to the extremely poor heat transfer capacity of gases, if no fluid is present in the circulating drilling media, extremely high rock-bit temperatures can be generated. This can result, when combined with connate water and rock dust generated from the drilling process in conjunction with high temperatures and the polishing action of the bit, in the formation of a thin but very low permeability ceramic pottery like glaze on the face of the formation. This phenomena can be observed on the face of sidewall cores cut in such situations and on the face of air drilled core. Like mud solids invasion, due to its extremely localized depth, glazing tends to be problematic specifically in open hole completion scenarios. Mashing, caused by poorly centralized strings and tripping, refers to mechanical damage caused by friction and motion of the string and centralizers, collars etc., against the formation face and results in the intrusion of a paste like layer of fines and drill solids into the formation face directly adjacent to the wellbore. Once again, a localized form of damage usually problematic only in open hole completions.

Rock-Fluid Interactions.

Clays. The low permeability associated with many tight formations is generally caused by small grain size sandstones or limited intercrystalline porosity development in carbonates, but in some formations, predominantly clastics, the permeability is also reduced by significant concentrations of clay. A variety of different types of clay can be present. Highly fresh water sensitive expandable clays such as smectite or mixed layer clays can occur in shallower tight gas formations. Examples include the Viking, Basal Colorado, Belly River and Milk River formations in Western Canada. When contacted by fresh or low salinity water these clays expand in size due to substitution of water into the clay lattice (Ref. 6). The physical expansion of the clay (up to 500% depending on the type of clay under consideration) can result in near total permeability impairment. Other types of clay, such as kaolinite are susceptible to electrostatic deflocculation (Ref. 6), where abrupt changes in salinity and pH can cause the clay to disperse and migrate to pore throat locations where it bridges, blocks and can cause permanent reductions in permeability (Cardium, Belly River, Glauconite, Halfway, Bluesky, Basal Quartz, Gething, Ostracod, Viking, Rock Creek and Montney are some formation types in Western Canada where this phenomena has been observed). Since filtrate invasion can extend a significant distance into the formation if fluid losses are appreciable, this type of damage may be of sufficient radius of penetration to partially impair productivity of limited scale subsequent fracture treatment in certain situations. If fresh water sensitive or reactive clays are present, care should obviously be taken to use inhibitive fluids or low fluid loss systems to minimize the depth of invasion.

Chemical Adsorption. Physical adsorption of high molecular weight polymers or oil wetting surfactants can reduce permeability significantly in low quality formations or preferentially elevate permeability to water if a free water saturation is present in the formation. The relative size of the large polymer chains, when adsorbed on the surface of the porous media, is significant in comparison to the relative diameter of the pore throats allowing gas to flow from the media. Thus a film of adsorbed polymer, which may only moderately reduce the permeability in a higher quality formation, can totally occlude available permeability in a lower quality zone. Once again, this is a wellbore localized phenomena. Adsorbed polymer can often be removed using oxidizing agents, but care should be taken to ensure that invasion of the oxidizing agent, and subsequent entrapment, does not occur when the sealing effect of the polymer filter cake is degraded by oxidant contact.

Fines Migration. Fines tend to move preferentially in the wetting phase and hence when only gas is flowing migration of particulates in the porous media should be minimized. Problems can occur when fluid invasion occurs due to relatively high spurt losses potentially encountered during drilling or fracturing process, due to motion of invaded fluids.

during high drawdown cleanup operations, or if the formation produces liquid at rates above the critical migration rate during overbalanced drilling operations

Fluid-Fluid Interactions Problems with fluid-fluid incompatibilities would include the formation of insoluble scales or precipitates caused by adverse chemical reaction of invaded drilling or completion fluid filtrates and in-situ water. The potential for stable emulsion formation also exists if hydrocarbon drilling and completion fluids are used, or if water based fluids are used in formations which contain an initial irreducible liquid hydrocarbon saturation. Acid compatibility issues may also be apparent if acid is used in the presence of an immobile liquid hydrocarbon saturation.

4. Formation Damage During Fracturing of Tight Gas Formations. The majority of tight gas formations, by their nature, require hydraulic or acid fracturing in order to obtain economically viable production rates. Although it has been suggested by various authors that fracture faces can tolerate a huge amount of damage and that the productivity of the treatment is still limited by the amount of fracture conductivity present, there is significant lab and field evidence present to indicate that formation damage occurring during fracturing treatments is still a major issue. If we consider factors which may impair the productivity of a fracture treatment, these would include,

- Physical mechanical problems with the fracture treatment
- Formation damage to the high conductivity fracture itself
- Formation damage to the fracture face

Physical problems with the fracture treatment. These would include such problems as poor mechanical propagation of the frac, sandoffs, fracturing out of zone or channelling behind casing, etc

Formation damage to the high conductivity fracture itself. No matter how large the treatment, if a very high conductivity fracture channel is not maintained, particularly if permeability is lost in the portion of the fracture directly adjacent to the well, the benefit of hydraulic fracturing is severely compromised. A variety of mechanisms can result in impairment of the permeability of fractures in propped or acid fracture treatments, including

- improper breaking of linear or crosslinked gels
- polymer adsorption and entrapment
- entrapment of produced formation fines/solids in the fractures
- emulsion blocks in the fractures
- compaction of the fracture and embedment effects associated with plastic formations and increasing overburden pressures during the depletion process
- physical production of proppant from the high conductivity fracture causing a loss in fracture conductivity

A common misconception is that fracture treatments are impervious to formation damage on the fracture face itself during the fracture treatment and it is only the fracture conductivity which must be maintained. Mathematical

modelling, plus considerable field experience, has indicated that this is not the case in many reservoir situations. The smaller the size and effective cross sectional area of the fracture treatment, the more significant the damage occurring on the frac face in impairing the ultimate productivity of the frac treatment. Large, (100-200 tonne for example) fracs, can tolerate a significant amount of permeability impairment on the fracture face, perhaps in excess of 95%, without appreciably reducing the productivity of the frac. A permeability reduction of 100%, however, cannot be tolerated. Some of the damage mechanisms mentioned previously, particularly fluid retention, are capable of causing 100% permeability reductions in tight gas formations and have been the result of significant reductions in well productivity. Companion tight gas well fracs of identical size (150 tonnes) have been placed in tight formations in the Permian basin in identical quality pay with the only variable being the break time and rheology of the cross linked water based fracture fluid used. When the crosslink was preserved to propagate the frac, followed by subsequent breaking, lab tests indicated a fracture face invasion depth into this 0.01 mD, 12% Sw_i formation of less than 2 mm with over 80% fluid recovery in the field and 7,000,000 scf/day flow rates. Wells in which premature breaking of the frac fluid occurred exhibited over 6 cm of invasion in the lab, less than 10% fluid recoveries in the field and uneconomic post frac flow rates of less than 50,000 scf/day.

For this reason, fracture fluid compatibility, from both a potential invasion depth and retention point of view, as well as from a chemical and mechanical point of view must be carefully considered to ensure that, not only can a viable frac be propagated, but that invasion into the formation at the high differential pressure gradients occurring during all frac treatments, particularly in pressure depleted formations, is minimized. If invasion does occur to a limited extent care must be taken that the invading fluids are compatible with the formation and designed with maximum ease of recovery in mind.

5. Formation Damage During Kill/Workover Treatments.

Mechanisms of damage to perforated, open hole or fractured wells that can occur during hydrostatically overbalanced kill or workover treatments are similar to those described previously for drilling and completion. Damage and invasion may be more severe in these cases as, similar to an underbalanced drilling operation, these formations lack any type of protective or sealing filter cake to prevent wholesale invasion of the water or oil based kill/workover fluid, so a significant amount of fluid invasion and damage may be incurred before a hydrostatic kill condition is achieved.

6. Formation Damage During Production Operations.

Potential damage which could occur during normal production operations of tight gas formations include,

- Physical fines migration
- Retrograde condensate dropout phenomena (rich gas systems)

- Paraffin deposition problems (waxy rich gas systems)
- Diamondoid and hydrate plugging problems
- Elemental sulphur precipitation (high H₂S concentration systems)

Fines Migration. Considerable research (Ref 7) has indicated that fines generally tend to preferentially migrate in the wetting phase. For most gas reservoir systems this would be water (the exception being sub-dewpoint rich gas systems or gas reservoirs containing an initial immobile conventional or heavy oil saturation in which case the liquid hydrocarbon phase may partially or totally wet the surface of the formation) and significant problems with fines migration do not occur during normal production operations unless the interstitial shear rate caused by extreme gas flow rates causes mobilization of the connate water. Water coning, caused by excessive production rates, or the high rate cleanup of invaded water based drilling, completion, stimulation or workover fluids from the formation, may result in a condition of mobile water saturation and hence movement of the wetting phase. This results in conditions where, if loosely attached particulate matter is present in the pore system and the critical rate for migration is exceeded, that mobilization of the fines and damage may occur. Many examples of this phenomena are present where wells produce at high gas rates until the first sign of water breakthrough. At this point massive reductions in gas rate, which cannot be solely attributed to relative permeability effects, can occur, including, in some cases, physical sand production and formation collapse (some higher quality Gulf Coast formations in the USA exhibit this phenomena).

Retrograde Condensation Phenomena Fig. 8 provides a schematic illustration of a pressure-temperature diagram for a hydrocarbon system. A "dry" gas formation (typically a gas having a liquid yield of less than about 10 to 15 bbl condensate per MMscf of gas) follows the depletion path A to B. It can be seen that this depletion path never intersects the two phase envelope and hence this type of system is not prone to problems associated with downhole condensate dropout effects. These types of reservoirs may still produce liquid condensate at surface as the depletion path through the production tubing often follows the path A to C with the separator temperature being sufficiently low that production at surface conditions is well within the two phase envelope.

"Rich" gas systems, being those with liquid yields of greater than approx 15 bbl of condensate per MMscf, fall more to the left on the P-T diagram (Figure 8), and it can be seen at reservoir temperature conditions that during the depletion operation (path D to E) these systems will pass through the dewpoint line and liquid hydrocarbon condensate, which often may represent the most valuable fraction of the reservoir gas, condenses out of solution in the gas. In a manner analogous to an aqueous phase trap, because these tight gas formations do not generally contain a pre-existing hydrocarbon saturation, a sufficient hydrocarbon saturation to build a continuous liquid film to allow flow of the liquid condensate to the wellbore

must occur. This is commonly called the critical condensate saturation and the value is very dependant on reservoir lithology, wettability, condensate composition and drawdown pressure and can vary from a very small value (less than 2%) to very large values in excess of 40%. Tight gas systems, due to adverse capillary effects, often tend to exhibit higher critical condensate saturations than their higher permeability counterparts making them more susceptible to this particular mechanism of damage. The presence of the trapped condensate saturation has a blocking effect, identical to that described previously for the aqueous phase trap, and can substantially reduce near wellbore gas permeability.

In many rich gas systems, gas cycling schemes are implemented as a mechanism to recover the majority of the condensate liquids from the formation. In these systems condensate dropout, although mitigated in the bulk of the reservoir volume due to a properly executed cycling operation, can still significantly impair the productivity of the production wells as in many tight rich gas systems, even with large frac treatments in place, drawdown below the dewpoint pressure of the gas in the near wellbore region is required to obtain economic production rates.

Solids Precipitation Problems (Paraffins, Hydrates, Diamondoids, Elemental Sulphur). A detailed discussion of these phenomena is complex and beyond the scope of this paper, but is discussed in the literature (Ref 8 & 9). The formation of all of these solid precipitates are generally initiated by reductions in temperature, and are also in some cases weaker functions of reductions in pressure. In most situations this results in the generation of these elemental solids being more of a production problem in tubing and surface equipment, rather than directly in the formation itself. Near wellbore problems are encountered in some waxy condensate systems which are producing at high rates due to a significant Joule-Thompson effect occurring at the perforations or in the fractures. The rapid expansion of gas in these zones, due to high drawdown effects, results in a significant localized temperature drop which can aggravate problems with solids precipitation. Diamondoids are granular solids, similar to their oil reservoir counterparts, asphaltenes, which are directly precipitated from natural gases (generally rich gases). These hard granular solids can result in erosion and plugging problems, most often in surface equipment. Elemental solid sulphur production can also occur downhole and in production equipment under certain temperature and pressure conditions in very sour gas systems which can result in both corrosion and plugging problems.

Techniques to Avoid Damage and Remediate Existing Damage to Low Permeability Gas Reservoirs

Many of the types of damage described previously can be avoided or their effect greatly reduced if a proper understanding of the reservoir and the types of problems that may be encountered is obtained prior to drilling, completion

and production. This section attempts to identify drilling and completion practices which may be useful in tight gas scenarios, as well as remediation techniques for wells with existing damage.

Fluid trapping/retention problems. This is a major mechanism of damage in many tight gas reservoirs. If we consider methods of minimizing the impact of this type of damage, they would include

Avoid the introduction of water based fluids into the formation during the drilling and completion operation in totality. This would include straight gas drilling or the use of hydrocarbon based drilling and completion fluids. Oil based fluids may also phase trap to a certain extent in the formation and reduce permeability, but due to the fact that the liquid hydrocarbon will generally be the non-wetting phase in most gas reservoirs, where no pre-existing liquid hydrocarbon saturation is present, the physical amount of trapping of the hydrocarbon phase may be significantly less than would be encountered if water was used in an equivalent situation and a large increase in gas phase relative permeability may be apparent. This phenomena is illustrated in Fig. 9. If a pre-existing liquid hydrocarbon phase saturation is contained initially within the porous media (as is common in many Montney, Rock Creek, Ostracod, Gething, Viking and Cardium formations) it is possible that the formation may be partially or totally wetted by the hydrocarbon phase, or the small pre-existing hydrocarbon phase saturation may act as a spontaneous adhesion site to trap additional hydrocarbons. In these types of reservoirs, oil based fluids may not be advantageous over water based systems as they may have equal or more trapping and damage potential. The use of straight CO₂ or highly CO₂ energized hydrocarbons has been successful as a frac fluid medium in some reservoirs of this type as an alternative to water. Alcohol fracs (i.e. gelled methanol) have been used with success in some situations. Care must be taken with the use of alcohol in very low (<0.1 mD) formations as adverse capillary pressure effects can also physically trap the alcohol. Low molecular weight alcohols, such as methanol, have a very low degree of miscibility with liquid hydrocarbons and can often suffer from incompatibility problems with respect to sludge formation with many crude oils. For these reasons, their use should be avoided in most situations where a liquid hydrocarbon saturation is known to exist in the reservoir in favour of higher molecular weight mutual solvents (i.e. IPA, EGMBE) which exhibit significantly greater miscibility with liquid hydrocarbons and fewer compatibility problems.

If water based fluids must be considered for technical or economic reasons, invasion depth should be minimized to the maximum extent possible to avoid significant aqueous phase retention problems. For drilling fluids this would include minimization of overbalance pressure, if possible, and rheology and bridging agents, if appropriate, to establish a protective filter cake to act as a barrier for significant fluid loss into the formation. Kill or workover fluids should be designed with

appropriate fluid additives to prevent losses to the formation under hydrostatic overbalance conditions. The use of cross-linked fracture fluids with appropriate breaker packages and as rapid recovery systems or poly-emulsions should be considered if water based frac fluids are considered.

Remediation of fluid retention problems. A number of basic approaches can be taken to removing existing phase traps, these would include

1. Increasing capillary drawdown. Trapped saturation is a direct function of applied capillary gradient, the higher the available capillary gradient, the lower the obtainable water saturation. Therefore, in the absence of fines migration problems, water coning potential or retrograde condensate dropout potential (rich gas systems) the higher the drawdown pressure which can be applied across the phase trapped zone, the lower the water saturation which will be able to be obtained. In a practical application, unless the invasion depth of the infiltrated aqueous phase is very shallow, or the reservoir pressure is extremely high, due to the vertically asymptotic nature of most gas-liquid capillary pressure curves near the irreducible saturation, extreme drawdown gradients, which cannot be realized in most normal field applications, are required to obtain an effective reduction in the trapped liquid saturation. For this reason this method does not tend to be of great efficacy in most situations.

2. Reduced IFT between the water-gas or oil-gas system. Capillary pressure, which is the prime mechanism for the entrapment of the oil or water based fluid within the pore system, is a direct linear function of the interfacial tension (IFT) between the trapped phase and the gas in the bulk of the pore space (Equation 1). If some means can be found to reduce the IFT between the gas and liquid phase, then at the available reservoir drawdown it may become easier to mobilise and produce a portion or all of the entrapped fluid. A variety of treatments are available to reduce the IFT in situations such as this:

- a) Chemical surfactants have been used in some cases, but due to the disparate molecular nature of gas and liquids, it is difficult to find liquid soluble chemical surfactants which are effective in obtaining the multiple orders of magnitude reduction in IFT (from say 70 to 0.1 dyne/cm) required in order to effectively mobilize a significant amount of trapped fluid from the system.
- b) Mutual solvents, such as methanol or higher molecular weight alcohols or materials such as EGMBE can significantly reduce IFT between gas and liquid and are mutually miscible in the trapped liquid phase and tend to reduce viscosity and increase volatility and vapour pressure extractive effects to remove a portion of the trapped liquid. As mentioned previously, careful selection of a mutual solvent is important to ensure miscibility and compatibility if a liquid hydrocarbon saturation is present within the porous media.
- c) Liquid carbon dioxide has been used for aqueous phase traps

due to its ability to reduce IFT, dissolve in the trapped liquid phase, physically extract a portion of the trapped water as a desiccant and provide a zone of localized high reservoir energy to obtain a high instantaneous capillary gradient on blowdown which might not normally be present in the formation (particularly in low pressure zones)

d) Liquid CO₂, LPG, Liquid ethane and dry gas have all been used as techniques to remove hydrocarbon traps in porous media. Depending in the available treatment pressure, temperature and gravity of the trapped hydrocarbons, one or more of these liquids will often be miscible with the entrapped hydrocarbons. The treatment is designed to either miscibly displace the trapped hydrocarbon a sufficient distance into the formation so that cross sectional flow area is increased to the extent that the zone of trapped fluid does not substantially reduce productivity, or produce the hydrocarbon saturated liquid back out of the formation at sufficient backpressure to keep the extracted hydrocarbons in solution to physically "scrub" a portion of the formation adjacent to the wellbore or fracture face clean of entrapped hydrocarbon. High treatment pressures are required for this treatment to be effective with conventional dry gas (natural gas or nitrogen) injection, generally in excess of 35 MPa. The treatment may be effective at much lower pressures (8 - 20 MPa) with gases such as liquid CO₂ or ethane, and at very low pressure (3 - 5 MPa) with very rich low vapour pressure gases such as LPG. In the case of a retrograde condensate trap, the treatment may be of only temporary utility as, if the well is continued to be produced in a high drawdown condition, further entrapment will occur as additional condensate is retrograded as the gas continues to be produced from the well.

3. Physical changes in the pore geometry. Since capillary pressure is also a direct function of the radii of curvature of the immiscible interfaces which are present in the porous media (Eq 1), which are forced by the geometry of the confining porous media (Fig 3), if the radii of curvature can be increased, by making the pore spaces less constrictive, capillary pressure will be reduced and it may become possible to mobilize the trapped fluid. While generally difficult to accomplish in clastic formations, unless HF acid is considered, this can be accomplished in some cases in tight carbonates with appropriate acid treatments. These stimulation treatments, however, are in some respects the proverbial "two edged sword" in that when the acid spends we simply have more water in the formation. If the spent acid is squeezed past the zone of effective reaction, it may become entrapped like any other invaded aqueous fluid and, in some cases, aggravate the production problem it was intended to cure. This is evident in many acid squeeze treatments in tight gas reservoirs where acid recoveries have been exceptionally poor and well productivity has often been further impaired, rather than improved, by the acid treatment. The use of nitrified or foamed acids has been useful in some situations of this type as the total volume of liquid introduced into the formation is reduced and localized

charge energy to recover the acid is introduced into the formation by the gaseous agent (often CO₂) used to foam the acid. Caution is required in implementing this procedure to reduce a hydrocarbon trap, as many acids are incompatible with hydrocarbons and de-asphalting or the formation of stable emulsions, particularly in the presence of high concentrations of unsequestered iron, could occur.

4. Direct physical removal of the trapped water or hydrocarbon saturation. This encompasses a rather wide range of potential techniques which include

a) *Dry gas injection* A common misconception is that merely flowing the reservoir gas for an extended period of time will result in evaporation and removal of a portion of the trapped water or hydrocarbon saturation. Since the produced reservoir gas is saturated with both water vapour (in all cases) and heavy hydrocarbons (for a rich gas reservoir) at reservoir temperature and pressure conditions as it passes by the trapped liquid, it can be seen that no additional water or hydrocarbon could be effectively absorbed into the gas phase. If pressure can be elevated significantly, some hydrocarbon liquid may revaporize, but this is obviously much easier accomplished in an injection rather than a production scenario. Dry, dehydrated, pipeline spec gas injection will result in the gradual desiccation of a portion of the reservoir directly adjacent to the injection zone, a phenomena well known in many gas storage wells. The objective of a dry gas injection technique is to inject dry gas for a short period of time (10 days at 1 to 3 MMscf/day typically) to attempt to dehydrate some of the higher conductivity channels in the reservoir and establish a conductive flow path to the bulk of the undamaged reservoir. The technique is relatively easy to apply and has particular application in damaged horizontal wells where large exposed pay zones may render other types of penetrating treatments impractical. Dry gas injection has been successfully combined, in some situations, with mutual solvents such as methanol to increase the potential extractive power of the treatment. Variations of the procedure would include the use of alternative dry gases such as nitrogen, oxygen content reduced air, dehydrated flue gas or carbon dioxide. Figure 10 provides a schematic illustration of the dry gas injection process. If highly saline brine is the trapped phase (i.e. - weighted drilling, completion or kill fluids or spent acid) laboratory investigation of this technique is often warranted as precipitation of the soluble salts from solution as evaporation occurs in the pore system can result in significant residual permeability impairment which may counteract the benefit of the removal of the trapped water saturation.

b) *Formation heat treatment* This is a relatively new experimental treatment which has been specifically designed to remove both aqueous phase traps as well as thermally decomposing potentially reactive swelling or deflocculatable clays (Ref 10). The treatment is applied using a specially designed coiled tubing conveyed downhole treating system. Electrical heaters in the downhole tool are used to heat

nitrogen, injected down the CT string, to very high temperatures which is then subsequently injected directly into the formation. If downhole temperatures can be elevated above 500°C, supercritical volatilization of water, regardless of the reservoir pressure, occurs as well as partial or total thermal decomposition and desensitization of reactive clays. In lab tests the technique has resulted in over 10 fold improvements in permeability in damaged zones. The technique has particular application to relatively shallow tight gas reservoirs where vertical wells penetrate thin, highly damaged sand layers. Treatment area is generally approximately two metres in length by 1 to 2 metres in radius in a single application. The most common application is potentially stimulating secondary target gas zones which were badly damaged using conventional water based fluids when targeting deeper primary zones. Fig. 11 provides an illustrative schematic of the FHT process.

c) Localized Combustion This has been a method suggested to remove hydrocarbon phase traps in tight gas. The technique involves short term air injection. If downhole temperature is sufficient, spontaneous ignition will occur, combusting the condensate saturation while simultaneously generating localized heat which may also vaporize a portion of the trapped connate water saturation and thermally decompose reactive clays. Wellbore flashback effects and extreme potential corrosion concerns are potential problems associated with the use of this method.

d) Time Nature abhors a steep capillary gradient. Thus, when a zone of high water saturation is induced into a water-wet formation, natural capillary action will tend to have a dispersing effect in gradually imbibing a portion of the water saturation away from the wellbore or fracture face. This phenomena is illustrated in Fig. 12. Due to the limitations of the capillary imbibition, the water saturation in the flushed zone will only be able to imbibe down to the irreducible saturation dictated by the capillary geometry of the system, therefore a significant residual aqueous phase trapping effect may still be apparent. This phenomena has been observed in many cases where tight gas wells have been drilled, tested and subsequently shut in or abandoned. After an extended period of time some of these wells have been retested and produced at order of magnitude or more greater rates than observed initially. Production of the well obviously counteracts, to an extent, this phenomena and may slow the speed of this process.

Countercurrent Imbibition. Countercurrent imbibition problems during underbalanced drilling operations can be minimized by increasing the magnitude of the apparent underbalance pressure to act as a greater deterrent to imbibition. If a significant difference exists between the initial and irreducible water saturations, however, such as in the case of many tight gas reservoirs, this technique is generally insufficient to counteract the extremely adverse capillary pressure gradients present in the porous media if a water based fluid is used. Better results are obtained in situations such as this by avoiding the use of water based fluids through either

straight gas drilling, or using a hydrocarbon based fluid as the drilling fluid medium (if the formation is water-wet). Since hydrocarbon is the non-wetting phase, no impetus will be present for spontaneous imbibition to occur. If the underbalance pressure condition is compromised, invasion and trapping of the hydrocarbon based fluid could still occur and be problematic.

Mud Solids Invasion. As mentioned previously, this is generally only a significant problem if an non-stimulated open hole completion is contemplated for the well under consideration. If this is the case, care must be taken in the design of the drilling fluid to ensure that significant invasion of solids into the formation does not occur. In general solids larger than about 30% of the median pore throat size will not invade a significant depth into the formation. Due to the small pore throat size associated with most tight gas reservoirs, natural exclusion of the majority of artificial (barite, bentonite, bridging agents, natural drill solids, etc.) occurs. Pore size distribution data (and fracture aperture sizing if fractures are present) should be obtained in this type of situation to allow mud engineers to ensure that the expected size distribution of solids present in the fluid system are appropriate to avoid invasion.

Due to the very small pore throat size, normal mud solids are too large to form a low permeability sealing filter cake in most low permeability gas reservoirs. This results in the solids being retained from invading into the formation, but because the filter cake is relatively coarse (in comparison to the small pore throats the cake is attempting to block) a considerable amount of fluid seepage into the pore system can still occur which can initiate a damaging phase trap or other fluid-fluid incompatibility problems. Proper sizing of the suspended particulate matter can generate a much lower permeability filter cake than would be obtained using naturally occurring solids and can act as an efficient barrier to damaging filtrate invasion. Sizing criteria vary depending on the system, but would range from 10-40% of the pore throat size for matrix systems and 10-100% of fracture aperture for fractured reservoirs. Specific size distribution for a fluid bridging agent can generally only be quantified after a detailed evaluation of the system under consideration.

Underbalanced drilling may also be considered as a technique to prevent this type of damage if a heterogenous formation exists where formulation of a single fluid system with effective bridging characteristics is impractical.

Glazing Classic glazing is generally motivated by heat associated with pure gas drilling operations in open hole completions in uniform, low permeability clastics or carbonates. Glazing can generally be avoided by the inclusion of a small amount of compatible fluid (i.e. mist drilling) in the system to increase lubricity and heat transfer from the bit.

Rock-Fluid and Fluid-Fluid Interactions. Initial analysis of the formation to investigate the presence of any potentially reactive clays (smectite, mixed layer clays, mobile kaolinite), is essential in tight gas reservoirs. This is generally conducted using a combination of thin section, XRD and SEM analyses. If reactive clays are present, this should act as a warning flag for the use of fresh or low salinity water in most situations. Detailed compatibility testing should be conducted, if water based fluids are to be used, to quantify inhibitors (i.e. - KCl, CaCl₂, etc.) which may stabilize reactive clays if invasion does occur. Chemical stabilizers (i.e. - high molecular weight polymers), while potentially efficient at stabilizing reactive and mobile clays, often may cause more damage due to physical adsorption of the polymer on the rock surface which may occlude the minuscule area available for flow in tight gas formations and hence should only be used after detailed lab evaluation has been conducted to ascertain their usefulness and degree of damage that they may cause.

Similar tests should be conducted between potential invading filtrates and formation fluids to ensure that they are compatible with respect to scale, precipitate or emulsion formation with in-situ water and liquid hydrocarbons which may be present in the porous media. If acid treatments are to be used in reservoirs which contain a trapped liquid hydrocarbon saturation, compatibility tests to ensure that asphaltenes, sludges and emulsions do not form between the acid and the in-situ oil should be conducted. Rock solubility tests should also be conducted in this case to ensure that a large concentration of insoluble fines (i.e. - quartzose rock fragments, pyrobitumen, anhydrite, etc.) are not released by acidization and allowed to subsequently be squeezed deeper into the formation where they may reduce permeability.

Fracturing Operations. Detailed modelling and geomechanical measurements can be undertaken to attempt to ensure that the mechanical propagation of hydraulic and acid fracturing treatments are acceptably achieved. Fluid retention, particularly water retention, is a significant problem in many tight gas fracturing operations. A variety of techniques have been utilized to attempt to reduce fluid losses to the formation in situations where water trapping is problematic including the use of pure oil fracs, CO₂ energized oil fracs, crosslinked water based fracs, poly-emulsion fracs and water based foam fracs. The selection of the appropriate fluid will be highly dependant on the size of the frac, formation characteristics and phase trapping potential and available drawdown pressure.

In formations which contain a pre-existing oil saturation and which may (or may not be) oil-wet, oil based fluids may react as adversely or worse than water. Pure CO₂ fracturing has been used successfully in some formations of this type (i.e. - Rock Creek, Ostracod, Gething, Montney), but obvious limitations exist with respect to the size of frac which can be effectively propagated (generally less than 20 tonnes with current technology) and depth constraints (generally less than

2000 metres, depending on tubing/casing size).

Kill/Workover Treatments. Many wells have been drilled with great care paid to formation damage, only, at some later date, to have poorly conceived kill jobs conducted which were very effective in achieving not a only temporary but permanent well control results. Water-based kill fluids generally react poorly in most tight gas situations and significant invasion generally occurs due to the unprotected nature of the fracture faces or open hole wellbore after production has been occurring for some period of time. Oil-based fluids with appropriate bridging agents may be a better choice for kill agents in some situations. Careful care with respect the composition, rheology, bridging character, filter cake building potential and removability should be taken in kill fluid design in a manner similar to designing a drilling fluid. In many cases the use of CT or snubbing equipment may be viable and the workover or recompletion can be conducted with the well in a live mode, underbalanced, to avoid significant additional damage effects.

Production Problems. A large majority of production problems with tight gas reservoirs, including fines migration, retrograde condensate dropout and solids precipitation are all associated with large pressure drops or rates associated with the low permeability nature of the reservoir. Means of reducing rate or pressure drop, including physical rate reduction increase in flow area by horizontal drilling, open completions or fracturing are the best techniques to counteract these problems.

Dual completions using downhole ESP's to pump off water in wet zones can prevent the premature coning of water in some gas reservoir situations, which may have adverse relative permeability and fines migration effects.

Solids precipitation problems are difficult to prevent, being inherent to the nature of the produced gas itself. But can often be minimized by judicious selection of the correct downhole operating temperature and pressure and the selective use of a variety of chemical inhibitors or treating agents (solids precipitation inhibitors, organic solvents, crystal modifiers, etc.). Detailed work has also been conducted recently in insulated and heat traced tubing, coupled with detailed numerical wellbore heat loss models for paraffin deposition, to optimize the production of deep waxy retrograde condensate gas reservoirs.

Canadian Formations Susceptible to Various Tight Gas Damage Mechanisms. This section provides an incomplete summary of a number of low permeability formations in Canada that have been investigated recently for tight gas damage mechanisms in the lab and the field. The results are site specific and can, of course, vary regionally with reservoir quality and saturation conditions, but provide some idea of type and scope of this problems in some common formations.

applications in Canada

Nomenclature

| | |
|-------|--|
| CCI = | Countercurrent imbibition |
| FFI = | Fluid-Fluid Interactions (precipitates, scales, emulsions, acid incompatibility) |
| FM = | Fines Migration |
| GL = | Glazing |
| MI = | Mud Solids Invasion |
| RFI = | Rock-Fluid Interactions (reactive clays) |
| OR = | Oil Retention |
| PP = | Production Problems (Condensate dropout, solids precipitation) |
| WR = | Water Retention |

Formation Name and Potential Damage Mechanism Susceptibility

| | |
|----------------|----------------------------------|
| Bakken - | WR, GL, CCI |
| Baldonnel - | WR, OR, MI, CCI, FFI |
| Basal Colorado | WR, OR, MI, GL, RFI, FM |
| Basal Quartz - | WR, OR, MI, GL, RFI, FM, PP |
| Belly River - | WR, MI, GL, CCI, RFI, FM |
| Bluesky - | WR, MI, GL, CCI, RFI, FM |
| Cadomin - | WR, MI, GL, CCI, RFI, FM |
| Cadotte - | WR, MI, GL, CCI, RFI, FM |
| Cardium - | WR, OR, GL, CCI, RFI, FM |
| Doig - | WR, GL, CCI, RFI, FM |
| thing - | WR, OR, GL, CCI, RFI, FM |
| Maunconite - | WR, GL, CCI, RFI, FM |
| Halfway - | WR, OR, GL, CCI, RFI, FM, PP |
| Jean Marie - | WR, GL, CCI, RFI, FFI |
| Medicine Hat - | WR, GL, CCI, RFI, FM, PP |
| Milk River - | WR, GL, CCI, RFI, FM, PP |
| Montney - | WR, OR, GL, CCI, RFI, FM, PP |
| Ostracod - | WR, OR, GL, CCI, RFI, FM, PP |
| Paddy - | WR, CCI, RFI |
| Rock Creek - | WR, OR, MI, GL, CCI, RFI, FM, PP |
| Taber - | WR, GL, CCI, RFI, FM |
| Viking - | WR, OR, GL, CCI, RFI, FM, PP |
| White Specks - | WR, OR, GL, CCI, RFI |

Conclusions

1 Significant reserves of natural gas and condensate liquids exist in low permeability formations throughout the world. Good engineering and evaluation is required in order to understand the initial reservoir quality and saturation conditions and accurately assess, at the current level of technology, if reserves exist and if those reserves are economically recoverable.

2 With advanced technology gas has been effectively and economically produced from many tight gas formations with permeabilities of less than 0.1 mD.

3 Tight gas formations are very susceptible to formation damage. Fluid retention is a major mechanism of damage in many of these situations. Means of minimizing damage effects

include understanding the wettability and initial saturation conditions of the reservoir and then minimizing invasion through the use of gas or gas energized fluids, ultra low fluid loss conventional systems or underbalanced drilling and completion techniques.

4 Significant damage can occur during fracturing treatments in tight gas due to improper fluid selection or mechanical problems with the frac. Fluid retention near the frac faces and fracture permeability impairment are major damage mechanisms in these cases. The smaller the fracture treatment, the more significant the effect of frac face damage on productivity. In some cases oil based, gas energized oil or pure CO₂ fracs have proven useful in minimizing damage. Success has also been achieved with very low fluid loss cross linked water based gel systems in some very low permeability formations which were highly susceptible to fluid retention effects.

5 Reducing drawdown rate can result in minimizing problems with retrograde condensation, water coning, fines migration and a variety of solids precipitation problems. This can be accomplished by reducing production rate, or more commonly by increasing cross sectional flow area by open hole completions, horizontal drilling or fracturing.

Acknowledgments

The authors wish to express appreciation to the Hycal Energy Research Laboratories for the database to publish this paper. Thanks also to Maggie Irwin and Vivian Whiting for their assistance in the preparation of the manuscript and figures.

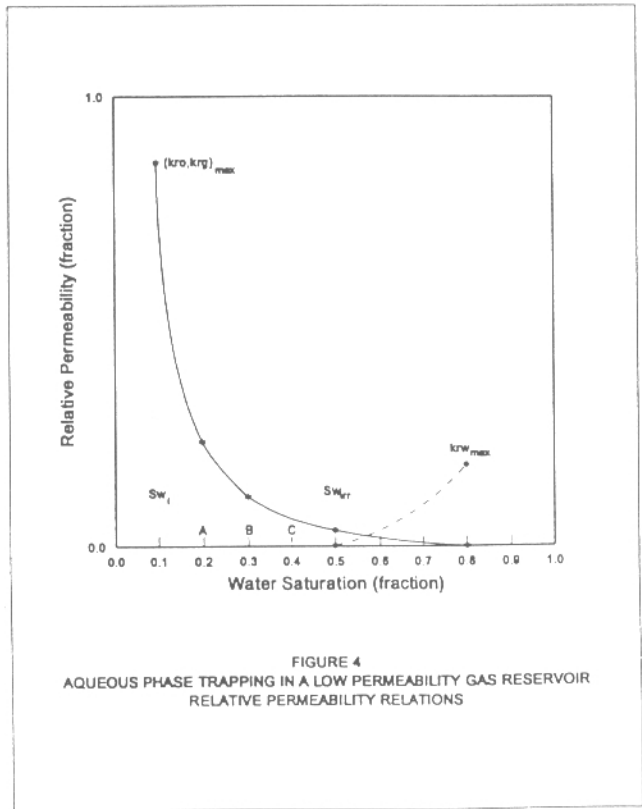
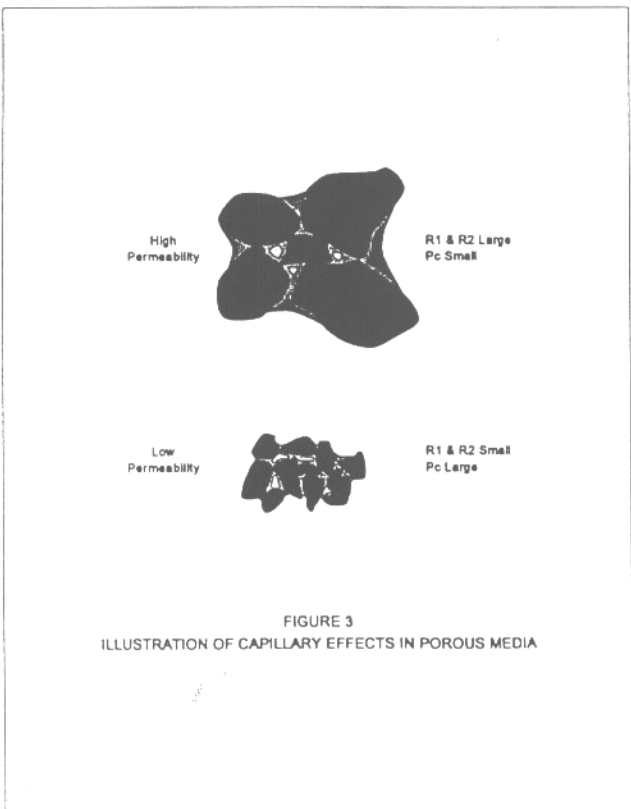
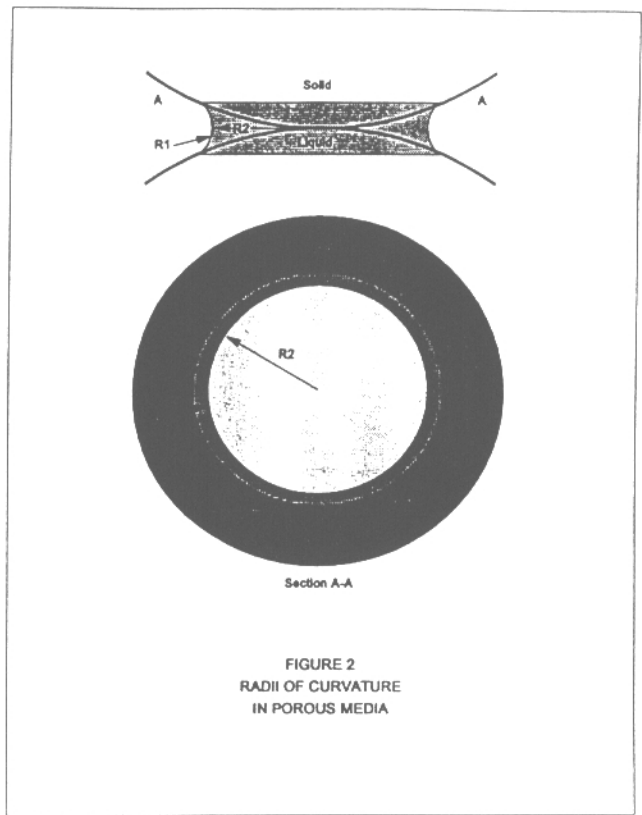
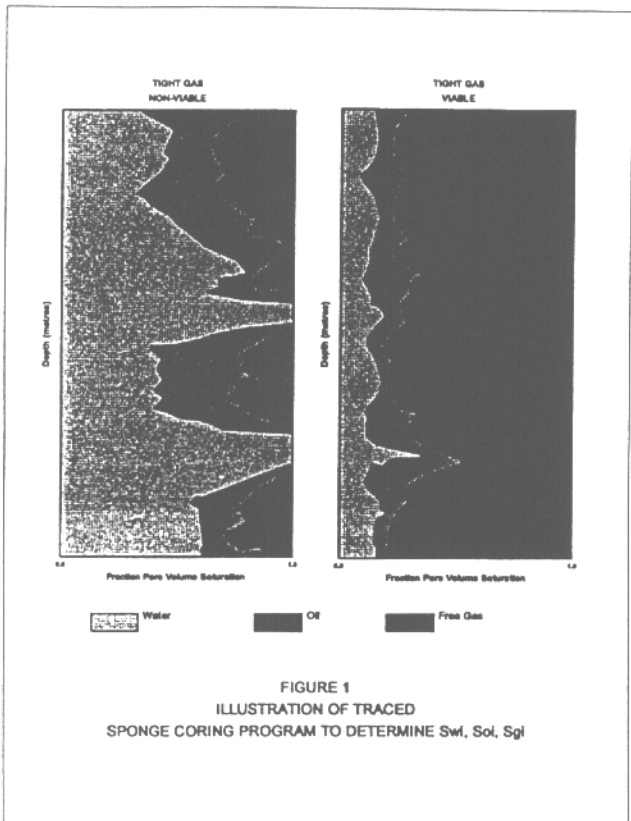
References

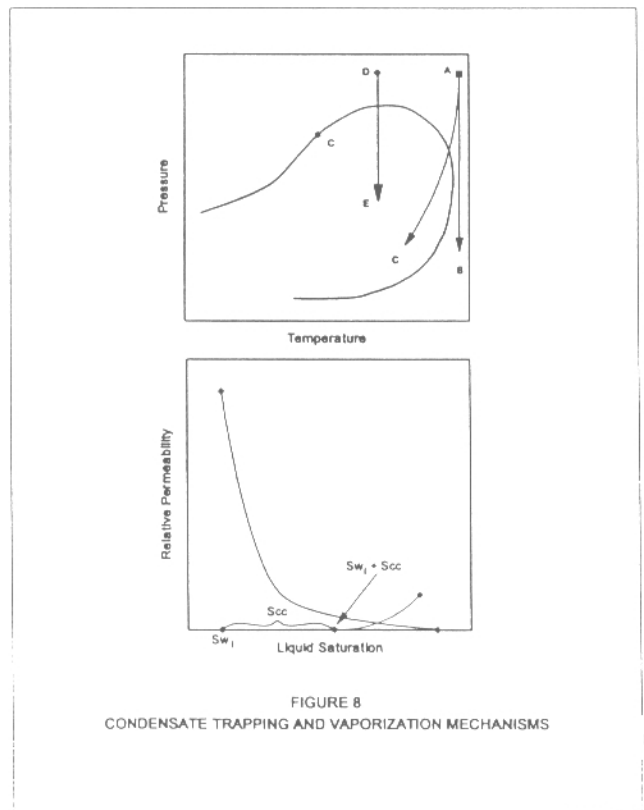
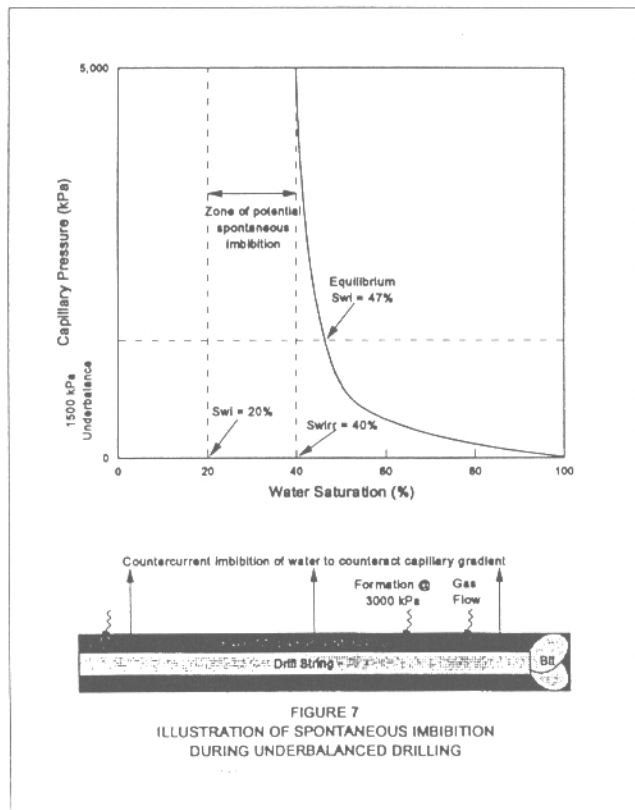
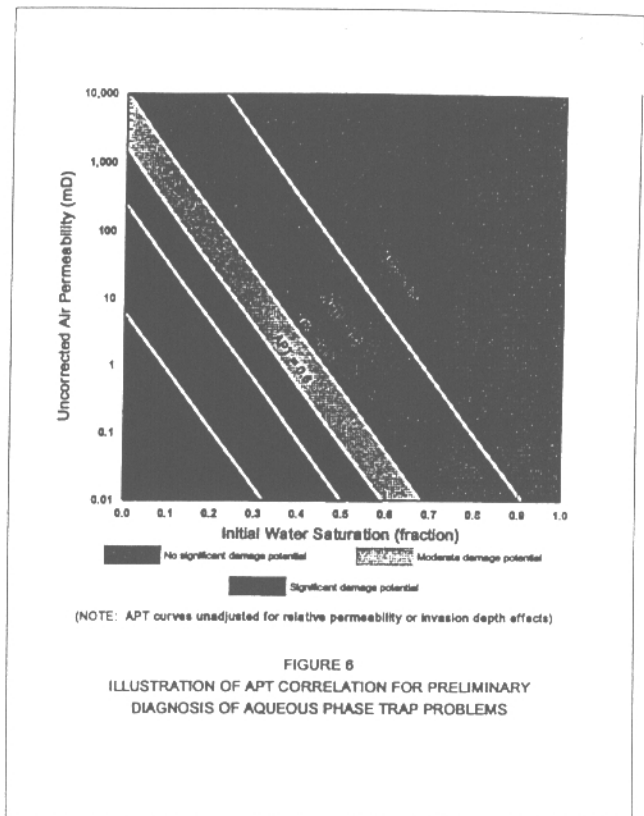
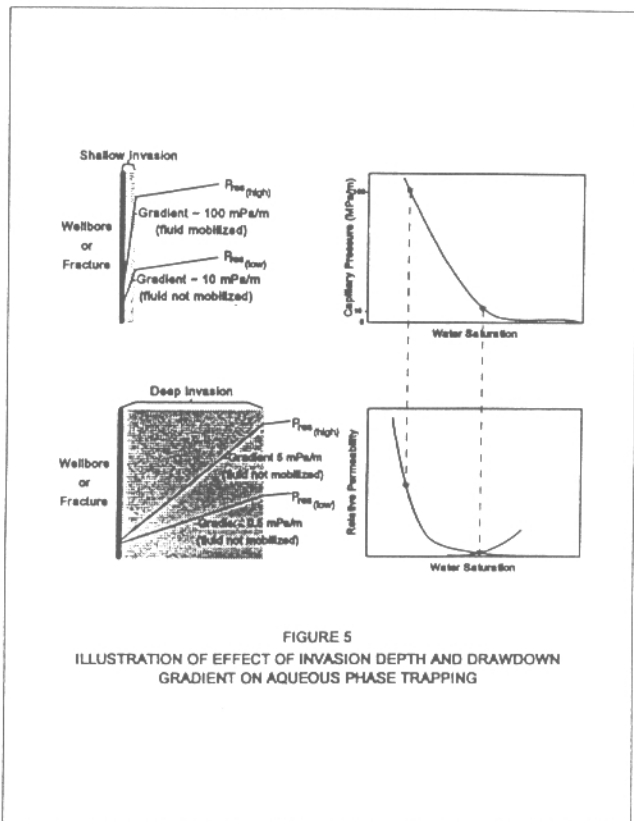
- Bennion, D B, Thomas, F B, Crowell, E C, Freeman, B "Applications For Tracers In Reservoir Conformance Predictions and Initial Saturation Determinations", presented at the 1995 1st Annual International Conference on Reservoir Conformance, Profile Control Water & Gas Shutoff, August 21-23, 1995, Houston, Texas
- Bennion, D B, Cimolai, M P, Bietz, R F; Thomas, F B "Reductions in the Productivity of Oil and Gas Reservoirs Due to Aqueous Phase Trapping", *JCPT*, November, 1994
- Bennion, D B, Thomas, F B, Bietz, R F, Bennion, D W "Water and Hydrocarbon Phase Trapping in Porous Media - Diagnosis, Prevention and Treatment", CIM Paper No 95-69 presented at the 46th Annual Technical Meeting at Banff, Alberta, May 14-17, 1995
- Bennion, D B, Thomas, F B "Underbalanced Drilling of Horizontal Wells - Does It Really Eliminate Formation Damage?" Paper SPE 27352 presented at the 1994 SPE Formation Damage Symposium, Feb 9-10, 1994, Lafayette, Louisiana
- Bennion, D B, Thomas, F B, Bietz, R F, Bennion, D W "Underbalanced Drilling, Praises and Perils", presented at the first international Underbalanced Drilling Conference and Exhibition, The Hague, Netherlands, Oct 2-4, 1995
- Bennion, D B, Bennion, D W, Thomas, F B, Bietz, R F "Injection Water Quality - A Key Factor to Successful Waterflooding", Paper CIM 94-60, presented at the May 1994 Annual Technical meeting of the Petroleum Society of CIM

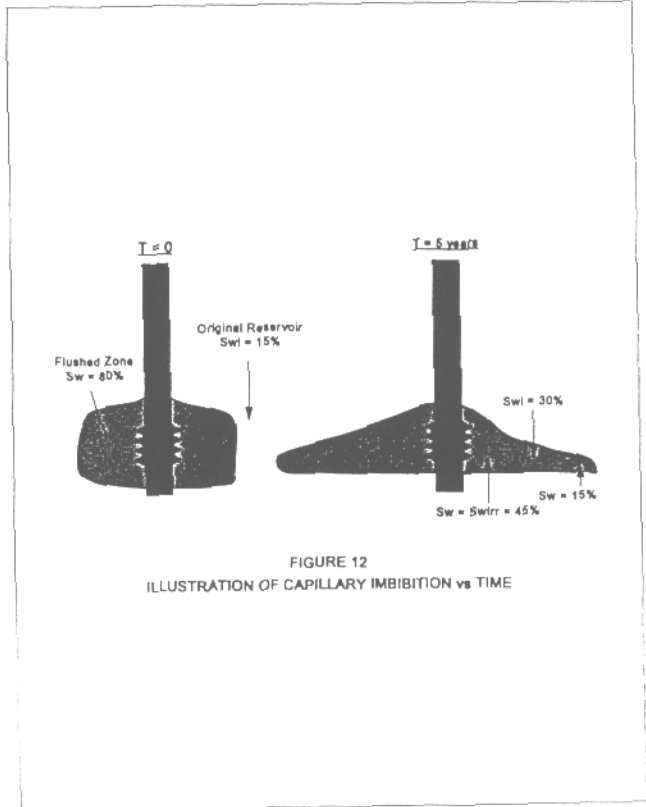
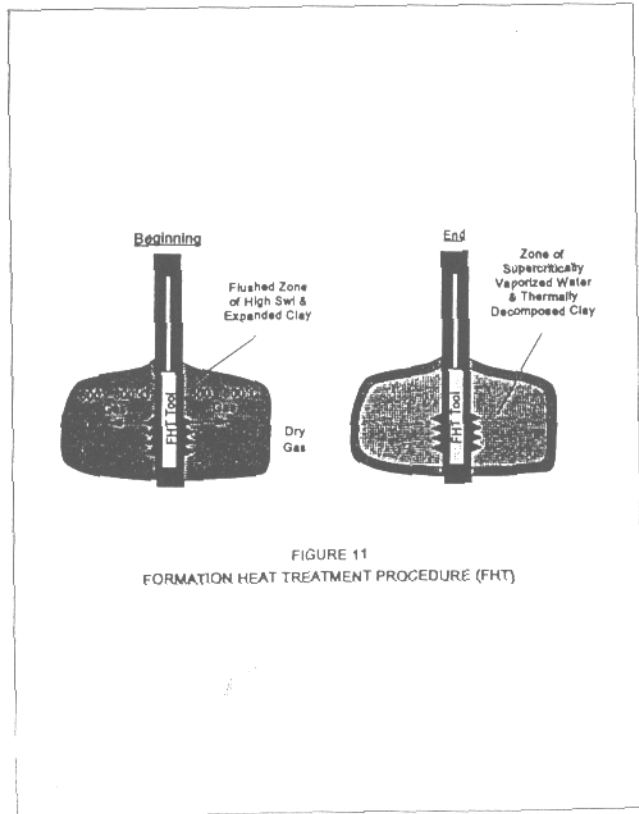
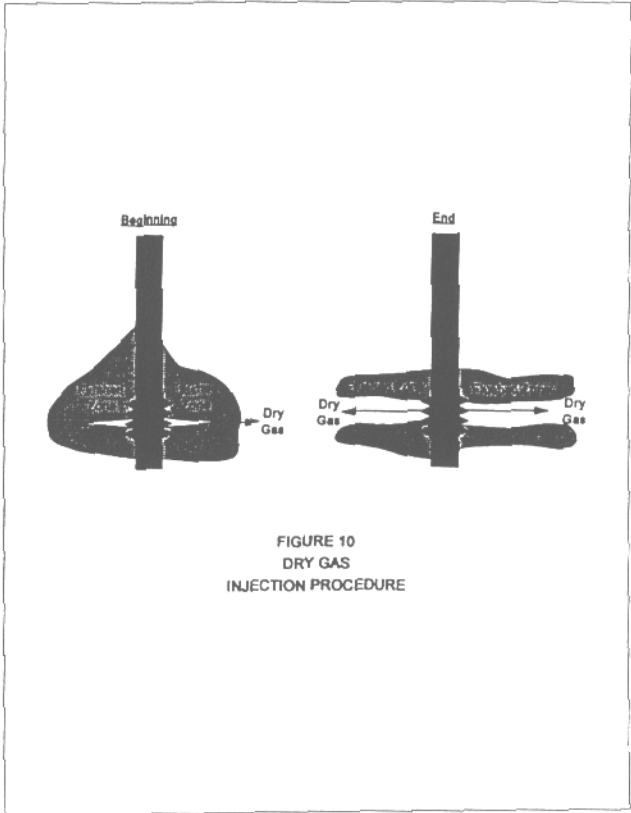
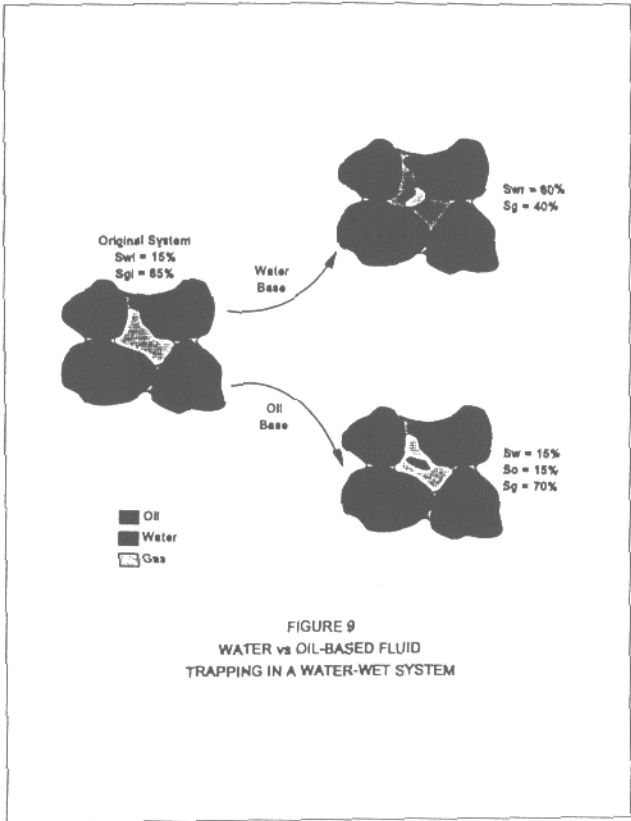
- 7 Eng, J H , Bennion, D B and Strong, J B : "Velocity Profiles in Perforated Completions," *Journal of Canadian Petroleum Technology*, (October 1993) pp 49-54
- 8 Thomas, F B , Bennion, D B and Bennion, D W "Experimental and Theoretical Studies of Solids Precipitation From Reservoir Fluids," *Journal of Canadian Petroleum Technology*, (January 1992)
- 9 Thomas, F B , Bennion, D B , Bennion, D W and Hunter, B E "Solid Precipitation From Reservoir Fluids: Experimental and Theoretical Analysis," Paper presented at 10th SPE Technical Meeting, Port of Spain, Trinidad and Tobago (June 27, 1991)
10. Jamaluddin, A K M , Vandamme, L M , Nazarko, T W , Bennion, D B "Heat Treatment for Clay-Related Near Wellbore Formation Damage", presented at the 46th Annual Technical Meeting of the Petroleum of CIM in Banff, Alberta, Canada, May 14-17, 1995

SI Metric Conversion Factors

1m = 0.3048 ft
1MPa = psi







RECENT IMPROVEMENTS IN EXPERIMENTAL AND ANALYTICAL TECHNIQUES FOR THE DETERMINATION OF RELATIVE PERMEABILITY DATA FROM UNSTEADY STATE FLOW EXPERIMENTS

D.B.Bennion, Hycal Energy Research Laboratories Ltd.
F.B. Thomas, Hycal Energy Research Laboratories Ltd

Copyright 1991, Society of Petroleum Engineers, Inc

This paper was prepared for presentation at the SPE 10th Technical Conference and Exposition held in Port of Spain, Trinidad, June 26 - 28, 1991

Summary. Accurate relative permeability data is an essential input parameter for many reservoir engineering applications, most significantly in the area of reservoir simulation. Methods of relative permeability determination are discussed with specific emphasis being given to the calculation of relative permeability curves from unsteady state displacement experiments. Recent advances in history matching techniques for the computation of relative permeability data from unsteady state displacement tests, including rigorous modeling of capillary effects, more flexible cubic and B spline functional forms for the relative permeability relations, and the simultaneous prediction of relative permeability and capillary pressure, are all discussed. Simple corrective techniques for correcting endpoint relative permeability values for in-situ capillary effects are also presented

Introduction

Relative permeability is an empirical parameter used to modify Darcy's single phase flow equation to account for the numerous complex effects associated with the flow of multiple immiscible phases within porous media¹

Relative permeability measurements are utilized extensively in many areas of reservoir engineering, and more particularly in recent years in the area of matching, predicting and optimizing reservoir performance and depletion strategies through the use of detailed numerical simulation models.

Those involved in numerical simulation realize the importance of good relative permeability data on the performance of reservoir simulation models. This paper discusses the evolution of relative permeability measurement techniques and reviews the current state of the art technology in the determination of relative permeability data. Recent experimental work and techniques for improving the acquisition of raw laboratory data for relative permeability calculations are also discussed

Factors Affecting Relative Permeability

Relative permeability can be affected by many physical parameters including fluid saturations,²⁻⁴ physical rock properties,⁵⁻⁷ wettability,⁸⁻¹⁰ saturation history (hysteresis effects),¹¹⁻¹² overburden stress,¹³⁻¹⁴ clay and fines content,¹⁵⁻¹⁶ temperature,¹⁷⁻¹⁸ interfacial tension,¹⁹ viscosity,²⁰ magnitude of initial phase saturations,^{21,22} immobile or trapped phases,^{21,22} and displacement rates and capillary outlet phenomena.²³⁻²⁶ A detailed discussion of the many factors affecting relative permeability is beyond the scope of this paper, but the general consensus of researchers is that in order to obtain the most representative relative permeability data that reservoir conditions during the tests be duplicated as closely as possible. This involves the use of well preserved or restored state reservoir core material, the use of "live" uncontaminated actual reservoir fluids in the tests, and operation at full reservoir conditions of temperature, pressure and confining overburden stress

Types of Relative Permeability Measurements

A number of researchers have postulated different methods for the experimental determination of relative permeabilities on reservoir core samples. The most popular of these fall into the category of "steady state" and "unsteady state" displacement tests. A number of centrifuge methods have also been proposed^{27,28} but in general have had limited acceptance due to the small size of the core samples which can be utilized and the inability to conduct those types of tests at reservoir conditions of temperature and pressure.

Steady State Measurements

Figure 1 provides an illustrative schematic of a typical steady state relative permeability apparatus.

In this type of test a fixed ratio of two or more immiscible fluids are simultaneously forced through a test sample until saturation and pressure equilibrium are established. The experiments are designed in such a way as to eliminate end effects. This is accomplished in a number of ways, the most common being the inclusion of an additional length of core or sandpack to the end of the test section of interest to absorb the capillary end effect. Various other methods such as the use of semi-permeable membranes and plates, or cone shaped core ends to increase production velocity at the outlet face to minimize the end effect, have also been investigated.

At each equilibrium point, in a steady state test, individual-phase permeabilities and relative permeabilities are computed based on the measured phase differential pressures and individual phase flow rates. Once one set of stable data is obtained the injection ratio of the two fluids is varied, stability is re-established and the relative permeabilities at the next saturation level are then determined.

The steady-state method is preferred by some investigators since end effects are negated and, since the test is not truly a displacement test but rather an equilibrium flow test, stability and rate effects associated with viscous instabilities are eliminated. The disadvantages of this method are:

- 1 Accurate determination of in-situ saturations is required after each displacement level which

can be difficult and expensive in reservoir condition tests.

- 2 Days or weeks are often required to achieve equilibrium at each saturation point. This can result in weeks or months being required to complete a simple relative permeability determination at an extremely high cost.
- 3 A considerable amount of expensive experimental equipment is required to conduct these tests, particularly at conditions of elevated temperature and pressure.

Unsteady State Measurements

These much simpler tests are conducted rapidly by the displacement of a single phase through a core which is initially saturated with wetting and non-wetting phase and is at the minimum saturation of the phase to be injected (ie S_{wi} for a waterflood in a water-wet core). The production history and pressure differential across the core are closely monitored during the displacement. Mathematical derivations of classical Buckley-Leverett²⁹ theory or more complex computer simulation techniques, (which shall be discussed shortly), can be used with this data to compute the relative permeability curves. Because this type of experiment can be conducted relatively rapidly and at a low cost, it is almost exclusively utilized in preference to the steady-state method for commercial relative permeability testing. The main disadvantages of this method are its susceptibility to end effects, rate-dependent instability effects, and potential non-equilibrium between displacing and displaced fluids.

Calculation Methods for Computation of Relative Permeability From Laboratory Data

Steady-State Methods

As discussed previously, relative permeabilities can be computed directly from two-phase steady-state relative permeability displacement tests at given saturation levels. This is a distinct advantage of the steady-state method as no special treatment or manipulation of the data is required. Due to the cost and complexity of steady state measurements, however, they are not often utilized with preference being given to the much simpler

and less expensive unsteady state test

Unsteady-State Methods

The fluid theory initially described by Buckley and Leverett²⁹ to describe fluid flow through porous media was later modified by Welge³⁰ to facilitate the prediction of relative permeability ratios at given saturation levels in laboratory scale core displacement tests. These classical flow equations are described in detail in the above references, to which the reader is referred.

For the case of horizontal flow and negligible capillary pressure, Welge illustrated that:

$$S_{w,av} - S_{w,2} = F_{o_2} Q_w \quad (1)$$

where

- $S_{w,av}$ = average core water saturation
- $S_{w,2}$ = outlet-face water saturation
- F_{o_2} = fractional flow of oil at outlet face
- Q_w = total pore volumes of water injected

Since $S_{w,av}$ and Q_w are known (from material balance and injection data respectively) and F_{o_2} can be determined from a plot of Q_w as a function of $S_{w,av}$ it can be calculated that:

$$f_{o_2} = \frac{1}{1 + \frac{\mu_o/k_{ro}}{\mu_w/k_{rw}}} \quad (2)$$

where:

- μ_o, μ_w - oil and water viscosities (cP)
- k_{ro}, k_{rw} - endpoint oil and water relative permeability values

This allows the relative permeability ratio to be computed at any saturation AFTER breakthrough of the water phase. Similar equations can be derived for gas-oil systems.

The work of Welge was extended by Johnson *et*

*al*³¹ to obtain a method (commonly called the JBN method) for calculating individual-phase relative permeabilities from unsteady-state test data. These equations are

$$k_{ro} = \frac{f_{o_2}}{d\left(\frac{1}{Q_w I_r}\right) / d\left(\frac{I}{Q_w}\right)} \quad (3)$$

$$k_{rw} = \frac{f_{w2}}{f_{o2}} \frac{\mu_w}{\mu_o} k_{ro} \quad (4)$$

$$I = \frac{\text{injectivity}}{\text{initial injectivity}} = \frac{Q_{wi} / \Delta P}{(Q_{wi} / \Delta P)_{nit}} \quad (5)$$

where.

- F_{w2} = outlet fractional flow of water
- ΔP = pressure differential across sample

The advantage of the JBN method over that of the Welge method was that for the first time individual phase relative permeabilities could be computed from unsteady state data instead of merely relative permeability ratios.

The JBN method has been popular since its inception, even though it suffers from some basic deficiencies, and is still used in many applications today.

Another fairly popular method is that of Jones and Roszelle³². This method is an extension of the JBN method and also utilizes graphical techniques (which can be computerized).

The basic assumptions of the Jones-Roszelle method are similar to that of the previously discussed JBN method. In this technique the oil produced is expressed as a change in the average water saturation within a core sample. The change in saturation is plotted vs the pore volumes of water injected to calculate the relative permeability ratios.

as a function of the water saturation

The Jones-Roszelle method has particular application late in waterfloods when oil production is very minimal and the slope of the oil recovery vs PV of injection graph becomes very slight. The methods involve plotting recovery vs the inverse of cumulative injection ($1/Q_{wi}$) which avoids long tangent extrapolations back to the y axis and also facilitates easy extrapolation back to the point of infinite water injection ($1/Q_{wi} = 0$), which is thought by the authors to yield a better estimation of the true residual oil saturation after a waterflood

Since all three methods discussed previously are based upon the same fundamental derivations of Buckley-Leveritt flow theory, they tend to be subject to the same limitations, namely

- 1 All methods neglect both capillary pressure and gravitational effects in their basic derivation. This means that the methods cannot account for end effect phenomena and the dispersing effect of capillary pressure on saturation shock fronts within porous media. Typically in the past these types of tests were run at very high displacement velocities to yield a large pressure drop across the core sample to minimize the contribution of capillary pressure effects. This can lead to severe problems with both fines mobilization and viscous instability effects
- 2 The Welge, JBN and Jones-Roszelle methods all assume perfectly dispersed flow with no core heterogeneities. Since these methods are based on the evaluation of derivatives of the fractional flow curves, if the fractional flow data is non-monotonic, which can often occur in heterogeneous core samples, this results in severe deviations in the computed relative permeability data. This phenomena is illustrated by Sigmund *et al*³³ and appears as Figure 3.
- 3 Since all of the methods are based upon the analysis of fractional flow data, they can only predict relative permeability data after water breakthrough. In strongly water wet core material, a water displacement results in an almost piston like flow of water through the core resulting in a very steep and localized

region of fractional flow. This, therefore, results in only a very small cluster of relative permeability data points being obtained at saturations near the maximum level. Thus significant extrapolation is required for the relative permeabilities at intermediate saturation levels

This last deficiency was commonly remediated by utilizing a viscous mineral oil in place of the hydrocarbon phase in the test. This, however, yields an improper viscosity ratio which can affect residual saturations and endpoint relative permeability values. Also, the use of refined or synthetic oils can affect core wettability due to the solubilization of asphaltic and heavy ends into solution and cause significant changes in the configuration of the resulting relative permeability curves

The drawback of the previous three calculation methods is that, since classical behavior is assumed in the method derivations (i.e., no capillary pressure, no end effects, perfectly dispersed flow with no heterogeneities), the accuracy of the obtained relative permeabilities can, in many instances, be questionable

The implicit history matching technique, first proposed by Archer and Wong³⁴ is an offshoot of the large advances recently made in reservoir simulation. The basis of the method is that, instead of using known relative permeability relationships in the solution of the partial differential equations which describe multi-phase flow in porous media to predict the pressure and production history, the pressure and production history is utilized to predict the relative permeability curves for a given system

The method begins by assuming certain functional relationships in the simulator for the wetting and non-wetting phase relative permeabilities and the capillary pressure functions. Initial estimates for adjustable parameters in these equations result in a certain production and pressure history being predicted. This production and pressure history is then compared to the input experimental lab data and the least-square error computed. Correction algorithms adjust the parameters in the functional relationships and the process continues to iterate in this fashion until the minimum least-square error is obtained. The resulting relative permeability curves obtained provide the best fit (within the

limits set by the form of the functional relationships utilized) to the experimental data

Since the numerical model can incorporate both gravity and capillary pressure effects, these can be incorporated directly into the simulation thus allowing the end effect to actually be simulated as a portion of the experiment. This facilitates running tests at low advance rates to eliminate stability problems. The method also provides a complete history match over the entire range of the saturation change, regardless of the fractional flow characteristics of the displacement, giving it specific application to heterogeneous and strongly wetted systems

The first published applications of the method were presented by Sigmund and McCaffery³³. They utilized relatively simple exponential formulations to define the functional form for the relative permeability curves as follows:

$$k_{rw} = k_{rwo} \left[\frac{(Se)^{\epsilon_w} + ASe}{1 + A} \right] \quad (6)$$

$$k_{rnw} = k_{rnwo} \left[\frac{(1-Se)^{\epsilon_n} + B(1-Se)}{1 + B} \right] \quad (7)$$

$$Se = \frac{S_w - S_{wmin}}{S_{wmax} - S_{wmin}} \quad (8)$$

where

- k_{rw} = Predicted wetting phase relative permeability
- k_{rnw} = Predicted non-wetting phase relative permeability
- k_{rwo} = Wetting phase endpoint relative permeability
- k_{rnwo} = Non-wetting phase endpoint relative permeability
- ϵ_w = Wetting phase adjustable shape exponent
- ϵ_n = Non-wetting phase adjustable shape exponent
- A, B = Linearization constants (0.01 in

- (Sigmund's work)
- S_c = Normalized wetting phase saturation
- S_w = Wetting phase saturation
- S_{wmin} = Minimum wetting phase saturation
- S_{wmax} = Maximum wetting phase saturation

Capillary pressure effects were expressed by

$$P_c = P_{cb} \left[\frac{1}{(S_{pc})^{1/\lambda}} - 1 \right] \quad (9)$$

where

$$S_{pc} = \frac{S_w - S_{wi}}{S_{wo} - S_{wi}} \quad (10)$$

- P_c = Capillary pressure
- P_{cb} = Measure of interfacial tension and mean pore size
- λ = Pore size distribution parameter
- S_{pc} = Normalized capillary pressure saturation value
- S_{wi} = Irreducible wetting phase saturation from a drainage capillary pressure test (Always must be less than S_{wmin}).
- S_{wo} = Maximum value of wetting phase saturation corresponding to zero capillary pressure.

The numerical model utilized to match the data incorporated the one-dimensional Buckley-Leverett, incompressible, two phase flow equations;

$$\frac{k}{\mu_w} \frac{\partial}{\partial x} \left(k_{rw} \frac{\partial P_w}{\partial x} \right) = \phi \frac{\partial S_w}{\partial t} + q_{iw} \quad (11)$$

$$\frac{k}{\mu_{nw}} \frac{\partial}{\partial x} \left(k_{rnw} \frac{\partial P_{nw}}{\partial x} \right) = -\phi \frac{\partial S_w}{\partial t} + q_{inw} \quad (12)$$

$$P_c = P_{nw} - P_w \quad (13)$$

where

| | | |
|-------------------|---|---|
| k | = | Absolute permeability |
| μ_w, μ_n | = | Viscosities of wetting and non-wetting phases |
| k_{rw}, k_{rnw} | = | Relative permeabilities of wetting and non wetting phases |
| P_w, P_{nw} | = | Pressures in the wetting and non wetting phases |
| ϕ | = | Porosity |
| S_w | = | Wetting phase fraction |
| q_{iw}, q_{inw} | = | Source terms for wetting and non wetting phases |
| P_c | = | Capillary pressure |
| ∂_x | = | Space co-ordinate |
| ∂_t | = | Time co-ordinate |

The model utilized by Sigumund et al utilized one-point upstream transmissibility weighting with linearized implicit transmissibilities (utilizing a secant method to estimate the derivatives) and a modified Newtons method to handle capillary pressure induced non linearities. A 40 gridblock one dimensional model was utilized.

The optimum relative permeability parameters were calculated using a least squares Gauss-Newton optimization routine. The error equation for the i^{th} observation in this routine can be written as

$$Error = \Delta P_{OBC_i}^q + \Delta E_{OBC_i}^q \quad (14)$$

where:

$$\Delta P_{OBC_i}^q (\epsilon_w, \epsilon_{nw}) = W_i \left(\Delta P_{D_i}^{obs} - \Delta P_{D_i}^{calc} \right) \quad (15)$$

and

$$\Delta E_{OBC_i}^q (\epsilon_w, \epsilon_{nw}) = W_i \left(E_{R_i}^{obs} - E_{R_i}^{calc} \right) \quad (16)$$

where

| | | |
|--------|---|------------------|
| W_i | = | Weighting factor |
| P_D | = | Pressure data |
| E_R | = | Recovery data |
| obs | = | Measured data |
| $calc$ | = | Calculated data |

obc = objective function

For a given set of "m" observations (data points) the algorithm attempts to find the values of ϵ_w and ϵ_{nw} which will minimize the error function.

$$E = \sum_{i=1}^m \left(\left(\Delta P_{OBC_i}^q \right)^2 + \left(\Delta E_{OBC_i}^q \right)^2 \right) \quad (17)$$

subject to the given constraints;

$$\epsilon_{min} \leq \epsilon_w, \quad \epsilon_{nw} \leq \epsilon_{max}$$

Details of the specific application of the Gauss-Newton correction algorithm can be found in the appendix of Sigumund et al³³

Batycky et al²⁴ and MacMillan³⁵ also utilized this technique using similar functional forms.

One disadvantage of this particular form of the history matching method is that the obtained relative permeability curves can conform to only the configurations possible under the constraints imposed by the given functional form. The exponential forms discussed previously are usually quite adequate for most systems, but cannot adequately model unusual relative permeability configurations, such as those obtained for dual porosity or very heterogeneous systems. Figure 4 provides an illustration of the various types of relative permeability curve configurations which can be obtained using different values of ϵ_w and ϵ_{nw} in the exponential formulation model.

The history matching technique, however, is not limited to the use of any one specific functional relationship. Research by Kerig et al^{36,37} indicated that free and clamped cubic spline formulations could provide superior fits to almost all types of relative permeability curves.

Kerig et al utilized a cubic spline functional form to represent the relative permeability curves defined by

$$k_{ri} = a_{ij} S_i^3 + b_{ij} S_i^2 + c_{ij} S_i + d_{ij} \quad (18)$$

For $S_{i,j} \leq S_i \leq S_{i,j+1}$

Where

J = number of total spline segments
 $S_{i,j}$ = Value of S_i at knot J
 $a_{ij}, b_{ij}, c_{ij}, d_{ij}$ = spline coefficients

Cubic splines are highly flexible functions which can, with a sufficient number of spline segments, represent any continuous function as accurately as desired³⁸. Figure 5 illustrates the flexibility of cubic splines in modeling relative permeability curves of a nonuniform nature which cannot be well described by simple exponential formulations. Examples of such system would include very heterogeneous reservoirs or systems characterized by multiple porosity types

Kerig et al³⁷ discussed sources of error in the relative permeability estimation technique via automatic history matching. They defined two possible sources of error:

- 1 Modeling Error - Results of inadequacy of the mathematical model of the displacement experiment in the exact representation of the experiment (ie effect of capillary pressure, heterogeneity or non-uniform initial saturation)
- 2 Estimation Error
 - a) Bias Error - Inability of the functional forms to represent the true, though unknown, relative permeability curves.
 - b) Variance Error - errors associated with statistical uncertainty of the data utilized (ie experimental error) and the number of parameters utilized in the functional form of the relative permeability curves. (Increasing the number of parameters in the functional form generally increases the variance error while reducing the bias error.)

The use of cubic spline formulations over simple exponential formulations can greatly reduce bias error while causing relatively small increases in variance error as illustrated in Figure 6

Kerig et al³⁹ did additional work in this area and

determined specific algorithms for the optimization of the many parameters required when cubic splines are utilized as functional forms in the relative permeability relations. The algorithms utilized incorporated inequality constraints to ensure that physically realistic relative permeability curves were maintained throughout the optimization process. The constraints utilized were such to ensure that the relative permeability curves obtained remained convex downward, remained monotonic, and had zero relative permeability at $S_i = 0$. The optimization program utilized in this work was a Gauss-Newton method with a Marquart modification^{40,41}. A detailed discussion of the model and operational constraints utilized can be found in Reference 39

Watson et al⁴² further extended this work to include the use of B Splines³⁸ as functional forms for the relative permeability curves using:

$$k_{ri}(\xi) = \sum_{j=1}^{N_i} C_j^i B_j^m(\xi) \quad i = w, nw \quad (19)$$

N_i = Dimensions of the Spline
 C_j^i = Parameters to be determined

The use of B Splines has an advantage over the use of Cubic Splines in that B Splines are not "piecewise" type polynomial approximations (ie. each spline segment is valid only over a certain saturation interval). B Splines retain a set of independent coefficients over the entire saturation range of interest making them easier to use while still retaining the flexible nature of cubic splines. The algorithms utilized and operational constraints employed during the optimization process are discussed in detail by Watson et al.⁴² Figure 7 illustrates the superior nature of spline estimated relative permeability data over that predicted by simple exponential models.

Richmond et al⁴³ further extended the work of Watson et al⁴² to include simultaneous optimization of capillary pressure data along with the prediction of relative permeabilities from displacement experiments. The functional form for the capillary pressure was also defined by B Splines as:

$$P_c(\xi) = \sum_{j=1}^{N_i} C_j^i B_j^m(\xi) \quad (20)$$

Richmond *et al*⁴³ utilized a Levenberg-Marquart Algorithm with linear inequality constraints in their optimization process. They also investigated the problem of convergence on multiple distinct local minima by variation of their initial optimization initialization point and covariance analysis of the Hessian matrix obtained from the solution of the data. Also proposed was a new procedure for the automatic selection of the optimum number and location of the spline knots to obtain the maximum accuracy in estimation with the minimum number of spline segments and resulting optimizations.

The work of Richmond *et al* utilized pure parameter adjustment for the history matching of the capillary pressure functions to optimize the error between the experimentally observed pressure and production history and the simulator predicted data. Recent research at Hycal has been involved in the actual measurement of in-situ capillary pressures during a dynamic displacement test through the use of pressure transducers equipped with special wetted membranes to sense specific individual phase pressures and the resulting capillary pressure.

The measurement of actual dynamic capillary pressure data allows the further extension of the history matching technique to the direct history matching of the capillary pressure curve allowing for the direct prediction of both reservoir condition relative permeabilities and capillary pressures accurately and inexpensively from a single test. Further testing and experimentation is still under way to continue to improve and refine this latest addition to the history matching method.

Simple Correction Techniques for Endpoint Relative Permeability Values

All of the history matching models previously discussed require that the user input both the wetting and non wetting phase endpoint relative permeability values. Relative permeability endpoint values, determined utilizing a standard unsteady state displacement technique, may often result in the measurement of endpoint values which are substantially lower than actual values measured

from steady state tests. Figure 8⁴⁴ illustrates this phenomena for displacement tests conducted at the same rate utilizing both a Penn-State type steady state approach vs the standard unsteady state test methodology.

The major cause of this type of phenomena is attributed to capillary effects. An excellent discussion of capillary and rate effects can be found in the work of Batycky²⁴, Osaba⁴⁵, and Rapoport and Leas⁴⁶.

Capillary pressure is simply defined as:

$$P_c = P_{nw} - P_w \quad (21)$$

where

- P_c = Capillary Pressure (kPa or Psi)
- P_{nw} = Non-wetting Phase Pressure (kPa or Psi)
- P_w = Wetting Phase Pressure (kPa or Psi)

When a single fluid is flowing in the porous media in the presence of other immobile residual immiscible fluid phases (i.e. the flow of water at a residual oil saturation), a certain portion of the applied force to move the fluid through the system is required to overcome the capillary forces which exist within the sample. Generally, the larger the capillary forces which exist within a sample, the larger the influence on the endpoint relative permeability data.

Typically in the past relative permeability tests were conducted at high rates which resulted in a relatively large pressure differential across the core sample which, in general was much larger than the capillary pressure force and thus tended to minimize its overall effect on the measured endpoint relative permeability value. Figure 9⁴⁴ provides an illustrative example of this phenomena.

The use of high rates in conducting unsteady state relative permeability tests has associated problems, these being:

- 1 The potential for fines migration
- 2 Unstable flow effects due to viscous instability²³

- 3 Erroneous pressure data due to non-Darcy flow caused by turbulent interstitial flow
- 4 Experimental data acquisition difficulties resulting from a very short test time

Recent work has illustrated that a simple correction technique can be accurately applied to correct for the effect of capillary effects on endpoint relative permeabilities while avoiding many of the aforementioned difficulties. The technique is applied as follows.

- 1 Conduct a regular, low rate unsteady state displacement test, measure the resulting endpoint relative permeability and residual fluid saturations
- 2 Use the computer history matching routine to generate the complete relative permeability curves
- 3 Conduct geometric rate increases of the displacing phase at 2 to 3 higher displacement velocities. Example, if the base displacement test was conducted at a rate of 10 ml/hr, conduct additional endpoint tests at 20, 40 and 80 ml/hr. The technique does not require the use of excessively high injection rates and these should be avoided to reduce the potential for fines mobilization or unstable flow
- 4 Record any additional production of the residual immobile phase caused by the increase in interstitial fluid shear force

The profile of the experimental results can have three configurations as illustrated in Figure 10, these being

CASE 1 - Endpoint permeability remains constant with rate illustrating perfect conformance to Darcies Law indicating an absence of capillary effects. This indicates that no correction of the endpoint relative permeability data is required and that capillary effects are negligible

CASE 2 - Endpoint permeability increases with increasing injection rate. This indicates the presence of capillary forces, a reduction in the

residual immobile phase saturation, or a combination of both phenomena. The endpoint correction technique, to be discussed shortly, should be applied here

CASE 3 - Endpoint permeability decreases or initially increases then decreases with increasing injection rate. This indicates either damage by fines mobilization or turbulent flow phenomena. These two phenomena can be easily differentiated by reducing to the base rate and observing if the permeability returns to the originally recorded value. In the case of fines migration the endpoint correction technique, in general, can still be applied if sufficient points (3 minimum) are available prior to the reduction in permeability. If turbulent flow occurs, lower rates should be selected to allow evaluation in the laminar flow regime

The correction technique is applied by fitting the non linear model

$$k_i = a_1(1 - e^{-a_2 q_i}) \quad (22)$$

where: k_i = measured endpoint permeability at flow rate "i" (mD or μm^2)
 q_i = flow rate at point "i" (cc/hr, cc/sec)
 a_1, a_2 = adjustable constants

to the experimentally determined data. In this work a non-linear finite difference Levenberg-Marquardt optimization routine^{41,47-49} was used to optimize the values of the constants a_1 and a_2 to yield the minimum least square error between the experimental and predicted data

By definition, as the flowrate, q_i approaches infinity, the pressure across the sample also becomes infinitely larger than any contribution associated with capillary effects. Thus,

$$\lim_{q_i \rightarrow \infty} a_1(1 - e^{-a_2 q_i}) = a_1 \quad (23)$$

Thus the value of the constant a_1 provides the simple final approximation to the final corrected

permeability value. Examples of the application of this technique for both water oil and gas-oil displacement tests appear as Tables 1 and 2 and Figures 11 and 12. The resulting relative permeability data is simply renormalized at this point to the higher endpoint relative permeability value.

If the residual immobile phase saturation is reduced by the elevated rate displacements, as may sometimes occur due to the increase in capillary number associated with the higher displacement velocity. This is accommodated by (See Figure 13):

- 1 Determine "new" final residual saturation
- 2 Using the previously derived and matched functional form for the relative permeability curve, extrapolate the existing relative permeability curve to the "new" residual saturation
- 3 Normalize the new set of relative permeability data up to the final corrected endpoint relative permeability

Use of this technique eliminates the use of high displacement rates during the actual two phase immiscible displacement test which obviates the potential for viscous instability effects. Since the method works upon an extrapolative technique, this also eliminates the need for extreme flow velocities to facilitate the endpoint correction, and thus has specific application to velocity sensitive core materials.

Conclusions

Recent advances in unsteady state displacement technology have allowed the data from these relatively simple and inexpensive tests to have much wider application and improved accuracy when correlated with the data from more expensive and time consuming steady state tests. Advances have been made in automatic history matching, particularly with the advent of more sophisticated cubic spline and B spline functional forms for the relative permeability and capillary pressure relations. Recent work also indicates the possibility of the prediction of accurate reservoir condition capillary pressures simultaneously during unsteady state displacement tests. Simple procedures for the

correction of endpoint relative permeability data by the use of parameter estimation techniques to match the results of multirate flow tests were documented and illustrative examples of the technique presented.

References

1. Muskat, M., and Meres : M W.: *Physics*, Vol 7, (1936) 346
2. Leverett, M C, and Lewis, W.B.: "Steady Flow of Gas-Oil-Water Mixtures Through Unconsolidated Sands," *Trans*, AIME, Vol 142 (1941) 107.
3. Sarem, A.M.. "Three Phase Relative Permeability Measurements by Unsteady State Methods," *SPEJ*, Vol 9 (1966) 199
4. Owens, W.W and Archer, D.E.: "The Effect of Rock Wettability on Oil-Water Relative Permeability Relationships," *Trans*, AIME (July 1971) 873-78
5. Maloney, D.R, Honarpour, M.M., Brinkmeyer, A.D.: "The Effects of Rock Characteristics on Relative Permeability," NIPER Report No FC22-83 FE 60149 (January 1990)
6. Morrow, N.R.: "Capillary Pressure Correlation for Uniformly Wetted Porous Media," *JCPT*, (Oct. 1976)
7. Arps, J.J. and Roberts, T.G : "The Effect of the Relative Permeability Ratio, the Oil Gravity and the Solution Gas-Oil Ratio on the Primary Recovery from a Depletion Type Reservoir," *Trans*, AIME Vol 24 (1955) 120
8. Craig, F.F., Jr.: "The Reservoir Engineering Aspect of Waterflooding," *SPE Monogram Series* (1971)
9. Wang, F.H.L "Effect of Wettability Alteration on Water/Oil Relative Permeability, Dispersion, and Flowable Saturation in Porous Media," *SPE Res Eng* (May 1988)

- 10 Morrow, N.R., Lim, H.T., Ward, J.S.: "Effect of Crude Oil Induced Wettability Changes on Oil Recovery," *SPE Form Eval.* (Feb 1986)
- 11 Geffen, T.M., Owens, W.W., Parrish, D.R., and Morse, R.A.: "Experimental Investigation of Factors Affecting Laboratory Relative Permeability Measurements," *Trans.*, AIME, Vol. 192, (1951) 99
- 12 Land, C.S.: "Comparison of Calculated and Experimental Imbibition Relative Permeability," *Trans.*, AIME, Vol. 251 (1971) 419.
- 13 Wei, K.K., Morrow, N.R., Brower, K.R.: "Effect of Fluid, Confining Pressure and Temperature on Absolute Permeabilities of Low Permeability Sandstones," *SPE Form Eval.* (August 1986)
- 14 Gobran, B.D., Brigham, W.E., Ramey, J.H. Jr.: "Absolute Permeability as a Function of Confining Pressure, Pore Pressure, and Temperature," *SPE Form Eval.*, (March 1987).
- 15 Soeder, D.J.: "Laboratory Drying Procedures and The Permeability of Tight Sandstone Core," *SPE Form. Eval.* (February 1986)
- 16 Selby, R.J., Ali, S.M.F.: "Mechanics of Sand Production and the Flow of Fines in Porous Media," *JCPT*, (May 1988).
- 17 Nakornthorp, K., Evans, R.D.: "Temperature Dependant Relative Permeability and Its Effect on Oil Displacement by Thermal Methods," *SPE Res Eng*, (May 1986) 230-242
- 18 Polikar, M., Ali, S.M.F., Puttagunta, V.R.: "High Temperature Relative Permeabilities For Athabasca Oil Sands," *SPE Res Eng* (Feb 1990)
- 19 Morrow, N.R., Chatzes, I., Taber, J.J.: "Entrapment and Mobilization of Residual Oil in Bead Packs," *SPE Res Eng* (1988)
- 20 LeFebvre duPrey, E.J.: "Factors Affecting Liquid-Liquid Relative Permeabilities of Consolidated Porous Medium," *SPEJ* 2, (1973) 39.
- 21 Caudle, B.H., Slobod, R.L., and Brownscombe, E.R.: "Further Developments in the Laboratory Determination of Relative Permeability," *Trans.*, AIME, Vol. 192 (1951) 145
- 22 McCaffery, F.G.: "The Effect of Wettability on Relative Permeability and Imbibition in Porous Media," Ph.D. Thesis, University of Calgary, Alberta, Canada (1973).
- 23 Sigmund, P., Sharma, H., Sheldon, D. and Aziz, K.: "Rate Dependence of Unstable Waterfloods," *SPE Res. Eng.* (May 1988)
- 24 Batycky, J.P., McCaffery, F.G., Hodgous, P.K. and Fisher, D.B.: "Interpreting Relative Permeability and Wettability from Unsteady State Displacement Measurements," *SPEJ*, (June 1981) 296
- 25 Peters, E.J., and Flock, D.L.: "The Onset of Instability During Two-Phase Immiscible Displacement in Porous Media," *SPEJ*, (April 1981) 249.
- 26 Bentsen, R.G.: "A New Approach to Instability Theory in Porous Media," *SPEJ*, (Oct 1985) 765
- 27 Van Spronsen, E.: "Three-Phase Relative Permeability Measurements Using the Centrifuge Method." Paper SPE/DOE 10688 Presented at the Third Joint Symposium, Tulsa, Okla. (1982)
- 28 O'Mera, D.J., Jr. and Lease, W.O.: "Multiphase Relative Permeability Measurements Using an Automated Centrifuge," Paper SPE 12128 Presented at the SPE 58th Annual Technical Conference and Exhibition, San Francisco (1983)
- 29 Buckley, S.E. and Leverett, M.D.: "Mechanism of Fluid Displacement in Sands," *Trans.*, AIME, Vol. 146 (1942) 107

- 30 Welge, H.J.: "A Simplified Method for Computing Recovery by Gas or Water Drive," *Trans*, AIME, Vol 195 (1952) 91
- 31 Johnson, E.F., Bossler, D P, and Nauman, V.O.: "Calculation of Relative Permeability from Displacement Experiments," *Trans*, AIME, Vol. 216, 2959, 370.
- 32 Jones, S.C. and Rozelle, W O "Graphical Techniques for Determining Relative Permeability from Displacement Experiments," *JPT*, Vol. 15 (1978) 807
- 33 Sigmund, P.M., and McCaffery, F G: "An Improved Unsteady-State Procedure for Determining the Relative Permeability Characteristics of Heterogeneous Porous Media," *SPEJ* (Dec 1973) 343
- 34 Archer, J.S., and Wong, S W "Use of a Reservoir Simulator to Interpret Laboratory Waterflood Data," *SPEJ*, (Dec 1973) 343.
- 35 MacMillan, D.J.: "Automatic History Matching of Laboratory Corefloods to Obtain Relative Permeability Curves," *SPERE*, (February 1987) 85
- 36 Kerig, P.D.: "Estimation of Relative Permeabilities from Displacement Experiments," PhD. Dissertation, Texas A & M Univ., College Station, Texas (1985)
37. Kerig, P.D., Watson, A.T.: "Relative Permeability Estimation from Displacement Experiments: An Error Analysis," *SPE Res Eng* (March 1986).
- 38 Schumaker, L.L.: *Spline Functions Basic Theory*, John Wiley and Sons Inc, New York (1981).
- 39 Kerig, P.D. and Watson, A.T "A New Algorithm for Estimating Relative Permeabilities From Displacement Experiments," *SPE Res Eng*, (1987)
- 40 Bard, Y.: *Nonlinear Parameter Estimation*, Academic Press, New York (1974)
- 41 Marquart, D W. "An Algorithm for Least Squares Estimation of Non-Linear Parameters," *Soc. Industrial Applied Math Journal*, (1963)
- 42 Watson, A.T., Richmond, P.C., Kerig, P.D. and Tao, T.M.: "A Regression Based Method for Estimating Relative Permeabilities from Displacement Experiments," *SPE Res Eng* (1988)
- 43 Richmond, P.C. and Watson, A T, "Estimation of Multiphase Flow Functions From Displacement Experiments," *SPE Res Eng* (1990)
- 44 Fassihi, M R, "Estimation of Relative Permeability from Low Rate Unsteady State Tests - A Simulation Approach," *JCPT*, (May 1989)
- 45 Osaba, J.S.. "Laboratory Measurements of Relative Permeability," *Trans*, AIME Vol 192 (1951) 47
- 46 Rapoport, L.A, and Leas, W.J.: "Relative Permeability to Liquid in Liquid-Gas Systems," *Trans*, Vol 192 (1951)
- 47 Brown, K.M., and Dennis, J.E.: "Derivative Free Analogues of the Levenberg-Marquardt and Gauss Algorithms for Nonlinear Least Squares Approximations," *Numerische Mathematik*, 18 (1972) 289-297
- 48 Brown, K.M.: "Computer Oriented Methods for Fitting Tabular Data in the Linear and Nonlinear Least Squares Sense," Department of Computer, Information, and Control Sciences, TR No 72-13, University of Minnesota
- 49 Levenberg, K.: "A Method for the Solution of Certain Non-Linear Problems in Least Squares," *Quart Appl Math.* 1, (1944) 164-168

TABLE 1
CORE AND FLUID PARAMETERS
FOR ENDPOINT CORRECTION TESTS

| | Core "A" | Core "B" |
|-------------------------|----------|----------|
| Length (cm) | 5.45 | 4.85 |
| Diameter (cm) | 3.80 | 3.80 |
| Porosity (%) | 21.0 | 17.2 |
| Water Viscosity (cP) | 0.581 | 0.581 |
| Live Oil Viscosity (cP) | 3.78 | 3.78 |
| Gas Viscosity (cP) | 0.0124 | 0.0124 |

TABLE 2
ENDPOINT CORRECTION TEST DATA

| CORE "A" | | | |
|---------------------------------------|--|---------------------------|---|
| Injection Rate (ml/hr) | Endpoint Permeability To Water (mD) | Injection Rate (ml/hr) | Endpoint Permeability To Gas (mD) |
| 10 | 1.85 | 20 | 0.825 |
| 20 | 2.37 | 50 | 2.79 |
| 50 | 4.07 | 100 | 3.56 |
| 100 | 6.82 | 200 | 4.69 |
| 200 | 10.98 | 500 | 7.69 |
| Extrapolated Endpoint Permeability | 14.50 | | 7.92 |
| CORE "B" | | | |
| Injection Rate (ml/hr) | Endpoint Permeability To Water (mD) | Injection Rate (ml/hr) | Endpoint Permeability To Gas (mD) |
| 5 | 2.55 | 10 | 3.61 |
| 20 | 4.43 | 20 | 7.10 |
| 40 | 6.62 | 50 | 9.35 |
| 80 | 9.59 | 100 | 9.90 |
| 200 | 13.17 | | |
| Extrapolated Endpoint Permeability | 13.27 | | 10.03 |

Figure 1 - Steady State Relative Permeability Apparatus

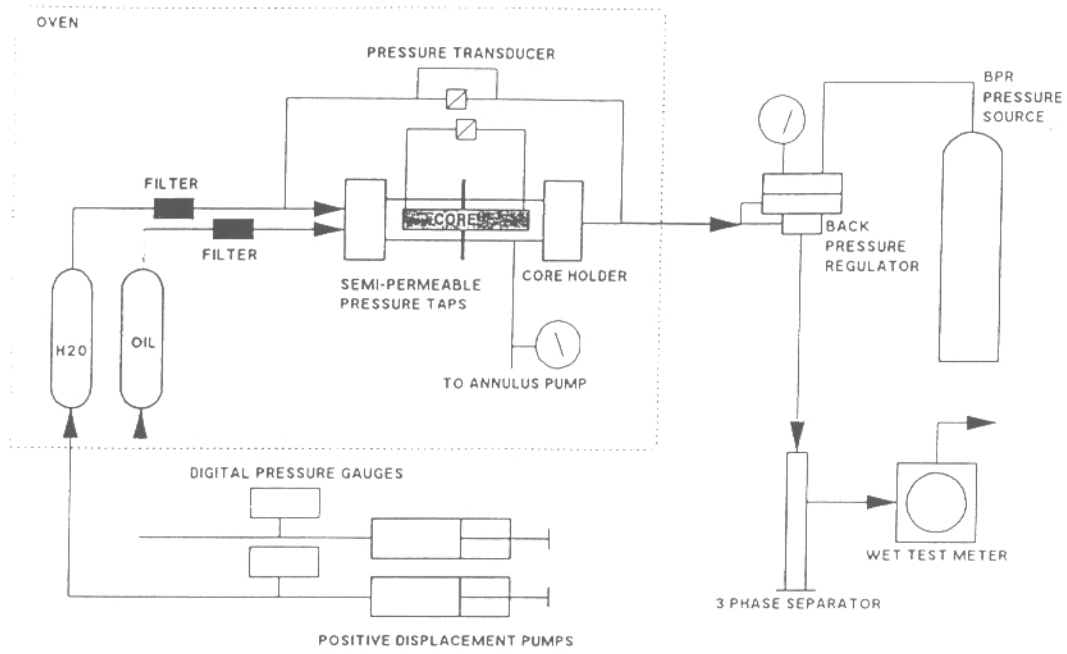


Figure 2 - Unsteady State Relative Permeability Apparatus

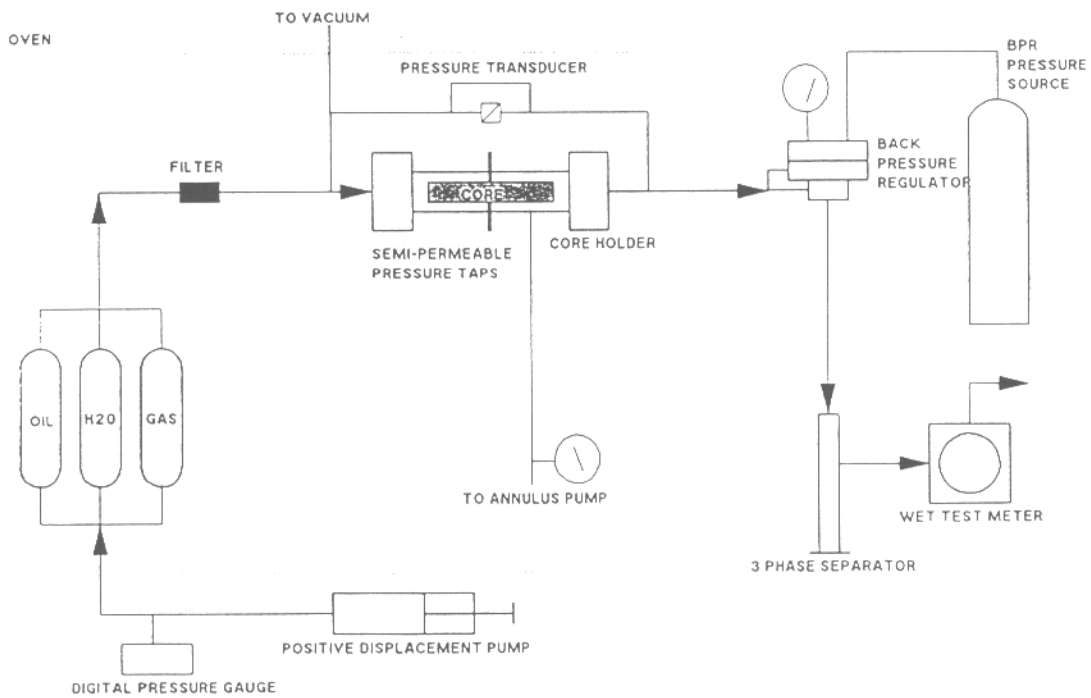
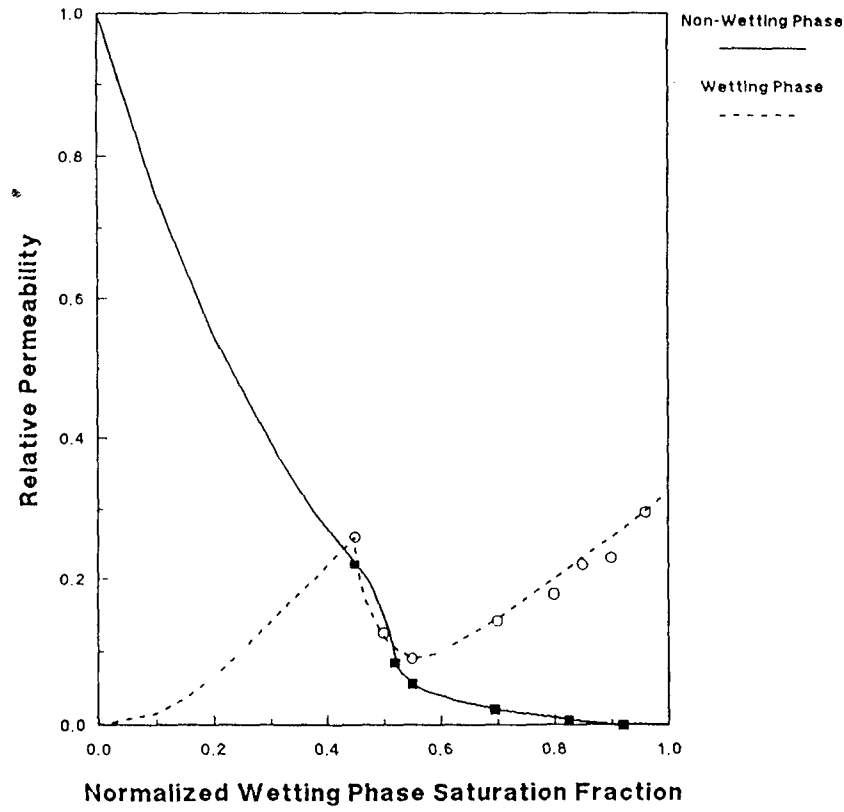


FIGURE 3

IMBIBITION RELATIVE PERMEABILITY - JBN METHOD
RELATIVE PERMEABILITY vs
NORMALIZED WETTING PHASE SATURATION FRACTION



From Sigmund et al (Ref 33)

FIGURE 4

COMPARISON OF VARIOUS RELATIVE PERMEABILITY
CURVE CONFIGURATIONS USING EXPONENTIAL
FUNCTIONAL FORMS

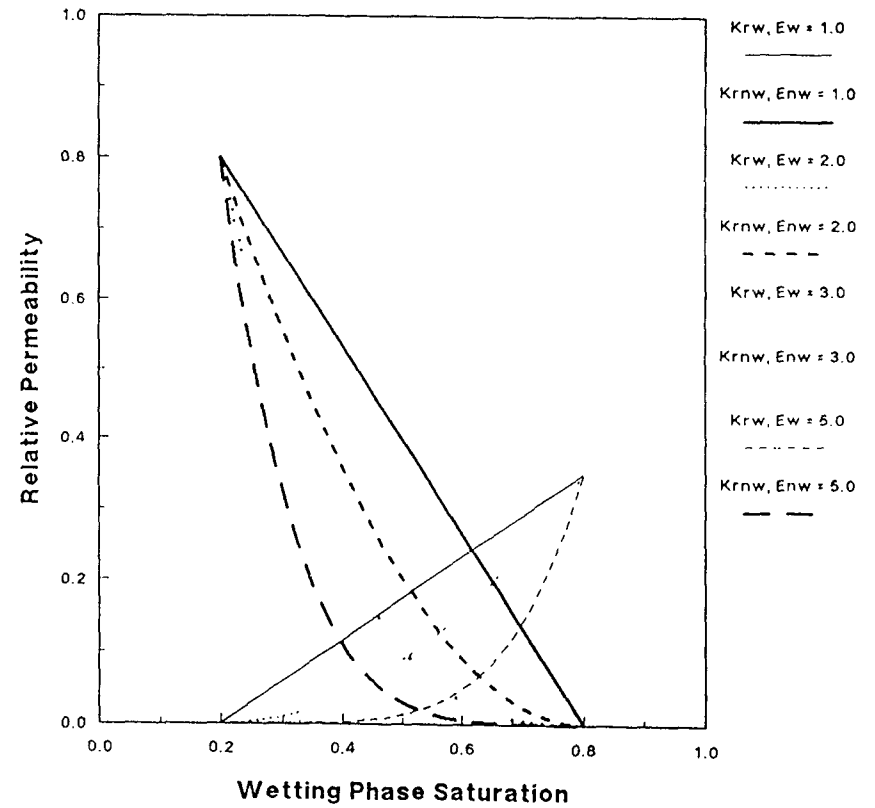


FIGURE 5
EXAMPLE OF RELATIVE PERMEABILITY CURVE
CONFIGURATIONS GENERATED USING CUBIC SPLINE
FUNCTIONAL FORMS

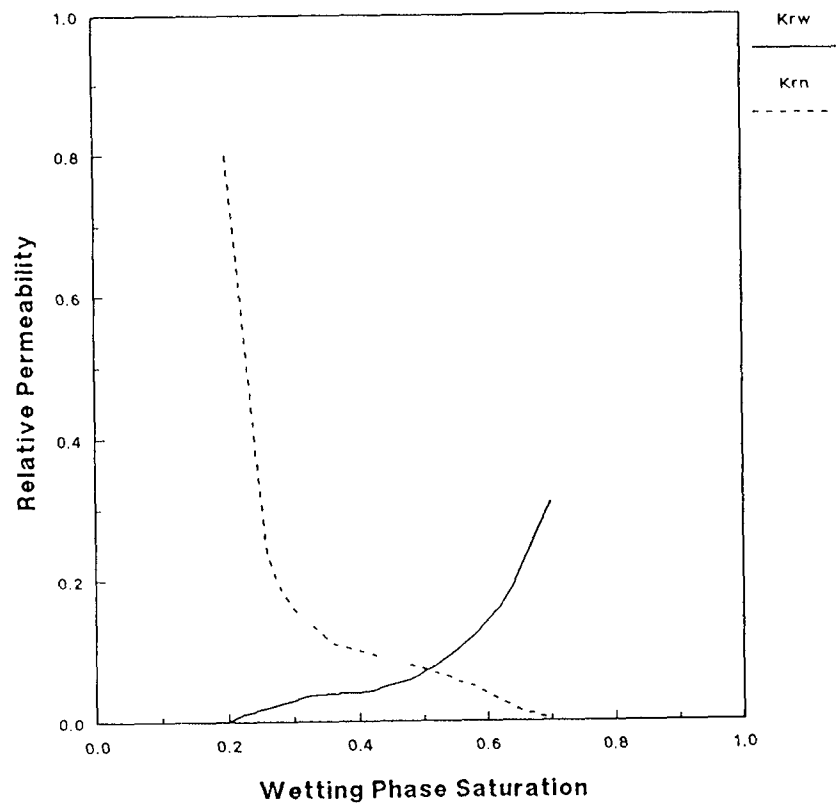
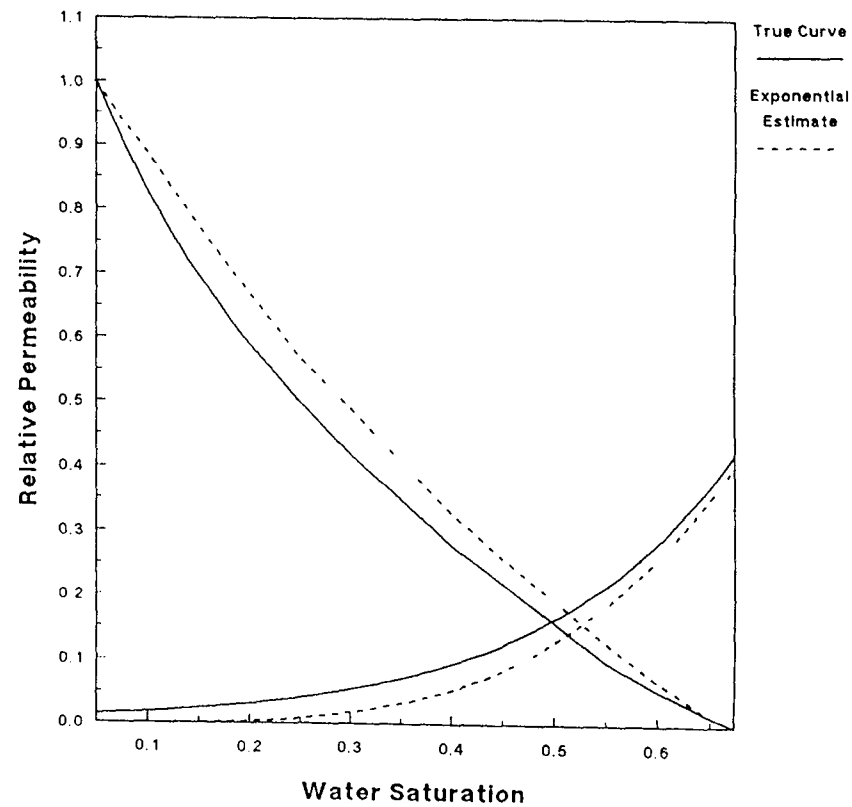


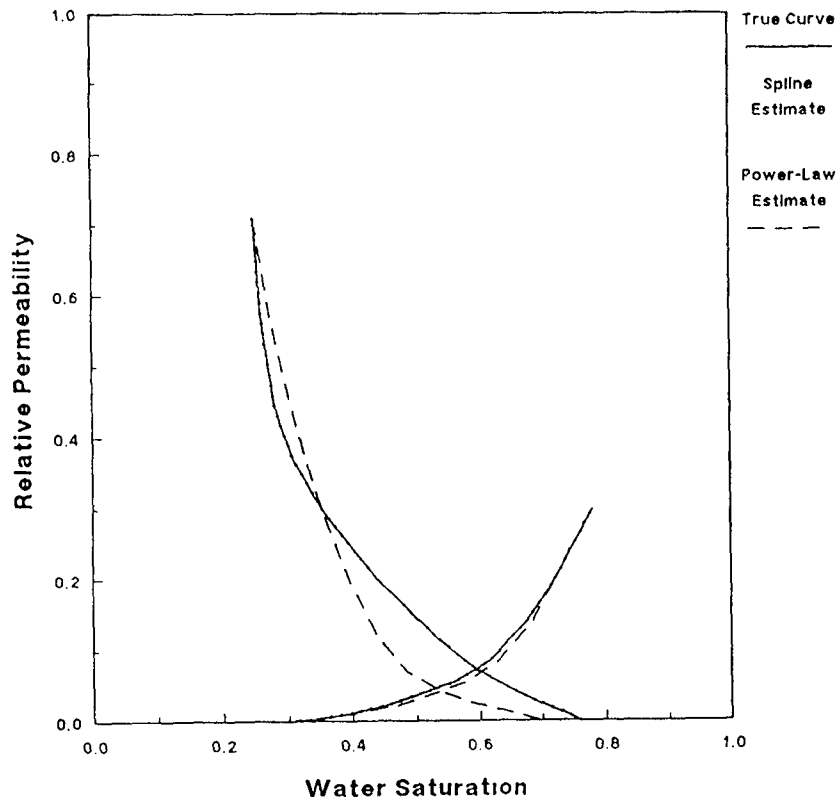
FIGURE 6
ILLUSTRATION OF BIAS ERROR ASSOCIATED WITH THE
USE OF EXPONENTIAL FUNCTIONAL FORMS FOR RELATIVE
PERMEABILITIES IN AUTOMATIC HISTORY MATCHING



From Kerig et al (Ref 37)

FIGURE 7

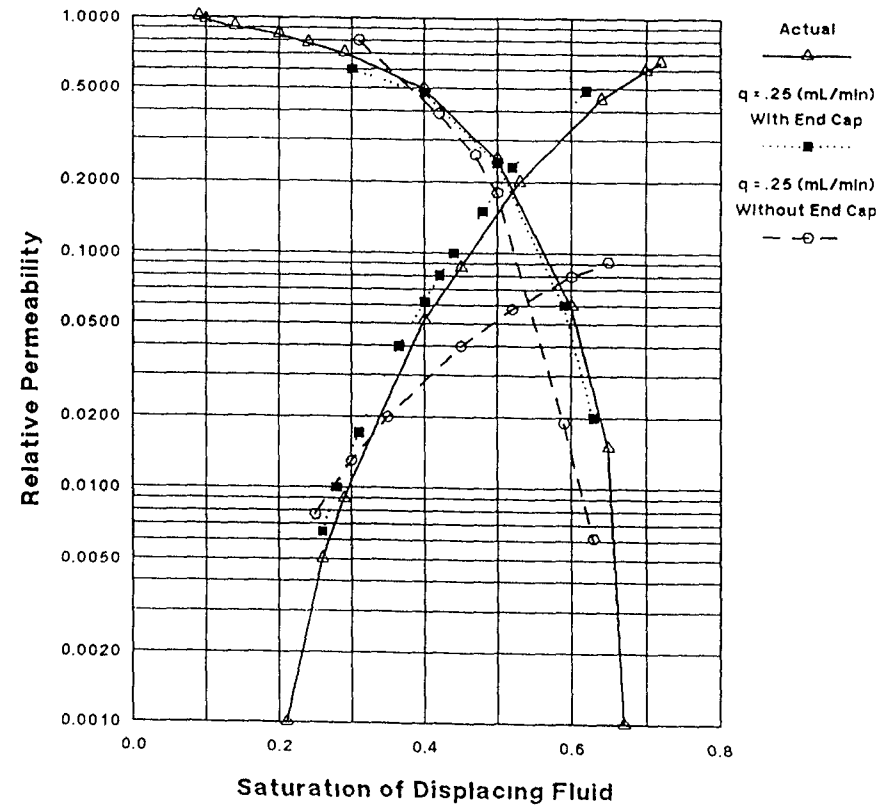
COMPARISON OF EXPONENTIAL AND SPLINE FUNCTIONAL FORMS FOR GENERATING RELATIVE PERMEABILITY CURVES BY THE AUTOMATIC HISTORY MATCHING METHOD



From Watson et al (Ref 42)

FIGURE 8

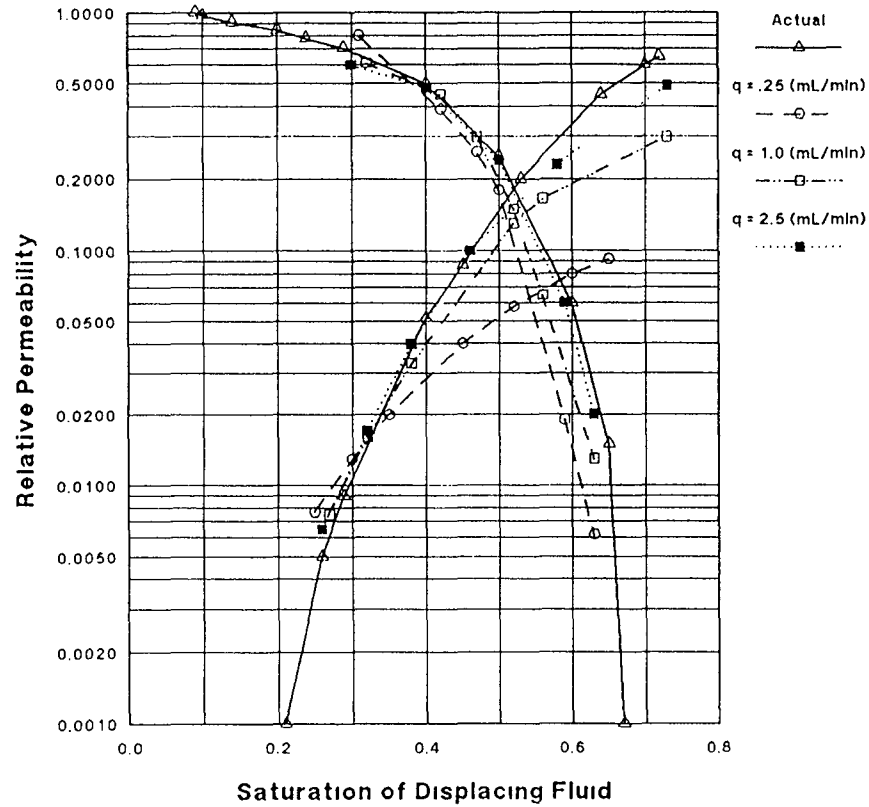
EFFECT OF AN OUTLET SECTION IN NEGATING CAPILLARY END EFFECT



From Fassihi (Ref 44)

FIGURE 9

**EFFECT OF RATE IN NEGATING
CAPILLARY END EFFECTS**



From Fassihi (Ref 44)

FIGURE 10

**ILLUSTRATION OF POTENTIAL CONFIGURATIONS OF
PERMEABILITY PROFILES FROM ELEVATED RATE
DISPLACEMENT TESTS FOR ENDPOINT CORRECTION**

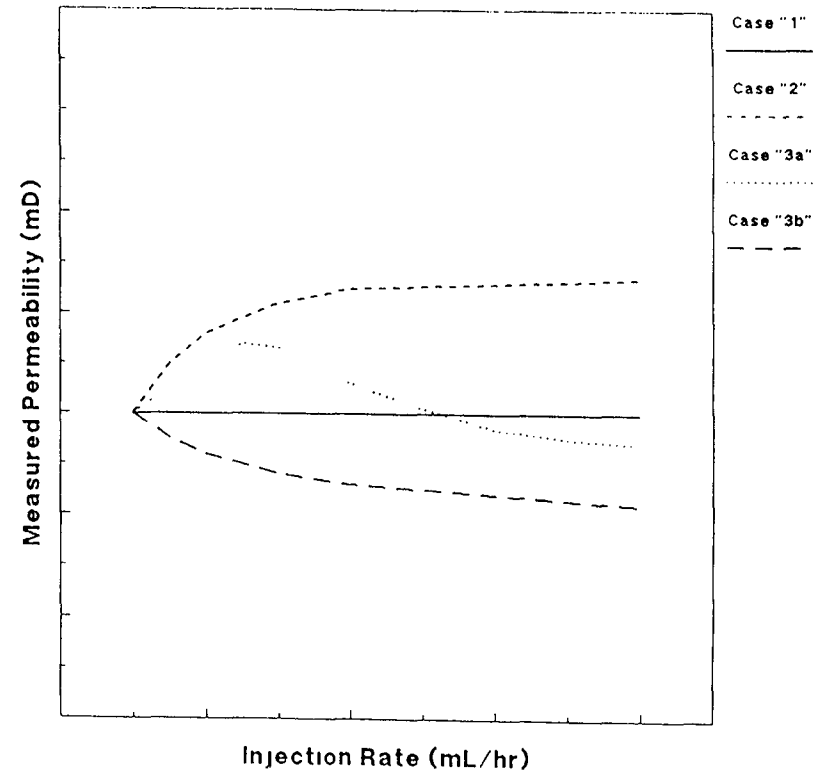


FIGURE 11
ENDPOINT CORRECTION TEST DATA
WATER-OIL TESTS

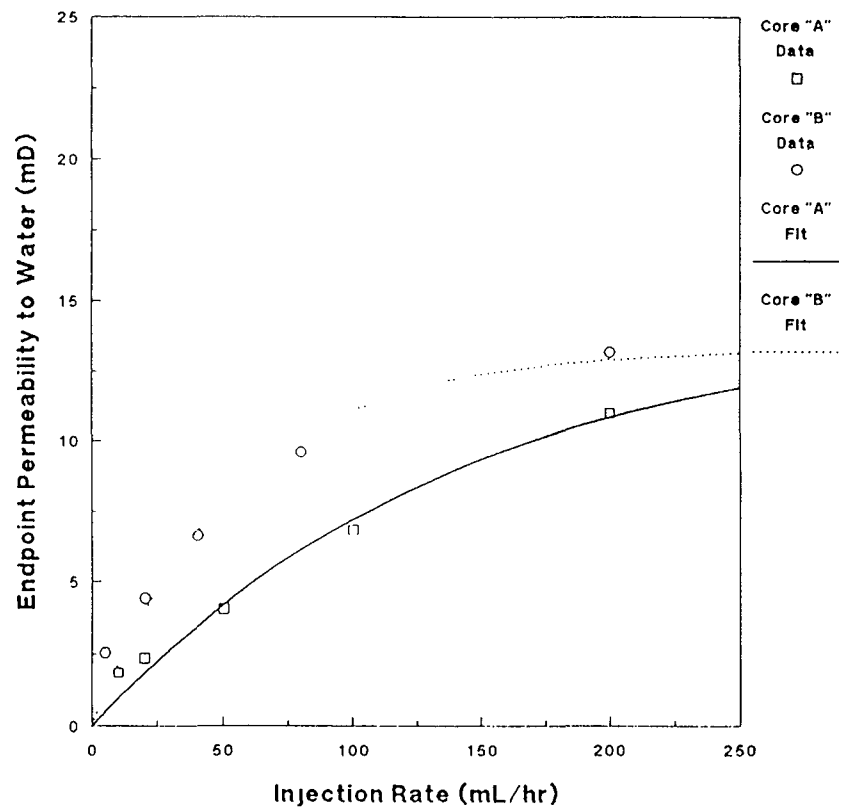


FIGURE 12
ENDPOINT CORRECTION TEST DATA
GAS-OIL TESTS

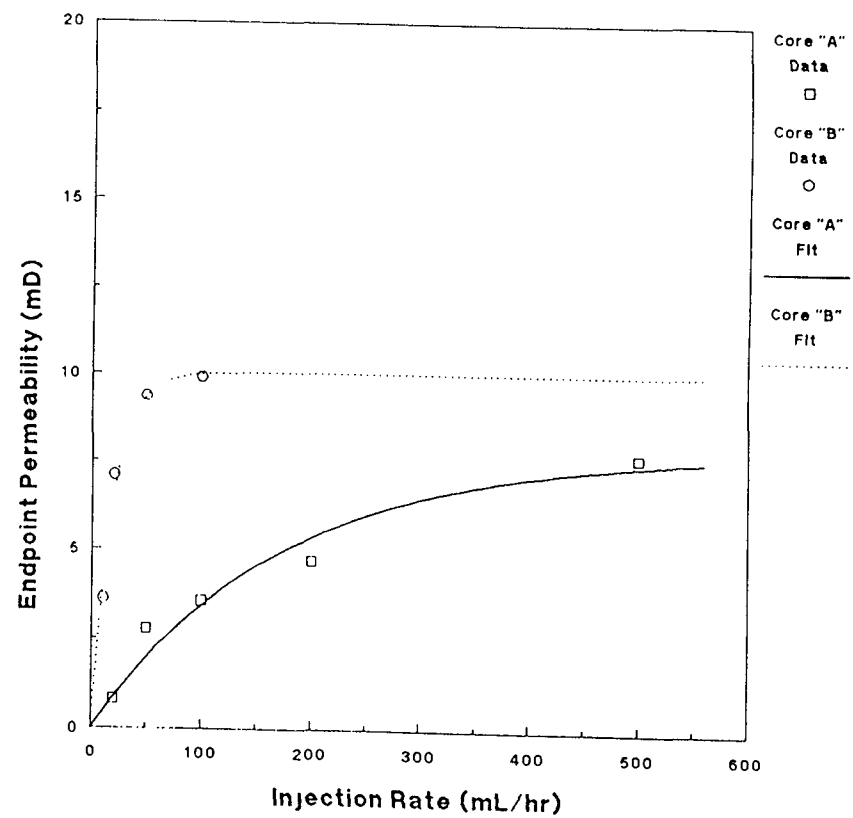


FIGURE 13
EXAMPLE OF APPLICATION OF ENDPOINT CORRECTION
METHOD FOR THE CASE OF A CHANGE IN ENDPOINT
RESIDUAL SATURATION

